



# Mercator Ocean

Ocean Forecasters



## Editorial – Apr 2014 – The Pre-operational PREVIMER system

Greetings all,

This new issue of the Mercator Ocean newsletter is dedicated to the Pre-operational PREVIMER system (see article 1, this issue for a general introduction to the Previmer system) which provides coastal observations and forecasts along French coasts: currents, waves, sea levels, temperature, salinity, primary production and turbidity. Previmer marine environment data come from in situ observations, satellite images, and numerical models. They are centralized and archived in Center for Data in Coastal Operational Oceanography, then published on website and finally disseminated to users. The present issue describes in details all the components of the PREVIMER users system.

The Previmer project was launched on 2006 to enlarge the French operational oceanography capability towards the coastal areas. The first phase (2006-2007) focused on various demonstrators (sea states, coastal circulation, primary production and water quality). The second phase (2008-2013) has ended last December 2013 and aimed at building infrastructures and tools in order to ensure an operational service for the benefit of a wide community (private companies, public organisms, defense, and citizens).

The four main components that constituted the Previmer project are:

- ❶ **in situ observations:** instrumental development, data acquisition, deployment and exploitation of optimized instrumental networks to produce specific coastal data. This component is illustrated in the 3 following papers by Charria et al., Beurret and Thomas as well as Beurret et al.
- ❷ **modeling tools:** development and evolution of numerical models, coupling of hydrodynamical (waves and circulation), sedimentological, biogeochemical models, data assimilation, tools for the chemical and toxicity risk analysis. This component is illustrated with 7 papers: see for example the papers in this issue by Pineau-Guillou et al, Arduin et al. and Garnier et al.
- ❸ **interface tools for users and advanced products:** satellite data processing, synthetic indicators, data, images, dissemination thanks to the web. This component is illustrated in this issue in the 2 following papers: Theetten et al. and Raynaud et al.
- ❹ **data center dedicated to coastal operational oceanography (CDOCO):** acquisition, quality control, diffusion of observations and model results, implementation of the models and data center, daily production of services and products. This component is illustrated in the following paper: Faillot et al., this issue.

Franck Dumas and Laurence Crosnier, Editors.

## Table of Content:

<b>1. GENERAL INTRODUCTION:</b>	
<b>PREVIMER, A FRENCH PRE-OPERATIONAL COASTAL OCEAN FORECASTING CAPABILITY .....</b>	<b>3</b>
<i>By Dumas F., L. Pineau-Guillou, F. Lecornu, J.-F. Le Roux, B. Le Squère</i>	
<b>2. PREVIMER: A CONTRIBUTION TO IN SITU COASTAL OBSERVING SYSTEMS . .....</b>	<b>9</b>
<i>By G. Charria, M. Repecaud, L. Quemener, A. Ménesguen, P. Rimmelín-Maury, S. L'Helguen, L. Beaumont, A. Jolivet, P. Morin, E. Macé, P. Lazure, R. Le Gendre, F. Jacqueline, R. Verney, L. Marié, P. Jegou, S. Le Reste, X. André, V. Dutreuil, J.-P. Regnault, H. Jestin, H. Lintanf, P. Pichavant, M. Retho, J.-A. Allenou, J.-Y. Stanisière, A. Bonnat, L. Nonnotte, W. Duros, S. Tarot, T. Carval, P. Le Hir, F. Dumas, F. Vandermeirsch, F. Lecornu</i>	
<b>3. OBSERVATION OF SURFACE CURRENTS BY HF RADARS .....</b>	<b>21</b>
<i>By S. Beurref, N. Thomas</i>	
<b>4. PAOLA: A NEW AUTONOMOUS AIR-DEPLOYED OCEAN PROFILER .....</b>	<b>23</b>
<i>By S. Beurref, P. Brault, A. David</i>	
<b>5. A NEW PROCEDURE FOR INTERPOLATING SATELLITE-DERIVED SUSPENDED PARTICULATE MATTERS WITHIN THE PREVIMER CONTEXT .....</b>	<b>25</b>
<i>By F. Gohin, P. Bryère, L. Perrot</i>	
<b>6. PREVIMER: IMPROVEMENT OF SURGE, SEA LEVEL AND CURRENTS MODELLING .....</b>	<b>29</b>
<i>By L. Pineau-Guillou, F. Dumas, S. Theetten, F. Arduin, F. Lecornu, J.-F. Le Roux, D. Idier, H. Muller, R. Pedreros</i>	
<b>7. NUMERICAL WAVE MODELING IN PREVIMER: MULTI-SCALE AND MULTI-PARAMETER DEMONSTRATIONS .....</b>	<b>39</b>
<i>By F. Arduin, M. Accensi, A. Roland, F. Girard, J.-F. Filipot, F. Leckler, J.-F. Le Roux</i>	
<b>8. DOWNSCALING FROM OCEANIC GLOBAL CIRCULATION MODEL TOWARDS REGIONAL AND COASTAL MODEL USING SPECTRAL NUDGING TECHNIQUES .....</b>	<b>44</b>
<i>By G. Herbert, Garreau, P., Garnier V., Dumas F., Cailleau S., Chanut J., Levier B., Aznar R.</i>	
<b>9. EVALUATION OF THE HYDROLOGY AND DYNAMICS OF THE OPERATIONAL MARS3D CONFIGURATION OF THE BAY OF BISCAY .....</b>	<b>60</b>
<i>By H. Berger, F. Dumas, S. Petton, P. Lazure</i>	
<b>10. MENOR: A HIGH-RESOLUTION (1.2 KM) MODELING OF THE NORTH-WESTERN MEDITERRANEAN SEA ROUTINELY RUN BY THE PREVIMER OPERATIONAL FORECAST SYSTEM .....</b>	<b>69</b>
<i>By V. Garnier, I.L. Pairaud, A. Nicolle, E. Alekseenko, M. Baklouti, B. Thouvenin, F. Lecornu, P. Garreau</i>	
<b>11. DEVELOPMENT AND VALIDATION OF A SEDIMENT DYNAMICS MODEL WITHIN A COASTAL OPERATIONAL OCEANOGRAPHIC SYSTEM .....</b>	<b>76</b>
<i>By F. Cayocca, R. Verney, S. Petton, M. Caillaud, M. Dussauze, F. Dumas, J-F. Le Roux, L. Pineau, P. Le Hir</i>	
<b>12. OPERATIONAL MODELLING OF NUTRIENTS AND PHYTOPLANKTON IN THE BAY OF BISCAY AND ENGLISH CHANNEL .....</b>	<b>87</b>
<i>By A. Ménesguen, M. Dussauze, F. Lecornu, F. Dumas, B. Thouvenin</i>	
<b>13. BMGTOOLS : A COMMUNITY TOOL TO HANDLE MODEL GRID AND BATHYMETRY .....</b>	<b>94</b>
<i>By S. Theetten, B. Thiébaud, F. Dumas, J. Paul</i>	
<b>14. VACUMM – A PYTHON LIBRARY FOR OCEAN SCIENCE .....</b>	<b>99</b>
<i>By S. Raynaud, G. Charria, J. Wilkins, V. Garnier, P. Garreau, S. Theetten</i>	
<b>15. A TOOL FOR COASTAL OCEAN FORECASTER .....</b>	<b>103</b>
<i>By M. Faillot, J. Lagadec, D. Jourdan, B. Le Squère, J.-M. Léculier</i>	

## GENERAL INTRODUCTION: PREVIMER, A FRENCH PRE-OPERATIONAL COASTAL OCEAN FORECASTING CAPABILITY.

By *F. Dumas<sup>(1)</sup>, L. Pineau-Guillou<sup>(1)</sup>, F. Lecornu<sup>(1)</sup>, J.-F. Le Roux<sup>(1)</sup>, B. Le Squère<sup>(2)</sup>*.

<sup>1</sup>IFREMER, Brest, France

<sup>2</sup>SHOM, Brest, France

### Abstract

Pre-operational system PREVIMER provides with coastal observations and forecasts along French coasts: currents, waves, sea levels, temperature, salinity, primary production and turbidity. These marine environmental data come from in situ observations, satellite images, and numerical models. They are centralized and archived in PREVIMER databases, then published on website (real time and historical data), and freely available to users, private companies as well as public administrations. This paper describes in details PREVIMER components and users.

### Outlines of Previmer

The Previmer project was launched in 2006 in order to extend the French operational oceanography capability towards the coastal areas. The first phase (2006-2007) focused on various demonstrators (sea states, coastal circulation, primary production and water quality). The second phase (2008-2013) aimed at building infrastructures and tools in order to ensure a pre-operational service for the benefit of a wide community (private companies, public administrations, defense, and citizens).

Previmer relies on the partnership of several public organisms: Ifremer, SHOM and Météo-France. The Previmer Project provides observations, ocean hindcasts and forecasts in real time to the users of coastal areas. It has been identified in the State/Region contracts (CPER 2000-2006 and 2007-2013) of Brittany and funded jointly by the organisms and the Region. The development and their exploitation are performed within the scope of the public partnership (Ifremer, SHOM, Météo-France) with assistance of private companies. All the numerical simulations and the data processing uses the supercomputer Caparmor, hosted on the Ifremer center located in Brest. All the teams that collaborate to the project are located at Ifremer and SHOM. This project is coordinated by Ifremer and SHOM.

### Previmer Components

The components of the Previmer project encompass various aspects involved and required for coastal operational oceanography:

- ❶ **in situ observations**: instrumental development, data acquisition, deployment and exploitation of optimized instrumental networks to produce specific coastal data,
- ❷ **modeling tools**: development and improvement of numerical models, hydrodynamical coupling (waves and circulation), sedimentological, biogeochemical models, data assimilation, chemical and toxicity risk analysis tools.
- ❸ **interface tools for users and advanced products** : satellite data processing, synthetic indicators, data, images, dissemination through internet, ...
- ❹ **data center dedicated to coastal operational oceanography (CDOC)**: acquisition, quality control, dissemination of observations and model results, models implementation, daily production of services and products.

These components are coordinated by a management team which also ensures the valorization of the project.

#### ❶ In situ observation

This task is focused on the development and acquisition of in situ instruments that must be reinforced to fill the gap in coastal observations networks. Here, sustainable and recurrent dedicated acquisitions are targeted to supply a database for analysis, validation and future data assimilation. For that purpose various observation sensors are on track:

- network of profilers (figure 1) fitted to coastal environment (shallow waters, high frequency dynamics, strong currents, intense foiling) from those deployed at global scale observation within ARGO or completely new concepts.
- Anchored multi-parametric platforms,
- Sensors mounted on trawlers, scientific or merchant fleet ships to pick up additional opportunity measurements,
- of the national tide gauges network (SHOM) with real time acquisition and transmission capacity,
- Extension of the CANDHIS network (CEREMA) of wave buoys.

The radar HF Observation which started at the very beginning of Previmer (2006) has been extended during the second phase of the project. Thus it gives a continuous database from then up to now of sea surface currents over the Iroise Sea, a work area of the project (See Beurret and Thomas, this issue). All the deployments of instruments were optimized considering a cost/benefit ratio with regards to investments and exploitation. All these systems and the data acquired are described by Charria et al (this issue).



Figure 1: Arvor-C profiler

## ② Modeling tools

This item concerns mostly the development and improvement of numerical ocean models used within the scope of Previmer (MARS, WaveWatch III® and HYCOM models). It deals with the integration of operational constraints requiring to evolve from research to operational tools (assessment of the numerical solution regarding available observation, confidence indicators, and descriptors of the state of the systems). It also includes the evolution of the state of the art of numerical modeling due to the progress in knowledge (mixing parameterization, wave/circulation interactions, data assimilation methods specific to the coastal zone, coherent interfacing with global numerical solutions like spectral nudging; for this last point, see Herbert et al this issue).

Data collections have been properly organized from different sources of information at the CDOCO in order to be integrated to the validation process. These information are sea surface temperature, sea states, radiative thermal fluxes, ocean color (chlorophyll a as an indicator of the total biomass and water clearance, phytoplankton and suspended particulate matter) and in a next future sea surface salinity.

Most of the questions that coastal operational oceanography intends to address are multidisciplinary and require beyond the ocean physics parameters (currents, hydrology,...) descriptions of the state of the system on sedimentology and biogeochemistry (see for example Menesguen et al this issue).

Regarding the sea state description, many evolutions of WaveWatch III® have been conducted (see Arduin et al, this issue) in order to enhance its performance in the coastal area (unstructured grid with adaptive time stepping, wave breaking parametrization...). This numerical model has also been adapted to be interfaced with ocean and atmospheric circulation models thanks to numerical coupling kit (OASIS/PALM).

## ③ Interface users tools

The project also aims at developing tools upstream and downstream of the numerical models. Upstream of the model, these tools (ie Bmgttools, see Theetten et al this issue) are designed to ease the building of new model configurations (generate model inputs such as atmospheric forcings, boundary conditions, river runoffs and in-situ observations) in order to be more efficient and shorten the time between their development and their operational use in particular in the context of environmental crisis or simply to minimize the development costs for new areas. Some user interfaces have been developed in order to integrate sedimentological, chemical or biogeochemical modules to the circulation models and to facilitate their broadcast and implementation for the project partners.

Downstream of the models, tool boxes, (e.g. like Vacuum, Charria et al this issue), have been developed as generic tools to facilitate the assessment of model performances, to detect possible deficiencies at different levels of the forecasting process, generate quality indicators or advanced products (indicators, bulletin - <http://www.previmer.org/newsletter>-, trends, anomalies) that suit better the societal request of information. It has been developed in cooperation with the private partners of the project to target downstream services.

The access to all the data and results of the different applications (mapped and commented data) which represents the daily update of the environment state is given through a dedicated website ([www.previmer.org](http://www.previmer.org), figure 2). It has been designed to fulfill a wide panel of user requirements. This site gives an access according to various criteria: the results can thus be viewed according to thematic criteria (sea level, current, wave, temperature ...), temporal criteria (short terms forecasts, present state, hindcasts), application criteria (according to the numerical model used) or geographical criteria.

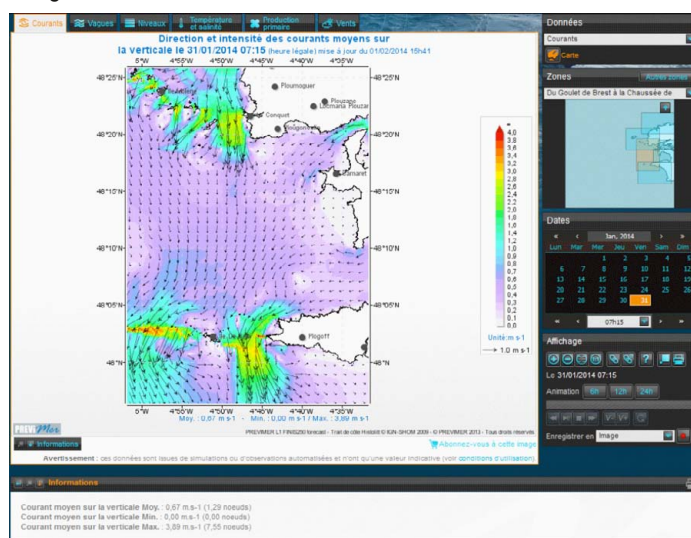


Figure 2: Website PREVIMER [www.previmer.org](http://www.previmer.org): currents in Iroise Sea the 31st of January 2014 at 07:15

## ④ Center for coastal operational oceanography

The operational center is divided into two parts: the data center for coastal operational oceanography (CDOCO) in real time itself and on the other hand a component which is in charge of the implementation and the supervision of all the modeling processes. For this purpose, it makes available in an optimal way all the information required for modeling according to the arrival time. This center also ensures a help to the Previmer users.

First CDOCO ensures collecting external data (Météo-France, SHOM, Direction de l'Eau, Mercator Océan, CETMEF...) with a conventional framework agreed by all the partners on a routine and sustainable basis. Data control procedures are applied according to international standards in order to guarantee the highest level of quality to the database thus built. Besides, the CDOCO ensures the archiving of the whole set of numerical results and products for retrospective analysis purposes.

The development of the CDOCO has been extended to operational treatments in order to gather, validate and provide the different time series required by the modeling activities:

- forcing data: meteorological forcings, open boundary and initial conditions (from Mercator Ocean), river runoffs (water, nutrients, sediments and organic matter),
- reference data: coast line, bathymetry, bottom sediment,
- in situ data: from campaigns, from operational networks. These are also archived in Coriolis database,
- satellite data: sea surface temperature, waves, water color, radiative thermal fluxes and wind products (archived at CERSAT).

The second part of the center for coastal operational oceanography is dedicated to the operational chains for the modeling processes. They are designed to facilitate the daily production of forecasts, analysis and advanced products derived from input data and model results. An effort has been put on the optimization of these chains, their safety and their ergonomics in order to ease their supervision and to reach the better service level agreement.

## Project Targets in terms of spatial and temporal scales

The Previmer project is focused on coastal areas. The spatial scales targeted within the scope of the project start at the regional scale down to the scale of the bay or the estuaries or even to the scale of the shellfish production or coastal fisheries areas. The resolutions of the various models start from a few kilometers (for the Bay of Biscay -see Berger et al this issue- or the North Western Mediterranean Sea -see Garnier et al this issue-) down to several hundreds of meters (see Pineau-Guillou et al this issue) for the coastal zones. All the metropolitan areas are thus covered.

The temporal scales associated extend from the present time to forecast at J+4 (for the circulation) to J+9 (for wave fields). On the one hand, the refreshing of the information provided is performed once a day for circulation, twice a day for waves. On the other hand, the hindcasts produced within Previmer cover the whole period of the project (2006/2013). The time steps with which the numerical solution is stored and broadcasted are compatible with the high and low frequency of the phenomenon relevant in the coastal dynamics, from the seasonal frequency (thermal and haline fronts, stratification) to 15 minutes period (tidal currents, surges).

## Previmer users

There are two types of PREVIMER users: those who access to information through the website, and those who access to digital products via a ftp server. Website allows viewing the data; it is quite difficult to describe who website users are, because they do not need to register. To access to numerical data, users need to register through a form, and receive access codes to download freely data. This methodology is not so much appreciated by users - who prefer to download data without registration, but allows collecting information about users and analysing who they are.

## Website users

PREVIMER website [www.previmer.org](http://www.previmer.org) (figure 2) publishes results from models, in-situ observations and satellite images split into different thematic: currents, sea levels, waves, temperature and salinity, primary production and turbidity. Users do not need to register so it is quite difficult to get their profiles. We have some indirect returns, showing that their profiles are very different:

- researchers consulting satellite images to validate models,
- forecasters (meteorological or flood forecasting services) consulting surges,
- ship pilots consulting waves and currents,
- fishermen consulting temperature to find hot water veins for fishing bass,
- biologists consulting primary production in case of toxic blooms,
- scientists consulting environmental conditions before sea surveys...

The website traffic has permanently increased since 2006 (figure 3). In 2013, the traffic reaches an average of 4000 visitors per day, with some peaks exceeding 6000 users per day, particularly during storms. For example in 2013, we noticed peaks at these dates:

- 27th of October 2013, 6379 visitors (Christian storm),
- 23rd of December 2013, 5767 visitors (Dirk storm).

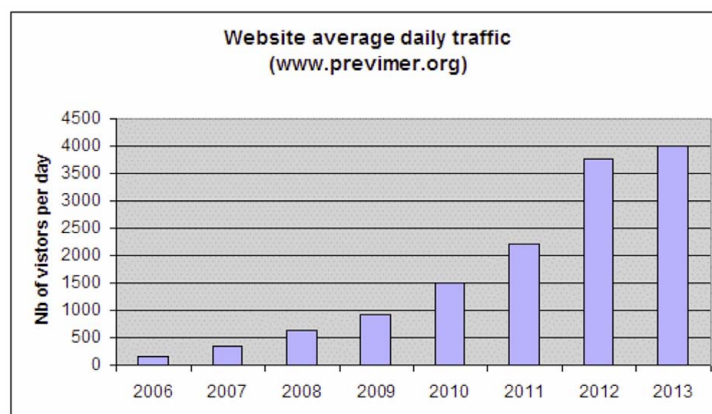


Figure 3: Website [www.previmer.org](http://www.previmer.org): average daily traffic

Users access to PREVIMER website in order to visualize mainly results from models (forecast and hindcast): observations (including satellite and in-situ) represents only 5% of consulted pages, wave models 71%, hydrodynamic models 22% and biogeochemical models 2%. The most viewed pages are wave models; however, concerning digital products, we will see in next part that it tends to reverse: users first ask for hydrodynamic models (46%), and wave models are only in second position (39%).

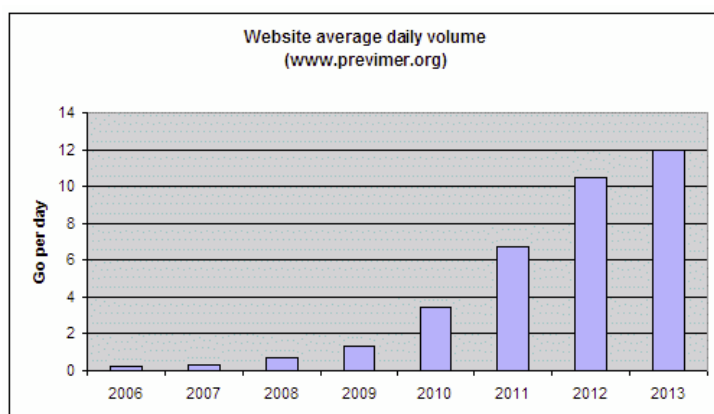


Figure 4: Website [www.previmer.org](http://www.previmer.org): average daily volume

Concerning website daily volume, it has never stopped increasing since 2006 (figure 4). The average daily volume of web consultations reaches 12Go in 2013.

## Numerical products users

Numerical products are described in PREVIMER products catalogue (PREVIMER Project team, 2014). They include:

- analysis and forecasts: results from hydrodynamic, wave and biogeochemical models,
- observations: currents from High Frequency radars over Iroise sea,
- atlases: harmonic constituents of tidal water levels and currents along Atlantic and English Channel French coasts (Pineau-Guillou 2013),
- hindcasts: sea-states hindcast HOMERE (1994-2013) over the Channel and the Bay of Biscay (Bouidière et al. 2013).
- 38 products are registered in the catalogue, there are described in table 1.

Product type	Product name	Geographical Area	Resolution
Hydrodynamic models MARS3D	PREVIMER_F1-MARS3D-MANGAE2500	Bay of Biscay & English Channel	2500 m
	PREVIMER_F2-MARS3D-MENOR1200	North West Mediterranean Sea	1200 m
Biogeochemical models ECOMARS3D	PREVIMER_B1-ECOMARS3D-MANGA4000	Bay of Biscay & English Channel	4000 m
Hydrodynamic models MARS2D	PREVIMER_L1-MARS2D-ATLNE2000	North East Atlantic	2000 m
	PREVIMER_L1-MARS2D-MANGA700	Bay of Biscay & English Channel	700 m
	PREVIMER_L1-MARS2D-MANE250	Eastern Channel	250 m
	PREVIMER_L1-MARS2D-MANW250	Western Channel	250 m
	PREVIMER_L1-MARS2D-FINI250	Finistère	250 m
	PREVIMER_L1-MARS2D-SUDBZH250	South Brittany	250 m
	PREVIMER_L1-MARS2D-AQUI250	Aquitaine	250 m
Hydrodynamic models HYCOM	PREVIMER_HYCOM-MANGASC60	Bay of Biscay & English Channel	~1800 m
Wave models WAVEWATCH III (regular grids)	PREVIMER_WW3-NORGAS-2MIN	Bay of Biscay & English Channel	~3700 m
	PREVIMER_WW3-MENOR-2MIN	North West Mediterranean Sea	~3700 m
	PREVIMER_WW3-PDC-200M	Pas de Calais	200 m
	PREVIMER_WW3-SUDBZH-200M	South Brittany	200 m
	PREVIMER_WW3-LOIRE-200M	Loire	200 m
	PREVIMER_WW3-AQUITAINE-200M	Aquitaine	200 m
	PREVIMER_WW3-NORMANDIE-200M	Normandy	200 m
	PREVIMER_WW3-COTENTIN-200M	Cotentin	200 m
	PREVIMER_WW3-ARMOR-200M	North Brittany	200 m
	PREVIMER_WW3-FINIS-200M	Finistère	200 m
	PREVIMER_WW3-ROUSSILLON-200M	Roussillon	200 m
	PREVIMER_WW3-LANUEDOC-200M	Languedoc	200 m
	PREVIMER_WW3-PROVENCE-200M	Provence	200 m
	PREVIMER_WW3-CHARENTES-200M	Charentes	200 m
	PREVIMER_WW3-ANTILLES-3MIN	West Indies	~5500 m
PREVIMER_WW3-POLYNESIE-3MIN	Polynesia	~5500 m	
PREVIMER_WW3-CALEDONIE-3MIN	Caledonia	~5500 m	
PREVIMER_WW3-REUNION-180M	Reunion	180 m	
Wave models WAVEWATCH III (unstructured grids)	PREVIMER_WW3-NORGAS-UG	Bay of Biscay & English Channel	Up to 200 m
	PREVIMER_WW3-MENOR-UG	North West Mediterranean Sea	Up to 200 m
	PREVIMER_WW3-IROISE-UG	Iroise	Up to 200 m
	PREVIMER_WW3-REUNION-UG	Reunion	Up to 200 m
Wave spectra WAVEWATCH III	PREVIMER_WW3-SPECTRA-1D	Global	-
	PREVIMER_WW3-SPECTRA-2D	Global	-
Current HF Radar Observations	SHOM_COURANT_RADARS-HF-VIGICOTE	Iroise sea	
Harmonic constituents atlases	PREVIMER_L1-ATLAS-HARMONIQUES	North East Atlantic	Up to 250 m
Sea-states hindcast HOMERE (1994-2013)	PREVIMER_HOMERE-NGUG	Bay of Biscay & English Channel	Up to 200 m

Table 1: PREVIMER products

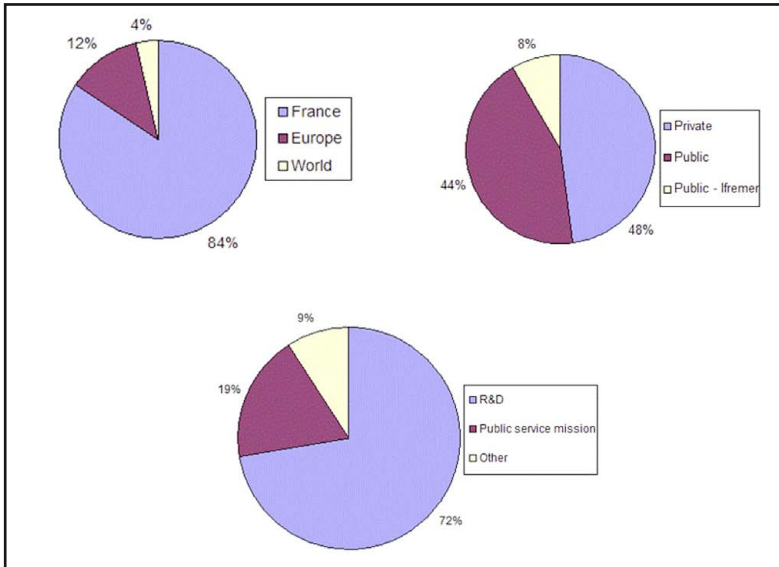


Figure 5: Origin of numerical products users

Users need to register to access to numerical products; they receive access codes and can access to data through ftp and OpenDap. PREVIMER registered 262 requests between February 2010 and December 2013, which means around 70 requests per year. Those registered between February 2010 and August 2012 (141 requests) have been analyzed, results are presented below.

Concerning the origin of users (figure 5), they come mainly from France (84%), but also from Europe (12%) and out of Europe (4%). There is a good repartition between private sector (48%) and public sector (52%). It appears that 8% of users come from Ifremer; however, this figure is largely underestimated because many Ifremer users access directly to PREVIMER data, without filling the PREVIMER form (and are not registered). Users are mainly involved in R&D activities (72%), only 19% are in charge of public service mission.

Concerning the type of products (figure 6), main part of requests concern hydrodynamic models (46%), followed by wave models (39%), observations (8%) and biogeochemical models (7%). The wave models are the most consulted on website, but are not the most downloaded (hydrodynamic models are the first downloaded). Among hydrodynamic models, the Bay of Biscay and Channel MARS3D model is the most downloaded (39%), then North West Mediterranean Sea MARS3D model (33%), followed by MARS2D high resolution models (28%). Users are mainly interested in delayed time (67%) instead of real time (33%).

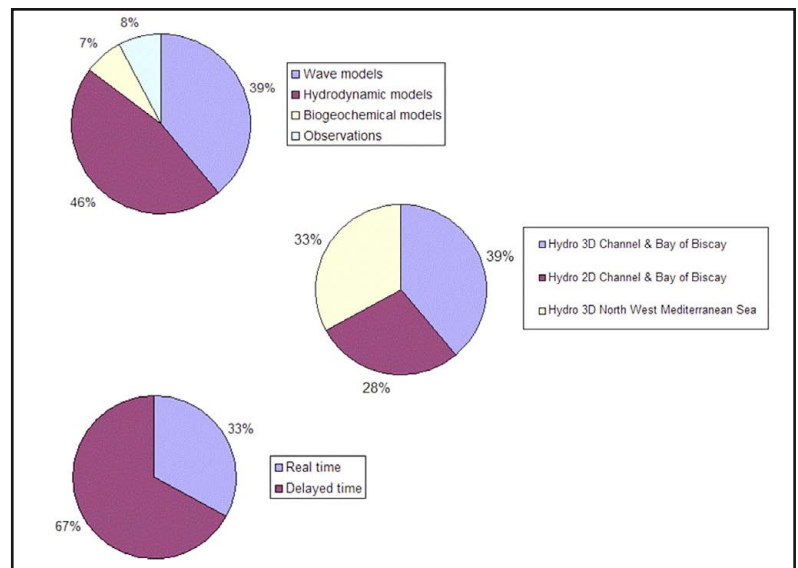
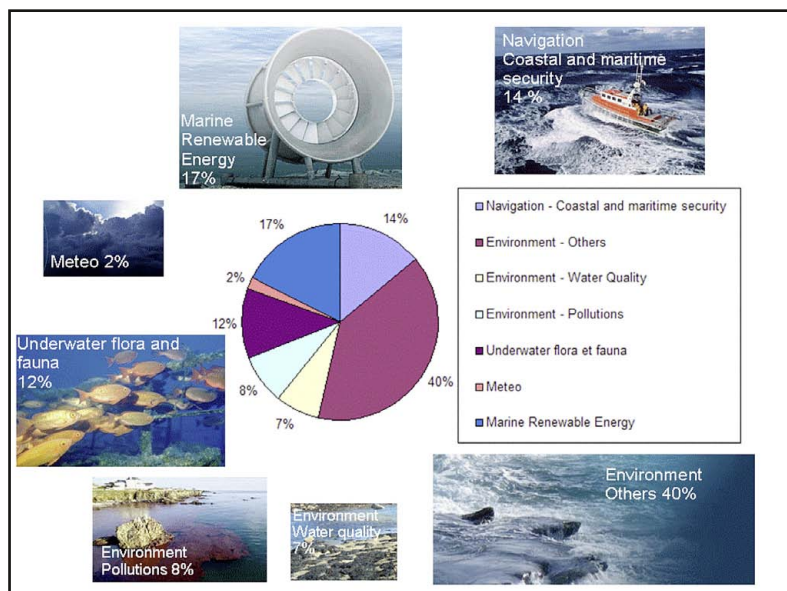


Figure 6: Type of numerical products repartition



Concerning activities sectors (figure 7), the main sector is from far environment (40%, not taking into account water quality and pollutions, counted separately), then Marine Renewable Energy (17%), followed by navigation and maritime security (14%), underwater flora and fauna (12%), pollutions (8%), water quality (7%) and meteo (2%). Some examples of requests are presented in table 2. All these activities have not the same real-time constraints: activities with the more constraints are pollutions (64% of these requests ask to access to real-time data) and navigation and maritime security (42% of these requests ask to access to real-time data), whereas for activities like underwater flora and fauna, only 13% of these requests ask to access to real-time data.

Figure 7: Activity sectors repartition

In 2013, a user satisfaction survey has been sent to users, 30 of them answered, with a good representation of private (46%) and public (54%) sectors. We noticed that only 71% of users have exploited the data they had asked; this is mainly due to problem linked with data format (some users do not know how to deal with NetCDF format) or data volume (often large volumes), or by lack of time from users. For those who have exploited data, 94 % of them are satisfied with data, and 88% find essential that this service goes on.

Activity sector	Organism	Object
Navigation Coastal and maritime security	Météo-France	Acces to modeled surges, in the context of Vigilance Waves Submersion
	Ministry of Ecology / CEREMA (ex-CETMEF)	Development of Le Havre maritime harbour
	ACTIMAR	PREVICOT project : routes optimization in the Mediterranean Sea
Environment	Ifremer Arcachon	Boundary conditions for Arcachon basin modeling
	ACRI	Statistic modeling of suspended matters concentrations in Bay of Biscay
Underwater flora and fauna	Ifremer Brest	Predictive cartography of coastal benthic habitats : application to laminaria algae of Breton sublittoral
	Ifremer Boulogne	Rational management of living marine resources
Renewable Marine Energy	Ifremer Brest	Climatologic characterization of testing sites for study and sizing of offshore wind turbines
	EDF	Setting up of tidal current turbines farm on Paimpol-Bréhat site
Environment / Water Quality	Rivage Pro Tech	Coastal numerical modelling of bathing water quality in Basque Country
	Rivage Pro Tech / Lyonnaise des eaux	Realization of bathing water quality profile for Carantec commune, North of Finistère
Environment / pollutions	Ifremer Bastia	Simulation tests of microplastics becoming depending on currents
	CEDRE	Crisis management in case of accidental pollution

Table 2: Example of PREVIMER users needs

## Conclusion

Pre-operational system PREVIMER provides coastal observations and forecasts along French coasts. These marine environment data are disseminated to users, thanks to website and services - allowing access to digital outputs. Website is very popular, and visited by about 4000 visitors per day. Catalogue of products describes available data; 262 requests have been registered between February 2010 and December 2013. Requests come from public (52%) and private (48%) sectors; they are mainly in charge of R&D activities (72%). Users are more interested in delayed mode (67%) than real time (only 33%). Data are used for many activity sectors; a large part of requests (17%) concerns marine renewable energy sector.

PREVIMER feedback conference took place the 17th of September 2013, at Ifremer Brest (Lecornu et al. 2013); half a day was dedicated to users and allowed showing many PREVIMER applications. According to users satisfaction survey realized in 2013, 94 % of users who exploited data were satisfied with it, and 88% of users find essential that PREVIMER service goes on.

## Acknowledgements

The authors wish to thank the users who answered the satisfaction survey. They wish also to thank the many users who participated to PREVIMER feedback conference (17<sup>th</sup> of September 2013, Ifremer Brest, more than 140 participants), and particularly those who deliver their feedback at the users' session: EDF, CEREMA (ex-CETMEF), Rivages Pro Tech, Actimar.

## References

Boudière, E., Maisondieu, C., Arduin, F., Accensi, M., Pineau-Guillou, L. and Lepasqueur, J. 2013: A suitable metocean hindcast database for the design of Marine energy converters. International Journal of Marine Energy, 3-4, e40-e52. <http://dx.doi.org/10.1016/j.ijome.2013.11.010>

Pineau-Guillou, L. 2013 : PREVIMER Validation des atlas de composantes harmoniques de hauteurs et courants de marée. Ifremer report, 89pp. <http://archimer.ifremer.fr/doc/00157/26801/>

Pineau-Guillou, L., Lecornu, F. and Le Roux, J.-F. 2014: Previmer Catalogue Produits Version 2.0, 105pp.

PREVIMER Project team 2014 : Catalogue Produits PREVIMER Version 2.0. <http://archimer.ifremer.fr/doc/00176/28703/>

PREVIMER Project team 2014 : Synthèse de la journée de restitution du projet PREVIMER Phase II. <http://archimer.ifremer.fr/doc/00176/28704/>

## PREVIMER: A CONTRIBUTION TO IN SITU COASTAL OBSERVING SYSTEMS

By G. Charria<sup>(1)</sup>, M. Repecaud<sup>(2)</sup>, L. Quemener<sup>(2)</sup>, A. Ménesguen<sup>(3)</sup>, P. Rimmelin-Maury<sup>(4)</sup>, S. L'Helguen<sup>(5)</sup>, L. Beaumont<sup>(6)</sup>, A. Jolivet<sup>(5)</sup>, P. Morin<sup>(7)</sup>, E. Macé<sup>(7)</sup>, P. Lazure<sup>(1)</sup>, R. Le Gendre<sup>(8)</sup>, F. Jacqueline<sup>(8)</sup>, R. Verney<sup>(1)</sup>, L. Marié<sup>(9)</sup>, P. Jegou<sup>(10)</sup>, S. Le Reste<sup>(10)</sup>, X. André<sup>(10)</sup>, V. Dutreuil<sup>(10)</sup>, J.-P. Regnault<sup>(2)</sup>, H. Jestin<sup>(1)</sup>, H. Lintanf<sup>(10)</sup>, P. Pichavant<sup>(10)</sup>, M. Retho<sup>(11)</sup>, J.-A. Allenou<sup>(11)</sup>, J.-Y. Stanisière<sup>(11)</sup>, A. Bonnat<sup>(12)</sup>, L. Nonnotte<sup>(13)</sup>, W. Duros<sup>(13)</sup>, S. Tarot<sup>(12)</sup>, T. Carval<sup>(14)</sup>, P. Le Hir<sup>(1)</sup>, F. Dumas<sup>(1)</sup>, F. Vandermeirsch<sup>(1)</sup>, F. Lecornu<sup>(1)</sup>

<sup>1</sup> IFREMER, ODE/DYNECO/PHYSED, Plouzané, France

<sup>2</sup> IFREMER, REM/RDT/LDCM, Plouzané, France

<sup>3</sup> IFREMER, ODE/DYNECO/BENTHOS, Plouzané, France

<sup>4</sup> IUEM-UBO, UMS CNRS 3113, Technopôle Brest-Iroise, Plouzané, France

<sup>5</sup> IUEM-UBO, UMR CNRS 6539, Technopôle Brest-Iroise, Plouzané, France

<sup>6</sup> CNRS/INSU, Division Technique, Meudon, France

<sup>7</sup> CNRS-UPMC, UMR CNRS 7144, Roscoff, France

<sup>8</sup> IFREMER, ODE/LITTORAL/LERN, Port-en-Bessin, France

<sup>9</sup> IFREMER, ODE/LPO, Plouzané, France

<sup>10</sup> IFREMER, REM/RDT/SI2M, Plouzané, France

<sup>11</sup> IFREMER, ODE/LITTORAL/LERMPL, La Trinité sur Mer, France

<sup>12</sup> IFREMER, IMN/IDM/SISMER, Plouzané, France

<sup>13</sup> ALTRAN, Brest, France

<sup>14</sup> IFREMER, IMN/IDM/ISI, Plouzané, France

### Abstract

To design a prototype for an Integrated Ocean Observing System (IOOS), at least three components are mandatory: a modeling platform, an *in situ* observing system and a structure to collect and to disseminate the information (e.g. database, website). The PREVIMER project followed this approach and in order to sustain model applications, PREVIMER has developed, funded and organized part of *in situ* observing networks in the Bay of Biscay and the Channel. For a comprehensive system, focus was addressed on fixed platforms (MAREL MOLIT, MAREL Iroise, Island network and D4 for sediment dynamics), ships of opportunity (RECOPECA program and FerryBoxes), and coastal profilers (ARVOR-C/Cm).

Each system is briefly described and examples of scientific results obtained with corresponding data are highlighted to show how these systems contribute to solve scientific multidisciplinary issues from the coastal ocean dynamics to the biodiversity including pelagic and benthic habitats.

### Introduction

The PREVIMER project has been a prototype of an integrated system including coastal ocean modeling systems, associated with *in situ* observing networks, and a data center with associated solutions for data visualization (e.g. web site) and distribution. The present paper aims to introduce how the PREVIMER project sustained coastal *in situ* observing systems in the Channel and the Bay of Biscay. Indeed, the project contributed to the development, deployment and setup of ongoing *in situ* platforms including fixed platforms, coastal profiling systems and programs of opportunity measurements. These three components contribute to an integrated observation of the 4D (longitude, latitude, time, and depth) coastal environment from high frequency time series (at fixed stations or onboard commercial cruises) to the sampling of the whole water column in targeted areas (using coastal profilers) or based on opportunity network (using fishing vessels).

Figure 1 shows the spatial distribution of the observing systems partly or fully funded through the PREVIMER project. These items have to be considered as a component of the French coastal observing system, part of the recent extent to the coastal regions of the Coriolis convention. This new convention is including other coastal observing networks with, for example, the SOERE MOOSE<sup>1</sup> in the Mediterranean Sea.

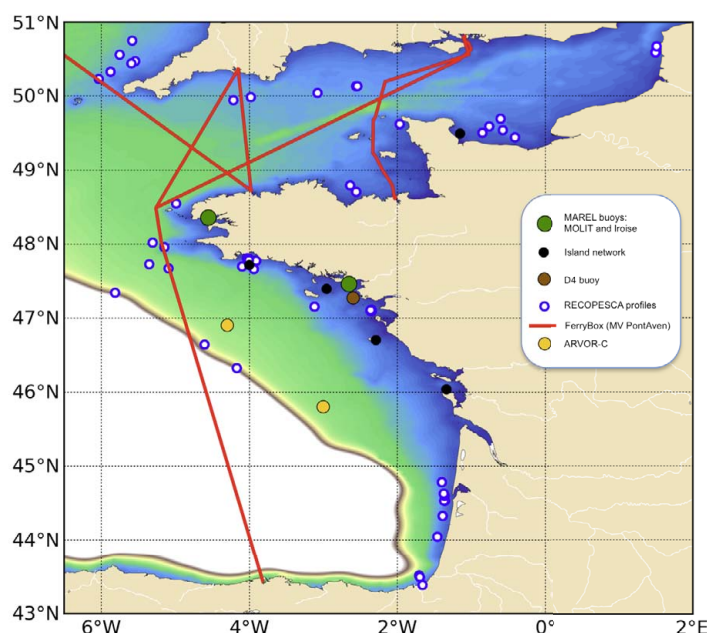


Figure 1: Observing systems in the frame of the PREVIMER project.

<sup>1</sup> SOERE MOOSE: Système d'Observation et d'Expérimentation pour la Recherche en Environnement - Mediterranean Ocean Observing System on Environment (<http://www.allenvi.fr/groupe-transversaux/infrastructures-de-recherche/moose>)

As fixed platforms, three categories can be described. First, MAREL buoys are complex platforms able to sample a wide range of parameters and to support the development of new sensors (see "Fixed platforms" section). In the PREVIMER project, MAREL MOLIT in the Vilaine Bay and MAREL Iroise in the Bay of Brest have been partly supported. Another network is the island network designed to monitor salinity evolutions near the main river plumes (see "Fixed platforms" section). Finally, a prototype of a fixed platform dedicated to sediment dynamics (called D4) studies has been implemented (see "Fixed platforms" section).

To extend the network of fixed platforms, generally near the coast, two observing systems based on measurements of opportunity have been improved in the frame of the project. The RECOPECA program aims to acquire hydrological variables with probes implemented on fishing vessels (see "Ships of opportunity" section). This program is initially planned to collect measurements for fishery science. FerryBoxes (see "Ships of opportunity" section) represent the other system of opportunity used in the frame of coastal observing networks. With high spatial resolution measurements, FerryBoxes provide detailed information about the surface ocean.

The last component of the current network is based on coastal profilers called ARVOR-C / ARVOR-Cm (see "Coastal Profilers" section). These platforms, designed as a coastal version of ARGO floats, allow observing the whole water column close to a given geographical point.

In addition to previous systems dedicated to long-term coastal ocean observation, the PREVIMER project also contributed to improve the knowledge of the coastal environment through the investment in sensors and platforms dedicated to scientific cruises (*i.e.* Scanfish - a remotely operated towed vehicle).

In the present paper, we will introduce the different systems through a short description and examples of results obtained exploring the corresponding collected data.

## Fixed platforms

The first pillar of coastal high frequency *in situ* observations is based on fixed platforms. MOLIT platform, MAREL Iroise buoy, the island network and the D4 systems are described.

### MOLIT platform

The scientific buoy MOLIT (Figure 2) was moored in the Vilaine Bay in October 2007 thanks to the PREVIMER and TROPHIMATIQUE projects:

- PREVIMER relies on Ifremer's computational cluster, linked to the coastal oceanography data center, which pools observations and stores the model outputs, which are put on-line daily.
- TROPHIMATIQUE project aimed the development of new operational sensors as chemical analyzers or multi parametric probes.

The MOLIT platform is very original regarding its functioning principle: sea water is pumped from two levels (sub surface and bottom) through an umbilical, which is also the mooring device. This means that surface and bottom measurements are performed alternatively by the instrumentation and the system can act as a docking station for the testing of new sensors, analyzers, samplers or measurement protocols.

A special aspect is also the protection of all the pipes, sensors and pumping devices by chlorination (sea water electrolysis).

The water collected is analyzed over the same probe avoiding by the way the possible discrepancy in case of a two probes measurement. MOLIT has a high-capacity instrument payload. It is specially streamlined for use in the open sea. It has sensors to measure nutrients and ammonium, as well as temperature, salinity, dissolved oxygen, chlorophyll and turbidity probes; the data are transmitted to the data center in real time.

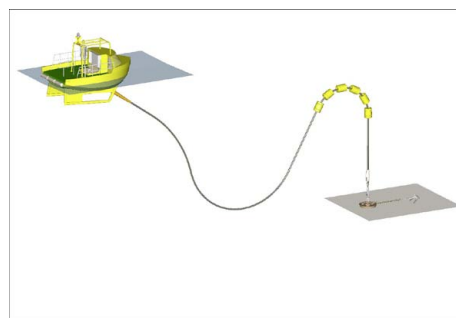


Figure 2: General view of MOLIT scientific buoy.

MOLIT buoy is a key system to observe the dissolved oxygen in the Vilaine Bay.

Indeed, oxygen depletion in the bottom waters is the more dangerous aspect of coastal eutrophication, because of its detrimental effects on the marine life (growth slow-down, increased vulnerability to fishing, reproduction impairment, reduction of the biodiversity) and the ultimate threat of ecosystem death in case of complete anoxia, leading to more and more numerous "dead zones" in the world (Diaz and Rosenberg, 2008). Along the French coast, the only spot where lethal anoxia has been recorded in July 1982 is the Vilaine bay (Merceron, 1988): due to a sudden sunny and calm period following a brief, but strong inflow of nutrient-rich freshwater from the Vilaine watershed, a large phytoplankton bloom developed in the surface layer of the strongly stratified bay, and its decay after sedimentation exhausted the total oxygen content of the bottom water, killing marine invertebrates and fishes (Figure 3). A model of the anoxia event of 1982 (Chapelle et al., 1994) has been recently applied to the whole Bay of Biscay and English Channel, with a zoom on the marine area in front of Vilaine and Loire rivers (Dussauze, 2011). This model reveals that a large part of this area is sensitive to bottom anoxia in summer (not shown). For that reason, in the framework of the PREVIMER and TROPHIMATIQUE projects, the MOLIT buoy has been moored in the northern part of the Vilaine bay to measure every 20 minutes the oxygen concentration in the surface layer as well as in the bottom one. Time-series obtained during the years 2008 to 2013 (Figure 4) show every spring and summer droops of bottom oxygen concentrations, occurring with a small delay after surface oxygen over-saturations (which sign important blooms in the surface layer). A strong effect of tidal regime on the oxygen content of the water column is visible on these records: weak currents during neap tides favour stratification and, hence, surface blooms and bottom decrease of oxygen content, whereas strong currents associated with the spring tides mix again the water column and restore a quasi-

saturation of oxygen in the whole water column. Hypoxia may be more severe near mussel farms, as shown by measurements made in June 2008 by Ifremer/La Trinité. The ecological effects of recurring hypoxias in the Vilaine area are not yet well described, but some seashell (*Mytilus edulis*) and crabs (*Carcinus moenas*) mortalities have been recorded during measured hypoxias in June 2008, and Stanisière et al. (2013) show arguments in favour of a decisive role of acute hypoxia in triggering the mortality of bottom cultivated oysters in the bay of Quiberon, not far from the Vilaine bay. Using the biogeochemical modelling of the decade 2000-2010, they show that in summer 2006, the year of exceptional oyster mortality, 3 abnormal droops of oxygen concentration in the oyster farm areas were simulated in July, August and September, and with a geographical distribution corresponding to the map of recorded mortalities. The fact that the biological response to oxygen deficiency is non-linear, and that lethal, very low, oxygen concentrations are short, impermanent phenomena, occurring mostly during a few hours at the end of the night, militates absolutely for the deployment of automatic sensors, in order to record these dramatic short events.

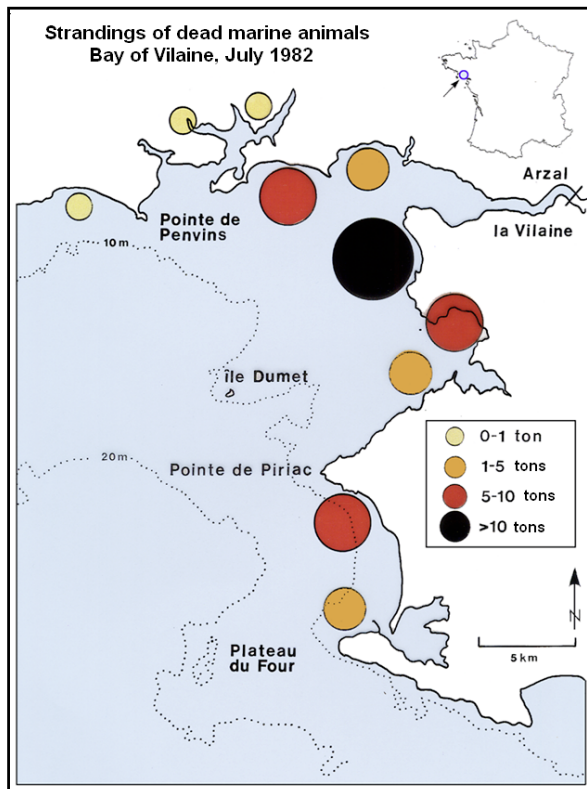


Figure 3: Geographic distribution of dead fish and invertebrates strandings in July 1982.

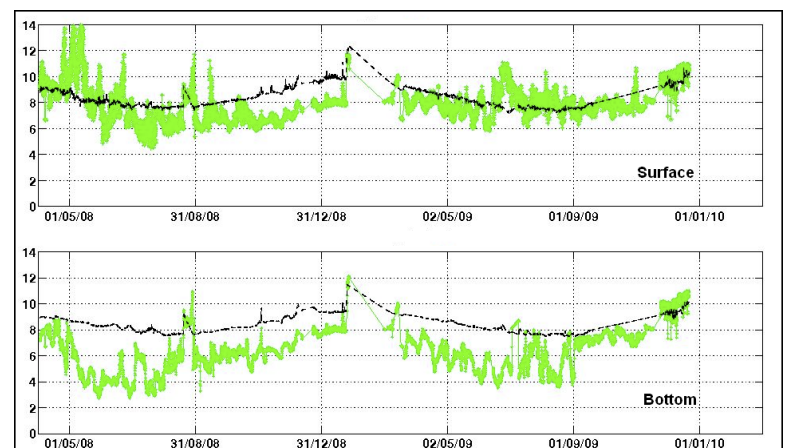


Figure 4: Measured surface and bottom oxygen concentrations (mgO<sub>2</sub> L<sup>-1</sup>) by the MOLIT buoy in the Vilaine bay, during 2008 and 2009 (green: measurements, black: computed oxygen saturation at local temperature and salinity).

## Marel Iroise



Figure 5: The "Marel Iroise" scientific buoy at the outlet of the Bay of Brest

The MAREL Iroise buoy is a key tool to observe at high frequency the temperate coastal ecosystem of the Bay of Brest, which is impacted by both continental and Iroise Sea inputs. This scientific buoy is property of IUEM (Institut Universitaire Européen de la Mer, <http://www-iuem.univ-brest.fr/fr/>) and Ifremer. It was moored in 2000 at the outlet of the bay (Figure 5) where manual sampling is also performed for the weekly observation network SOMLIT (French coastal monitoring network, <http://somlit.epoc.u-bordeaux1.fr/fr/>). MAREL Iroise records several parameters at a 20 minutes frequency: temperature ( $\pm 0.05^\circ\text{C}$ ), conductivity ( $\pm 0.05\text{mS/cm}$ ), dissolved oxygen ( $\pm 5\%$ ), in vivo fluorescence ( $\pm 5\%$ ), and turbidity ( $\pm 5\%$ ) of superficial waters. By the mean of two additional sensors, these core parameters are completed by aerial Photosynthetic Activated Radiation (PAR) and  $\text{pCO}_2$  ( $\pm 3\text{ppm}$ ). The principle of this automated measurement station is to pump the sea water through a multi parametric probe in order to guaranty the quality of the collected data. Thanks to this method, and to the chlorination of the water circuit, the quality of the collected data is guaranteed over three months without any maintenance. The whole installation is controlled by an autonomous embedded computer, which regulates all functions, including the daily data transmission to an inshore station. The data are available on the website: <http://www.ifremer.fr/difMarelstanne/>. The computer can be called over a GSM system in order to modify the parameters or transfer the logged data to the shore station. Nutrient concentrations (Nitrate, Ammonium, Silicate and Phosphate) can be also measured for special studies. The MAREL Iroise *in situ* instrumentation has been deployed for 13 years and has produced a data collection with a mean success ratio of 79%. Such data set has already been explored in multidisciplinary studies. Some of them are briefly presented hereby.

The biological significance of this tool can be illustrated by the study of inter-annual growth variations during the first year of life of the Great scallop (*Pecten maximus*). Since 1987 (EVECOS Series, PI L. Chauvaud), the observing service of IUEM measures daily growth of this animal (Figure 6). How temperature affects the growth of these species in the highly variable environment of the Bay of Brest is analyzed by using the low - frequency records of temperature (1 measurement per week).

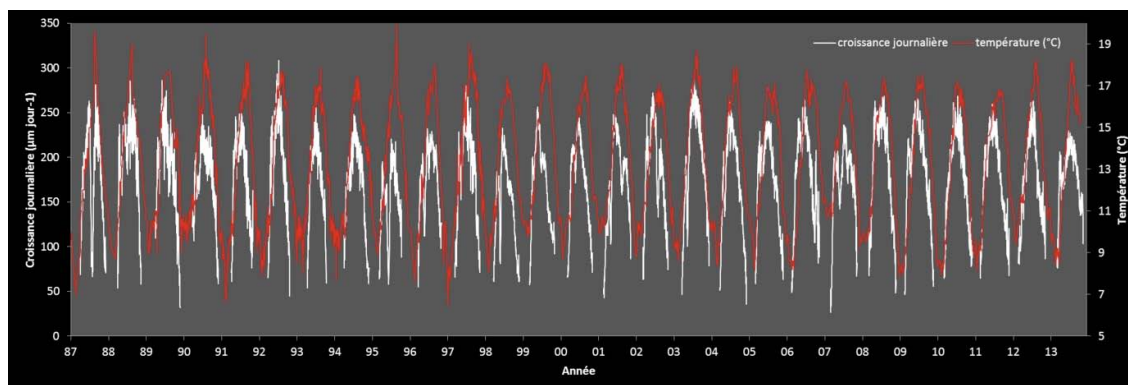


Figure 6: Interannual growth variations of Great scallop *Pectenmaximus* during their first year of life from 1987 to 2013 (EVECOS, Observing service-IUEM).

The daily formation of the growth striae on the Great scallop valves also provides, by measuring its chemical composition, an access to several proxies. In this context, the use of high - frequency environmental data (1 measure per day) produced by MAREL Iroise allows calibration and subsequent use of these sclerochemical data as environmental proxies.

A more biogeochemical use of MAREL Iroise data has been achieved through the study of high frequency record of  $p\text{CO}_2$  (since 2003) in order to investigate the variability and the evolution of  $\text{CO}_2$  flux exchanged at the ocean-atmosphere interface (PI Y. Bozec). The authors showed that biological processes like photosynthesis and respiration are the main controller of diurnal and seasonal  $p\text{CO}_2$  variations and that diurnal variability can reach 70% of the average seasonal variation (Figure 7). This underlined the need to consider high frequency variation to avoid an 8 to 36% error in the monthly budget estimation. The seven years budget also showed a relatively equilibrated  $\text{CO}_2$  emission of  $0.4 \pm 0.7 \text{ mol.m}^{-2}\text{yr}^{-1}$  with a low interannual variation so that coastal temperate ecosystem of Bay of Brest seems to act as a buffer interface between estuarine sources and oceanic sinks.

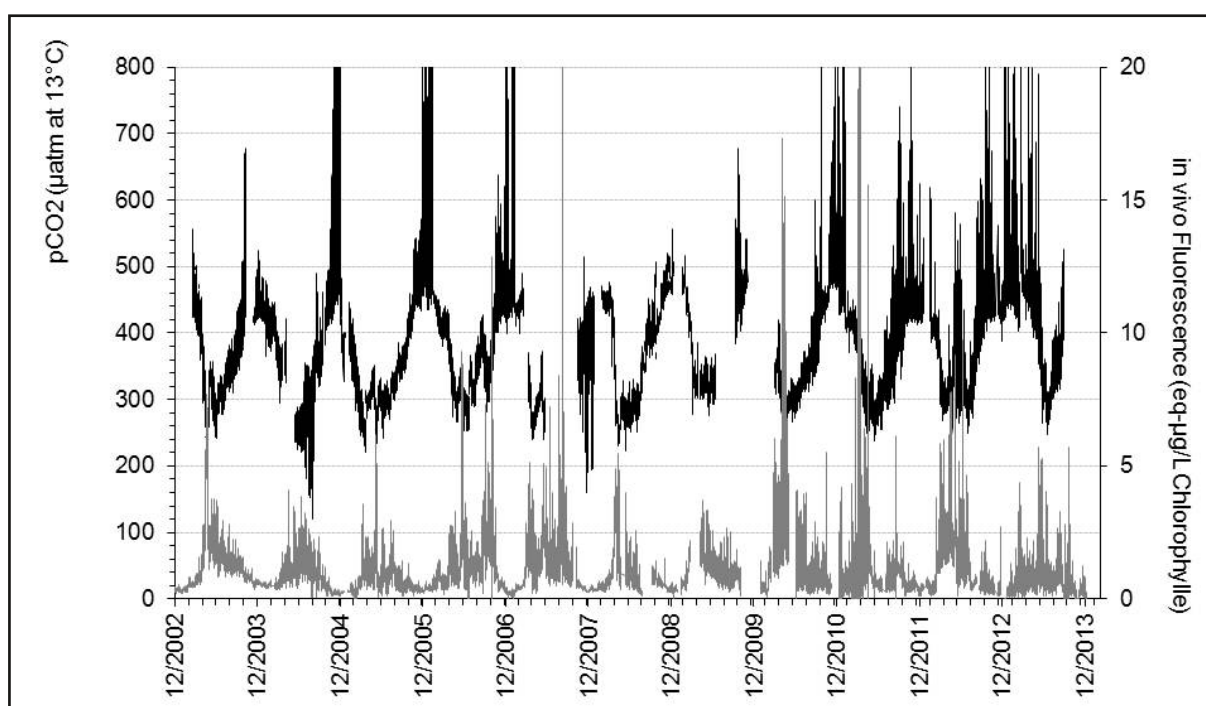


Figure 7: Temporal variation of  $p\text{CO}_2$  (normalized at  $13^\circ\text{C}$ , grey line) and in vivo fluorescence ("Marel Iroise" data, black line).

In a more physico-chemical interest, Tréguer et al. (2013) used the MAREL Iroise data to investigate the temporal variability of physico-chemical features of the Bay of Brest waters during winter in relation with large and local scale weather processes over the 1998-2013 period. These authors examined the relationships between sea surface temperature, sea surface salinity and nutrient concentration, river discharges, precipitation and climatic index data (North Atlantic Oscillation, NAO; East Atlantic Pattern, EAP; Atlantic Ridge, AR). Mainly focused on winter months, the study reveals that the variability in the coastal water characteristics is impacted by both the large-scale North Atlantic atmospheric circulation and local river inputs. While the NAO is strongly correlated to changes in sea surface temperature, the EAP and the AR have a major influence on precipitations, which in turn modulate river discharges that impact sea surface salinity. A future dominance of a positive EAP phase could support an increase in precipitations and therefore, the delivery of high nutrient standing stocks leading to a high new production during the following spring.

These studies highlight the scientific significance of this high frequency *in situ* monitoring, which allows the observation of the long-term evolution of coastal marine ecosystems. They also show that it is essential to continue the high frequency acquisition of physical, chemical and biological parameters in order to predict the responses of coastal systems to climatic changes and anthropogenic forcing.

## Island network

The island network was initially designed in 2000 (Lazure et al, 2006) to track the fate of the large river plumes in the Bay of Biscay. The continental shelf is under the influence of two major rivers, the Loire and Gironde with annual mean discharges of  $900\text{m}^3\text{ s}^{-1}$ . Numerous smaller rivers spread also along the coast and may dramatically affect the local salinity patterns. To avoid these local effects, conductivity probes have been deployed as far as possible from estuaries but not too far to allow regular maintenance operations. To cope with these constraints, probes have been deployed along the coast of several small islands (Glénan, Houat, Yeu and Oléron) and the times series of coastal salinity have been used as validation data for the operational regional MANGA model (Lazure et al, 2009).

Since the end of 2010, the network has been renewed to allow direct time access to the data and better calibration and validation procedures.

The Island network is now formed by a set of four small autonomous small buoys named MAREL SMATCH (Figure 8).



Figure 8: A MAREL SMATCH buoy.

MAREL SMATCH buoy is an operational remote transmission multiparametric probe: temperature (accuracy:  $0.02^\circ\text{C}$ ), conductivity (accuracy:  $0.05\text{mS}$ ) and pressure (accuracy:  $0.1\text{m}$ ). The included principle of local chlorination protects the sensors against bio fouling and therefore guaranties the quality of the measure for a period of three months without any maintenance. An autonomous embedded computer deals with the logging, and transmission of data (GPRS modem) once a day. This small buoy weights only 9 Kilograms and can be easily moored by a rope and a small dead weight for coastal operations. Data can be downloaded from: <http://www.coriolis.eu.org/Data-Services-Products/View-Download/Eulerian-networks-fixed-buoys>.

A new mooring has been deployed near Saint Marcouf island (Bay of Seine, English Channel), mainly to monitor the fate of freshwater inputs from the Seine river and four secondary watersheds flowing in the Bay of Veys (*i.e.* Vire, Douve, Aure, Taute). The Bay of Seine receives large freshwater inputs, mainly from the Seine River (mean flow around  $500\text{ m}^3/\text{s}$ ) whereas cumulated mean flow from the Bay of Veys does not exceed  $40\text{m}^3/\text{s}$ . It covers around  $3500\text{ km}^2$ , with a tidal range varying from 3 m at neap tide to 7.5 m at spring tide. The mean depth is around 20 m and the bay is striated by a deeper channel corresponding to the paleovalley of the Seine River. Tidal residual circulation in the Bay of Seine have been well described (Ménéguen and Gohin, 2006) and exhibits important meso-scale features such as two anticyclonic gyres, induced by the presence of capes; one offshore of "Barfleur" ( $49.67^\circ\text{N}/-1.25^\circ\text{W}$ ) and the second near "Antifer" ( $49.66^\circ\text{N}/0.12^\circ\text{E}$ ). Saint Marcouf mooring is located approx 100km west from the Seine mouth, and 15km north from the Bay of Veys. Prevailing wind in this part of the English Channel are usually southwesterlies but intense northeasterly wind sequences frequently occur.

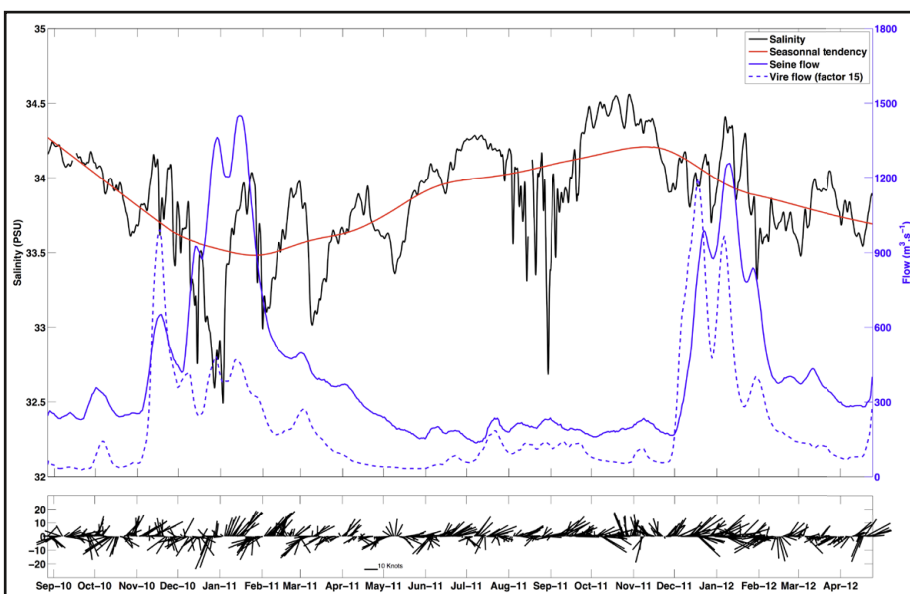


Figure 9: Salinity data recorded at St Marcouf mooring between the end of August 2010 and April 2012 (black). On black curve, tidal signal has been removed to rub out high frequency variations, and red solid line represents the seasonal component. Solid blue line corresponds to the Seine instantaneous flow whereas dotted line is the Vire flow ( $\times$  factor 15). Wind barbs (2 days averaged) are shown on the bottom panel (scale 10 knots).

Salinity ranges from 32.5 to 34.5 psu. Minimum was recorded at the beginning of winter 2010-2011. This figure exhibits interesting features to help us apprehend the functioning of the bay. We can first note that Seine and Vire flow evolutions are not necessarily concomitant with larger runoffs from the Vire observed few days before peaks in the Seine flow. The salinity decreases, as during winter 2010-2011, occur generally after Northeasterlies sequences resulting in an extension of the Seine freshwater plume to the mooring position. However, in winter 2011-2012, the decrease is less pronounced (until 34 psu instead of 32.5 psu during winter 2010-2011). The different wind regime can partly explain this difference. More generally, the seasonal cycle is also strongly dependent on the wind regimes.

Beyond the use of these data to observe and to explain local processes, the island network measurements are key observations to qualify model simulations contributing to reduce the lack of observations (specifically for salinity and in a near future for turbidity) close to river plumes.

## D4 : a platform to quantify suspended sediment concentration in the water column

### Context

Suspended sediment in the water column and related turbidity constitute driving parameters of the coastal ecosystems. They are associated to sediment fluxes, sedimentary habitats, and influence the productivity of ecosystems as limiting the euphotic depth and hence the primary production. Quantifying suspended sediment concentration (SSC) in the entire water column in quasi real-time is a challenging issue. It requires operating top research measuring techniques and pre-process, collect and transmit a limited volume of data.

### Platform overview

The Previmer-D4 measuring platform (Figure 10) was designed in collaboration with iXSurvey and operated to provide key hydrodynamic and sediment features in the coastal seas, i.e. current and SSC profiles, waves, seabed sediment altimetry and temperature/salinity time series. The system is composed of two non-contact interconnected principal modules. The benthic module consists of an anti-trawl frame receiving a detachable basket containing the following instruments: a 1MHz Nortek® AWAC Doppler acoustic profiler (measuring waves, current/acoustic backscatter signal profiles (0.50m cells), seabed temperature and pressure), a WETLabs® ECO-NTUS pole mounted turbidity sensor, a Tritech® PA500-6 bed millimetric altimeter vertically fitted on a firmly grounded external T-shaped frame, and a Sercel® MATS211 acoustic modem for data transmission from the bed to the surface. At the surface the buoy supports a Sercel® MATS251Z7-MATS231/P acoustic modem, a Hydrolab MS5 multi-sensor probe (temperature, salinity, turbidity), a GPS, a radio modem with UHF antenna, solar panels and batteries, and an embedded micro-PC collecting, buffering and transmitting data from all instruments. Data are sent every half an hour for all parameters except waves each hour through GSM protocol and collected on the CORIOLIS server in Ifremer Brest.



Figure 10: Schematic view of the Previmer-D4 platform (left) and a photograph of the real buoy (right).

### Measuring SSC profiles

Two optical backscatter sensors are operated on the Previmer-D4 platform, but measurements are only collected at 1.70m below the surface and 1.75m above the bed. Quantifying SSC on the entire water column requires analysing the AWAC acoustic backscatter signals (Thorne and Hanes, 2002). We decided to apply a semi-empirical method to correct the acoustic signals from water attenuation and calculate SSC profiles (Tessier et al., 2008), using the near bed SSC time series (from the calibrated optical turbidity sensor located in the second AWAC cell).

### Previmer-D4 observations

The measuring platform was deployed twice in 2007-2008 2nm S/SW off Le Croisic and in 2009-2010 close to Quiberon in the bay. Focusing on the first deployment (November 2007-March 2008), the system successfully recorded several winter storms characterised by 3 to 4m wave height. These wave events resuspended sediments, with SSC up to 100g.l<sup>-1</sup> close to the bed, and impacted the entire water column. As an example, 30mg.l<sup>-1</sup> SSC was regularly recorded 10m above the bed while the ambient calm weather concentration is around 5mg.l<sup>-1</sup> (according to calibration of simultaneous measurements/water samples - Figure 11). The quasi real-time data collection enables to evaluate the coastal sea dynamics, and compare with both satellite ocean colour data and model results.

From this experience several technical improvements would be necessary to lower uncertainties on quantitative SSC measurements. The first issue is related to the calibration of the optical sensors, which requires ground truth water sample on the full signal range. However, operations at sea are mainly conducted with small boats under calm weather for safety and do not allow to collect sample during high turbid (waves) events, hence limiting

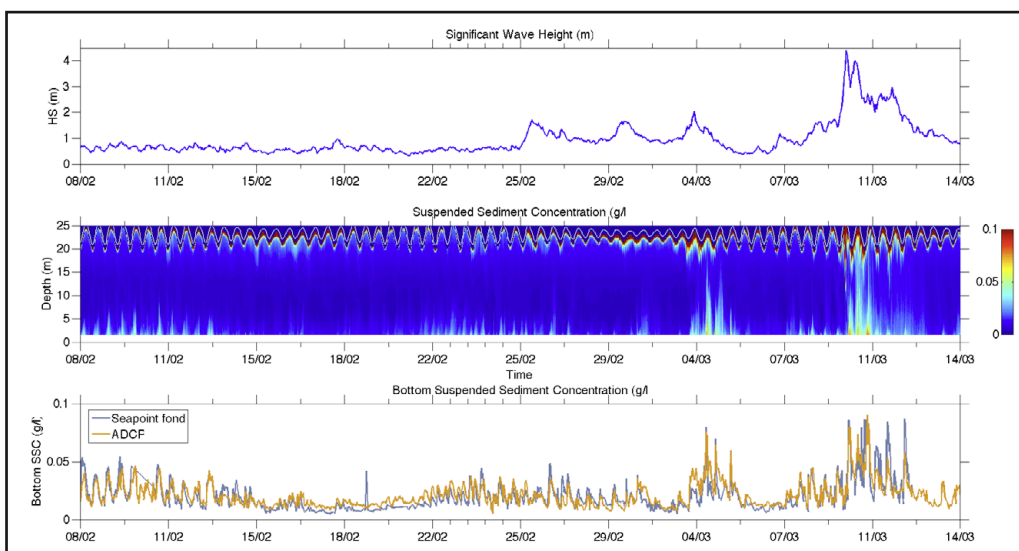


Figure 11: Wave and suspended sediment time series from the 8th February 2008 to the 14th March 2008 at Le Croisic (France).

the calibration range to low SSC. The second limitation is associated to the acoustic signal and its validity close to the surface: the mixing at the air/sea interface contributes to introduce bubbles in the water column, the depth depending on wave intensity. These bubbles are intense scatterers that produce noise in the acoustic signal. In consequence, part of the acoustic signal is discarded, as bubbles/suspended sediment signals cannot be separated. Research works are currently in progress in order to improve the quality of the measurements.

## Ships of opportunity

The second part of coastal observing systems is based on the use of ships of opportunity to collect frequent observations with an optimal cost/quality ratio. In the present manuscript, data collected in the RECOPECA project and from FerryBox are presented.

### RECOPECA project

The aim of the RECOPECA project (Leblond et al., 2010) is to achieve accurate spatial distribution (GPS monitoring of boat and timestamp) of catches (weight with anti-rolling weigh-scale), fishing effort (working duration of the fishing gear) and environmental (depth, temperature, salinity, turbidity) characterization of fisheries area required for an ecosystem approach to fisheries. The collected data are available for fishery scientists and physicists who dispose of continental shelf dataset from 2 to 300m depth. The physical data are stored and shared in two data centers (i) The Fisheries Information System of Ifremer and its database *Harmonie* (ii) the *Coriolis* database for operational oceanography. A real time quality control is applied on collected data.

RECOPECA is a mean based on a participative approach, where the voluntary fishermen team up with fishery scientists. This successful collaboration is possible because we used equipment, which doesn't need interventions of the fisherman team during several months. For this, we developed rugged probes that can be directly fixed on fishing gears (trawl, net, fishing trap...), self-powered, autonomous, with accurate and fast response time sensors for profiling function during way down.

Onboard basic equipment is comprised with:

- A probe with depth (3% full scale precision) and temperature sensor (precision less than 0.05°C in the range 0°C to 20°C) without or with an additional sensor such as conductivity sensor (precision  $\pm 0,05$  mS/cm in the range 10 to 60 mS/cm) or turbidity sensor (precision less than 2%). The probe records only during immersion stage and the data are timestamp. The record time frequency is configurable. Typically we use two frequencies. The first is set to 1 second during the way down period (profiling period) and the second set to 2-10 minutes during the fishing gear bottom working period. The probe is equipped with a radio device for transmitting automatically its data to the *concentrator*.
- A receiver on-board hub called *concentrator*, placed outside on the vessel bridge. The *concentrator* is equipped with a GPS 3D patch, a GPRS modem for transferring all the data to the Ifremer data center in Brest, a radio device for bi-directional communication with the probes. The probes are set to time at each data transfer with the *concentrator*. The *concentrator* has 6 months memory capacity.

In addition, specific equipment can be added:

- A turn-counter placed on the gear hauler in order to measure the length of passive gears hauled at each fishing operation. A radio device is present for data transfer to the concentrator.
- An anti-rolling weight-scale recording the catches per species and fishing operation. A radio device is present for data transfer to the concentrator.

At the end of 2013, around 80 vessels are equipped and 28181 profiles have been collected in the Bay of Biscay and the Channel (domain: 43°N/52.5°N - 12°W/2°E). The deployment plan, at the national scale, is in accordance with the diversity and representativeness of the fishing fleets (fishing area, vessel length and work experience).

The geographical distribution of vertical profiles (Figure 12) from 2006 to 2013 translates the preferential areas for fishing activities (in agreement with the fishery science aim of the project). We can notice very well sampled areas as the South of Brittany or the western Channel and undersampled regions as the South of the Bay of Biscay off Landes coast, where profiles (less profiles than in the northern part) are distributed in an area very close to the coast where the hydrology is very sensitive (e.g. upwelling activity) and then profiles are potentially supporting a stronger variability.

**Figure 12: Map of RECOPECA Temperature profiles since 2006. The rectangle highlight the studied region (46.2°N/48.6°N - 6°W/2.8°W).**

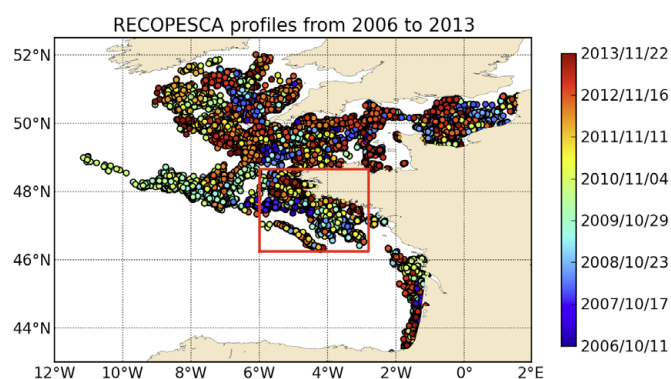


Figure 13 displays the average vertical profiles South of Brittany (46.2°N/48.6°N - 6°W/2.8°W) in winter (Figure 13, left) and summer (Figure 13, right) for the different years from 2007 to 2013. This result highlights an interannual variability observed for the first time in this region from ship of opportunity measurements. In winter (January to March, Figure 13-left), we can notice that the number of profiles is very different for each year with large number of profiles in 2009 and 2011 and less than 100 available profiles for the other years. However, these average profiles show clearly that the bottom temperature is larger than the surface temperature. For example, more than 0.5°C difference between bottom and surface waters is observed in 2013. This trend is also observed (with a smaller amplitude < 0.5°C) during the other observed years except in 2012 and 2007, which are also the only years when the number of profiles is lower than 50 profiles. In summer (July to September, Figure 13-right), vertical profiles describe the seasonal stratification with surface waters ranging in average from 15.8°C to 18.3°C (depending the considered year) in surface waters and from 10.8°C to 12.5°C around 100m depth. The thermocline lies between 20m and 40m depth. This layer related to the thermocline is also the zone where the standard deviation in profiles is the most important (not shown) related to local and high frequency processes (e.g. internal waves) able to upwell or downwell the thermocline with an amplitude reaching several meters. The interannual variability can be ranged from the year 2013 (with a smooth stratification) to 2009 (with a well marked summer stratification). The shape of these summer profiles has to be related to weather conditions (*i.e.* wind, precipitations and heat fluxes) and the previous winter conditions in the water column. These results highlight the ability of RECOPECA profiles to catch the interannual variability.

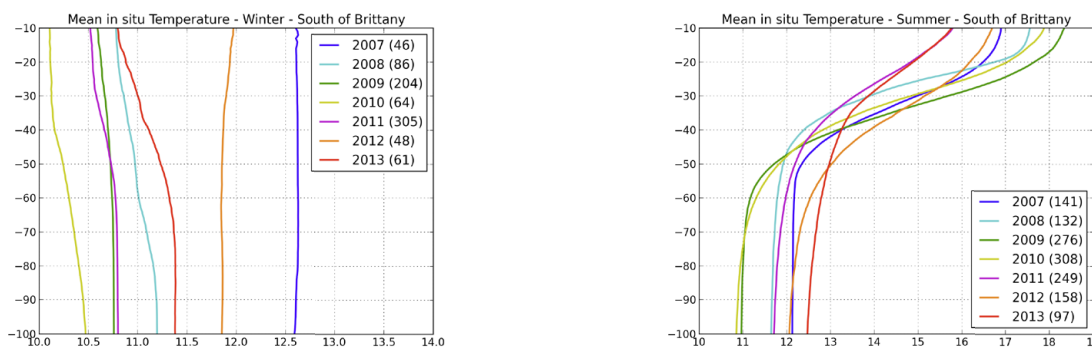


Figure 13: Mean in situ temperature for winter (January-February-March - left) and summer (July-August-September - right) from available vertical profiles for each year South of Brittany ( $46.2^{\circ}\text{N}/48.6^{\circ}\text{N} - 6^{\circ}\text{W}/2.8^{\circ}\text{W}$ ). Only profiles with measurements deeper than 100m depth are considered. Number in brackets is the number of profiles used to compute the mean profile.

### FerryBox

Marine ecosystems are exposed to increasing anthropic perturbations due mostly to the development of industrial activities and urbanisation of the coastal zones. The functioning of marine ecosystems responds to complex interactions between physical and biogeochemical processes depending on natural climatic cycles and are influenced since the last decades by anthropic perturbations, which can modify natural cycles. To distinguish between the natural variability of the biogeochemical cycles and changes induced by anthropic activities, long term time series of observation of physical, biogeochemical and biological parameters are necessary to get a better knowledge of the sensitivity of the ocean to the global change. To address this important question, it is necessary to develop long term studies based on regular sampling. Since 2008, Station Biologique de Roscoff and Ifremer Brest have launched high frequency measurements of hydrological and biological parameters in surface waters on repeated sections in the Bay of Biscay, Celtic Sea and Western Channel. These repeated measurements will contribute to a better knowledge of the seasonal, interannual and decadal variations in these areas and will give access to a better documentation of extreme events (e.g. phytoplankton blooms, Loire outputs on the continental shelf) which amplitude and duration are not well known with low frequency observations from classical oceanographic cruises.

The main objective of FerryBox project is to achieve surface measurements of oceanographic parameters using an automatic platform installed on commercial ferries operating regular lines.



Two ferry box systems have been installed on

Brittany Ferries M.V. "Armorique" and "Pont Aven". Complementary sampling strategies have been chosen for an optimal spatio-temporal coverage of the western European seas (Figure 14). A high frequency spatio-temporal sampling is realized with M.V. "Armorique" ferry box along two daily transects in the Western English Channel between Roscoff and Plymouth whereas a spatial coverage of the Western English Channel, Celtic Sea and Bay of Biscay with a weekly sampling is realized with M.V. Pont Aven along transects between U.K., Spain, France and Ireland (Portsmouth and Santander lines, Portsmouth and Saint Malo, Roscoff and Cork and between Roscoff and Plymouth). These lines contribute to the coverage of the European continental shelf by FerryBox lines (<http://www.ferrybox.org/routes/>) and are integrated in the FP7 EU Jerico program.

### Western Channel and bay of Biscay Network

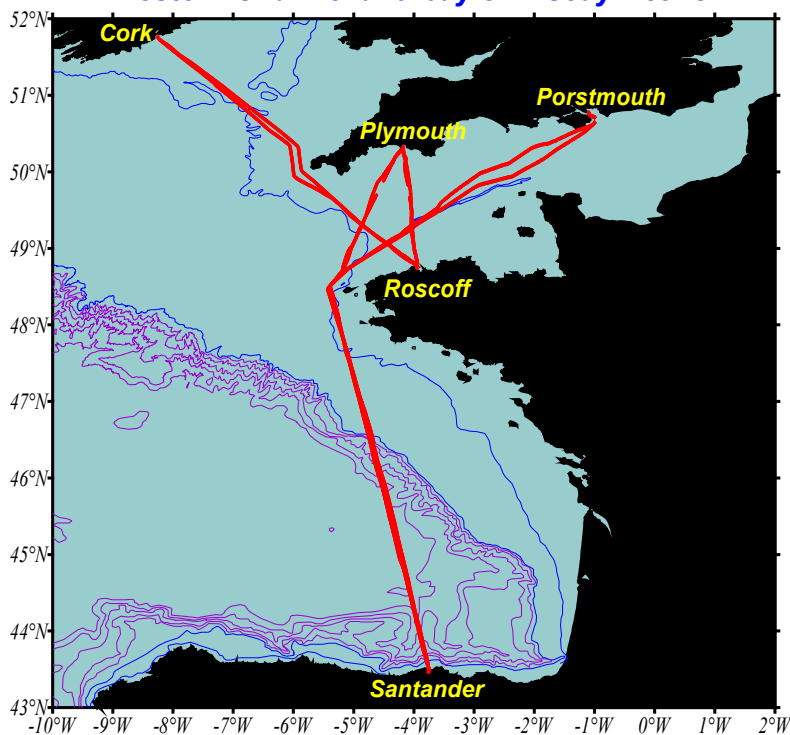


Figure 14: FerryBox routes in the Western Channel, Celtic Sea and Bay of Biscay operated on MV "Pont Aven" and "Armorique" ferries of the Brittany Ferries.

The two ferries are equipped with the same systems and sensors. Six parameters (temperature, salinity, dissolved oxygen, chlorophyll fluorescence, turbidity and Colored Dissolved Organic Matter CDOM) are sampled with a 1 minute frequency. Acquisition frequency is a mean value every 1 minute corresponding to a distance of approximately 500m. The different sensors are regularly calibrated with water samples taken from an output valve of the FerryBox system. Temperature and salinity are measured using a Seabird SBE45 thermosalinograph (precisions:  $\pm 0.02^{\circ}\text{C}$ ,  $\pm 0.02$  PSU), an Aanderaa 3835 optode (precision:  $\pm 3.4 \mu\text{Mole L}^{-1}$ ) and a Turner Designs C3 fluorometer for chlorophyll fluorescence, turbidity and CDOM. A set of additional sensors is available and can be installed immediately in case of failures of sensors to ensure permanent measurements at sea. Availability of an additional set of sensors is crucial for operational measurements at sea.

Data collected are transmitted automatically through a GPRS modem to the Roscoff data base at the arrival of ferries in the ports and data are made available through a website (<http://abims.sb-roscoff.fr/hf/>) where they can be visualized in quasi real time. Data are immediately transmitted to the Coriolis and MyOcean data center for operational oceanography where quality codes are given for the physical parameters.

In the frame of the French FerryBox project, the repeated lines are maintained since May 2010 (MV "Armorique") and February 2011 (MV "Pont Aven"). Examples of results obtained along the Santander – Porstmouth line during 2011 are presented on Figure 15.

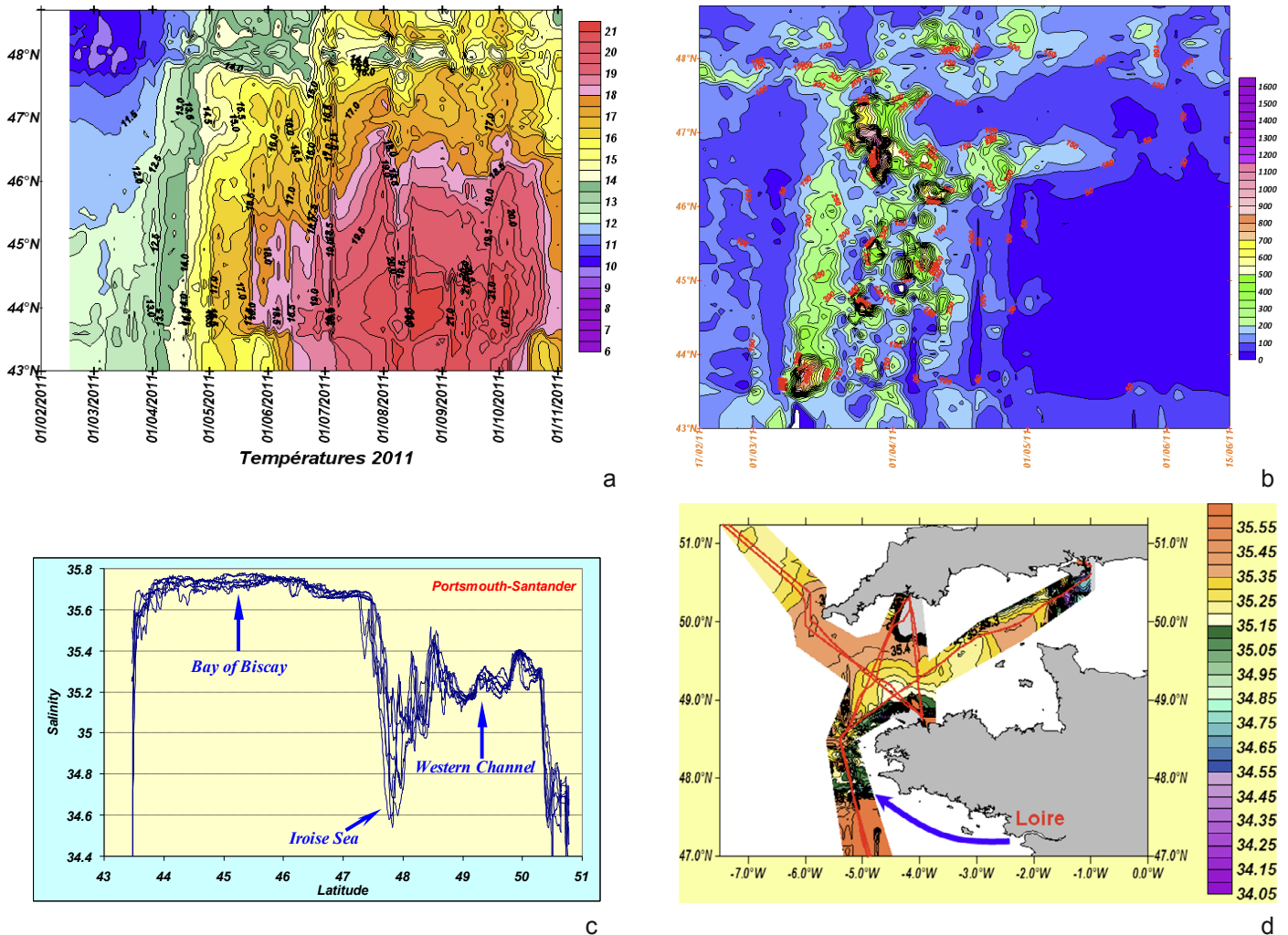


Figure 15. Seasonal evolution of subsurface temperatures during 2011 (a) and chlorophyll fluorescence during spring 2011 (b) along the Santander-Porstmouth line. Evolution of surface salinity in April 2011 along the Santander-Porstmouth line (c) and off Brittany (d) with a salinity minimum at 48°N corresponding to the low salinity waters of the Loire river plume.

Sequential development of the spring phytoplankton bloom in the Bay of Biscay, Celtic Sea and Western Channel:

Important differences in surface temperatures ( $>4^{\circ}\text{C}$ ) were clearly visible during the whole year leading to a late spring heating of the surface waters north of 47°30N (Figure 15a). Due to the early heating of surface waters, the spring phytoplankton bloom was firstly initiated in early March in the southern Bay of Biscay (Table) and then propagated progressively northwards. Three chlorophyll fluorescence maxima were observed during spring 2011 (43°46N, 44°34N and 46°48N). In Celtic Sea, the spring phytoplankton bloom was initiated later in early April (when surface waters became warmer leading to a vertical stratification of the water column) and then propagated southwards (Figure 15b). Two maxima of chlorophyll fluorescence were observed at 49°53N and 49°34N. In the Western Channel, the spring bloom developed firstly in the early beginning of April in the northern stratified side whereas the maximum of chlorophyll fluorescence were observed later in the southern part (in late April and May). In this area, the water column is well-mixed over the whole year due the tidal currents and development of phytoplankton is light-limited leading to a late seasonal development. In the Bay of Biscay-Celtic Sea-Western Channel area, the permanent measurements using the FerryBox systems have shown that the spring phytoplankton bloom developed sequentially in space and time over more than two months.

Area	Latitude	Date maximum Fluorescence	Maximum Fluorescence
Bay of Biscay	43°46.8 N	10/03/2011	985
Bay of Biscay	44°34.2 N	24/03/2011	944
Bay of Biscay	46°48.0 N	28/03/2011	1604
Celtic Sea	50°38.4 N	02/04/2011	594
Western Channel	49°53.4 N	05/04/2011	242
Western Channel	49°33.6 N	22/04/2011	642
Western Channel	49°31.8 N	22/05/2011	895

Table 1. Areas, latitudes, dates and maximum fluorescence values of the spring phytoplankton bloom in the Bay of Biscay, Celtic Sea and Western Channel areas.

#### Loire plume extension on the Armorican Shelf:

Low salinity waters (< 34.6 PSU) were observed off the western coasts of Brittany at 48°N between March and June 2011 (Figure 15c). These low salinity waters were clearly lower than those observed in the Western Channel ( $\approx$  35.2-35.3 PSU) and in the Bay of Biscay ( $\approx$  35.7 PSU). They correspond to the northwestward extension of the Loire river plume on the Armorican shelf. These low salinity waters flow along the south coasts of Brittany and enter the Iroise Sea and the Western Channel as a narrow current. Despite relatively low inputs in 2011 (mean river discharge was 3 times lower than the usual mean discharge), the signature of the low salinity Loire was clearly visible in the entrance of the Western Channel (Figure 15d) and their influence could be even observed in the center of the Western Channel (49°30N – 3°W).

## Coastal profilers

Finally, coastal profilers (ARVOR-C/Cm in the present case) form the last pillar of our coastal observing system.

### Arvor-C

The Arvor-C is a vertical untethered profiling float, easy to set up and ready to be deployed. It behaves like a virtual mooring, for short to long term observations. It can take measurements at the same location for each profile thanks to the optimized time of ascent and descent through the water column, the short time of transmission at the surface, and its anti-drift capability when grounded on the seabed. The Arvor-C provides a standard set of measurements (pressure, temperature and conductivity), as well as a set of technical information. Multidisciplinary sensors can be integrated on this vertical vehicle, which is designed as an open platform. Additional sensors are being currently fitted to measure dissolved oxygen, turbidity and fluorescence. The Arvor-C is a coastal profiling float, designed to withstand pressures up to 450 meters depth. It can perform up to 320 profiles when cycling at 200 meters depth. The profile repetition rate can be configured from 1 profile every hour. Its ascending speed reaches 15 to 20 centimeters/second. For instance, a 2-second sampling period provides one single measurement every  $\sim$ 35 centimeters. Data are then averaged into 1-meter high slices to reduce transmission duration (André et al., 2010).

In the frame of the ASPEX project, two ARVOR-C coastal profilers have been maintained in the Bay of Biscay (Figure 16) for years 2009 to 2013. The deployment positions, one in the Northern part and one in the Southern part, have been chosen to collect profiles representing hydrological properties of the "cold pool" (usually names "bourrelet froid" in French) extending above Armorican and Aquitaine shelves. Ten deployments have been operated among which six profilers have been recovered and reused. Four profilers have been lost. The origin of two of these four losses, which happened during the same deployment in 2009, has been associated to a minor design fault of the sensor, which has been corrected. One loss, in 2010, is due to a software bug, corrected today. The last lost profiler is due to destruction during a trawling.

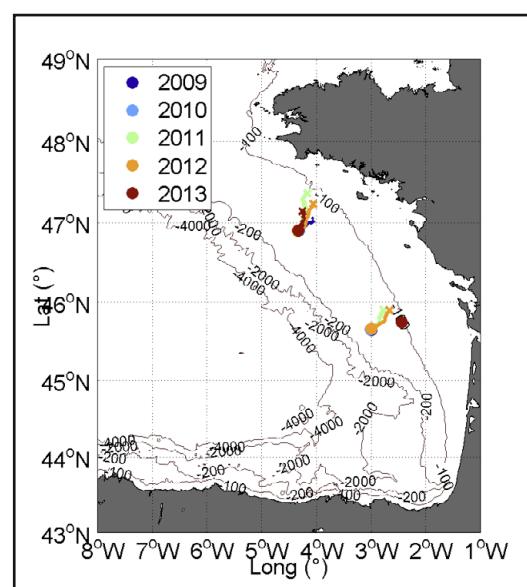
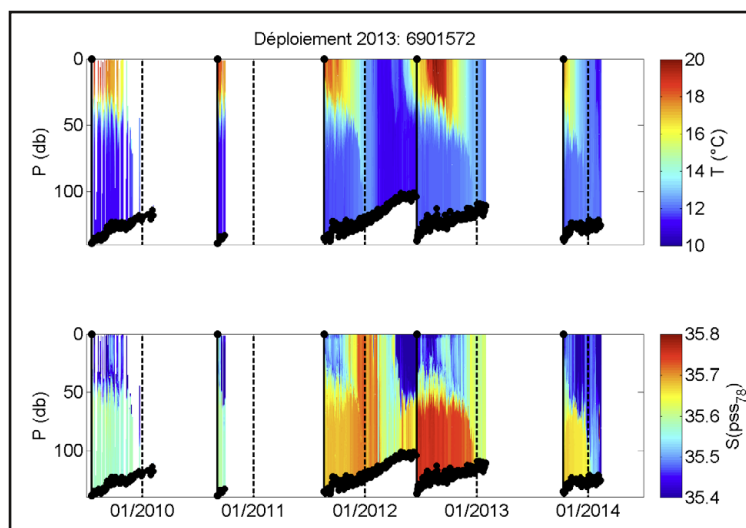


Figure 16

Deployed profilers in the Southern site have been strongly perturbed due to the fishing activity and, then, the corresponding dataset is fragmented. In the Northern part, Figure 17 presents temperature and salinity profiles. We observe on these profiles a good visualization of the annual cycle and the seasonal stratification over the Armorican shelf from 2011. These profiles from 2011 provide the first observations with a high temporal resolution of a full annual cycle of the thermal (Figure 17-up) and haline (Figure 17-down) stratification in this region. During the deployment of the profiler, begin of September 2011, the profiler meets classical stratified conditions with a layer around 40m depth of fresh and warm water at surface, and a layer of saltier and colder water at bottom. The propagation of internal waves, aliased by measurements, is clearly visible through an important noise

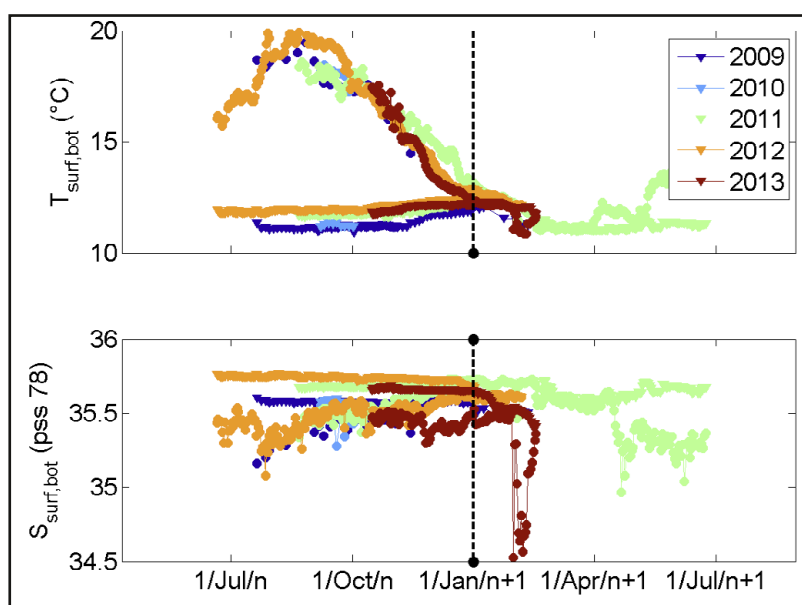


on the position of the seasonal thermocline. During the autumnal cooling in 2012, the surface layer cools quickly and becomes saltier. The seasonal pycnocline deepens quickly and is associated to a density contrast, which will decrease until it disappears, around the 1st January 2012. Surface salinity values are larger than those observed in the bottom layer during summer, showing a contribution of the horizontal advection because the only vertical mixing cannot explain these salinity values. During spring, haline stratification appears quickly in the middle of April. This stratification is used as a precondition for the setup of the thermal stratification reinforcing the haline stratification. The jump in salinity observed mid-June 2012 during the profiler replacement is not due to drift in sensor calibration (confirmed with CTD profiles with differences lower than  $0.05^{\circ}\text{C}$  and  $0.02$  psu after one year of deployment) but to different hydrological properties between the recovery point and the deployment point. The seasonal cycle observed by the profiler during the 2012-2013 deployment follows broadly similar evolutions.

Figure 17: Temperature and Salinity profiles collected by the ARVOR-C profiler in the Northern part of the Bay of Biscay (see Figure 16). Deployment dates are corresponding to the black continuous vertical lines. Black dashed lines are representing the beginning of each civil year.

Figure 18 shows that even if the temperature and salinity evolutions are similar each year, interannual variations can be observed. Then, the 2012 deployment displays warmer temperature than other years (at surface and at the bottom). Bottom salinity values present interannual variations reaching  $0.2$  (pss 1978). Summer surface salinity, even if they have a short-term variability more marked, seems on seasonal average less variable from one year to the next one. The series of storms, end of winter 2013, seems to induce an unusual early decrease in the surface salinity. This minimum has been later removed joining bottom values due to winter vertical mixing.

Figure 18: ARVOR-C profilers temperature (up) and salinity (bottom) observed at surface (circles) and bottom (triangles).



## Conclusion

This letter describes an overview of the coastal *in situ* high frequency systems developed and operated with the help of the PREVIMER project. Few illustrations show examples of results obtained with the data collected from these different platforms: fixed platforms, ships of opportunity and coastal profilers.

Through this network, the PREVIMER project contributed to develop coastal *in situ* observing systems along French coasts and to setup solid components of a future French Integrated Ocean Observing System.

## Acknowledgements

"Marel Iroise" data are collected and processed according to the terms of the framework agreement jointly signed by IFREMER, CNRS (INSU) and UBO (on behalf of IUEM) n°11/2-210922.

## References

- André, X., S. Le Reste, J.-F. Rolin, Arvor-C: A Coastal Autonomous Profiling Float, *Sea Technology*, 51(2), 10-13, 2010.
- Bozec, Y., L. Merlivat, A.-C. Baudoux, L. Beaumont, S. Blain, E. Bucciarelli, T. Danguy, E. Grossteffan, A. Guillot, J. Guillou, M. Répécaud, P. Tréguer. Diurnal to inter-annual dynamics of pCO<sub>2</sub> recorded by a CARIOCA sensor in a temperate coastal ecosystem (2003–2009). *J. Mar. Chem.*, 126, 13-26, 2011.
- Chapelle A., Lazure P., Ménesguen A., Modelling eutrophication events in a coastal ecosystem. Sensitivity analysis. *Estuar., Coast. and Shelf Sci.*, 39, 529-548, 1994.
- Chauvaud, L., R. B. Dunbar, A. Lorrain, Y.-M. Paulet, G. Thouzeau, F. Jean, J.-M. Guarini, D. Mucciarone. The shell of the Great Scallop *Pecten maximus* as a high frequency archive of paleoenvironmental change. *Geochemistry Geophysics Geosystems* 6, 2005.
- Diaz R.J., Rosenberg R., 2008. Spreading dead zones and consequences for marine ecosystems, *Science*, 321, 926-929.
- Dussauze M., 2011. Simulation de l'effet d'une variation réaliste des apports azotés et phosphorés de la Loire et de la Vilaine sur la production primaire dans la zone Loire/Vilaine. Rapport Ifremer RST DYNECO/EB/11-05/AM, 50 p., 2011.
- Lazure P., Jegou AM, Kerdreux M., Analysis of salinity measurements near islands on the French continental shelf of the Bay of Biscay. *Scienca Mar.*, 70 Suppl. 1 7-14, 2006.
- Lazure P., Garnier V., Dumas F., Herry C., Chifflet M., Development of a hydrodynamic model of the Bay of Biscay. Validation of hydrology. *Cont. Shelf Res.* doi: 10.1016/j.csr.2008.12.017, 2009.
- Leblond, E., P. Lazure, M. Laurans, C. Rioual, P. Woerther, L. Quemener, P. Berthou, RECOPECA: A new example of participative approach to collect in-situ environmental and fisheries data, *Joint Coriolis-Mercator Ocean Quarterly Newsletter*, 37, 40-55, 2010.
- Ménesguen A. and Gohin F., Observation and modelling of natural retention structures in the English Channel. *J. Mar. Sys.* 63(3-4): 244-256, 2006.
- Merceron, M., Baie de Vilaine: juillet 1982. Mortalité massive de poissons. L'analyse des causes et des mécanismes du phénomène, les propositions d'action. *Equinoxe* 21, 4-9, 1988.
- Stanisière J.-Y., Mazurié J., Bouget J.-F., Langlade A., Gabellec R., Retho M., Quinsat K., Leclerc E., Cugier P., Dussauze M., Ménesguen A., Dumas F., Gohin F., Augustin J.-M., Ehrhold A., Sinquin J.-M., Goubert E., Dreano A., Les risques conchyliques en Baie de Quiberon (3<sup>ème</sup> partie) : le risque d'hypoxie pour l'huître creuse *Crassostrea gigas*. Rapport final du projet Risco 2010-2013. Rapport Ifremer RST/LER/MPL/13.21, 73 p. 2013.
- Tessier, C., P. Le Hir, X. Lurton, and P. Castaing, Estimation of suspended sediment concentration from backscatter intensity of Acoustic Doppler Current Profiler, *Comptes Rendus Geoscience*, 340(1), 57-67, 2008.
- Thorne, P. D., and D. M. Hanes, A review of acoustic measurement of small-scale sediment processes, *Continental Shelf Research*, 22(4), 603-632, 2002.
- Tréguer, P., E. Goberville, N. Barrier, S. L'Helguen, P. Morin, Y. Bozec, P. Rimmelin-Maury, M. Czamanski, E. Grossteffan, T. Cariou, M. Répécaud, L. Quémener. Large and local-scale influences on physical and chemical characteristics of coastal waters of Western Europe during winter, *J. Mar. Sys.*, submitted, 2013.

## OBSERVATION OF SURFACE CURRENTS BY HF RADARS

By **S. Beurret<sup>(1)</sup>**, **N. Thomas<sup>(2)</sup>**

<sup>1</sup>SHOM, Brest, France

<sup>2</sup>ACTIMAR Brest, France

### Abstract

A WERA (WavE RADar) High Frequency (HF) radar system has been set up by SHOM in 2006 in order to measure surface currents, wave and wind parameters over a large area off the western coast of Brittany (France), which are then used for tuning and validating PREVIMER ocean and wave forecasting models. Under contract with SHOM, ACTIMAR<sup>(2)</sup> operates the HF radar and provides the real time validated data to the PREVIMER partners. These data were also available on the PREVIMER website.

### The WERA Radar

The WERA system is a shore based remote sensing system used to monitor ocean surface currents, waves and wind parameters. This long range, high resolution monitoring system is based on short radio wave radar technology. The vertical polarised electromagnetic wave is coupled to the conductive ocean surface and follows the earth's curve. This trans-horizon radar can detect back-scattered signals (Bragg effect) up to 200 km.

### Advantages of HF Radars

- Current and sea state measurements in real time (data available in 15 min)
- Wide coverage area (about 100km x 100km)
- High measurement density (about 1km resolution)
- Wave height and direction measurements

### The SHOM WERA radar

The SHOM WERA radar has 2 implantations in order to measure 2D scattering: Garchine site at Porspoder (R1) and Brezellec site at Cleden-Cap-Sizun (R2) – See Figure 1.

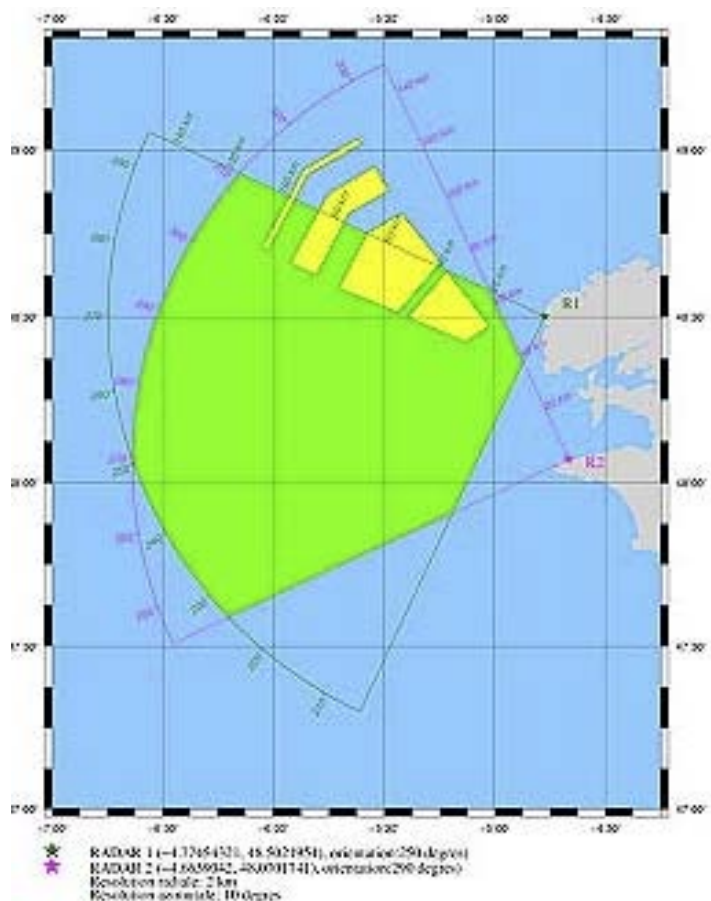


Figure 1: Implantation position and theoretical observation area

These 2 sites are equipped with the same material: one transmitter with 4 antennas, and one receptor with 16 antennas (see Figure 2 and Figure 3).



Figure 2: Garchine reception antennas

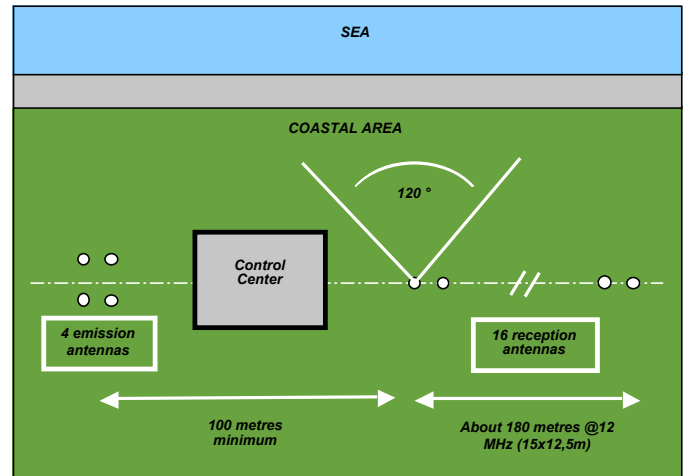


Figure 3: SHOM WERA Radar Synoptic

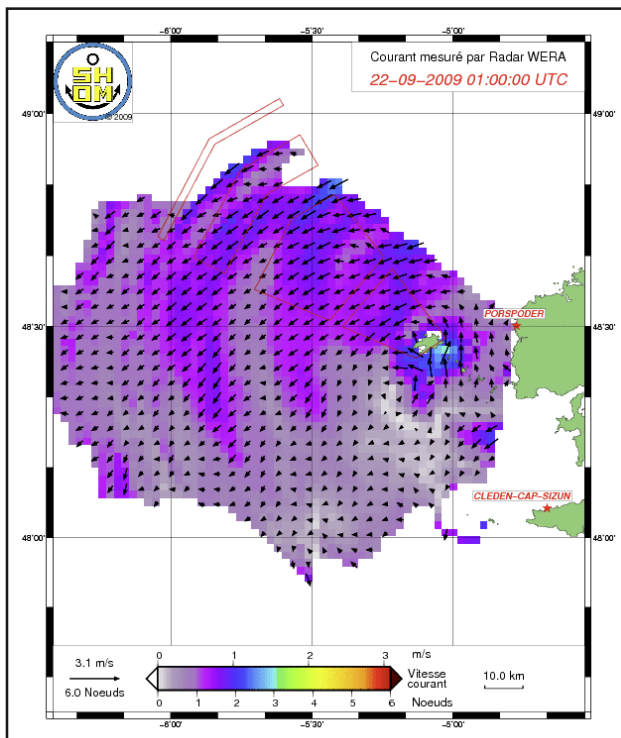


Figure 4: Example of currents measurement by SHOM WERA Radar

An example of currents measurement is given in Figure 4.

SHOM HF radar data were available in quasi real time on the PREVIMER website.

A snapshot is given in Figure 5.

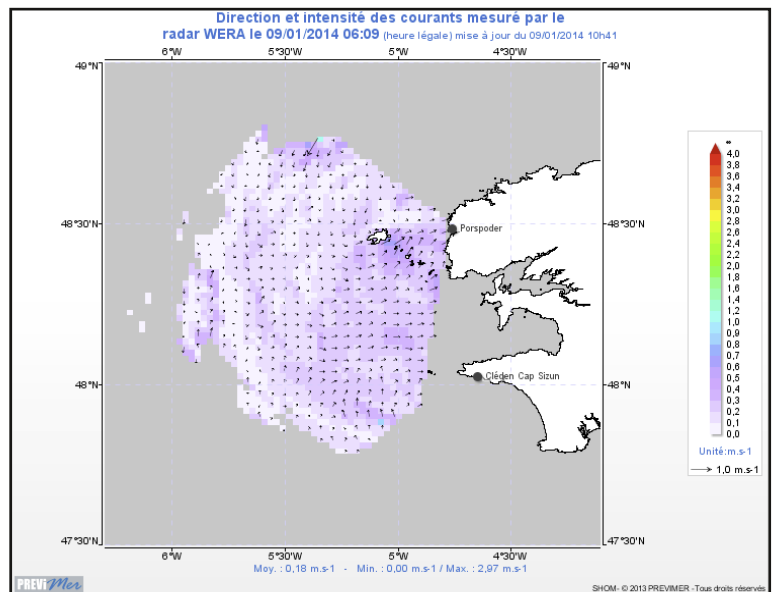


Figure 5: Snapshot of PREVIMER website

## Conclusion

The SHOM HF radar provide high resolution data in real time over a large area off the coast of Brittany, that are very useful for studying high frequencies oceanographic processes and also for tuning and validating ocean forecasting models in that area. This technology should be used by SHOM in other coastal areas depending on next project fundings.

## PAOLA: A NEW AUTONOMOUS AIR-DEPLOYED OCEAN PROFILER

By S. Beurret<sup>(1)</sup>, P. Brault<sup>(2)</sup>, A. David<sup>(2)</sup>

<sup>1</sup>SHOM, Brest, France

<sup>2</sup>NKE, Hennebont, France

### Abstract

In the framework of PREVIMER, the French Hydrographic and Oceanographic Office (SHOM) has developed a new low-cost air-deployed ocean profiler to be used as a "rapid environmental assessment" system for measuring temperature profiles and ambient noise with a high density in space and time. This system named PAOLA has been industrialised by NKE<sup>2</sup> and is on its way to be marketed soon.

### General specifications

The PAOLA profiler has been designed to be launched by an aircraft equipped with a standardised A-sized launcher (eg: maritime surveillance aircraft). A parachute is used to slow down the drop. When the profiler touches the sea surface, the parachute locked to the top end cap is released. So when the profiler is in the water, it can start cycling by changing its buoyancy using a piston. When going up, it makes measurements of pressure and temperature in the full water column, and of ambient noise at 3 depths. When it is on surface, it sends data via Argos (the profiler is also located by the Argos system). Then, depending on the operating mode, it waits until the next cycle (every 12 or 24 hours) or it goes down immediately (continuous mode). The profiler is designed to operate at least 50 cycles up to 500 metres depth (configurable). Figure 1 shows photos of the profiler with and without the cap and a schematic deployment illustration.

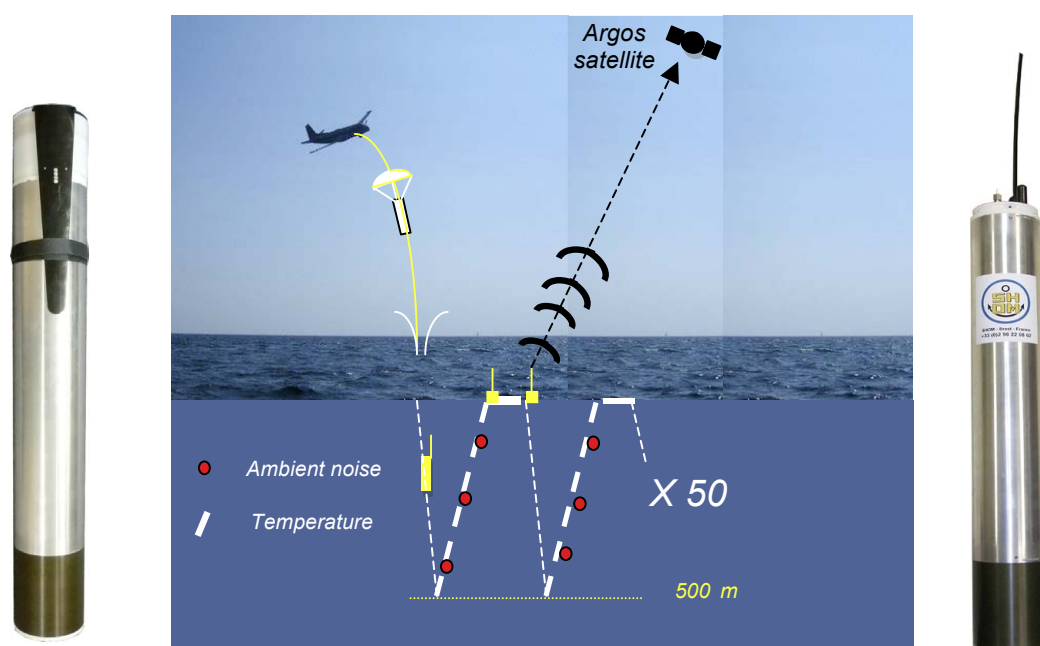


Figure 1: Deployment illustration

### Technical specifications

Main specifications are:

- 50 cycles up to 500 m depth (configurable)
- Aircraft droppable by a standardized A-sized launcher
- Pressure & Temperature Accuracy: 0.1 bar (~1m), 0.1 °C
- 3 operating modes: 12h cycle, 24h cycle, or continuous mode
- Data transmission by Argos satellites

Acoustic specifications:

- 10 frequency bands from 30 Hz to 2400 Hz
- 3 possible measurement depths (configurable)
- Acoustic sensitivity order of magnitude: 0 sea state



Figure 2: Details of PAOLA profiler

## Experiment results in Bay of Biscay in July 2013

Different trial tests have been achieved in order to validate the system. The latest was in July 2013 in the Bay of Biscay. Comparisons with other probe measurements (AXBT) showed that the profiler had a good behaviour after aircraft launching and that temperature measurements were correct. This profiler achieved 86 cycles in 43 days.

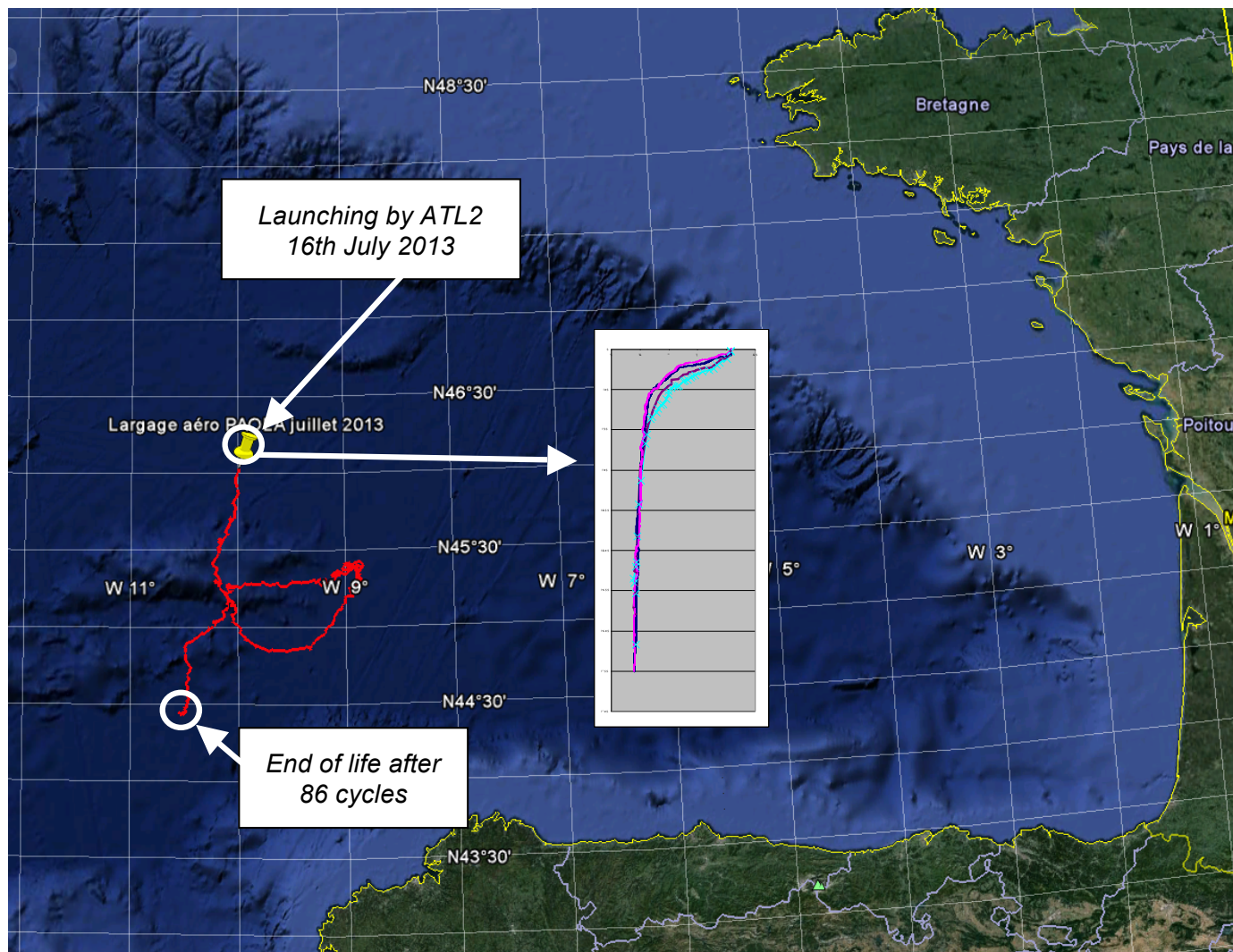


Figure 3: Example of a test in the Bay of Biscay

## Conclusion

The collaboration between SHOM and NKE has led to a new type of ocean profiler for in-situ observations. Some final improvements are under way to get a robust and reliable system.

# A NEW PROCEDURE FOR INTERPOLATING SATELLITE-DERIVED SUSPENDED PARTICULATE MATTERS WITHIN THE PREVIMER CONTEXT

By *F. Gohin*<sup>(1)</sup>, *P. Bryère*<sup>(2)</sup>, *L. Perrot*<sup>(1)</sup>

<sup>1</sup>IFREMER Brest, Plouzané, France

<sup>2</sup>ACRI-ST, Brest, France

## Abstract

After several years of experience in providing daily merged products of non-algal Suspended Particulate Matters (SPM) for forcing the light in the ecological model of Previmer ECO-MARS-3D, we have often observed poor quality SPM fields in winter due to the cloud cover. For this reason we propose a new interpolation scheme, multisensor and multitemporal, based on a first-guess field of daily SPM derived from a biweekly satellite climatology modified to take into account dynamically the effects of waves and tides. The contribution of waves and tide is simulated through a simple statistical model (multiplicative effects of the significant wave heights and tidal intensity) summing up the information coming out from the historical data set of SPM. On an operational basis, this also provides a pre-analysis tool very useful for writing bulletins.

## Introduction

The forcing of light based on  $K_{PAR}$  fields derived from non-algal SPM is particularly useful at the end of winter and at the beginning of spring when light limits the phytoplankton growth and when the hydro-sedimentary models fail to retrieve correctly the surface SPM. At the end of winter, the load of non-algal SPM in the water column and the bottom configuration have been deeply impacted by the successive winter storms, leading to resuspension processes which may be difficult to model. Building up complete fields of surface SPM from the remote-sensing reflectances provided by the Ocean Colour sensors (now MODIS or VIIRS) is particularly difficult on the European North-West Shelf at the end of winter when the cloud cover may persist several days. The task is harder still in real-time production as we can only rely on the satellite images preceding the current day. Up to now in Previmer the merged fields of SPM have been produced by kriging the SPM anomalies over a ten-day period, five days before and five days after the considered day, on the 1.2 km satellite "Atlantic" reference grid of Ifremer (Saulquin et al., 2011). In real time, only the five preceding days can be used. The anomaly is defined as the deviation of the daily SPM relatively to a mean value obtained by a bilinear interpolation applied to monthly averaged SPM. Five days can be considered as a short period if the availability of clear pixels is looked for and ten days is a long period if we considered the time scale of the variability of the effects of waves and tides on surface SPM. Rivier et al. (2012) have shown that a large part of the variance in the satellite-derived SPM signal can be explained by a simple statistical model based on the seasonal mean corrected by a very simple formulation of the variability of the surface SPM resulting from the bottom shear stress induced by the wave and the tidal current. The wave indicators are the daily maximum significant wave heights provided by the Previmer-IOWAGA System (Arduin 2010) within the Data Centre for Operational Coastal Oceanography and the tidal intensity is approached through the tidal coefficient provided by SHOM/Navy. This model, with coefficients defined pixel by pixel, takes into account only indirectly the advection of SPM. It is a very simple model which doesn't aim at providing 3-D SPM fields as a hydro-sedimentary model but daily fields of surface SPM consistent with the historical time series of satellite observation. The daily anomalies of satellite SPM relative to this dynamical underlying SPM are likely to respect the hypothesis of stationarity which is the basic condition in ordinary kriging. That is why we are proposing a new interpolation scheme based on a dynamical underlying field evolving in relation with the wave height provided by Previmer and the tidal coefficient of the SHOM.

## Biweekly means of surface Suspended Particulate Matter

From the time series of daily merged SPM images processed through the Ifremer method (Gohin 2011) over the period 2003-2013, a database of 26 biweekly maps has been constructed. The strong seasonal cycle is visible on the images, with a maximum at the end of February to a minimum in July. Although the SPM are considered as non-algal by construction (the role of phytoplankton biomass in the optical properties of the water being considered as known from the chlorophyll-a concentration in the inversion from the marine reflectance in the green and the red) strong phytoplankton bloom may have a residual effect in the retrieval of the non-algal SPM. The coccolithophores are the most significant living contributor to these errors due to their calcite 'scales', the coccoliths. A special attention has therefore to be paid to coccoliths and 26 biweekly maps have been also produced without coccoliths.

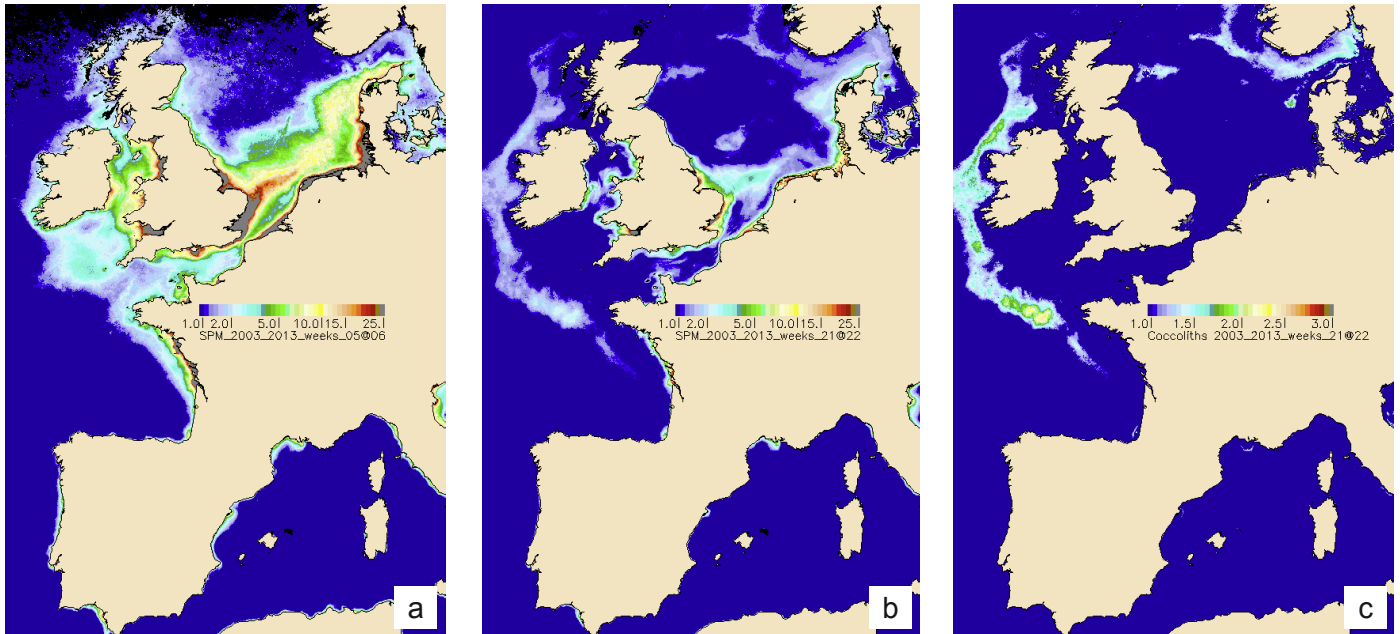


Figure 1 : Images of the climatology corresponding to (a) weeks 5-6 (beginning of February), (b) weeks 21-22 (end of May), (c) coccoliths (scale modified) extracted for weeks 21-22

## Dynamical underlying model

The underlying model giving the simulation of the first-guess field is expressed pixel by pixel  $SPM_j = a_0 SPM_{Mj} Tide_j^\alpha Hsj^\beta$  (1) where  $SPM_{Mj}$  is the mean SPM at day  $j$ ; the 3 unknown parameters  $a_0$ ,  $\alpha$ , and  $\beta$  are calculated for every pixel after log-transformation of the satellite-derived SPM over the period 2007-2010. The Tide parameter is the average of the tidal coefficients provided by SHOM on the last three days, including the current day  $j$ . The significant height of the wave,  $Hsj$ , is a weighted integration of the daily maximum  $Hs$ . Higher weights are applied to  $Hs$  of the latter days. The integration time for  $Hs$  is determined for each pixel, depending on the determination coefficient of the model, for two integration times of ten and twenty five days. For the Bay of Biscay and the Celtic Sea, facing directly the wavefronts, the integration time is generally 10 days whereas it is 25 days in the Eastern Channel where the effects of the waves and the advection from the western Channel are observed with delay.

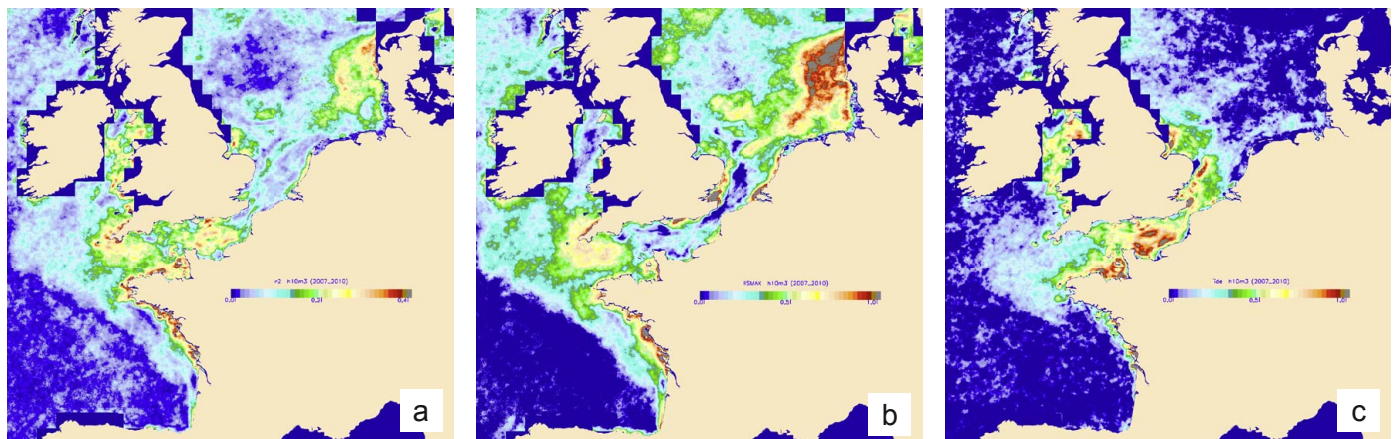
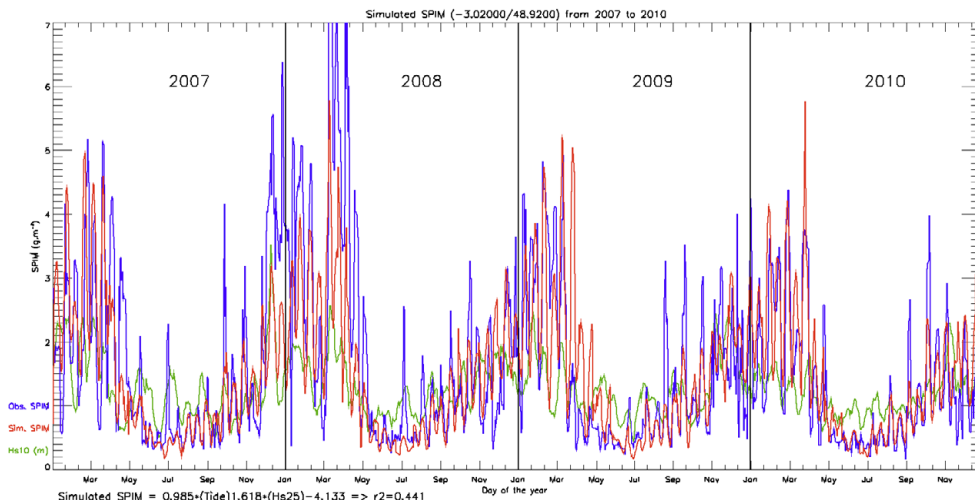


Figure 2 : Coefficient of determination and coefficients of the model for  $Hs$  cumulated over 10 days; (a) coefficient of determination, (b) power coefficient for  $Hs$ , (c) power coefficient for the tide

Figure 2 shows the map of the determination coefficient calculated by pixel and the coefficients  $\alpha$  and  $\beta$  for an integration time of ten days. The SPM of the central English Channel are highly sensitive to tide whereas, at the entrance of the Channel, the Eastern North-Sea and on the continental shelf of the Bay of Biscay they appear to be particularly sensitive to waves.

Figure 3 shows the time series of observed (daily merged products of SPM as provided up to now within Previmer) and simulated SPM (by applying formula (1)) north of the Isle of Bréhat in Northern Brittany, a location particularly sensitive to the tidal cycle. The Neap/Spring cycle of 14 days is apparent on both the observed and the simulated time series.

Figure 3 : Observed (blue) and simulated (red) non-algal SPM concentration north of the isle of Bréhat (3.02W, 48.92N) in Northern Brittany from 2007 to 2010



### The interpolation procedure

The interpolation procedure is based on the daily simulations of the statistical model over an eleven-day period centered on the day of interest. Relatively to these simulations, the daily deviations are averaged on a grid of 10\*10 pixels. Only the locations where a minimum of 20 points are observed are kept, to eliminate the isolated observations on the boundary of a cloud-flagged area, often dubious. Then, a simple 2-D interpolation by kriging is carried out, using a spherical covariance with a range of 80 pixels (about 100 km) and a ratio nugget (noise) on total variance of 25%. Figure 4 illustrates the procedure for February 1<sup>st</sup>, 2014. Figure 4(a) and (b) presents the maximum Hs for January 30<sup>th</sup> and February 1<sup>st</sup> when a storm hurt the eastern Atlantic. Figure 4(c) shows the simulation for February 1<sup>st</sup> and Figure 4(b) the mean anomaly relatively to the 11 simulations. The SPM anomaly is particularly high in February 2014 as a relentless succession of strong storms hurt the area since December 2013. The estimated field for February 1<sup>st</sup> is obtained from the simulation of the day to which is added the interpolated anomaly. The SPM field on February 1<sup>st</sup> of 2014 can be compared to the average map for the season, much lower, shown on Figure 1(a).

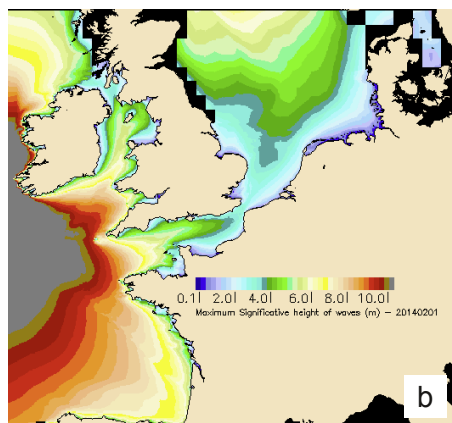
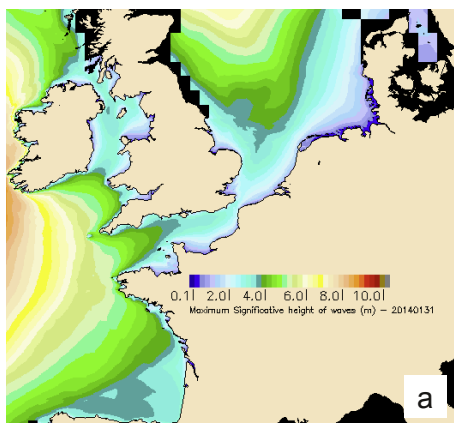
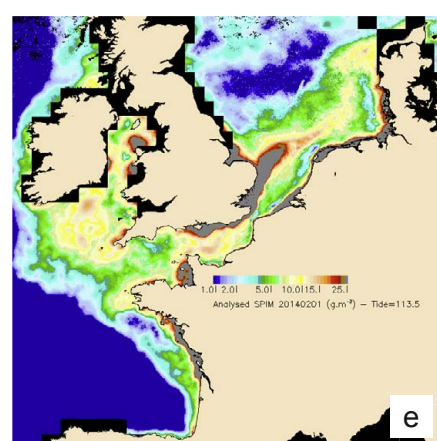
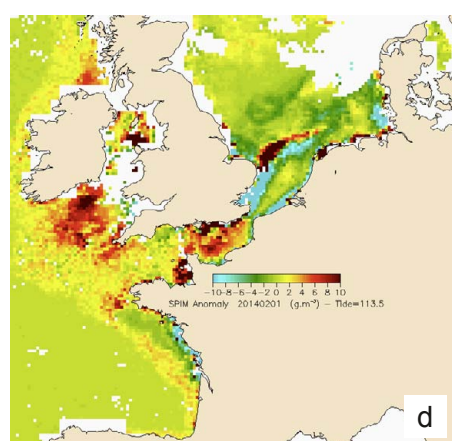
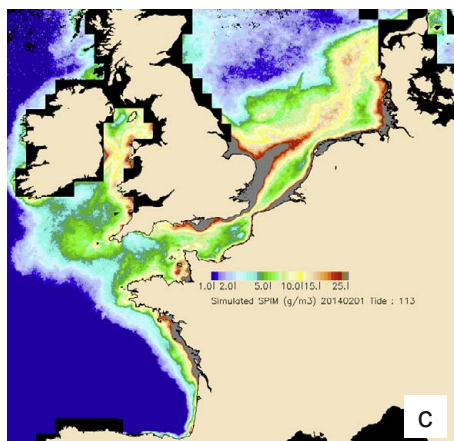


Figure 4 : Interpolation on 1 February 2014 (a) and (b) maximum Hs on 31/01 and 01/02; (c) simulation, (d) anomaly, (e) interpolated map on 1 February



## Conclusion

Besides its contribution to operational coastal oceanography, this product may improve our methods for investigating the spectral marine reflectance. The first improvement concerns our knowledge of the mineral SPM particles, whose shape and size are sensitive to the turbulence of the water. It is known that turbulence affects flocculated particles in shelf seas by tearing them apart, creating clouds of smaller particles with high refractive index (Bowers et al., 2005). It is likely that this process will change the backscattering:mass ratio of the particles and affect the algorithm for deriving suspended sediment load from remote sensing reflectance in these waters. The second improvement concerns the identification of phytoplankton groups from space in turbid coastal waters. Conversely to the estimation of the non-algal SPM from the reflectance in the green and the red as it is done today in the Ifremer method, we may infer the backscattering properties of the mineral content of the water from the simulated fields of non-algal SPM, therefore leading, by subtraction, to a better estimation of the optical properties of the second compartment optically active in these waters: the phytoplankton.

Several levels of satellite-derived products are available from Level-0 (sensor level) to Level-4 (multi-temporal, multi-sensor), and all these products have their own characteristics and utility. This new product could be considered as belonging to another category, a kind of L5 product, which uses external information in the merging procedure, and eventually could be able to provide with realistic fields even in case of lack of data due to a persistent cloud cover. If we would have to define a Level-5 product for remote-sensing data, the underlying model should be simple and robust, otherwise it should rapidly lead to a Bayesian approach, Kalman filtering or any other assimilation method which is beyond the scope of a satellite-derived product. However, the method could be improved by taking into account the river outflows and the wind intensity and direction, particularly in spring when the plumes of the rivers contribute significantly to the overall SPM on the continental shelf. This could be obtained relatively easily by adapting the formulation of the model (1) pixel by pixel.

Another advantage of this product is that it suits perfectly the goals of the coastal oceanography within an operational context. In practice, the daily anomalies relative to the simulated maps keep memory of the major "residual" effects of the past storms on the situation of the day, without the confusion brought by the Neap/Spring tidal cycle which is nothing but regular. This also contributes to make it easier writing the Previmer bulletins.

## Acknowledgements

The authors thank Previmer and Fabrice Arduin for providing wave heights, NASA and ESA for providing MODIS, VIIRS and MERIS data. Part of This work has been carried out within the MCGS project (Marine Collaborative Ground Segment) of the Pôle Mer Bretagne and PACA.

## References

- Arduin, F. 2010: Wave hindcasting and Forecasting: Geophysical and Engineering Applications. Examples with the Previmer-IOWAGA System, Mercator Ocean Quaterly Newsletter, #38, July 2010, 14-22.
- Bowers, D.G., K.M.Ellis and Jones S.E.J. 2005: Light scattered by particles suspended in the sea: the role of particle size and density. *Continental Shelf Research*, 25, 1071-1080.
- Gohin, F. 2011: Annual cycles of chlorophyll-a, non-algal suspended particulate matter, and turbidity observed from space and in-situ in coastal waters, *Ocean Sci.*, 7, 705-732, <http://www.ocean-sci.net/7/705/2011/>
- Rivier, A., Gohin, F., Bryère, P., Petus, C., Guillou, N., and Chapalain, G. 2012: Observed vs. predicted variability in non-algal suspended particulate matter concentration in the English Channel in relation to tides and waves. *Geo-Marine Letters*, 32, 2, 139-151.
- Saulquin, B., Gohin, F., and Garrello, R. 2011: Regional objective analysis for merging high-resolution meris, modis/aqua, and seawifs chlorophyll-a data from 1998 to 2008 on the european atlantic shelf, *IEEE Transactions on Geoscience and Remote Sensing*, 49, 143-154.

## PREVIMER: IMPROVEMENT OF SURGE, SEA LEVEL AND CURRENTS MODELLING

By **L. Pineau-Guillou<sup>(1)</sup>**, **F. Dumas<sup>(1)</sup>**, **S. Theetten<sup>(1)</sup>**, **F. Ardhuin<sup>(1)</sup>**, **F. Lecornu<sup>(1)</sup>**, **J.-F. Le Roux<sup>(1)</sup>**, **D. Idier<sup>(2)</sup>**, **H. Muller<sup>(2)</sup>**, **R. Pedreros<sup>(2)</sup>**

<sup>1</sup> IFREMER, Brest, France

<sup>2</sup> BRGM, Orléans, France

### Abstract

The pre-operational system PREVIMER provides coastal observations and forecasts along French coasts. It provides, among other variables, currents, sea levels, surges and waves. This paper describes the development and validation of a high temporal (15 minutes) and spatial (250 m) resolution modeling system, based on MARS hydrodynamic model (Lazure and Dumas 2008), along the Atlantic and English Channel coasts. Models benefit from experiments developed during the PREVIMER project by: (1) taking better into account wind and wave actions (improving surface drag coefficient parameterization), (2) taking into account a better meteorological forcing (improving spatial and temporal meteorological resolution). These high resolution models have been integrated in PREVIMER modeling system since 2013.

### Introduction

Being able to properly forecast surges and sea level is essential for many applications, particularly for prevention of marine submersion risk. The developments of sea level and currents models answer many other needs: (1) improvements of wave models, taking into account currents influence on waves (Bouidière *et al.* 2013), (2) prediction of presence or absence of some habitats (aquatic plants, laminaria algae); indeed, correlation between observation data and physical parameters linked with their developments (currents for example) allow to set up statistic models, which allow to predict habitats; (3) computation of boundary conditions for higher resolution coastal models (a few tens of meters), (4) study of transport by currents (microplastics, pollutants, larvae, harmful algae)...

The pre-operational system PREVIMER provides currents, sea levels and surges along Atlantic and English Channel coasts. The modeling system is based on MARS (2DH) hydrodynamic model, developed by Ifremer (Lazure and Dumas 2008). This study aims at developing high resolution spatial (250 m) and temporal (15 minutes) hydrodynamic models. The paper presents the model configuration, the improvement of parameterization, the validation and the results.

### Models configuration

In order to reproduce surges dynamics, the model extension must be sufficiently extended up to the North and West, in order to properly take into account depressions, generating surges which will propagate in the English Channel and Bay of Biscay. Models are nested models (figure 1), of resolution:

- 2 km for the rank 0 model, covering North East Atlantic,
- 700 m for the rank 1 model, covering the Channel and Bay of Biscay,
- 250 m for the five rank 2 models, covering Eastern Channel, Western Channel, Finistère, South Brittany and Aquitaine areas.

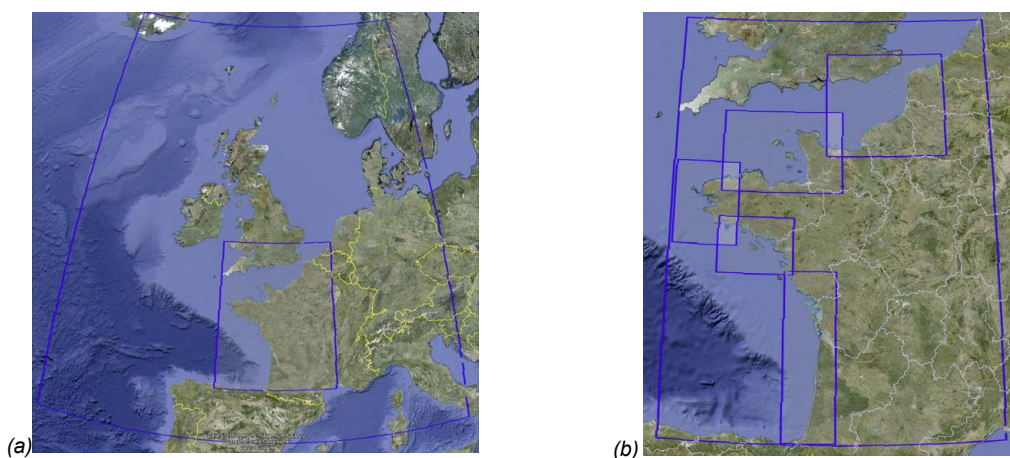


Figure 1: Extension of 2D models: rank 0 (North East Atlantic), rank 1 (English Channel and Bay of Biscay) and 5 rank 2 models (Eastern Channel, Western Channel, Finistère, South Brittany and Aquitaine)

Bathymetry comes from NOOS (North-West Shelf Operational Oceanographic System), EMODNET (European Marine Observation and Data Network), and Digital Terrain Models from Ifremer and SHOM (French Hydrographic Office) at 500 m and 100 m.

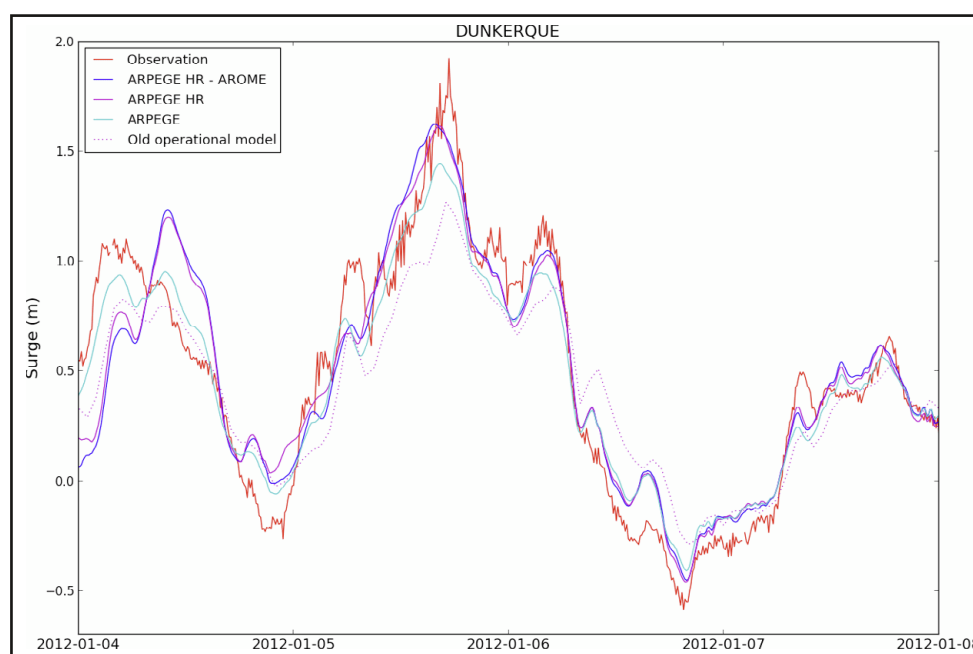
Meteorological forcing is provided by Météo-France, based on the meteorological models Arpege (Courtier *et al.* 1991, 1994) and Arome (Seity *et al.* 2011).

Each model runs twice, with and without meteorological forcing. Surges are calculated by subtracting the water level computed without meteorological forcing from the one computed with meteorological forcing. In both runs, the tide is taken into account. First, the tide is imposed at the boundary of the rank 0 model, using the FES2004 database (Lyard *et al.* 2006), which includes 14 harmonics constituents. Then, rank 1 is forced by the rank 0 water levels. Finally, the rank 2 models are forced (1) by tidal model cstFRANCE, developed by SHOM (Simon 2007), which includes 115 harmonic constituents (2) by surges from rank 1.

## Parameterization improvement

A sensitive study has been carried out on meteorological forcing. Meteorological data, provided by Météo-France are outputs from Arpege High Resolution (HR) and Arome models. Their temporal resolution is of 6 hours for Arpege and 1 hour for Arpege High Resolution and Arome; their spatial resolution is respectively of 0.5°, 0.1° and 0.0025°. The sensitivity study to meteorological forcing (Pineau-Guillou 2013, Muller *et al.* 2014) showed the influence of temporal and spatial resolution. Comparisons have been made in January 2012 over rank 0 configuration (2 km). The 5<sup>th</sup> of January 2012, Andrea storm crossed North of France, generating surges up to 2 meters in Dunkerque (figure 2). Three meteorological forcing have been tested: Arpege HR merged with Arome, Arpege HR alone, Arpege alone. Results showed that there is no significant improvement in merging Arpege HR with Arome at this resolution (2 km), because results are very similar with these two forcing: RMS errors are respectively of 12 cm and 11 cm, maximal surge respectively of 1.63 m and 1.62 m. Concerning comparison between Arpege HR and Arpege: results showed also that RMS errors are very similar: respectively 11 and 10 cm at Dunkerque. However, storm surge peaks modelling is really improved with high resolution: maximal surge reaches 1.62 m with Arpege HR, instead of 1.45 m with Arpege, an improvement of 17 cm. Statistics clearly show a diminution of peak error with Arpege HR, and an improvement of maximal surges (Muller *et al.* 2014). The resolution of meteorological forcing improves mainly the storm surge modelling associated to energetic events.

Figure 2: Surges at Dunkerque from 4 to 8 January 2012 (Andrea storm): influence of different meteorological forcing (Arpege HR merged with AROME, Arpege HR, ARPEGE) - Old operational model is forced with ARPEGE



Sea surface drag coefficient used for former PREVIMER operational model was a constant with value equal to 0.0016. Different parameterizations have been tested: wind dependant formulations (Wu 1982), (Moon *et al.* 2007), (Makin 2005) but also a wave and wind dependant formulation (Charnock 1955), inside PREVIMER working group on surges modeling (Idier *et al.* 2012). Charnock formulation takes into account surface roughness due to waves. By definition, the drag coefficient is expressed as:

$$C_d = \frac{u_*^2}{U_{10}^2} = \kappa^2 \left[ \ln \frac{z}{z_0} \right]^{-2} \text{ at } z=10 \text{ m (height above surface)}$$

with  $u_*$  the friction velocity,  $U_{10}$  10 m-wind,  $\kappa$  Von Karman's constant, and  $z_0$  surface roughness.

Surface roughness is expressed as  $z_0 = a_c \frac{u_*^2}{g}$ , where  $a_c$  is the Charnock dimensionless parameter.

In this study, the Charnock parameter can be constant (0.014), or variable and in this case, issued from WAVEWATCH III® (Tolman 2008, Ardhuin *et al.* 2010, Tolman *et al.* 2013), computed from the IOWAGA modeling system (Raschle and Ardhuin 2013) or from PREVIMER wave models. Sensitivity tests to drag coefficient formulation (constant, Wu, Moon, Makin, Charnock) show that taking into account wind and wave action (Charnock formulation with variable coefficient) give the best results, improving surge peaks modeling (Idier *et al.* 2012, Muller *et al.* 2014). During the Xynthia storm (28<sup>th</sup> February 2010), the differences using a constant drag coefficient (0.0016) and a Charnock formulation with a variable Charnock coefficient, on rank 0 model, reach 18 cm at La Rochelle (Pineau-Guillou *et al.* 2012b). These results are consistent with results obtained by (Bertin *et al.* 2012). A sensitive study has also been carried out on rank 2 models for the Petra storm (4<sup>th</sup> February 2014). Comparisons have been made between different drag coefficient parameterization: constant one (0.0016), Charnock formulation with a constant parameter (0.014) and Charnock formulation with a variable parameter,

issued from PREVIMER wave models. Results at Brest (figure 3) show an improvement of modeled surge up to 6 cm between constant value and Charnock formulation with constant parameter, and up to 12 cm between constant value and Charnock formulation with variable parameter. These improvements concern mainly peak surges. Generally, surges are still underestimated, compared to observations. However, the particular parameterization of the wave model (Rascle and Ardhuin 2013) improves short wave properties, but removes most of the wave-induced variability in the Charnock coefficient, and limits in our case the impact on results. Such results could still be improved, with different parameterization in the wave model.

Figure 3: Surges at Brest from 4 to 6 February 2014 (Petra storm): influence of drag coefficient parameterization (Charnock formulation with a variable or constant Charnock parameter, constant drag coefficient)

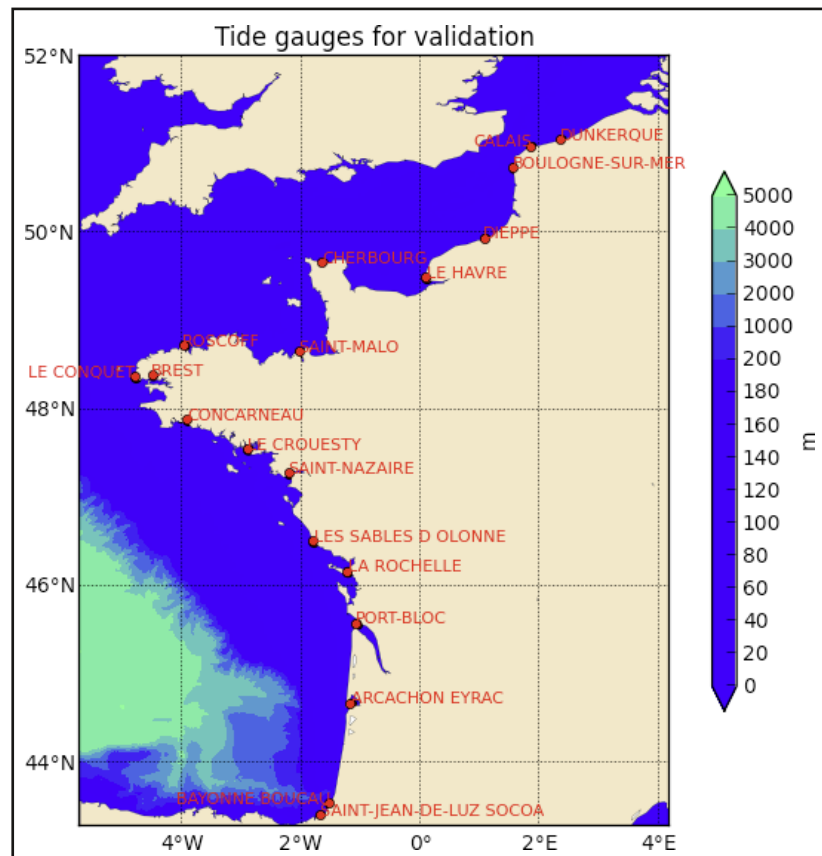
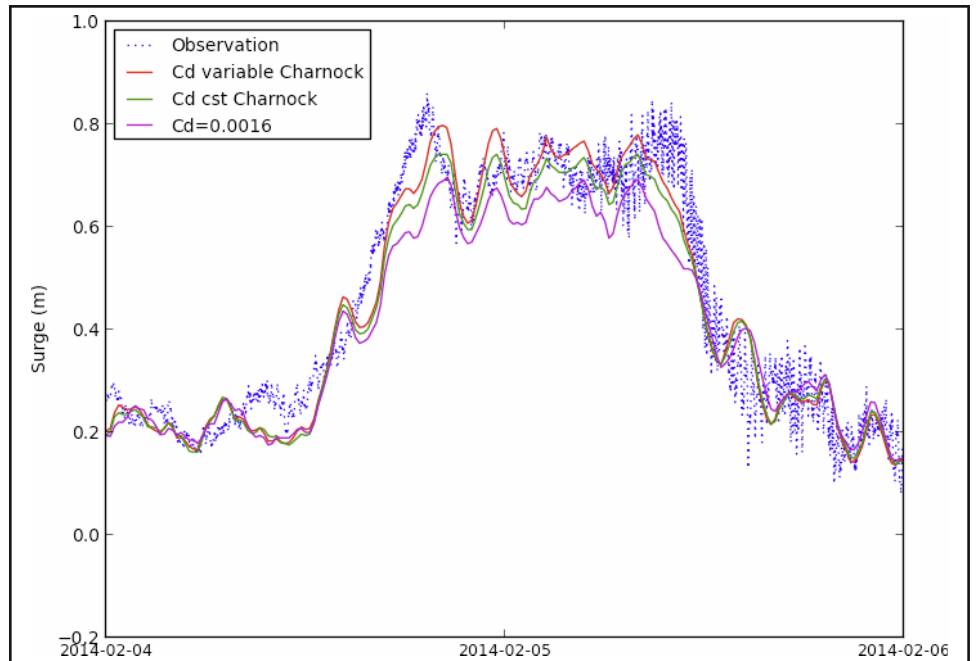


Figure 4: Tide gauges locations for tide, sea level and surges validation

### Validation

Validation has been carried out (Pineau-Guillou 2013) in 19 tide gauges (figure 4) from permanent network RONIM (French Sea Level Observation Network, managed by SHOM). For each site, data from numeric tide gauges have been collected through REFMAR ([www.refmar.shom.fr](http://www.refmar.shom.fr)), and analyzed in order to compute harmonic components. From these components, tidal predictions have been made, and used to extract the observed storm surge from the water level measurements.

Models have been validated in February 2010, during Xynthia storm (28 February 2010) (Pineau-Guillou *et al.* 2012a). Simulations have been carried from 15<sup>th</sup> to 28<sup>th</sup> February 2010 (Pineau-Guillou 2013). Meteorological forcing is a merge between Arome, Aladin and Arpege models outputs every 3 hours (Arpege High Resolution was not available in February 2010).

Tide has been validated by comparing modeled tide (from simulations without meteorological forcing) with predictions (based on observations harmonic analysis) at the 19 points presented figure 4. An example of validation is presented figure 5. RMS errors have been computed for each gauge and each model (table 1). They are on average of 22 cm for rank 0, 21 cm for rank 1 and 11 cm for rank 2 models; biases are on average of 3 cm for ranks 0 and 1, and null for rank 2 models. Tide is clearly improved for rank 2 models, which comes from the introduction at rank 2 boundary conditions of cstFRANCE tidal model (115 harmonic constituents, instead of 14 with FES2004 for rank 0), but also from the improvement of spatial resolution (250 m instead of 2 km for rank 0). Comparison between modeled tide with tidal predictions at Le Conquet between 22<sup>nd</sup> and 25<sup>th</sup> February 2010, shows clearly improvements between rank 0, rank 1 and rank 2 (figure 6).

Location	RMS Error (cm)			Bias (cm)			Rank 2 model
	Rank 0	Rank 1	Rank 2	Rank 0	Rank 1	Rank 2	
							MANE
Dunkerque	15	14	10	3	3	-3	MANE
Calais	17	17	11	4	5	0	MANE
Boulogne-sur-Mer	20	20	13	2	2	-4	MANE
Dieppe	22	23	14	5	5	0	MANE
Le Havre	20	21	13	0	1	-4	MANE
Cherbourg	13	15	6	0	2	-1	MANW
Saint-Malo	28	30	15	2	2	-3	MANW
Roscoff	20	21	7 8	3	4	0 3	MANW FINI
Le Conquet	19	18	7	1	-4	-4	FINI
Brest	32	15	10	1	1	0	FINI
Concarneau	14	14	8 7	-2	-2	-5 -5	FINI SUDB
Le Croesty	18	18	7	2	2	-1	SUDB
Saint-Nazaire	20	21	10	-1	-1	-6	SUDB
Les Sables d'Olonne	18	19	6	-2	-2	-2	AQUI
La Rochelle-Pallice	24	26	10	3	4	4	AQUI
Port-Bloc	34	19	13	1	0	1	AQUI
Arcachon	56	55	35	31	34	24	AQUI
Boucau-Bayonne	19	19	10	1	1	2	AQUI
Saint-Jean de Luz	12	13	8	3	3	4	AQUI
<b>Mean</b>	<b>22 cm</b>	<b>21 cm</b>	<b>11 cm</b>	<b>3 cm</b>	<b>3 cm</b>	<b>0 cm</b>	

Table 1: Root Mean Square errors and biases of water levels from different ranks (0, 1 and 2) without meteorological forcing (tide only) - Computed from 17<sup>th</sup> to 28<sup>th</sup> of February 2010

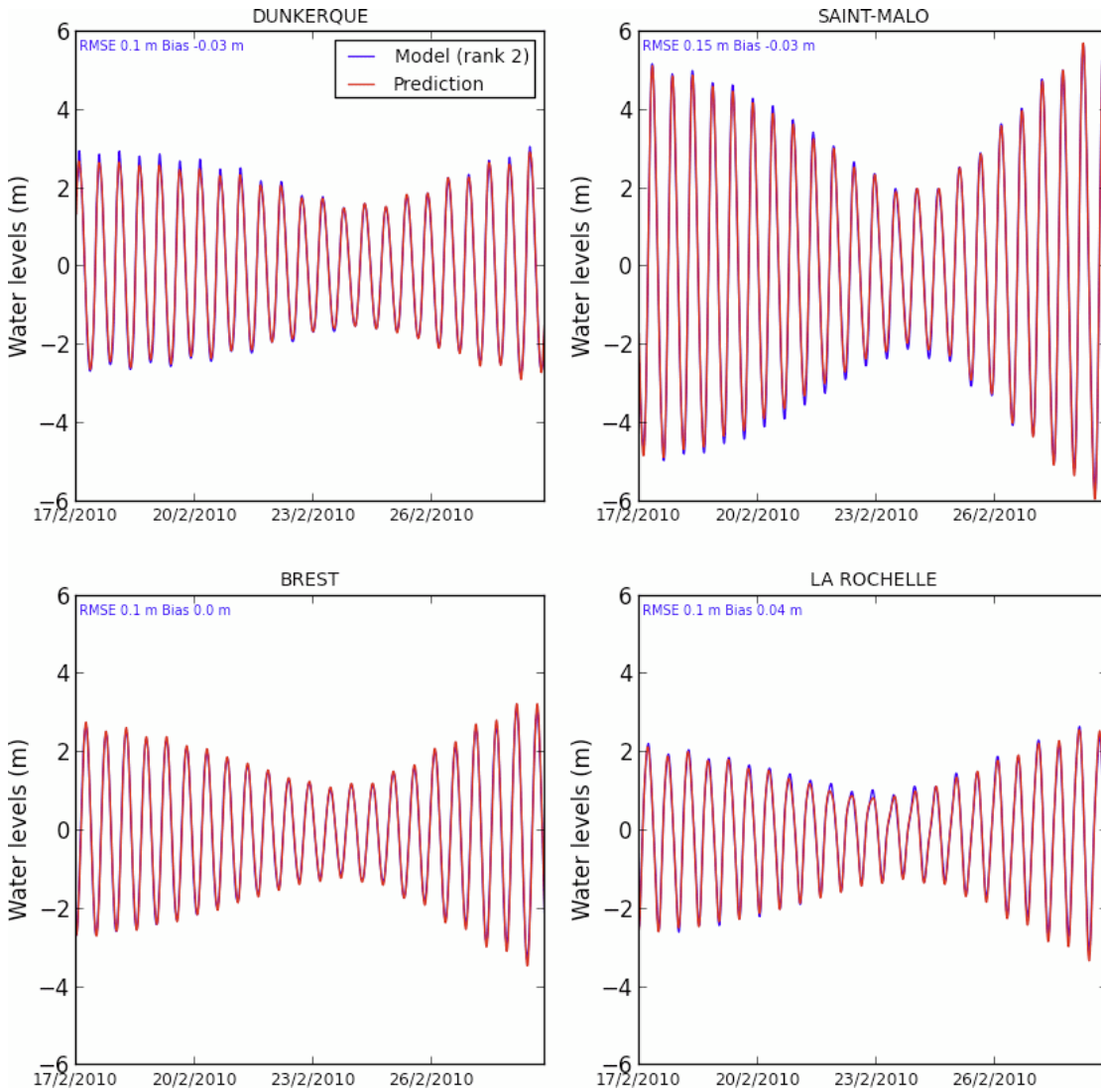


Figure 5: Comparison between modelled tide from rank 2 (without meteo) and predicted tide from observation at Dunkerque, Saint-Malo, Brest and La Rochelle, from 17 to 28th February 2010.

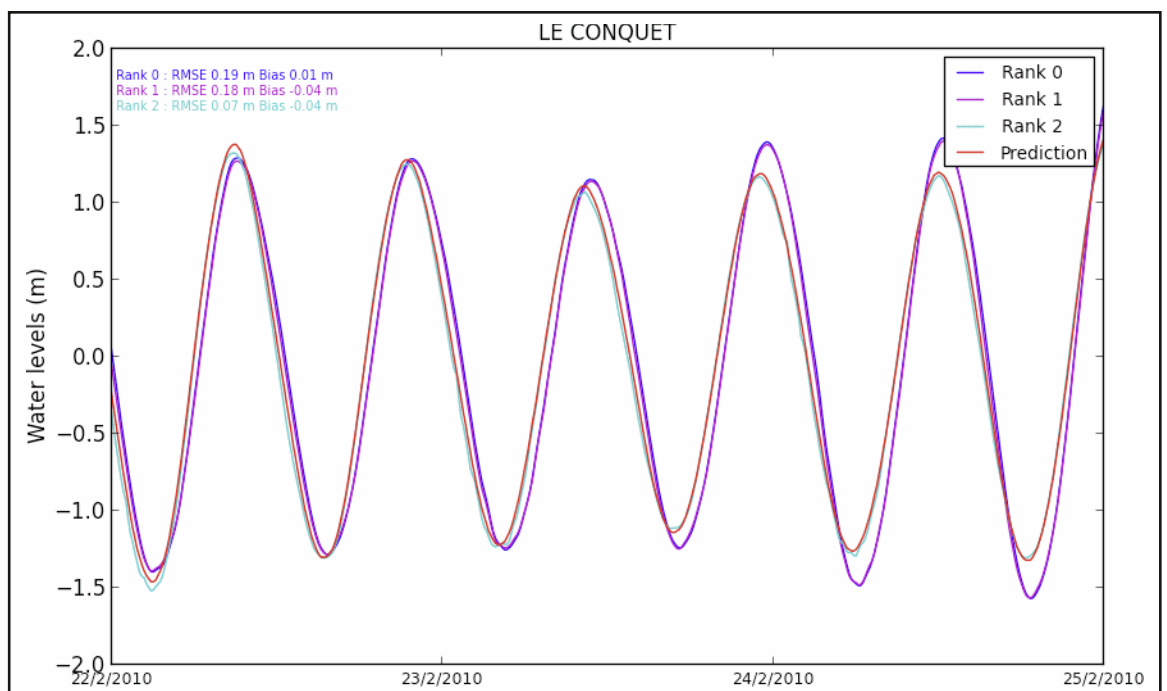
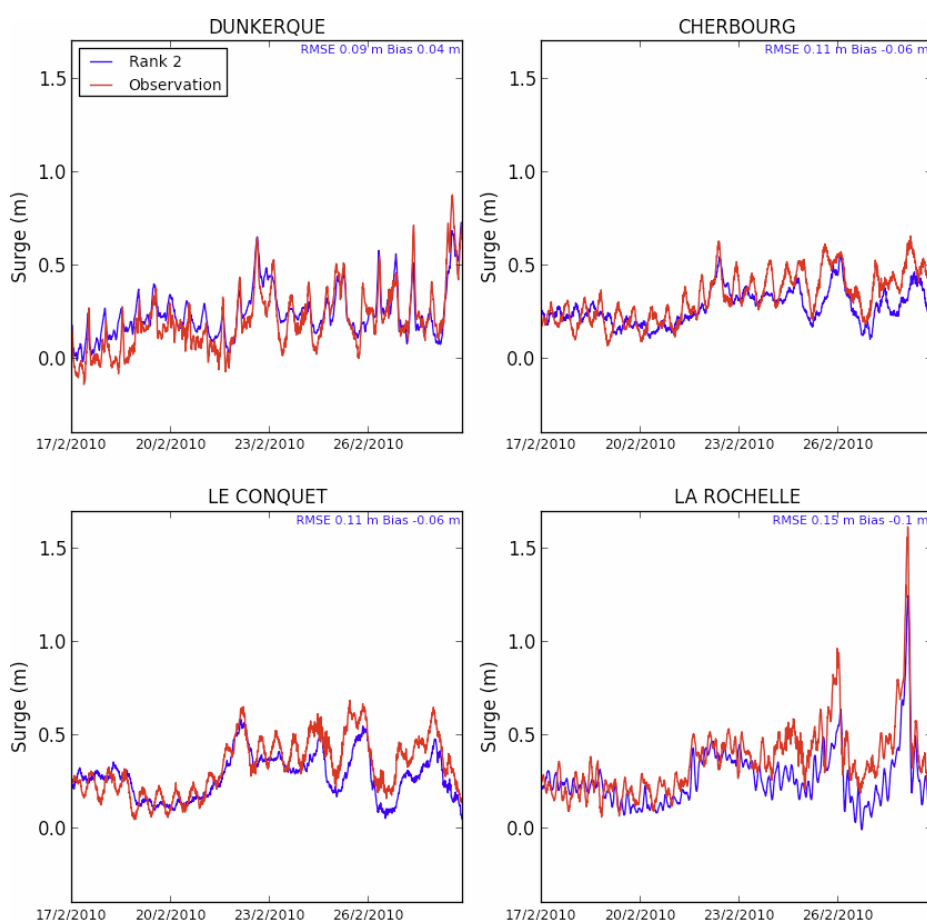


Figure 6: Comparison between modelled tide from rank 0, 1 and 2 models (without meteo) with predicted tide from observation at Le Conquet, from 22nd to 25th February 2010

The total sea levels (including tide and surge) have been validated by comparing modeled sea levels (from simulations with tide and meteorological forcing) with observations at 18 points presented figure 4 (no observations available at Boulogne-sur-mer). RMS errors are on average of 26 cm for rank 0, 24 cm for rank 1 and 16 cm for rank 2 models; biases are on average of -5 cm for ranks 0 and 1, and -7 cm for rank 2 models. Improvement of sea levels at rank 2 comes mainly from tide improvement (explained before).

Surges have been validated by comparing modeled surges (difference of simulations with and without meteorological forcing) with observed surges (differences between tide gauges observations and predictions) at 18 points. An example of validation figure is presented figure 7, at Dunkerque, Cherbourg, Le Conquet and La Rochelle. RMS errors and biases are the same for the three ranks: 13 cm and -8 cm. This result shows that the improvement of spatial resolution does not allow improving significantly surges modeling; surges from these 3 ranks are very similar, even if a small improvement is noticed on rank 2 models. Globally, modeled surges are inferior to measured ones, with a mean bias of 8 cm. This can be explained by the parameterization (drag coefficient can still be improved, see above), but also by wave set-up, which is not modeled here, and is far from being negligible – from few centimeters up to several tens of centimeters in the total surge (Idier *et al.* 2012, Bertin *et al.* 2012), depending of the site configuration.

Figure 7: Comparison between modelled surge from rank 2 model and observed surge at Dunkerque, Cherbourg, Le Conquet and La Rochelle, from 17 to 28 February 2010



Comparisons have been made between the old operational model used in the PREVIMER system (rank 0, 5.6 km, forced with Arpege, constant drag coefficient of 0.0016) and the new one (rank 0, 2 km, forced with Arpege HR, variable Charnock formulation for drag coefficient). RMS errors and biases have been computed for the January 2012 period. RMS errors of water levels are, on average, improved, with a reduction from 40 cm to 22 cm. Surges modeling is not significantly improved, with similar RMS errors on average of 9 cm; however, peak storm surges are really improved with differences up to 25 cm (162 cm instead of 127 cm in Dunkerque) (cf Table 2).

Location	Water levels RMSE		Surges RMSE		Maximal surges		
	Old model	New model	Old model	New model	Old model	New model	Observation
Dunkerque	40 cm	18 cm	14 cm	11 cm	<b>127 cm</b>	<b>162 cm</b>	193 cm
Saint-Malo	43 cm	29 cm	8 cm	9 cm	<b>32 cm</b>	<b>61 cm</b>	63 cm
Le Conquet	50 cm	17 cm	5 cm	5 cm	<b>11 cm</b>	<b>17 cm</b>	27 cm
La Rochelle	26 cm	23 cm	7 cm	10 cm	<b>14 cm</b>	<b>37 cm</b>	31 cm
<b>Mean</b>	<b>40 cm</b>	<b>22 cm</b>	<b>9 cm</b>	<b>9 cm</b>			

Table 2: Water levels and surges RMS errors and maximal surges for old operational model and new one (in production since 2013) – Computed for the January 2012 period

Finally, tidal currents have been validated by comparing modeled mean spring tide currents (from simulations without meteorological forcing, the 27<sup>th</sup> of February 2010, tidal coefficient of 94) with observations (tidal currents in mean spring tide), provided by SHOM (locations on figure 8). Tidal roses have been plotted. Examples of current validation figures are presented figures 9 and 10. They show quite good correlation between model and observations.

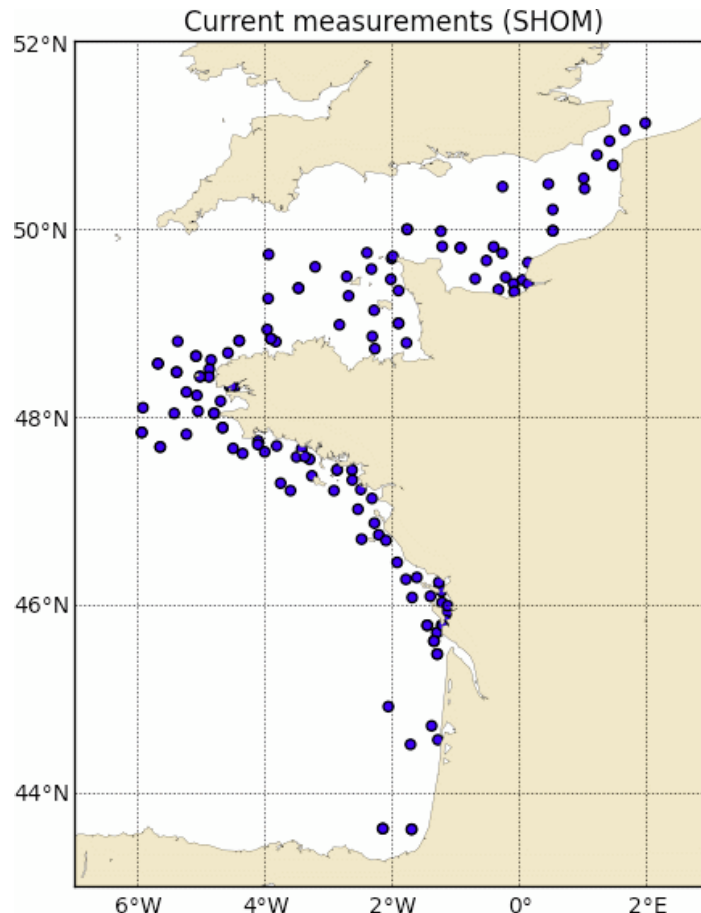


Figure 8: Current measurements location provided by French Hydrographic Office (SHOM)

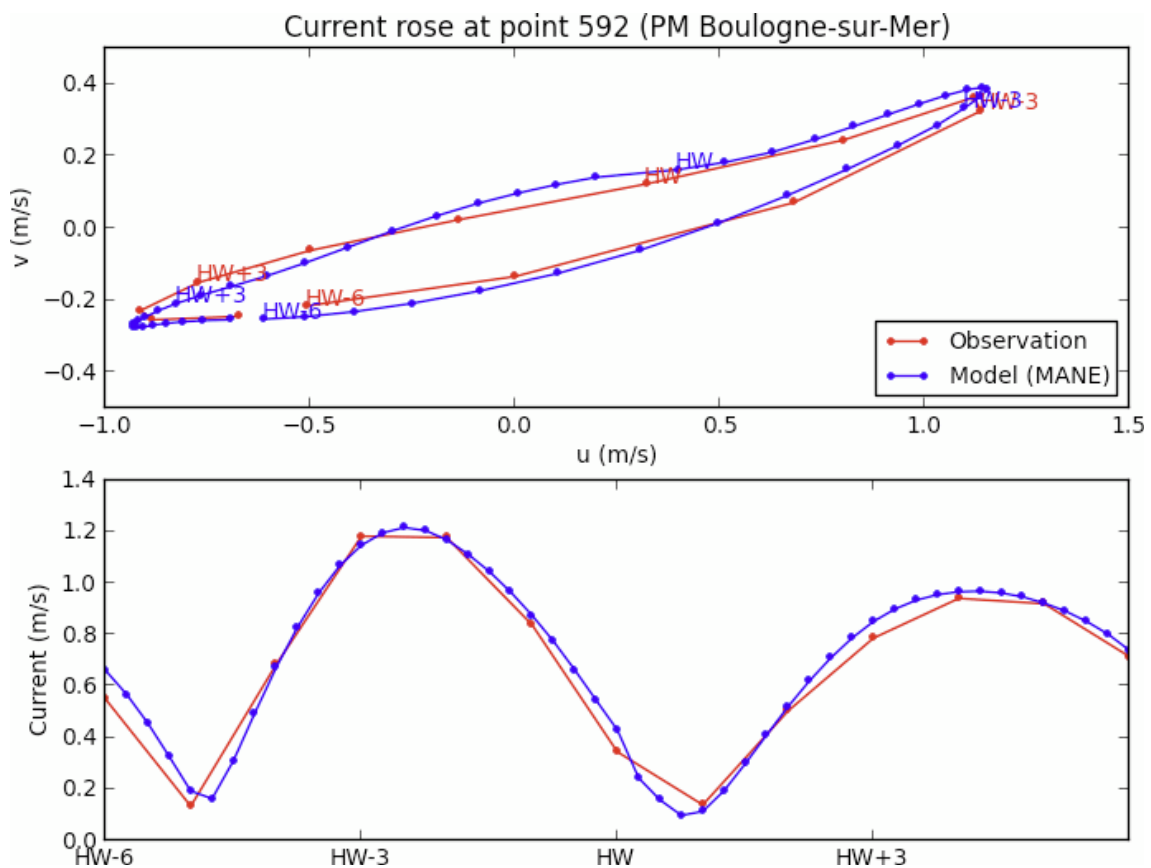


Figure 9: Comparison between modelled and observed mean spring tide currents and observed at point 592 in Eastern Channel

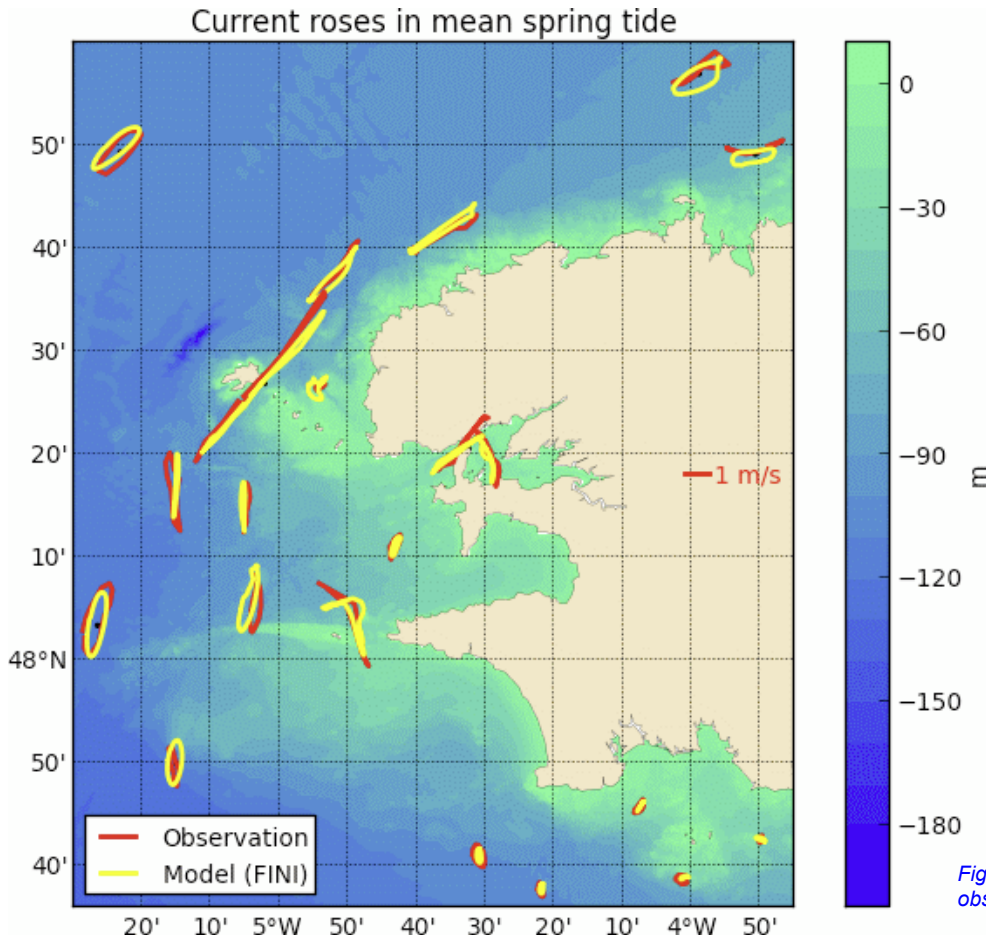


Figure 10: Comparison between modelled and observed current roses in mean spring tide

## Results

The operational model is in production since 2013. Every day, MARS simulations are made from the day before up to 4 days in advance (simulation over 5 days). Charnock coefficients are issued from PREVIMER WAVEWATCHIII® operational configuration. 14 simulations are computed (7 models with and without meteorological forcing in order to compute surges) on 64 processors. The data volume represents daily 15Go (for 5 days simulation), a year represents 1.2 To. Hindcasts have been computed from 2006. Data are used by many users: Ifremer for its own needs (detailed in introduction), but also PREVIMER partners like Meteo-France to access to modeled surges, CEREMA (ex CETMEF) for harbour management, or external users like private companies for studies on renewable marine energy or water quality. The website [www.previmer.org](http://www.previmer.org) shows historical and real-time results, but also comparisons between models and measurements. As illustrations of the PREVIMER system outputs, surges at Brest and Calais during Petra storm (4<sup>th</sup> of February 2014) are presented figure 11, whereas currents in Iroise Sea are presented figure 12.

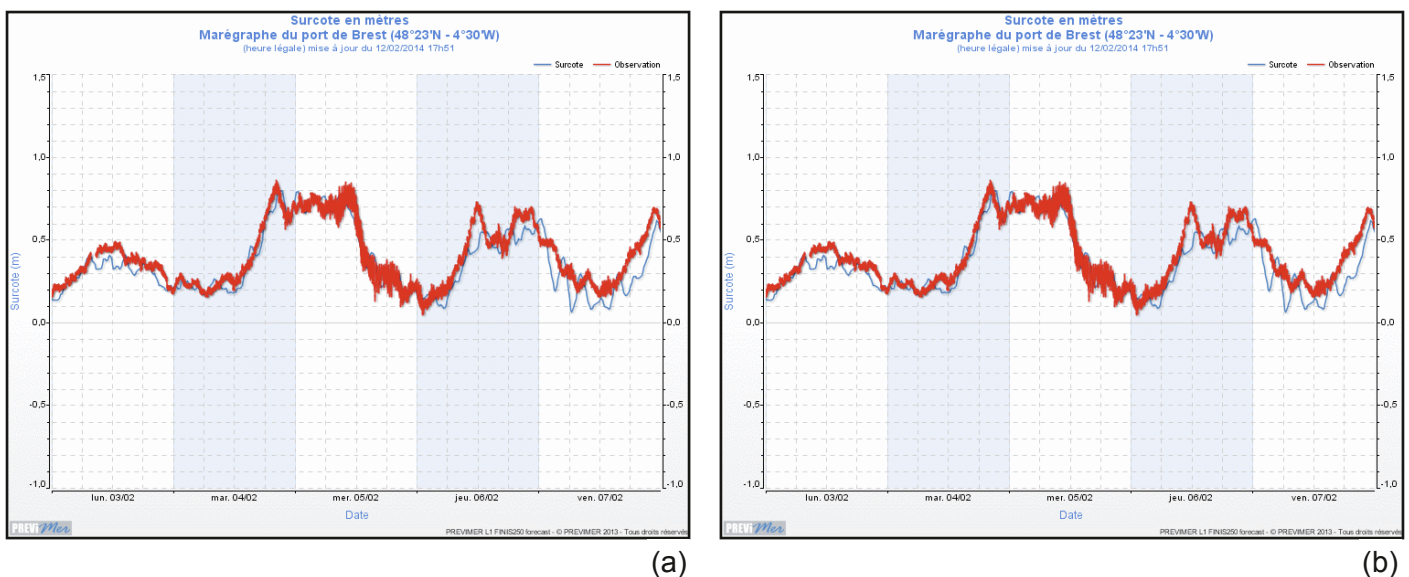


Figure 11: PREVIMER website [www.previmer.org](http://www.previmer.org): comparison between modelled and observed surges at Brest (a) and Calais (b) from 3 to 7th February 2014

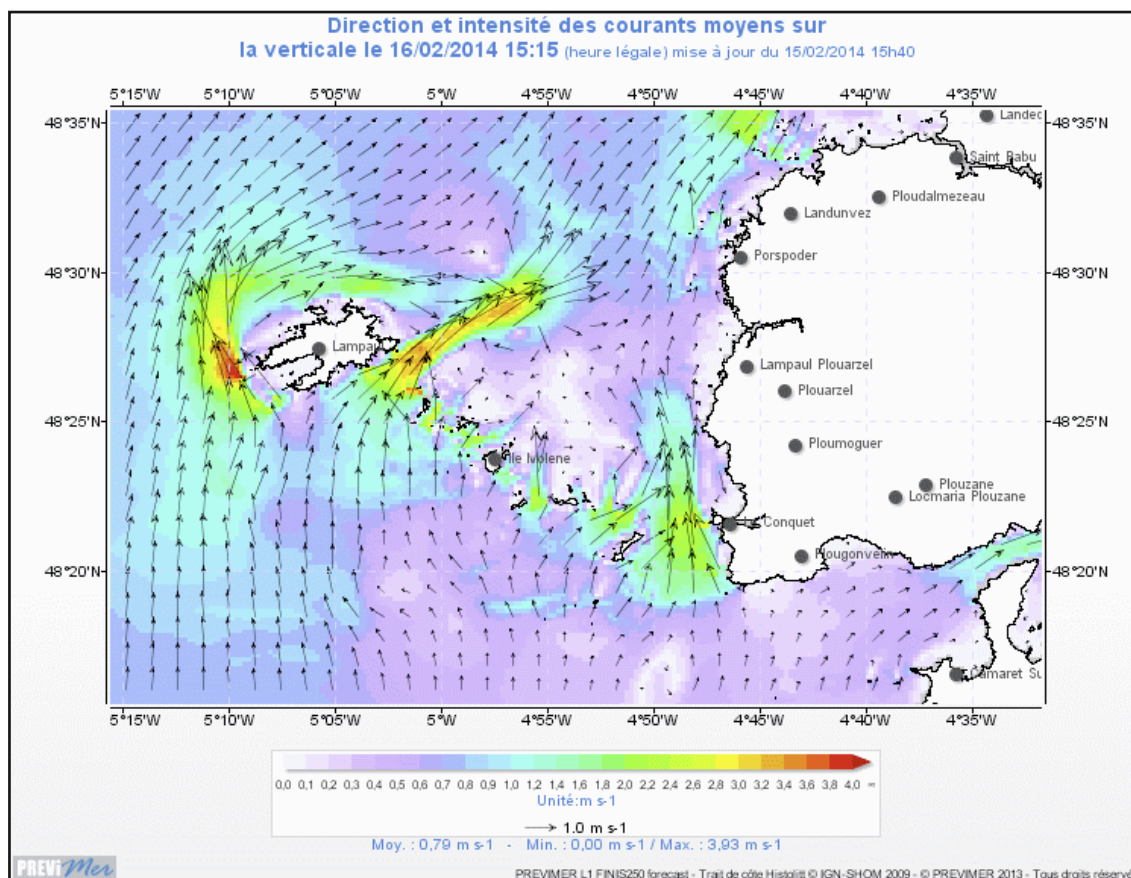


Figure 12: PREVIMER website [www.previmer.org](http://www.previmer.org): currents in Iroise sea the 16th of February 2014 at 15:15

## Conclusion

Sensitivity studies showed the influence of temporal and spatial meteorological forcing in storm surge modeling. Modeled surges have also been improved taking into account a better parameterization of surface drag coefficient. Wave effects on sea surface roughness is taken into account through a Charnock formulation, with a Charnock parameter variable and issued from PREVIMER wave models (WAVEWATCH III®). This parameterization allows improving peak surges, through an error reduction up to around 20 cm.

New parameterization (better space resolution, meteorological forcing and surface drag parameterization) has clearly improved results, dividing by two RMS errors of the water levels on rank 0 model. For rank 2 models, RMS errors for water levels are on average of 11 cm, and biases are null, which is satisfying. Concerning surges, the improvement of space resolution between rank 0 (2km) and rank 2 (250 m) did not allow improving significantly results. Main improvements came from surface drag parameterization and better meteorological forcing.

However, models still underestimate surges. A perspective is the improvement of Charnock parameter: the particular parameterization of the wave model (Raschle and Arduin 2013) improves short wave properties, but removes most of the wave-induced variability in the Charnock coefficient, and limits in our case the impact on results. Another improvement will be to take into account wave setup (surge due to wave breaking). This process is generally not taken into account in (pre-)operational coastal modeling systems, but its effect is far from being negligible, up to several tens of centimeters in the total surge (Idier *et al.* 2012, Bertin *et al.* 2012), especially on open coast (eg. Aquitanian coast) or basins (eg. Arcachon basin) sites; it can represent in some area, as Aquitaine coast, 50% of surge (Idier *et al.* 2012). This wave setup can be computed with a wave-current coupling model, or with a wave model, taken into account water level and currents, and then added to the atmospheric surge issued from the circulation model.

## Acknowledgements

The authors wish to thank SHOM for sea levels and currents data furniture and Météo-France for meteorological models furniture. They also would like to thank participants to PREVIMER surge steering committee (Ifremer, BRGM, SHOM, Météo-France).

## References

- Ardhuin, F., Rogers, E., Babanin, A. V., Filipot, J., Magne, R., Roland, A., van der Westhuysen, A., Queffelec, P., Lefevre, J., Aouf, L., and Collard, F. 2010: Semi empirical Dissipation Source Functions for Ocean Waves. Part I: Definition, Calibration, and Validation. *J. Phys. Oceanogr.*, 40, 1917–1941, doi:10.1175/2010JPO4324.1. 2418, 2425, 2431, 2441.
- Bertin, X., Bruneau, N., Breilh, J.-F., Fortunato, A.B., and Karpytchev, M. 2012: Importance of wave age and resonance in storm surges: The case Xynthia, Bay of Biscay. *Ocean Modelling*, vol. 42, pp 16–30. doi:10.1016/j.ocemod.2011.11.001
- Boudière, E., Maisondieu, C., Ardhuin, F., Accensi, M., Pineau-Guillou, L. and Lepasqueur, J. 2013 : A suitable metocean hindcast database for the design of Marine energy converters. *International Journal of Marine Energy*, 3-4, e40-e52. <http://dx.doi.org/10.1016/j.ijome.2013.11.010>.
- Charnock, H. 1955: Wind stress on a water surface. *Quart. J. Roy. Meteor. Soc.*, 81,639–640.
- Courtier, P., Freyrier, C., Geleyn, J.-F., Rabier, F. and Rochas, M. 1991: The ARPEGE project at Météo-France. In *ECMWF 1991 Seminar Proceedings: Numerical methods in atmospheric models; ECMWF, 9 - 13 September 1991, Vol. II*, 193-231.
- Courtier, P., Thepaut, J. and Hollingsworth, A. 1994: A strategy for operational implementation of 4D-VAR, using an incremental approach. *Q J R Meteorol Soc* 120:1367–1387.
- Idier, D., Muller, H., Pedreros, R., Thiébot, J., Yates, M., with collaboration of Créach, R., Voineson, G., Dumas, F., Lecornu, F., Pineau-Guillou, L., Ohl, P. and Paradis, D. 2012 : Système de prévision de surcotes en Manche/Atlantique et Méditerranée : Amélioration du système existant sur la façade Manche/Gascogne [D4]. Final report BRGM/RP-61019-FR, 165 p..
- Lazure, P., and Dumas, F. 2008: An external-internal mode coupling for a 3D hydrodynamical model for applications at regional scale (MARS). *Advances In Water Resources*, 31(2), 233-250.
- Lyard, F., Lefèvre, F. and Letellier, T., Francis, O. 2006: Modelling the global ocean tides: modern insights from FES 2004. *Ocean Dynamics* 56 (5-6), 394-415.
- Makin V. K. 2005: A note on the drag of the sea surface at hurricane winds. *Boundary-Layer Meteorol.*, 115, 169-176.
- Muller, H., Pineau-Guillou, L., Ardhuin, F. and Idier, D. 2014 : Atmospheric storm surge modeling methodology along the French (Atlantic and English Channel) coast. *Ocean Dynamics*, accepted (major corrections).
- Moon, I.-J., Ginis, I., Hara, T. and Thomas, B. 2007: A Physics-based parameterization of air–sea momentum flux at high wind speeds and its impact on hurricane intensity predictions. *Mon. Wea. Rev.* 135, 2869–2878.
- Pineau-Guillou, L., Lathuilière, C., Magne, R., Louazel, S., Corman, D. and Perherin, C. 2012a : Sea levels analysis and surge modelling during storm Xynthia. *European Journal Of Environmental And Civil Engineering*, 16(8), 943-952. <http://dx.doi.org/10.1080/19648189.2012.676424>
- Pineau-Guillou, L., Theetten, S., Dumas, F., Lecornu, F. and Idier, D. 2012b : Prévision opérationnelle des niveaux de la mer, surcotes et décotes sur les côtes de la Manche et de l'Atlantique. *XXIIèmes Journées Nationales Génie Côtier – Génie civil. Proceedings*, pp. 957-964. DOI:10.5150/jngcgc.2012.105-P
- Pineau-Guillou, L. 2013: PREVIMER Validation des modèles hydrodynamiques 2D des côtes de la Manche et de l'Atlantique. Ifremer report, 115pp.
- Rasclé, N. and Ardhuin, F. 2013: A global wave parameter database for geophysical applications. Part 2: model validation with improved source term parameterization, *Ocean Modelling*, 70, 174–188.
- Seity, Y., Brousseau, P., Malardel, S., Hello, G., Bénard, P., Bouttier, F., Lac, C. and Masson, V. 2011: The AROME-France convective scale operational model. *Mon Wea Rev* 139:976–991.
- Simon B. 2007 : La marée océanique côtière, Oceanographic Institute Editions, Paris, 433pp.
- Tolman H.L. 2008: A mosaic approach to wind wave modeling. *Ocean Modelling*, 25, pp 35-47.
- Tolman, H. L., Banner, M. L. and Kaihatu, J. M. 2013: The NOPP operational wave model improvement project,” *Ocean Modelling*, 70, 2–10.
- Wu, J. 1982: Wind-stress coefficients over sea surface from breeze to hurricane. *J. Geophys. Res.* 87, p. 9704-9706.

# NUMERICAL WAVE MODELING IN PREVIMER: MULTI-SCALE AND MULTI-PARAMETER DEMONSTRATIONS

By F. Ardhuin<sup>(1,2)</sup>, M. Accensi<sup>(1)</sup>, A. Roland<sup>(3)</sup>, F. Girard<sup>(4)</sup>, J.-F. Filipot<sup>(2,5)</sup>, F. Leckler<sup>(2)</sup>, J.-F. Le Roux<sup>(6)</sup>

<sup>1</sup>IFREMER/LOS, Brest, France

<sup>2</sup>SHOM/HOM, Brest, France

<sup>3</sup>Technical University of Darmstadt, Germany

<sup>4</sup>Actimar, Brest, France

<sup>5</sup>France Energie Marine, Brest, France

<sup>6</sup>IFREMER/DYNECO, Brest, France

## Abstract

Since 2006, PREVIMER has provided a unique context for testing and demonstrating new capabilities in terms of numerical wave modelling. These include three aspects: the development of physical parameterizations, numerical schemes on triangular meshes, and the extension of wave model use to new applications ranging from seismology to remote sensing, besides the more traditional marine forecasting, ocean and coastal engineering. All these features are now contained in the new version 4.18 of WAVEWATCH III that has just been released. On the parameterization side, the participation to the JCOMM wave verification exercise has led to the rapid demonstration of improved performance compared to other systems, including ECMWF. This has led to parameterization changes in operational centers, at Meteo-France, NOAA/NCEP and even ECMWF. On the numerics the use of residual distribution schemes on triangular meshes has allowed a seamless integration of the wave action equation from the global scale to the nearshore scale, with the French mainland coastline now resolved at 300 m, including forcing by the barotropic currents provided by PREVIMER. In turn the wave models provide important output for sediment dynamics and wind stress parameterizations. These are two examples of a broader multi-parameter demonstration. Over the coming years we will rise to the challenge of "surf-zone resolving" models, while enriching the physics of wave evolution, and broadening the spectrum of accurate model results.

## Introduction: why did we put waves in PREVIMER?

The main goal of PREVIMER was to demonstrate an operational oceanographic system with services to both the private sector and the general public (figure 1).

In 2005, few forecasting centers catered for small scales variations of the waves that matter to activities ranging from fishing and aquaculture to water sports. Puertos del estado, with its historical focus on harbors, had a distributed system with harbor approaches covered by SWAN configurations forced by their basin-scale WAM model (Gomez and Carretero 2005). In France, Meteo-France was only following the resolution of the atmospheric models, around 10 km at that time. Given the many islands that are 10 to 20 km away from the shoreline, such a coarse model did not resolve the variability of waves on the coast for most of the French coasts. Our first driver was thus resolution.

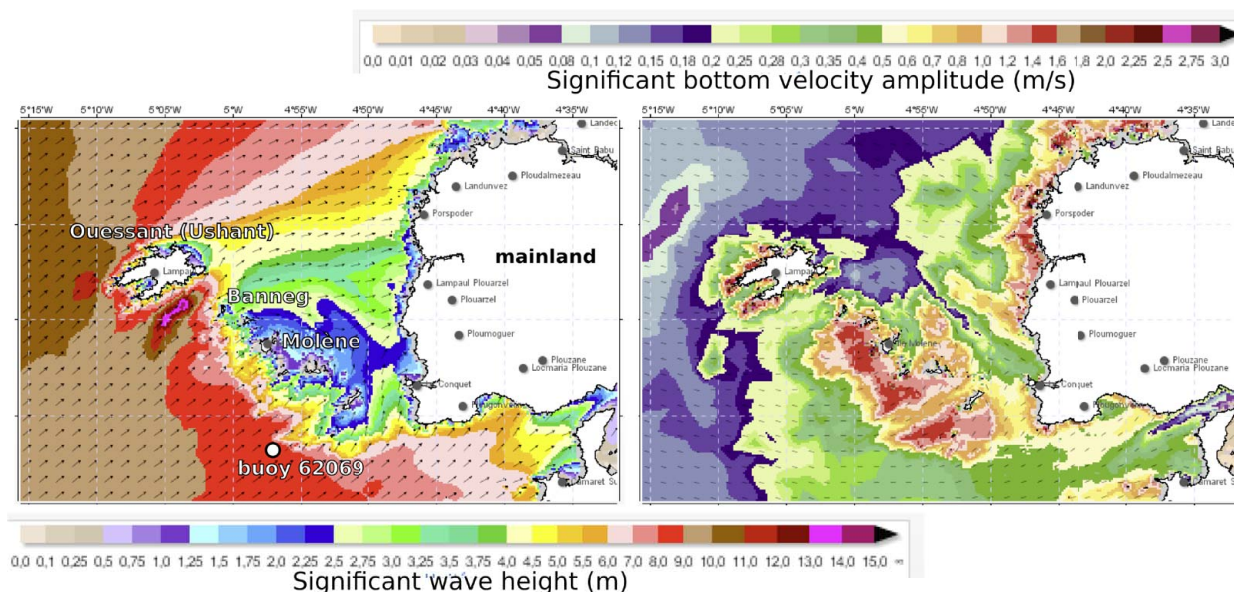


Figure 1: Example of two different sea state parameters modeled in the Previmer system: left, wave height, and right, bottom agitation. This snapshot corresponds to the peak of the Ulla storm, at 21 UTC on February 14, 2014. The offshore wave height was underestimated by 15%, in line with global-scale biases for high waves using uncorrected ECMWF winds (Rascle and Ardhuin 2013)... which highlights the need for a wind bias correction. The strong amplification of wave height in the Fromveur passage between Ouessant and Molène is caused by tidal currents (see Ardhuin et al. 2012). This is obtained with a triangular mesh using WAVEWATCH III, which replaced the regular grid SWAN models on October 21, 2009. This "Iroise" grid is now due for replacement, taking advantage of the detailed bathymetry data now available from SHOM and Ifremer with the support of the Brittany regional council and the Iroise Marine Natural Park (<http://www.parc-marin-iroise.com/>). Wave information at high resolution is needed to better understand coastal inundation and damage, or the dynamics of kelp beds.

The second driver was the forcing and the importance of currents for wave forecasting. Although this is often ignored in national centers that focus on global and regional scales, it is an obvious question for anyone living on the coast, in particular in Brittany. Building on the research funding provided as part of the ECORS project by the French Procurement Agency (DGA), the impact of currents on waves led us to work on parameterizations that would provide a reasonably steepness-induced breaking, and reproduce the measured modulations of waves over currents which are due to several factors (Arduin et al. 2013), and that can lead to a doubling of the wave height at some phase of the tidal cycle, as shown in figure 2.

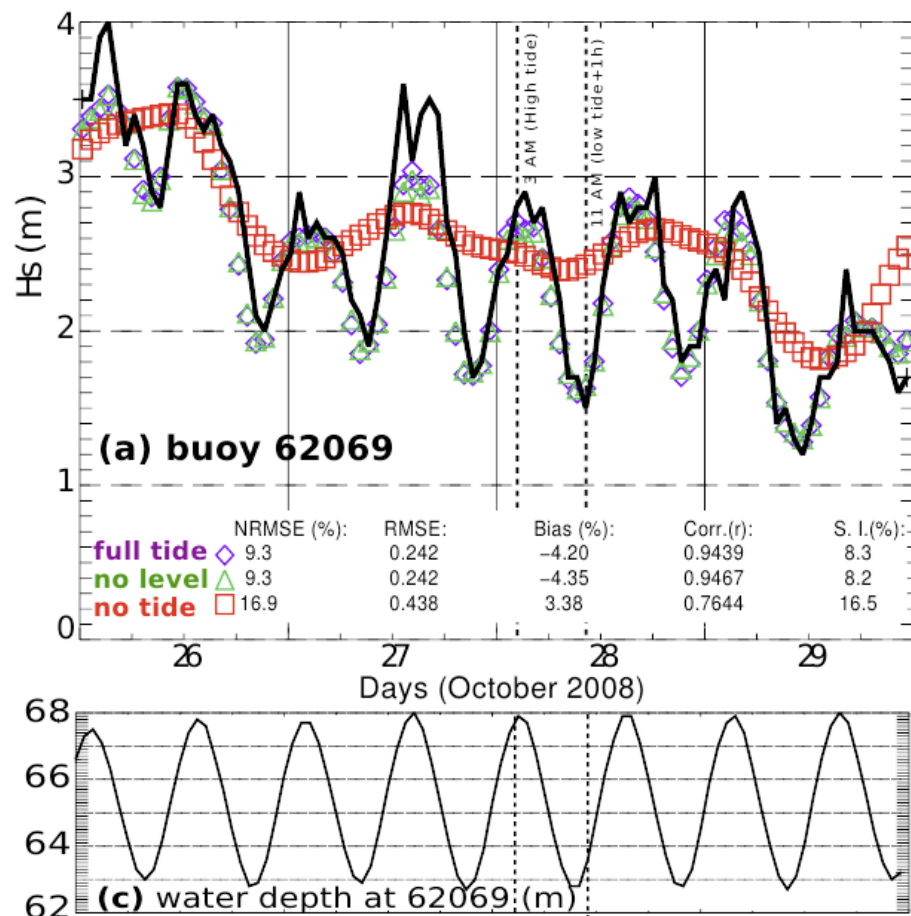


Figure 2: Observed (solid line) and modeled wave heights at the buoy (a) 62069 from October 26 to 29, taking into account both water levels and currents (full tide, blue diamonds), only the currents (no level, green triangles), or no tidal effects at all (no tide, red squares, meaning that the water level is fixed and the currents are set to zero). (c) Modeled water level at 62069. Error statistics correspond to the data shown on the figure. (Adapted from Arduin et al. 2012). See figure 1 for the buoy location. The purchase of this buoy was funded by the Previmer project.

This update of the model parameterization for dissipation, together with large-scale estimation of swell dissipation from satellite radar data (Arduin et al. 2009) lead to a large improvement in model performance at global scale which directly provided better coastal results. First tested in the WAVEWATCH III code ran in Previmer, and adopted by NOAA/NCEP in 2012, the new parameterization has quickly been ported to WAM at Météo-France, and is now tested at ECMWF in the framework of the MyWAVE project. The capability to demonstrate performance in PREVIMER was a key asset in making this quick transition from research to operations.

The third driving question was: what will people use wave information for, what kind of product do they need? That question proved irrelevant as soon as we started getting feedback from surfers happy to cut on their driving, finding the best spot for the day's wave-wind-tide combination, or fishermen who could for the first time see the island shadow in the lee of islands (see figure 1) and plan the deployment and retrieval of crab traps accordingly, or kayakers, or scuba divers ... The question was rather turned into: what is all the relevant and accurate information that we can squeeze out of a wave model? ... People will find their own use for it. As a result we did not try to favour one type of usage compared to another. While early model output focused on the usual significant wave height and direction, the number of output parameters was increased to include air-sea flux parameters relevant for upper ocean modelling (air-side Charnock parameter, energy flux to the ocean), bottom parameters (displacements and velocities as shown on figure 1, which are also visible on the PREVIMER web page), and a large range of sea state parameters (wind sea and swells partitions...). Another important output of the model has been full wave spectra, needed for boundary conditions in higher resolution models set up by users or partners of the project. One example is the LOREA project (Dugor et al. 2010), with an output integrated into the PREVIMER web site.

## Multi-scale

Since running a global ocean wave model is relatively cheap compared to the coastal models, and because we were planning from the start to cover French overseas region and other regions of interest for model validation, PREVIMER started off with a nested series of models from the global scale to the local scale, initially using SWAN at 200 m resolution around the Brest area, nested into WAVEWATCH III at resolutions of 3 to 50 km. This was modified in 2009 to take advantage of developments on unstructured grid modelling in WAVEWATCH III (Arduin et al. 2009, Roland and Arduin 2014). That approach proved to be faster, more efficient, and more accurate. Every day, twice a day, the following models are run on the Caparmor cluster located in Brest, an ICE 8200 EX SGI, based on Intel Xeon X5560 quad core at 2.8 GHz. Each forecast cycle (from -12 hours to +6 days) use about 3 hours on 256 processors. The following configurations are used:

- global multi-grid:  $0.5^\circ$  global +  $1/6^\circ$  on the margins of the Americas (both Pacific – including Hawaii - and Atlantic + Gulf of Mexico),  $1/20^\circ$  over New Caledonia, Tuamotus and West Indies,  $1/30^\circ$  over the Southern North sea and Bay of Biscay. All these domains are two-way
- Mediterranean multi-grid:  $1/10^\circ$  for the Mediterranean and Black sea,  $1/30^\circ$  around the French coasts.
- Several stand-alone triangular meshes with typical resolutions of 300 m at the coast: 110 k nodes for the Channel and Bay of Biscay, 12 k nodes for the "Iroise Sea", 55 k nodes for the French Mediterranean coast, 25 k nodes for the French West Indies. (Figure 3).

Work is under way to

- Add an Arctic grid (12 km polar stereographic grid), this will also reduce the overall cost of the global multi-grid system by allowing larger time steps on the "pseudo-refraction" caused by the turning of great circles in a longitude-latitude grid. This will also provide the opportunity to add zooms around Svalbard to support Arctic research activities.
- Replace the Iroise mesh with a much finer mesh with 30 k nodes or more to demonstrate new model capabilities.

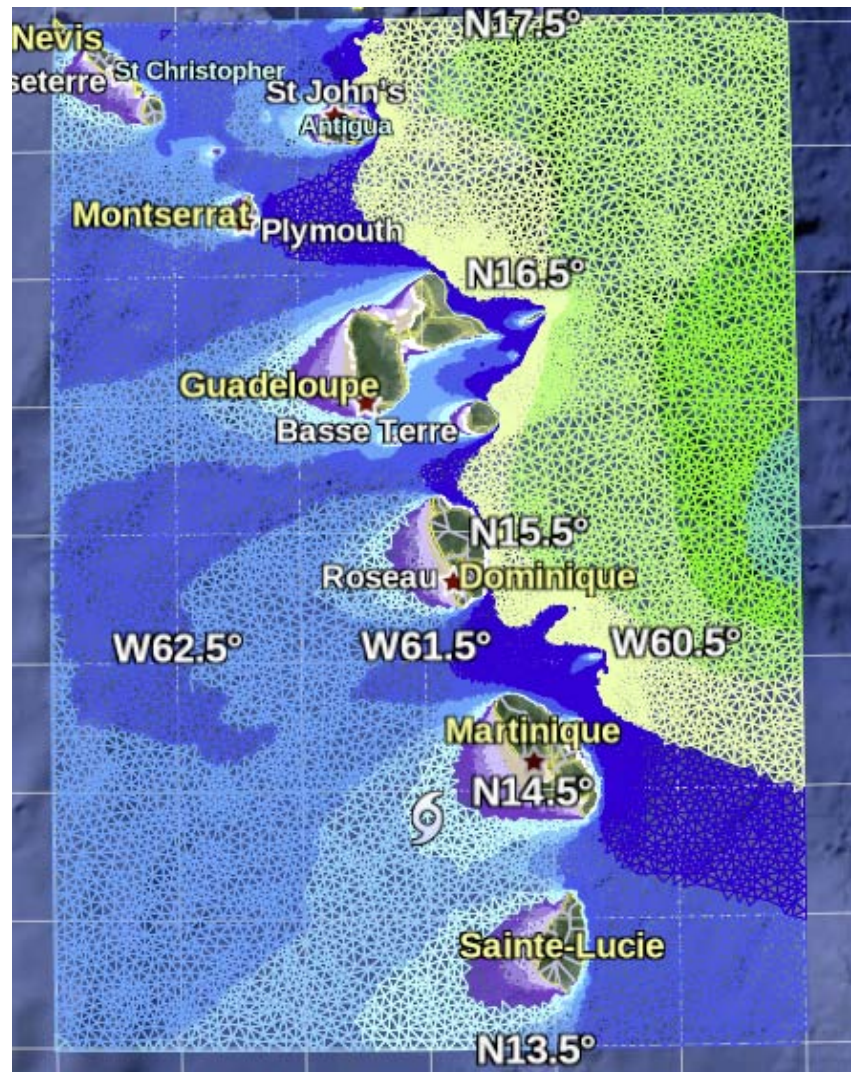


Figure 3: The first real-time output of the new West Indies Mesh, just in time for Tropical Storm Chantal on July 9, 2013. See Figure 1 for wave heights associated to the color scale. The output of that model should be available shortly on the Previmer web pages.

At present, one of the limitations in coastal applications are the very different space and time scales in and around surf zones, making it difficult to go to resolutions below 100 m while still covering a large area. The present approach is that people that really want the high resolution will set up their own system to do so, which is a common practice for impact studies. However, with data available at 300 m resolution covering up to 20 years (e.g. Boudière et al. 2013), the paradigm of impact study may be shifting with more focus on the transfer functions from the waves to their impact, rather than on running the wave models. Statistical downscaling method can also be used successfully to refine to the desired scale (e.g. Gutierrez et al. 2013). Efforts are ongoing as part of the French Department of Defense program PROTEVS (ran by SHOM) to go around the limitations deterministic wave models. PREVIMER will be, again, a good framework to demonstrate this kind of new capability.

## Multi-parameter for multiple applications

A wave model generally computes wave-related parameters that can be derived from the spectrum, but it can also provide fluxes of energy and momentum that are forcing terms for the ocean circulation. Coastal dynamics have been known to be largely forced by waves since the pioneering work of Longuet-Higgins and Stewart (1964), and the complexity of three-dimensional wave-forced flows in the nearshore (e.g. McWilliams et al. 2004, Arduin et al. 2008, Bennis et al. 2011) is only being addressed now (e.g. Michaud et al., 2012, Delpy et al. 2014). At the same time, the importance of ocean waves is now also recognised for their geophysical effects, either in defining the air-sea momentum and energy fluxes with a controlling influence on weather prediction (Janssen et al. 2002) and upper ocean dynamics (Rascle and Arduin 2009).

The support of the ERC and ONR for the IOWAGA and Wave-DB projects have been the occasion to expand the wave model output, outside of PREVIMER, towards seismic noise sources, whitecap properties (not very successfully yet) and surface slope variances. Maps of sea surface slope variance from PREVIMER are ingested daily by NASA to help the analysis of Aquarius brightness temperatures in terms of wind and salinity, and will be used for the planning of the CYGNSS mission. We could imagine similar uses for the correction of sea-state biases in space-borne altimeter range measurements (Tran et al. 2010), or direct measurements of surface current from Doppler in radar systems (Chapron et al. 2005), which will be first provided routinely by the soon to be launched Sentinel-1. PREVIMER will provide wave model output as ancillary data and for the validation of wave and current products from Sentinel-1.

The confrontation of “exotic modeled parameters” to observations, such as acoustic noise sources, has been a very effective method for detecting deficiencies in the wind-wave generation and dissipation terms (Rascle and Arduin 2013, Arduin et al. 2013), and we are every year finding new ways to use the model output. Surely other users will find even more, which is why we are making every effort to make the model output as comprehensive and easily accessible as possible. A recent example is the extension of a forecasting capability towards the very long 30s to 5 minute period “infragravity waves” (Arduin et al. submitted) that are very important for coastal hazards (e.g. Sheremet et al. 2014), and can be an important signal in the coastal sea level variability at scales of a few kilometers. This could be an interesting aspect to include ongoing efforts to enhance warning systems for high waves at the coast.

## Conclusion and perspectives

Because the developments of wave models used in PREVIMER have been performed thanks to other projects funded by DGA, ERC and ONR, they have tended to favor many different applications besides the simple demonstration of a coastal operational oceanographic system. At the same time, the routine operation and confrontation to observations has made it easier to detect bugs – and there were many – in the algorithms and model configurations. PREVIMER has also been a way to reach out to the public and push operational centers to improve on their model performance. The many researchers that use our output for mapping benthic habitats or geomorphologic changes also show that routine wave hindcasts are a very useful tool for the academic community. These multiple uses will eventually lead to improved model performance because they provide many more constraints on the quality of the output. In the short run, however, the performance for one particular application may not be optimal. For example we are well aware that our predicted air-side roughness – in the form of the Charnock parameter – is lacking most of the expected variability with wave age, which is not so good for driving a storm surge or ocean circulation model. This and an overestimation of energy for the high frequencies are important items that should be looked at.

## Acknowledgements

The authors wish to thank all contributors to the PREVIMER project, including support on the Nymphaea and Caparmor clusters, measurements at sea provided by many including CETMEF and SHOM, and generous funding from ERC for the IOWAGA project, ONR for the Wave model improvement project, and CNES through the ALTIBERG and IGALTI projects.

## References

- Ardhuin F., Marié L., Rasclé N., Forget P., and Roland A., 2009: Observation and estimation of Lagrangian, Stokes and Eulerian currents induced by wind and waves at the sea surface," *J. Phys. Oceanogr.*, 39(11), 2820–2838.
- Ardhuin, F., Rasclé, N., and Belibassakis, K. A., "Explicit wave-averaged primitive equations using a generalized Lagrangian mean, 2008: *Ocean Modelling*, 20, 35–60.
- Ardhuin, F., Lavanant, T., Obrebski, M., Marié, L., Royer, J.-Y., d'Eu, J.-F., Howe, B. M., Lukas, R., and Aucan, J., 2013: A numerical model for ocean ultra low frequency noise: wave-generated acoustic-gravity and Rayleigh modes, *J. Acoust. Soc. Amer.*, 134, 4, 3242–3259.
- Ardhuin, F., Rawat, A., and Aucan, J., in revision: A first generation infragravity wave model: definition and validation at regional and global scales," *Ocean Modelling*.
- Bennis, A.-C., Ardhuin, F., and Dumas, F., 2011: On the coupling of wave and three-dimensional circulation models : Choice of theoretical framework, practical implementation and adiabatic tests, *Ocean Modelling*, 40, 260–272.
- Boudière, E., Maisondieu, C., Ardhuin, F., Accensi, M., Pineau-Guillou, L., and Lepesqueur, J., 2013: A suitable metocean hindcast database for the design of marine energy converters, *Int. J. Mar. Energy*, 28, 3–4, e40–e52.
- Chapron, B., Collard, F., and Ardhuin, F., 2005: Direct measurements of ocean surface velocity from space: interpretation and validation, *J. Geophys. Res.*, 110, C07008. doi:10.1029/2004JC002809.
- Delpey, M. T., Ardhuin, F., Otheguy, P., Jouon, A., and Ardhuin, F., 2014: Effects of waves on coastal water dispersion in a small estuarine bay, *J. Geophys. Res.*, 119, 1–17.
- Dugor, J., Riouhey D., Ardhuin F., 2010: Développement d'un modèle opérationnel de prévision de houle à petite échelle sur le littoral transfrontalier des Pyrénées Atlantiques – Gipuzkoa, Proceedings of Xièmes Journées Nationales Génie Côtier – Génie Civil, Les Sables d'Olonne, 22-25 juin 2010. DOI:10.5150/jngcgc.2010.010-D.
- Gomes Lahoz, M, and Carretero Albiach J.C., 2005: Wave forecasting at the Spanish coasts, *J. of Atmos. and Ocean Sci.*, 10(4), 389–405.
- Gutiérrez, J. M., San-Martín D., Brands S., Manzanos R., Herrera S., 2013: Reassessing Statistical Downscaling Techniques for Their Robust Application under Climate Change Conditions. *J. Climate*, 26, 171–188.
- Janssen, P. A. E. M., Doyle, J. D., Bidlot, J., Hansen, B., Isaksen, L., and Viterbo, P., 2002: Impact and feedback of ocean waves on the atmosphere, in *Advances in Fluid Mechanics, Atmosphere-Ocean Interactions*, Vol. I (Perrie, W., ed.), pages 155-197, MIT press, Boston, Massachusetts.
- Longuet-Higgins, M. S. and Stewart, R. W., 1964: Radiation stress in water waves, a physical discussion with applications," *Deep Sea Research*, 11, 529–563.
- McWilliams, J. C., Restrepo, J. M., and Lane, E. M., 2004: An asymptotic theory for the interaction of waves and currents in coastal waters, *J. Fluid Mech.*, 511, 135–178.
- Michaud, H., Marsaleix, P., Leredde, Y., Estournel, C., Bourrin, F., Lyard, F., Mayet, C., and Ardhuin, F., 2012: Three-dimensional modelling of wave-induced current from the surf zone to the inner shelf," *Ocean Sci.*, 8, 657–681.
- Rasclé N. and F. Ardhuin, 2009, "Drift and mixing under the ocean surface revisited. stratified conditions and model-data comparisons," *J. Geophys. Res.*, vol. 114, p. C02016, 2009. doi:10.1029/2007JC004466.
- Rasclé, N. and Ardhuin, F., 2013: A global wave parameter database for geophysical applications. part 2: model validation with improved source term parameterization," *Ocean Modelling*, 70, 174–188.
- Roland A. and F. Ardhuin, 2014 (in press): On the developments of spectral wave models: numerics and parameterizations for the coastal ocean, *Ocean Dynamics*.
- Sheremet, A., Staples, T., Ardhuin, F., Suanez, S., and Fichaut, B., 2014: Observations of large infragravity-wave run-up at Banneg island, France," *Geophys. Res. Lett.*, 41.
- Tran N., D. Vandemark, S. Labroue, H. Feng, B. Chapron, H. L. Tolman, J. Lambin, and N. Picot, 2010, "The sea state bias in altimeter sea level estimates determined by combining wave model and satellite data," *J. Geophys. Res.*, vol. 115, p. C03020, 2010.

# Downscaling from Oceanic Global Circulation Model towards Regional and Coastal Model using spectral nudging techniques: application to the Mediterranean Sea and IBI area models

By *Herbert<sup>1</sup> G., Garreau<sup>1</sup> P., Garnier<sup>1</sup> V., Dumas<sup>1</sup> F., Cailleau<sup>2</sup> S., Chanut<sup>2</sup> J., Levier<sup>2</sup> B., Aznar<sup>3</sup> R.*

<sup>1</sup>Ifremer/DYNECO-PHYSED, Brest, France

<sup>2</sup>Mercator Ocean, Toulouse, France

<sup>3</sup>Puertos del Estado

## Abstract

In order to favour the downstream from the European MyOcean service of large scale ocean forecasts to the national service of coastal ocean forecasts, studies of new methods improving the downscaling between global or regional ocean models and coastal ones are in progress. In the framework of PREVIMER and MyOcean projects respectively, IFREMER and Mercator Ocean studied in parallel the impact of the spectral nudging method.

In the present work, the performance of spectral nudging was assessed using two regional hydrodynamic models: one of Mediterranean Sea and one of the Iberia-Biscay-Ireland (IBI) area. They are both forced by a coarser global circulation model (GCM) (PSY2V4/Mercator Ocean). This technique prevents large and unrealistic departures between the global circulation model (GCM) driving fields and the regional model fields at the GCM spatial scales.

Regarding the Med Sea application, the model's temperature  $T$  and salinity  $S$  are spectrally nudged towards PSY2V4 solution using nudging terms in the model tracer equations: a semi prognostic approach has been chosen. The simulated fields are then compared with those estimated by no-nudged model and confronted to observations. Results show that the spectral nudging is able to constrain error growth in large-scale circulation without significant damping of the meso-scales eddy fields.

Regarding the IBI application,  $T$ ,  $S$  as well as current speed  $U$ ,  $V$  have been nudged towards PSY2V4 solution: the increments are directly added as source and sink terms in the model prognostic equations. PSY2V4, nudged IBI and no-nudged IBI models as well as the present operational IBI model weekly restarted by PSY2V4 are compared and confronted to observations. The large scale and meso-scale structures are better represented off the shelf area where IBI is nudged and the bias significantly decreases on the shelf where the high frequency and high resolution physics of free IBI is better resolved than the assimilated PSY2V4 model one.

## Spectral nudging method: general description

The spectral nudging aims at forcing the regional child model solution to be close to the global parent forcing model at large scales, for which the highest quality in the forcing can be expected (thanks to data assimilation), while regional features are unconstrained. The nudging term depends on the difference of large spatial scales between the regional and global result. This term can be either positive or negative elsewhere and « nudges » the regional model solution so that it remains next to the large-scale global field. The general spectral nudging equation for a given variable  $X$  may be written as:

$$X(t+1)=X(t)+dt\{M(t)+\delta\} \text{ with } t_0 < t < t_0+T \quad (1)$$

Where  $M(t)$  is the free child model solution,  $\delta$  is the increment of  $X$  between the parent and the child models and  $T$  the assimilation window (period of the analysis cycle).

An IAU (Incremental Analysis Update, Bloom et al, 1996) process is applied for the time integration of the child model as it shown in the Fig. 1. After a forecast  $i$ -cycle of the child model, the increment  $\delta_i = \langle X_p - X_c \rangle_i$  between the parent model analysis  $X_p$  and the child model forecast  $X_c$  is calculated for a chosen state variable  $X$  (typically: the current  $U$ ,  $V$ , the temperature  $T$  and the salinity  $S$ ). The brackets " $\langle \rangle$ " consist in a time and space low pass filters which allows to take into account the only best part of the signal resolved by the parent model. A tapering function  $f(x,y,z)$ , (a spatial weight function), is applied to  $\delta_i$  in order to define where  $X_c$  has to be nudged. Then, the child system is restarted back for a 2nd  $i$ -cycle which can be called "analysis cycle". During the analysis  $i$ -cycle,  $X_c$  is nudged by  $X_p$  in following the IAU function  $g(t)$ , (a time weight function).

So, to sum up the method: after each forecast cycle of the child system, a corresponding analysis cycle is re-launched and the child system is nudged by the following final spectral nudging increment  $\delta X_{SN}$  such as:

$$\delta X_{SN} = g(t) \cdot f(x,y,z) \cdot \langle X_p - X_c \rangle = g(t) \cdot f(x,y,z) \cdot \delta$$

(2)

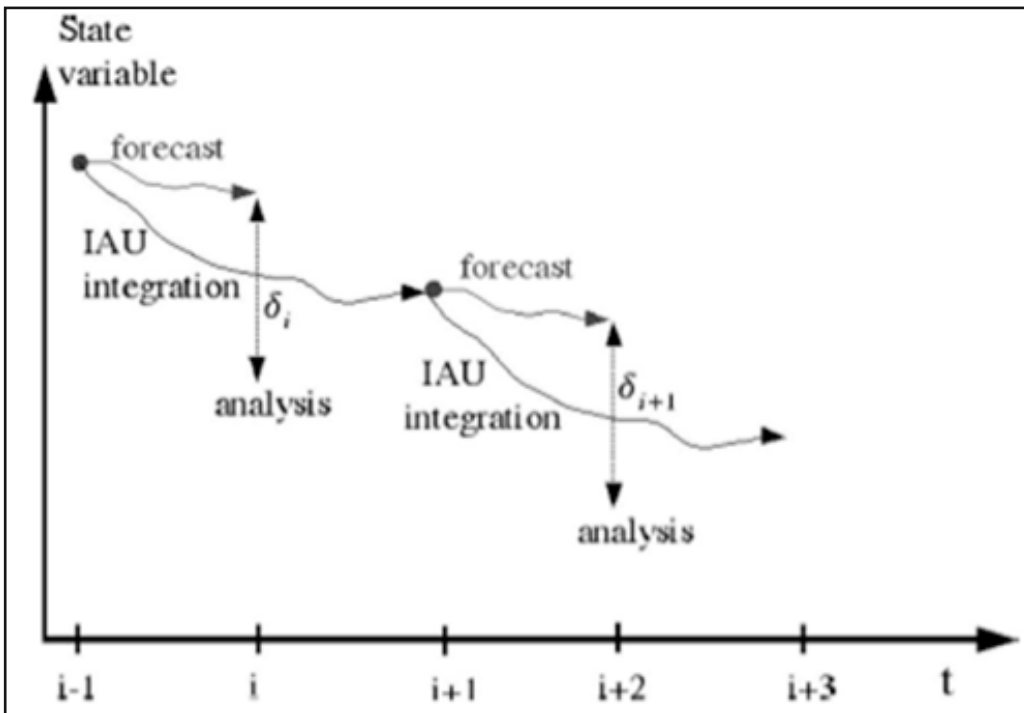


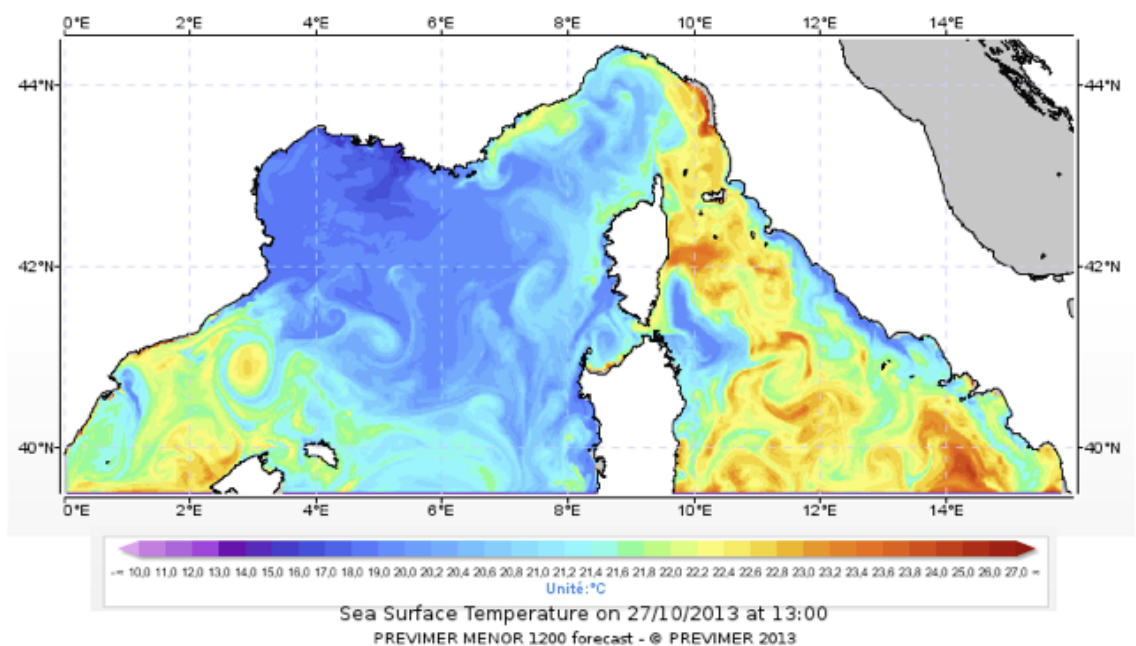
Figure 1: IAU method from Bloom et al, 1996.  $\delta_i$  is the increment of the  $i$ -cycle.

## Application to a Mediterranean Sea model

### Model configuration

The regional model used here is the MARS3D (Model for Applications at Regional Scale) developed at IFREMER, which is fully described in Lazure and Dumas (2008). The domain covers the western part of Mediterranean Sea between 39.5°N – 44.5°N and 0°E – 16°E (figure2) with a horizontal resolution of 1.2 km. There are 40 vertical levels, formulated using generalised sigma coordinate system. The open boundaries and initial conditions are provided by the global solution from Mercator Ocean (PSY2V4), at a horizontal resolution of 6 km, which is assimilated with SLA, SST and (T, S) profiles. The global solution is prescribed along the southern open boundary conditions without any nudging within the domain's body. The atmospheric forcing was specified according to the ALADIN (Aire Limitée Adaptation dynamique Développement InterNational) model from Météo-France. The fields were provided with a time resolution of 3 hours. This configuration is similar to the MENOR configuration proposed by PREVIMER for the regional Mediterranean forecast. Additional details about the MARS3D numerical code can be found in previous papers (<http://www.ifremer.fr/mars3d/References/Publications>).

Figure2: Domain of interest.



## Downscaling from Oceanic Global Circulation Model towards Regional and Coastal Model using spectral nudging techniques: application to the Mediterranean Sea and IBI area models

### Experiments

The specific spectral nudging method chosen to nudge this Med Sea model is based on the semi-prognostic method described by Eden and al. (2004) and revisited by Sheng and al. (2005). The authors achieved the implementation by adding nudging terms to part of the model equations such as motions equation (nudge on density gradient term) or thermodynamic equation (nudge on temperature and salinity) (von Storch et al. 2000; Alexandru et al. 2009). In our case, the spectral nudging was applied only for temperature and salinity. The spatial filter used here is a 2D convolution filter, which spatially smooths the misfits between global and regional model in temperature and salinity and filters out the wavelengths smaller than a cut-off scale. Regarding the time integration function  $g(t)$ , the increment  $\delta$ , which acts as an external forcing, is time constant over the temporal window  $t$ . In the present analysis, the spectral nudging increments are built over a period of  $t=7$  days and spatially filtered over a window of 50 km. Regarding the tapering function  $f(x,y,z)$ , the nudging was set to zero for water depths smaller than 500 m, so that the regional processes on the shelf are not affected, and a nudging coefficient  $\alpha$  can be defined.

The year 2010 has been chosen for the practical numerical experiences. The first simulation is a free run (i.e. without spectral nudging), leaving its temperature and salinity fields free to evolve all along the year. It is considered as the reference simulation, according to which the efficiency of the assimilation method will be assessed. The different steps of the 'nudged run' are depicted on the flow chart on figure 3: MARS3D is first freely run over a time-window, which determines the frequency bands selected for the increment. The difference of the regional/global temperature and salinity fields averaged over this time-window is computed from the global model fields interpolated on the regional model grids. The field of the differences is then spatially filtered out through a 2D convolution filter. This nudging term is finally introduced in temperature and salinity transport equation of the regional model as a constant sink or source term. The controlled solution of the regional model is then integrated over 7-days time-window. We repeat this from time to time over the year 2010. The effect of spectral nudging on the realism of the numerical solutions is afterwards evaluated by comparison with satellites and in-situ observations.

The main characteristics of the free simulation and the nudged simulation are listed in table 1.

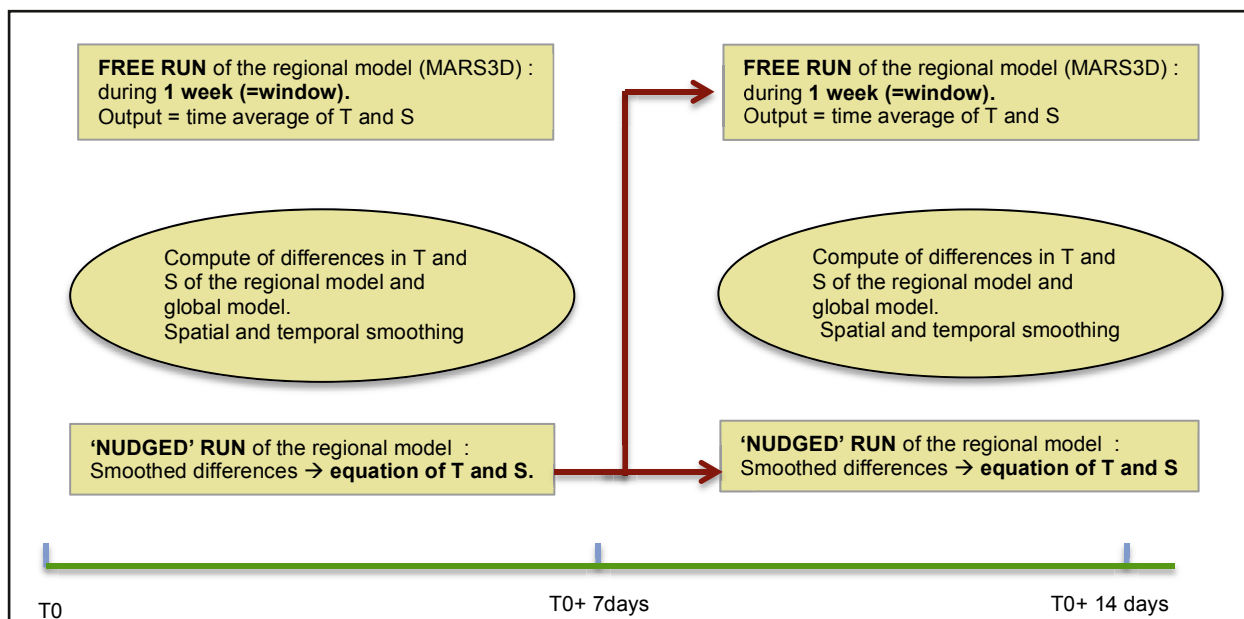


Figure 3 : Diagram presenting the spectral nudging method in temperature and salinity applied to the regional model MARS3D. February 2014 at 15:15

Simulation ID	Spectral nudging	Time window	Nudging coefficient $\alpha$	Nudging Applying	Spatial window
1- Nudged run	Yes	7 days	1/7.5	Bottom > 500 m	50 km
2- Free run	No	----	----	----	----

Table 1: Nudging parameters applied to the 'nudged simulation' (with applying of spectral nudging), in contrast with the 'free simulation' (i.e. without applying of spectral nudging).

Downscaling from Oceanic Global Circulation Model towards Regional and Coastal Model using spectral nudging techniques: application to the Mediterranean Sea and IBI area models

Results - Discussion

Comparison with SST from SEVIRI data.

In order to determine how the assimilation method impacts the sea surface temperature, we compare SST data from SEVIRI to simulated SST from the regional model, with and without spectral nudging applied over the year 2010. Figure 4 shows the time series of the spatial average of SST over the year 2010 of the nudged solution, the free simulation and from the global model PSY2V4, as well as the root mean square errors (RMSE) of each. Although the free simulation captures rather correctly the basic SST evolution, we notice a negative bias compared to the SEVIRI data from July to September. Indeed, the RMSE during this period reach 2.8°C whereas they are ranged from about 0.5 to 1.5°C the rest of the time (see table 2). The match is better for the global simulation where the RMSE does not exceed 1.5 °C in summer in agreement with the fact that the global solution is an analysis including SST observations. The use of spectral nudging reduces noticeably the biases and the RMSE and succeeds in maintaining the regional model next to the global analysis. On the contrary, in June and August, it performs less efficiently and even hardly improves the regional solution whatever the quality of the global analysis: the RMSE in August is slightly increased from 1.17 °C (free run) to 1.22 °C (the nudged run). It might be due to a link between this observed bias and the small scales activity.

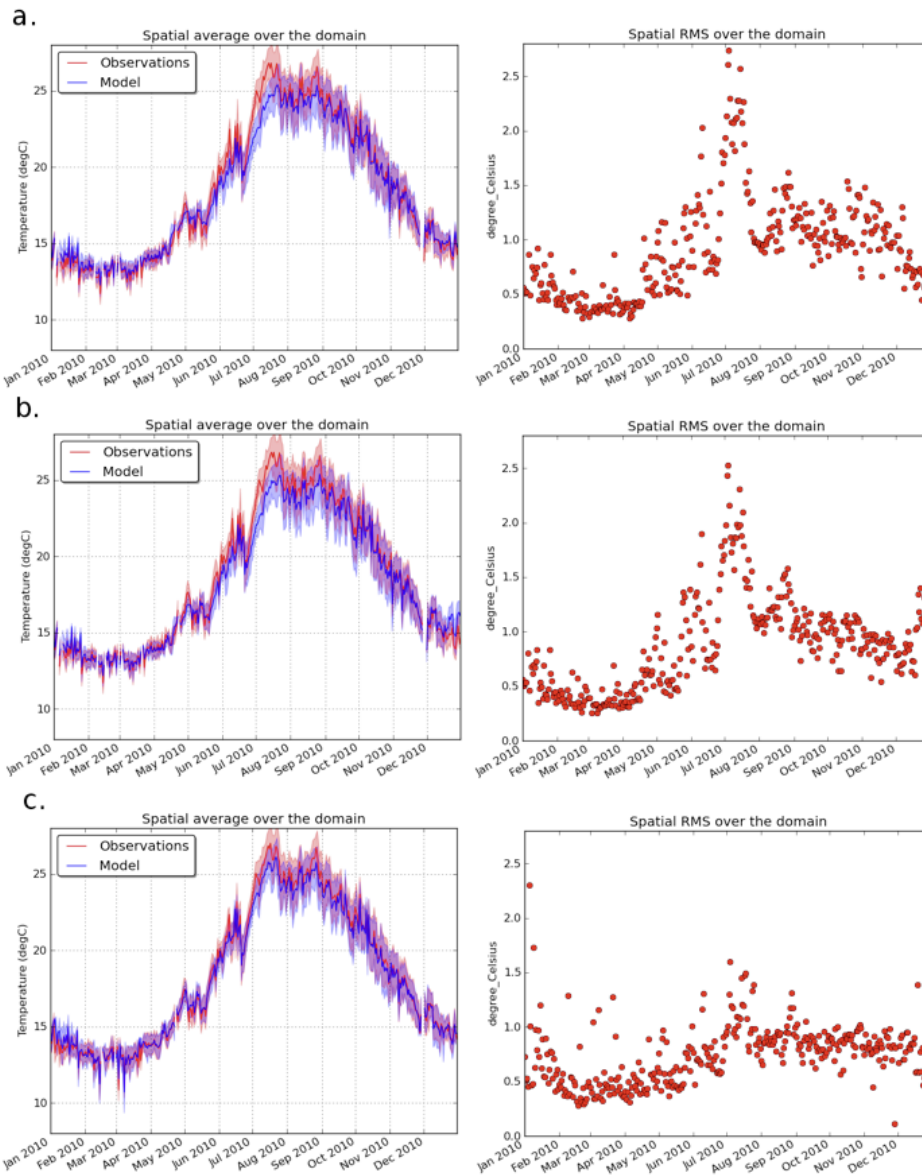


Figure 4 : Observed (red line) and simulated (blue line) daily sea surface temperature (°C) (left panel), and spatial rms over the domain (right panel) from the free simulation (a), the nudged simulation (b), and the global model PSY2V4 (c), over the year 2010. Observed daily SST data are provided by Spinning Enhanced Visible and InfraRed Imager (SEVIRI).

Table 2: Monthly rms errors between observed and simulated SST (in °C) provided by the nudged simulation, the free simulation and the global model PSY2V4 over the year 2010.

Month	Nudged run	Free run	PSY2V4
Janv.	0.54	0.60	0.61
Feb.	0.39	0.42	0.43
Mar.	0.36	0.40	0.48
Apr.	0.51	0.51	0.47
May	0.75	0.81	0.60
Jun.	1.10	1.14	0.73
Jul.	1.69	1.77	1.09
Aug.	1.22	1.17	0.91
Sep.	1.00	1.09	0.83
Oct.	0.98	1.10	0.87
Nov.	0.86	1.08	0.77
Dec.	0.98	0.74	0.71

## Downscaling from Oceanic Global Circulation Model towards Regional and Coastal Model using spectral nudging techniques: application to the Mediterranean Sea and IBI area models

Figure 5 shows an example of mean SST over November 2010 from SEVIRI observations, from the free regional model and from the nudged model, as well as the monthly mean bias (difference between observation and model field) associated. The results show that the regional model driven only at its lateral boundaries presented a warm bias in the middle of the domain (at the east of Baleares islands and at the north-west of Corsica). These biases that may reach  $-4^{\circ}\text{C}$  are largely reduced thanks to the nudging. However, some biases remain. Some of them are also present in the global model, as the warm bias observed at the east of Corsica. These cold waters result in intense mixing induced by strong westerly winds channelled between Corsica and Sardinia. They are clearly visible on satellite observations but missing in regional and global model. The nudging of the regional solution towards global solution will have a negative effect in this case. Other biases are specific to regional model dynamic, as the cold bias associated to river discharge (the « Rhone », at the east coast of Gulf of Lions, and the « Ebre », at Spanish coast), visible in the free simulation and maintained in nudged simulation since the spectral nudging is not applied on the shelf. These too cold waters has the effect the destruction of the warm surface signature associated to the North Current (i.e. Liguro-Provençal Current), which goes along the coast along the  $\sim 200\text{m}$  isobath and which is well visible in satellite observation and in the global simulation field.

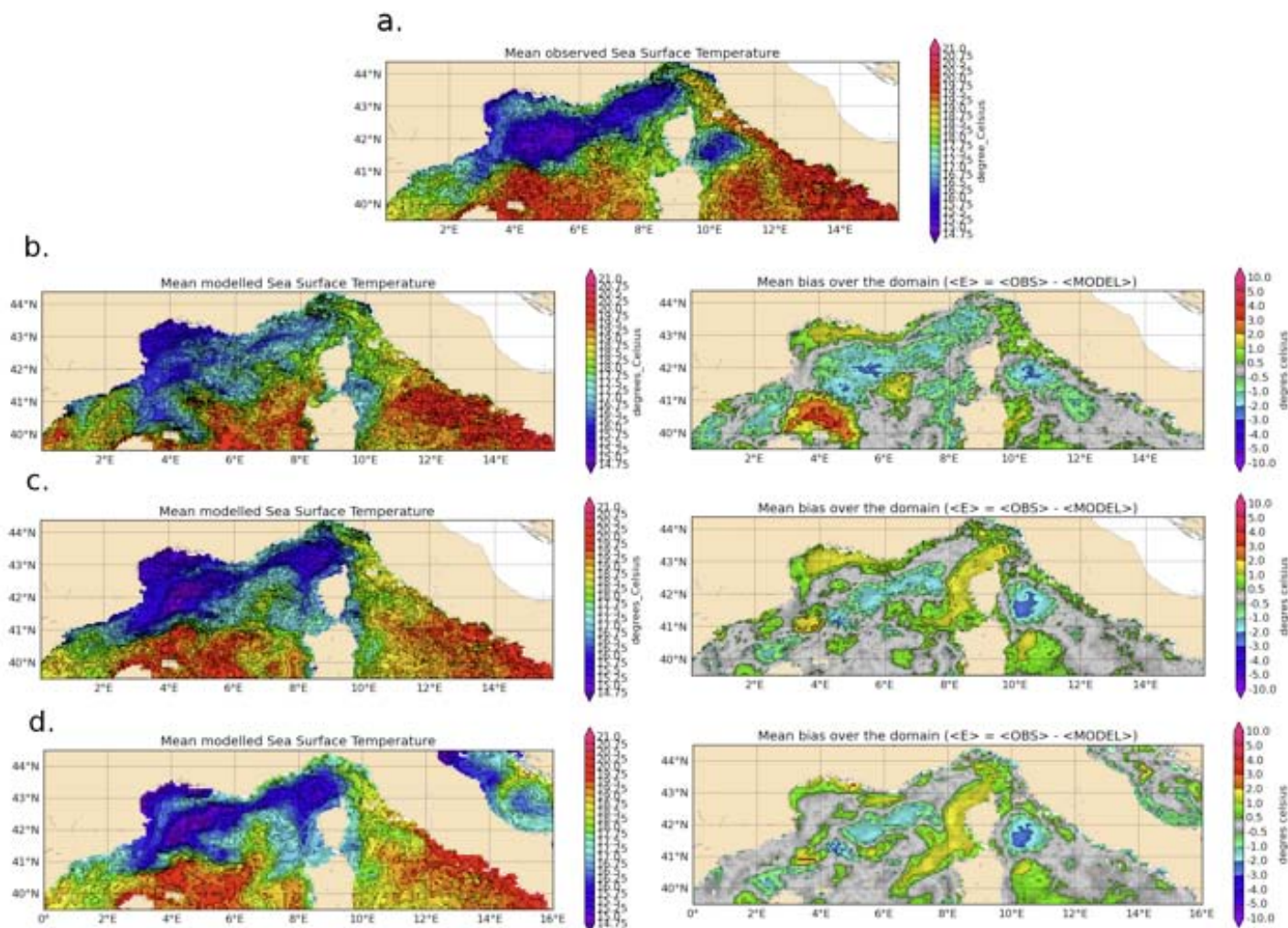


Figure 5 : SST ( $^{\circ}\text{C}$ ) over November month 2010 from SEVIRI satellite data (a), the free simulation (b), the nudged simulation (c), the global model PYS2V4 (d), and the mean bias (observation-model) associated.

### Modelling of Levantine water.

The Levantine Intermediate Water (LIW) is an important water mass for the overall hydrology and processes of the north-western of the Mediterranean Sea. They are formed in the Levantine Basin (easternmost Mediterranean area) during winter (Wüst, 1961; Lascaratos et al., 1993) and are characterised by a subsurface maximum of salinity (ranging from 39.0 psu in the Levantine basin to 38.5 psu in the Western Mediterranean), separating deep water from surface waters. One part contributes to the Liguro-Provençal Current (LPC) along French and Spanish coast, which is one of dominant process of the coastal dynamic of North Mediterranean region. The second part spreads in the whole areas at a depth ranging from 400 to 600 m. A realistic representation of these waters is essential in order to get a correct dynamic over the north-western basin, particularly the dense water formation during winter (MEDOC group, 1970, Millot, 1987, 1990, 1999, etc). The analysis of the volume of this water mass over 2010 is conducted in order to estimate the realism of each model and the efficiency of the spectral nudging with respect of the LIW preserving ability. Figure 6 shows a vertical section of salinity characteristic of LIW (i.e. ranged between 38.48 psu and 38.86 psu) along the latitude  $42^{\circ}\text{N}$  on January 15<sup>th</sup> 2010 (i.e. 15 days after the start of the simulation) and on December 11<sup>th</sup> 2010, from the PSY2V4 model, and from the regional model MARS3D without and with applying of spectral nudging.

## Downscaling from Oceanic Global Circulation Model towards Regional and Coastal Model using spectral nudging techniques: application to the Mediterranean Sea and IBI area models

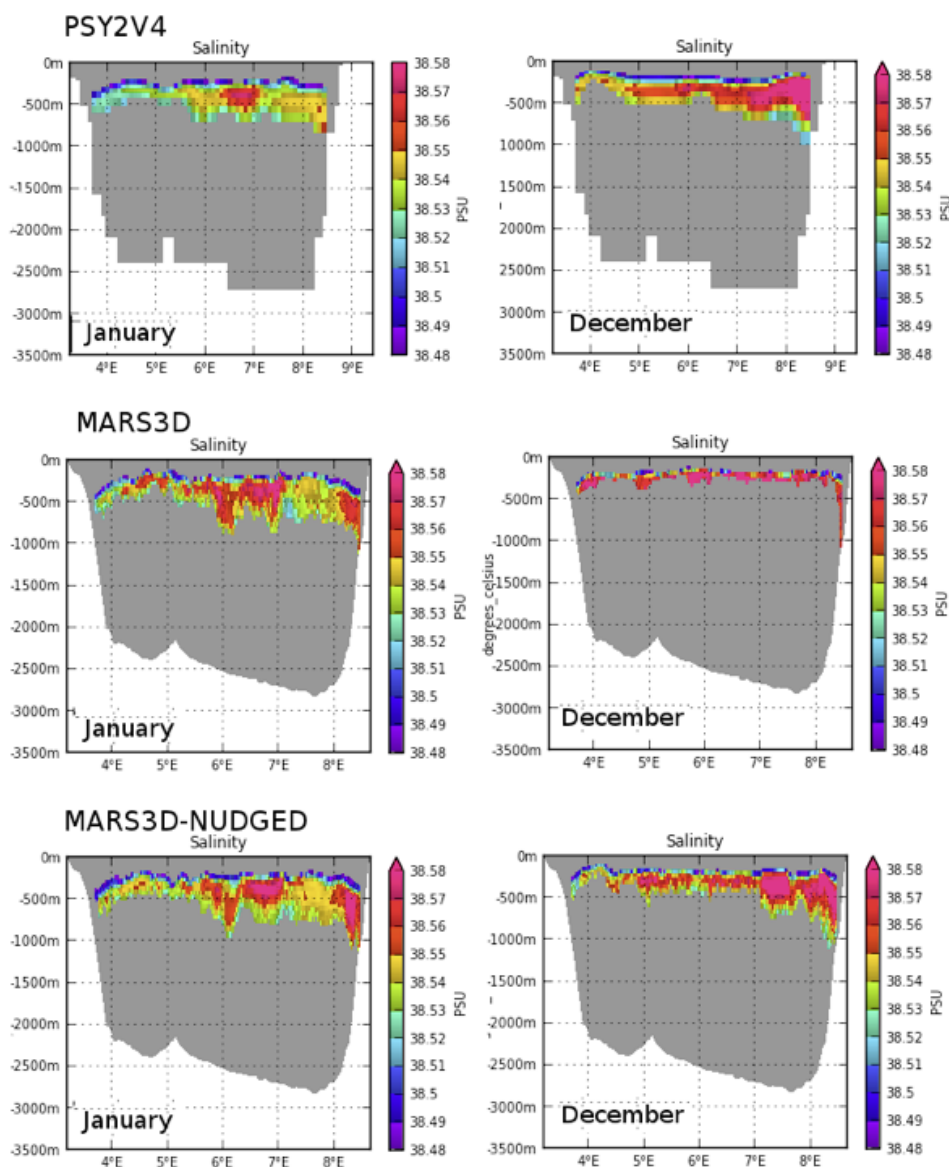
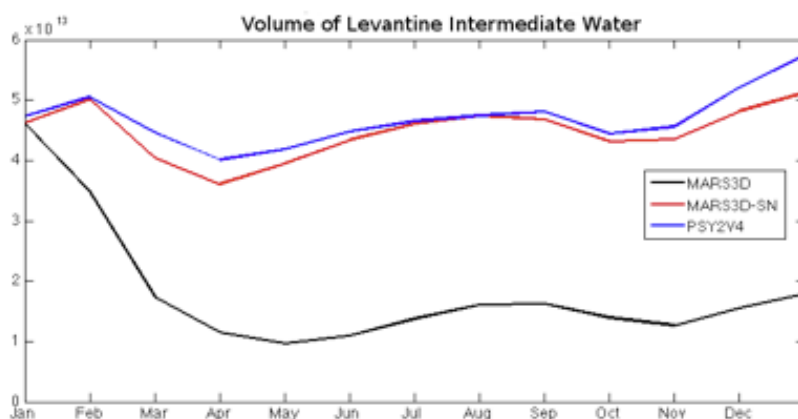


Figure 6: Vertical section of the salinity (psu) at the latitude 42°N on January 15th 2010 (left panel) and on December 11th 2010 (right panel), from the global model PSY2V4, and the regional model MARS3D without and with using of spectral nudging technique. Only the temperature ranged between 13.2°C and 14.2°C, the salinity ranged between 38.48 psu and 38.88 psu, and the depths 300m to 600m, characteristics of Levantine waters, are shown.

It can be seen in the global analysis PSY2V4 that the LIW extends from the Ligurian Sea to the Liguro-Provencal basin, between 300 m to 600 m depths. In January, the LIW represent 11% of the total volume of water masses (figure 7). The volume of LIW introduced into the basin fluctuates over months between a minimum on April (around  $4.10 \cdot 10^{13} \text{ m}^3$ ) and a maximum of  $5.8 \cdot 10^{13} \text{ m}^3$  at the end of the year. The restoration of LIW volume is not correctly represented by the regional model MARS3D (figure 6 right panel). Indeed, results show that the volume of LIW in December is not as high that in January: the volume of LIW decreases from  $4.6 \cdot 10^{13} \text{ m}^3$  (i.e. 11% of the total volume of water masses) at the start of the simulation (January 2010) to  $1.8 \cdot 10^{13} \text{ m}^3$  (i.e. 4% of the volume total of water masses) at the end of the simulation (December 2010) (figure 7). This water mass, which percentage could be considered as weak, plays an essential role in the constitution of dense and deep water in north-eastern Mediterranean Sea. A good control of these waters allows maintaining a realist cyclonic circulation in the northern part of the basin. The spectral nudging by putting the regional solution on the tracks of the global analysis allows to improve the seasonal variations of the LIW (see figure 6 and figure 7). This result is confirmed by the time evolution of the LIW's volume shown in figure 7: the variations of the volume of LIW over 2010 from the nudged simulation (red curve) are of an order of magnitude very close as the global model ones (blue curve) with values ranged from  $3.6 \cdot 10^{13} \text{ m}^3$  to  $5.2 \cdot 10^{13} \text{ m}^3$ .

Figure 7: Time evolution (one value every 30 days) of the volume of Levantine Intermediate Water (in  $\text{m}^3$ ) over the year 2010 from the free simulation MARS3D, the nudged simulation (noted 'MARS3D-SN') and the global model PSY2V4.



## Downscaling from Oceanic Global Circulation Model towards Regional and Coastal Model using spectral nudging techniques: application to the Mediterranean Sea and IBI area models

### Impact on mesoscale eddy field

In this section we assess the effect of the procedure on small scale features. A spectral analysis of the kinetic energy over a rectangular domain is performed (figure 8). The monthly mean SSH spectrum over February for the free simulation, the nudged simulation and from the global analysis give an idea of the 'effective resolution' of each model. It corresponds to the smallest small scales correctly resolved by the model and for which the dissipation terms in space and time become active (Skamarock, 2004). It is defined by the wavelength from which the spectrum of the model deviates to the slope of the energy cascade. The SSH spectrum of both simulations follow approximately the  $k^{-5/3}$  slope (dashed line on the figure 8) for the large scale (wavelengths > 100km) and the  $k^{-4}$  slope (blue line on the figure 8) for the mesoscale range, in agreement with recent development in very high resolution model (Klein, 2008). For the free model, the energy cascade leaves the  $k^{-4}$  slope for wavenumber of 0.09 cycles/km indicating an effective resolution of around 11 km. In the same way, we obtain an effective resolution of 45 km for the global model.

As far as the nudged model is concerned, the spectrum tends to follow the global model one for the large scales (wavelength > 100 km) and the free model for the smallest scales, with a similar effective resolution. We notice that the energy associated to scales smaller than 50 km is not significantly reduced by the nudging process; the spectrum of the nudged model exhibits a similar spectral slope behaviour to the SSH  $k^{-4}$  slope, just as the free model. This results are confirmed on the figure 9 which presents the time evolution over 2010 of the energy associated to wavenumbers lower than 0.01 cycles/km, (i.e. wavelength > 100 km) (figure 9.a), and to wavenumbers ranging between 0.02 cycles/km and 0.03 cycles/km (i.e. wavelength between 33 km and 50 km) (figure 9.b), for the free model (blue line) and for the nudged model (red line). The time series of energy associated to scales higher than 100 km from the nudged model tends to follow the global model one whereas the time series of energy associated to scales ranging between 33 km and 50 km tends to follow the free model one.

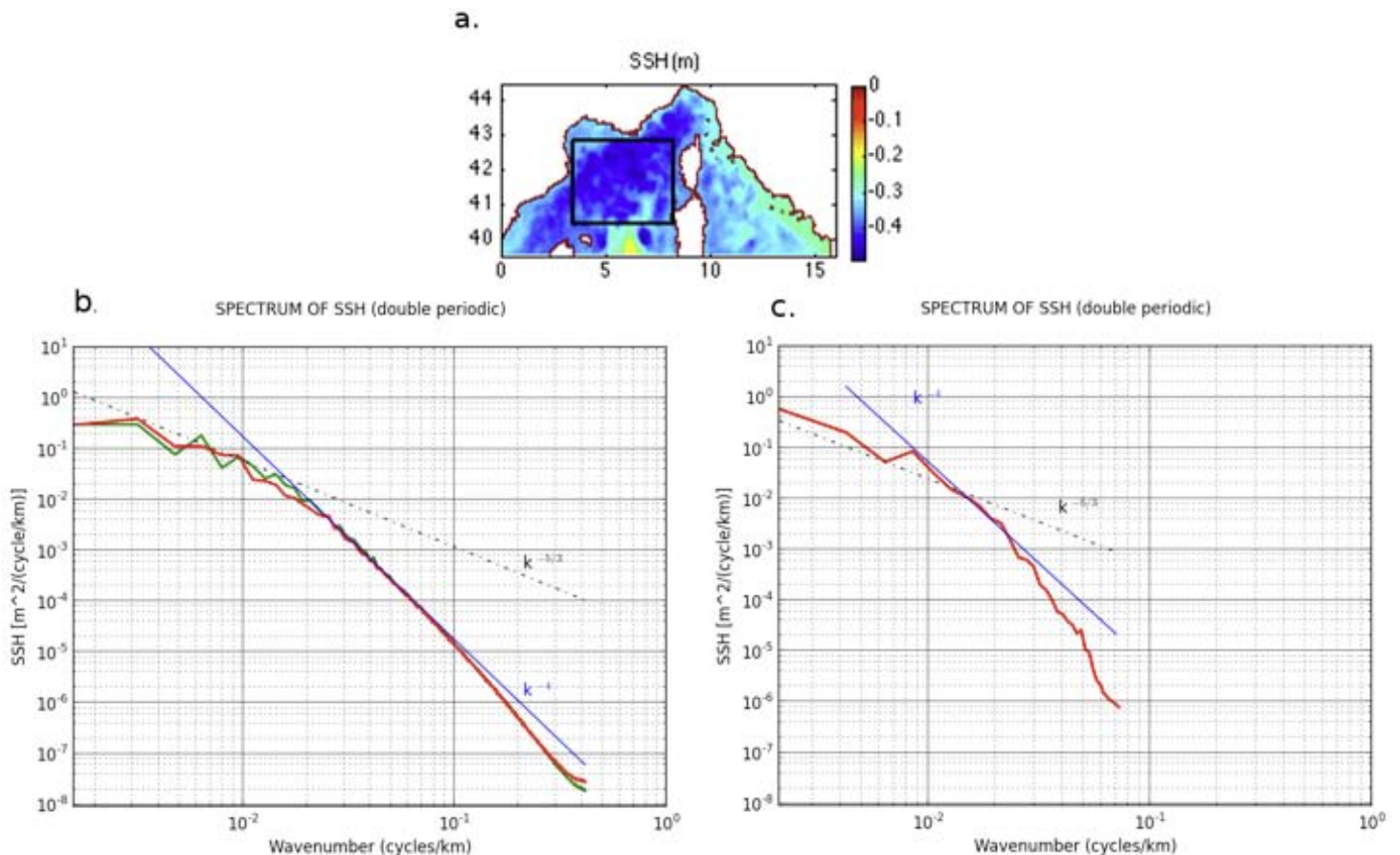


Figure 8: SSH spectrum mean over February month, from the free simulation (b; green curve), the nudged simulation (b; red curve), and the global model PSY2V4 (c). The lines indicate the  $-5/3$  (dashed) and  $-4$  (solid) slopes. The area on which the SSH spectrum has been computed is indicated by the black square on a) (the color field represents the SSH (m) on Feb.15th)

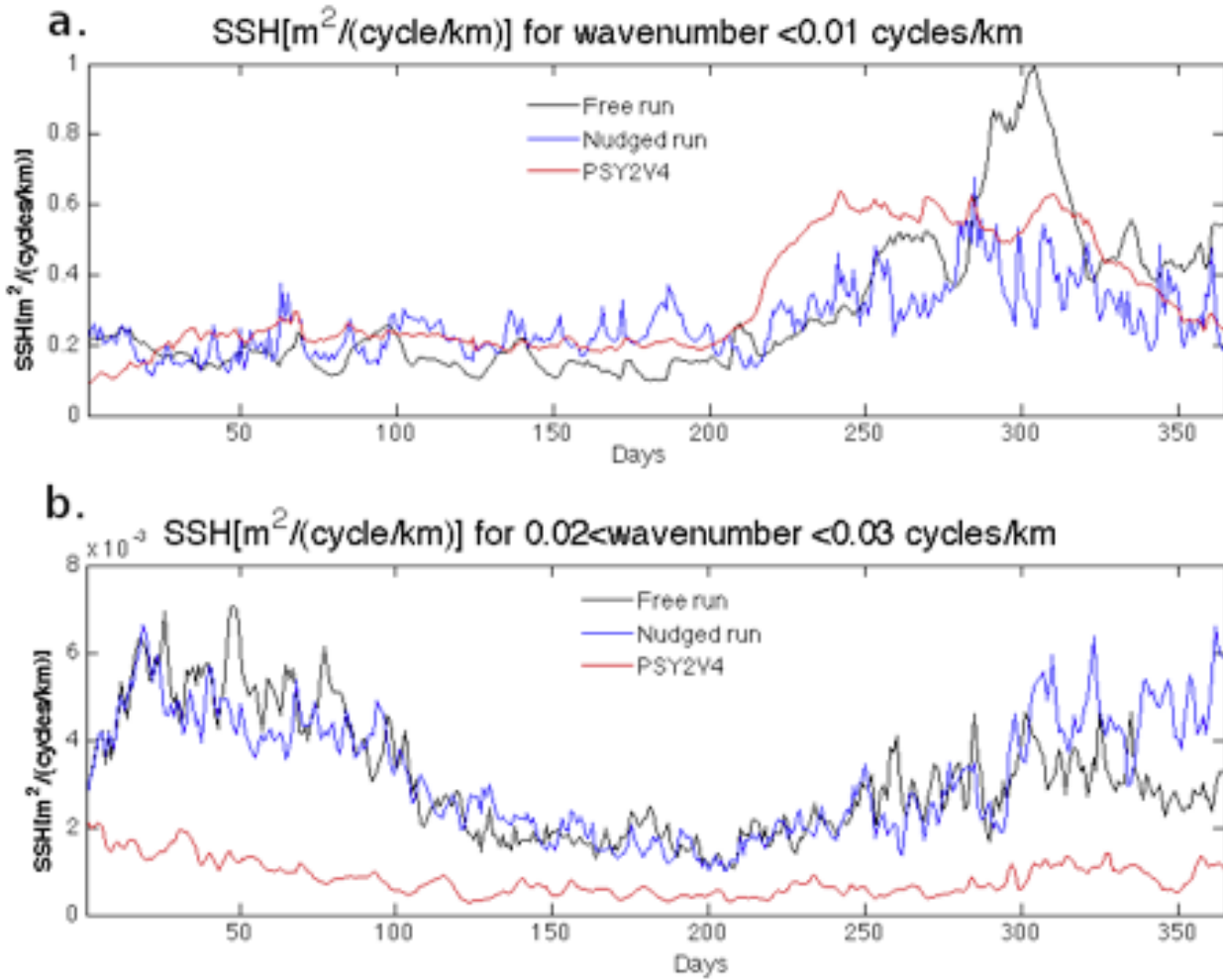


Figure 9: Time series of SSH energy associated to wavenumber a)  $< 0.01 \text{ cycles/km}$  and b) ranging between  $0.02 \text{ cycles/km}$  to  $0.03 \text{ cycles/km}$  (i.e. wavelength between  $33 \text{ km}$  to  $50 \text{ km}$ ) over the year 2010, from the free simulation (black curve), the nudged simulation (blue curve) and the global model PSY2V4 (red curve).

The kinetic energy over the domain, representative of the mean and mesoscale activity, is computed from geostrophic velocities deduced from sea surface height. The results obtained for March 2010 are presented on figure 10 and 11, which shows the monthly mean Total Kinetic Energy (TKE), the Mean Kinetic Energy (MKE) and the Eddy Kinetic Energy (EKE), from the simulations MARS3D with and without spectral nudging and from the global model. The Total Kinetic Energy is the time averaged kinetic energy. It is calculated as:

$$TKE = \frac{1}{2} (u_g^2 + v_g^2) \quad (3)$$

Where  $u_g$  and  $v_g$  are respectively the zonal and meridian component of geostrophic velocities, calculated as follows :

$$u_g = -\frac{g}{f} \frac{\partial \eta}{\partial x} \quad \text{and} \quad v_g = -\frac{g}{f} \frac{\partial \eta}{\partial y} \quad (4)$$

With  $\partial \eta$  the slope of sea level anomaly. The Mean Kinetic Energy is computed from the time-averaged velocities, and the Eddy Kinetic Energy is the difference between the TKE and the MKE. From both simulations, high EKE is associated with the variability of the along slope Liguro-Provencal Current. EKE values are of the order of  $100 \text{ cm}^2/\text{s}^2$  in the regional simulations and around  $40 \text{ cm}^2/\text{s}^2$  in the global one. Another region of high intensity (locally  $> 90 \text{ cm}^2/\text{s}^2$  in the regional simulation), at the west of Sardinia corresponds to the Balearic front well-known for its mesoscale activity. As expected, this region is much less energetic in the global model. In the regional model, some patches of activity (around  $70 \text{ cm}^2/\text{s}^2$ ) are found in many places in the whole basin due to the occurrence of sporadic and recurrent eddies or gyres (such as Bonifacio Gyres). The lowest energies ( $< 50 \text{ cm}^2/\text{s}^2$ ) are observed in the Liguro-Provencal basin and in the Tyrrhenian Sea.

## Downscaling from Oceanic Global Circulation Model towards Regional and Coastal Model using spectral nudging techniques: application to the Mediterranean Sea and IBI area models

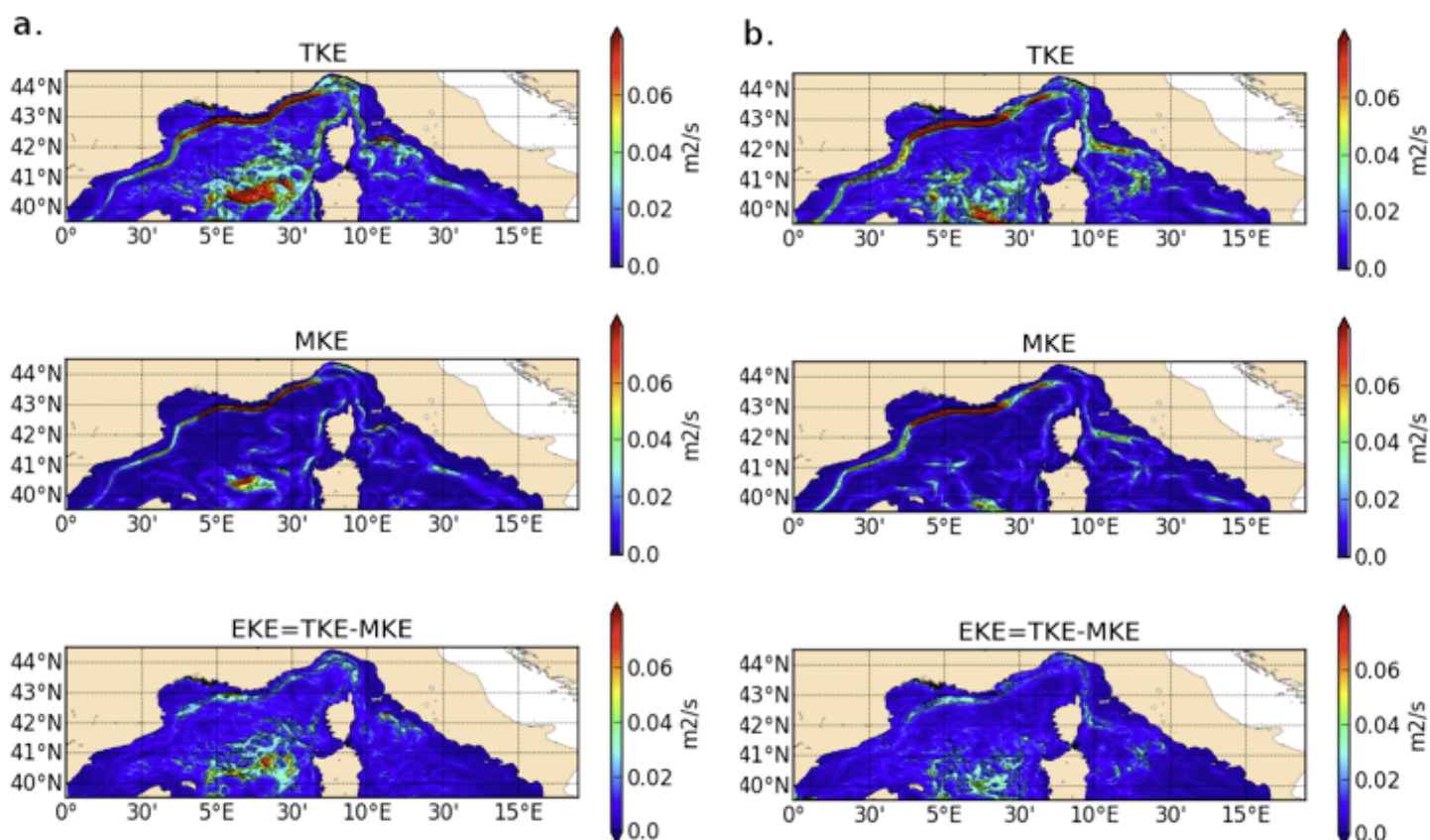


Figure 10: Mean of Total Kinetic Energy (TKE), Mean Kinetic Energy (MKE) and Eddy Kinetic Energy (EKE) in  $m^2.s^{-1}$  over March 2010, from the free simulation (a) and from the nudged simulation (b).

The spatial distribution of high and low patches of EKE is similar from both (free and nudged) simulations: slightly smaller values are present in the nudged simulation than in the free simulation, especially at the south of the domain, in the area of eddies formation. The reduction in the whole of the domain is not significant: -4.5% of the spatial average of TKE. Thus, the smallest scales, which were not driven by the spectral nudging, were not significantly affected by scale interaction.

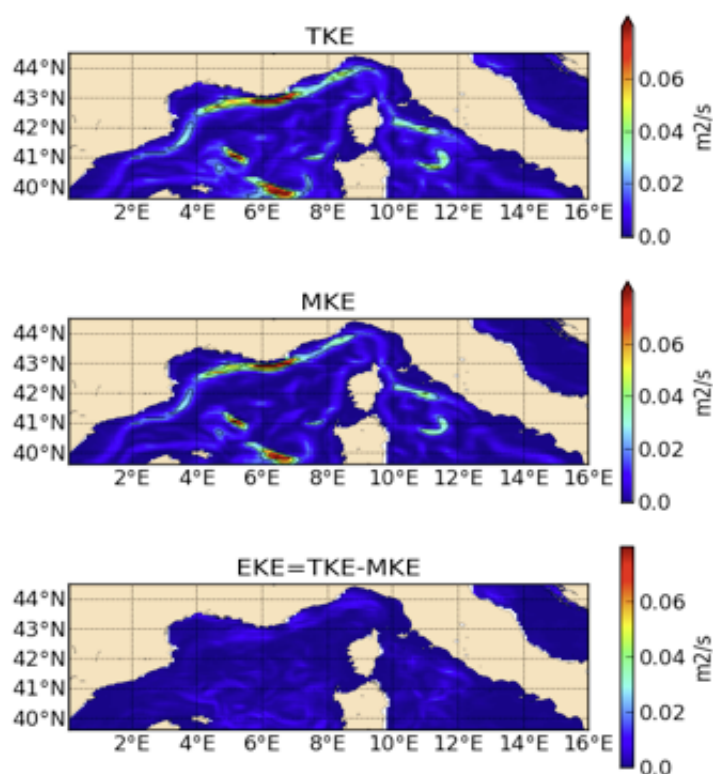


Figure 11: Same as figure 8 but from the global model PSY2V4.

## Application to an Iberia-Biscay-Ireland area (IBI) model

### Model configuration

The regional model used here is based on NEMO code (Madec et al., 1998; Madec, 2008). The model domain covers part of the North East Atlantic ocean, going from the Canary Islands to Iceland. It encompasses also part of the Western Mediterranean Sea and the North Sea, reaching to the Skagerrak Strait that connects the Baltic Sea to the North Sea. The primitive equations are discretized on a  $1/36^\circ$  ( $\sim 2$  km) curvilinear ORCA grid and on 50 z-levels in the vertical. Vertical resolution decreases from  $\sim 1$  m near the surface to more than 400 m in the abyssal plain. The open boundaries and initial conditions are provided by the global solution from Mercator Ocean PSY2V4 system. The global solution is prescribed along the open boundary conditions without any nudging. The atmospheric forcing was specified according to the 3-hourly. This configuration is similar to the configuration of MyOcean operational IBI system which runs in nominal mode at Puertos Del Estado and in backup mode at Mercator Ocean. Additional details about IBI system, its configuration description and its assessment can be found in Maraldi et al. 2013, Cailleau et al. 2012.

### Experiments

In this case, the spectral nudging is applied for  $T$  and  $S$  as well as the current speed components  $U$ ,  $V$ . As the large scale parent system PSY2V4 is supposed to resolve the meso-scale structures (up to the mid-latitudes at least) and as the representation of these structures in term of geostrophic turbulence are improved by the data assimilation of the sea level anomalies among other, IBI system must be nudged by the PSY2V4 resolved scales from large scale to meso-scale. So the space and time filters have been chosen in order to keep these scales and remove the smaller ones. Regarding the time filter, as the week is the typical characteristic time scale of the meso-scale structures, the chosen time smoothing consists in a simple weekly mean of  $X_p - X_c$ . Regarding the space filter, the spectral analysis allows to define the energy injection scale of a system ie. The wave length where the energy spectrum of the system leaves the slope of the energy cascade, and the system starts to become dissipative. In theory, the large scale follows the  $k^{-5/3}$  power law and the mesoscale follows the  $k^{-3}$  power law (see in Fig. 12). Finally, the energy injection scale could be defined as the effective resolution of a system, and can be used as the cutoff length  $T_c$  for the space low pass filter. So the parent system is able to resolve structures from the large scale to the energy injection scale. As it is presented in Fig. 12, a preliminary study has shown that  $T_c \sim 7\Delta x \sim 45\text{Km}$  can be chosen for PSY2V4 in mid latitude, between  $30^\circ$  and  $40^\circ\text{N}$ , (with  $\Delta x = 1/12^\circ$  the horizontal resolution of PSY2V4).

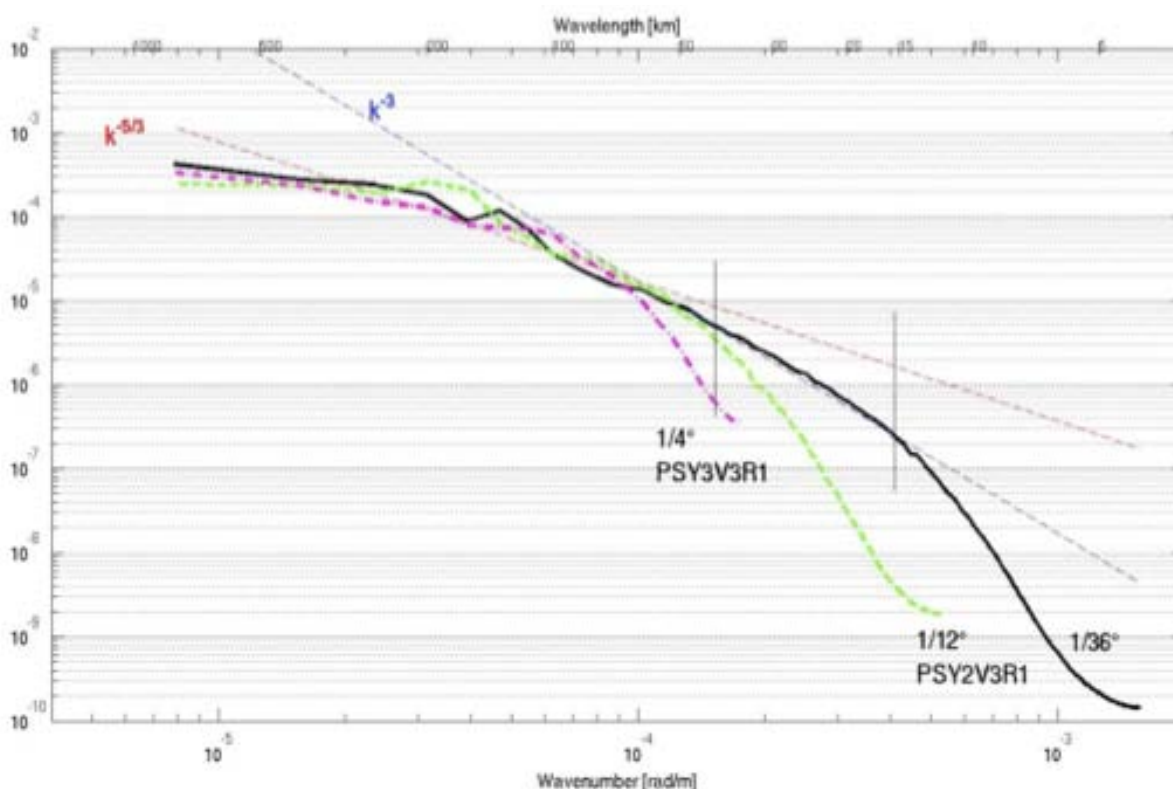
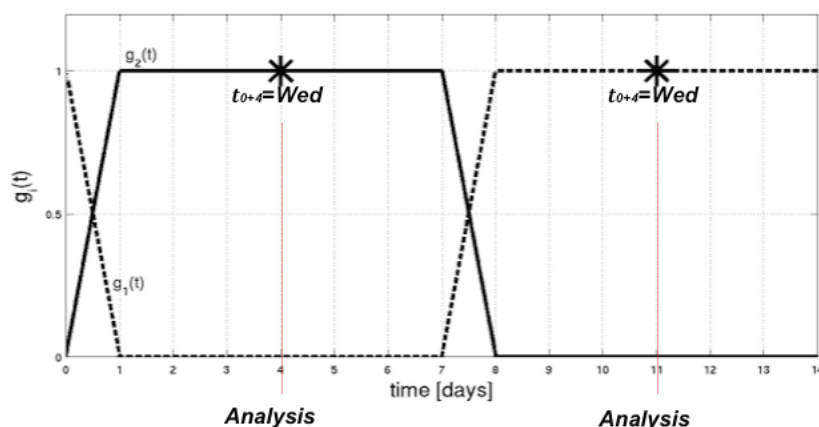


Figure 12: Spectral analysis of the large scale  $1/4^\circ$  system PSY3 (dotted and dashed pink spectrum), the eddy resolving/permitting  $1/12^\circ$  system PSY2 (dashed green spectrum) and the high resolution regional  $1/36^\circ$  IBI system (solid black spectrum). For each system, this spectra has been calculated off the Iberian coast  $s$  between about  $30^\circ$  and  $40^\circ\text{N}$  of latitude. The red dashed line corresponds to the energy cascade of the large scale and the blue one corresponds to the mesoscale energy cascade. The vertical solid black lines indicate the energy injection scale of PSY2 and IBI which is  $7\Delta x$  here (with  $\Delta x$  = horizontal resolution of each system).

## Downscaling from Oceanic Global Circulation Model towards Regional and Coastal Model using spectral nudging techniques: application to the Mediterranean Sea and IBI area models

During the analysis cycle of  $t=7$  days, the increment  $\delta$  is applied to the IBI model at each time step, by following the IAU function  $g(t)$  shown in Fig. 13. In order to prevent a discontinuity between the increments  $\delta_{i-1}$  and  $\delta_i$  of two successive analysis cycles  $i-1$  and  $i$  and so to ensure the transition between two cycles, a 1-day overlap is applied which corresponds to the linear decrease in the weight on  $\delta_{i-1}$  and the linear increase in the weight on  $\delta_i$ . The nudging was applied off the shelf (for the bottom depth  $> 200\text{m}$ ), off the coasts (from  $30\text{Km}$ ) and above depths from  $3000\text{m}$ .

Figure 13: Mercator IAU function  $g(t)$



We simulated the period from 2010/03/30 to 2010/10/18 with and without spectral nudging. So as the previous study in Med Sea, we launched a free run IBI-REF as a reference and a nudged run IBI-NUDG. The impact of the spectral nudging has been assessed by comparing the results of IBI-REF, IBI-NUDG, PSY2V4 as well as the present operational IBI system (called here IBI-OPER). The comparison with satellites and in-situ observations has been also done.

The main characteristics of the free simulation and the nudged simulation are listed in table 3.

Simulation ID	Spectral nudging	Time window	Nudging Applying	Spatial window
1- Nudged run IBI-NUDG	Yes	7 days	1- Bottom $> 200$ m 2- $30\text{km}$ off coast 3- Depth $> 3000\text{m}$	45 km
2- Free run IBI-REF	No	----	----	----

Table 3: Nudging parameters applied to the 'nudged IBI simulation' (with applying of spectral nudging), in contrast with the 'free IBI simulation' (i.e. without applying of spectral nudging).

## Results - Discussion

We have assessed the chosen spectral nudging method by comparing the free simulation IBI-REF, the simulation IBI-NUDG nudged by PSY2V4 off the coasts and shelf, the PSY2V4 simulation and the operational simulation IBI-OPER which is restarted every weeks with a 2-week spin up. The solutions are compared to observations. One of the main objectives of this work is to study whether IBI-NUDG solution is better than IBI-OPER, in which case we could then apply the spectral nudging method to the next IBI operational version.

IBI-OPER is able to keep track the large scale baroclinic patterns of the PSY2V4 system, and therefore, take benefit from the assimilation used on the large scale. But this simple restarting method has 2 significant drawbacks: (i) the time discontinuity inherent to the periodic re-initialization and (ii) the dependency to the large scale system on the shelf where water properties are largely biased by the missing physics. Thus, the solution of IBI-OPER is strongly constrained by the global one. But contrary to the large system, the IBI model configuration allows to resolve regional physical processes by taking into account higher frequency signals (such as tide, diurnal cycle ...) and their nonlinear interactions with the low-frequency circulation. Also the coastline, coastal bathymetry and coastal forcings (runoff) are better represented in the regional system. So the solution IBI-REF is better in the shelf area where most of high frequency processes occur. The spectral nudging method chosen for IBI-NUDG has permitted to "nudge" the low frequency IBI system solution towards the large scale PSY2V4 solution where this one is supposed to be better (off the shelf) and has permitted to let free the IBI solution on the shelf where the regional model physics is better adapted.

The IBI-REF, PSY2V4 and IBI-NUDG daily mean Sea Level Anomaly (SLA) has been qualitatively compared to AVISO one off the Gibraltar straight. In Fig. 14, the date of 2010-09-16 is taken as an example. PSY2V4 solution is obviously coarser than IBI-REF one but the meso-scale structures are better positioned due to the SLA assimilation. In this area, IBI-NUDG solution is closer to the AVISO SLA than IBI-REF by taking benefit of PSY2V4 solution with a best resolution of eddies and SLA gradients.

Downscaling from Oceanic Global Circulation Model towards Regional and Coastal Model using spectral nudging techniques: application to the Mediterranean Sea and IBI area models

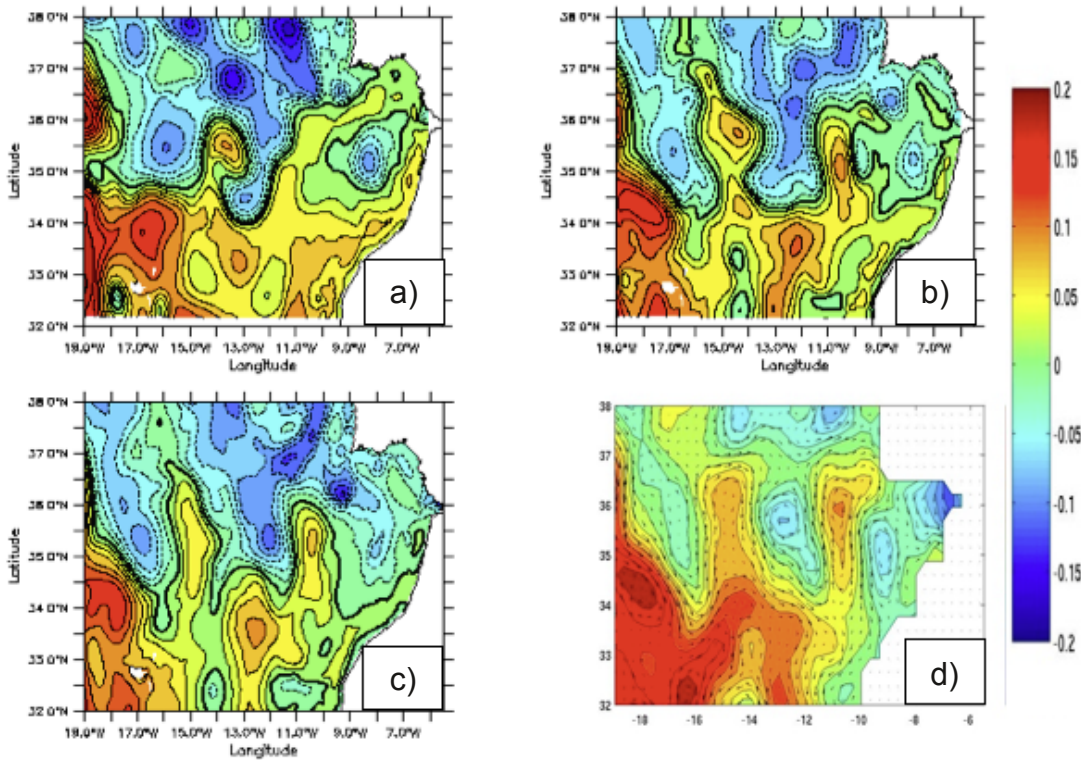
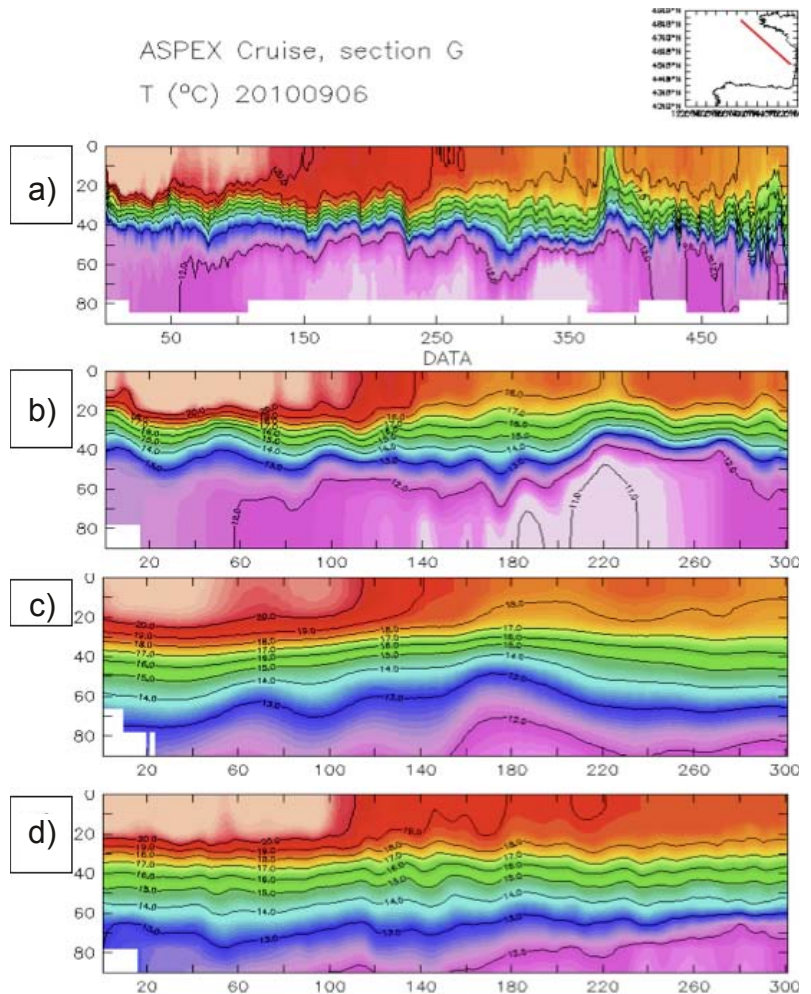


Figure 14:  
SLA comparison between  
a) IBI-REF,  
b) IBI-NUDG,  
c) PSY2 and  
d) AVISO.

In Fig. 15, the IBI-OPER, PSY2V4 and IBI-NUDG daily mean temperature of 2010-09-06 is compared to the ASPEX Cruise section one (Le Boyer et al, 2013), on the shelf in the Bay of Biscay off the Aquitaine and Britain French coasts. The thermocline as well as its associated temperature gradient is better resolved in IBI-NUDG with a depth between about 20m and 40m. The strongest observed eddies seem to be noticeable in the IBI-NUDG solution when the thermocline goes up for the anticlockwise eddies (cyclones) or down for the clockwise eddies (anticyclones). In this area, IBI-NUDG is free since the nudging from PSY2V4 is switched off above the shelf due to chosen tapering function. So the high frequency and small scale physical processes which are dominating in the shelf region, are better resolved by IBI-NUDG than PSY2V4 or IBI-OPER. Indeed, the physics, the resolution as well as the data used for the assimilation of PSY2V4 aren't adapted for this area, and the weekly restarting of IBI-OPER by PSY2V4 prevents small structures to develop on the shelf area.

Figure 15:  
Comparison of the temperature  
along the ASPEX Cruise  
section G (ASPEX campaign 2010, Louis  
Marié) on the 2010-09-06:  
a) observation,  
b) IBI-NUDG,  
c) PSY2,  
d) IBI-OPER.



Downscaling from Oceanic Global Circulation Model towards Regional and Coastal Model using spectral nudging techniques: application to the Mediterranean Sea and IBI area models

In Fig. 16 the SST bias significantly decreases from IBI-OPER to IBI-NUDG on the shelf for the same reasons explained above. This decrease is particularly noticeable in the English Channel and the Ireland Sea where the strong tidal fronts prevail. A nudging in this area would be obviously useless since PSY2V4 can't resolve tide processes.

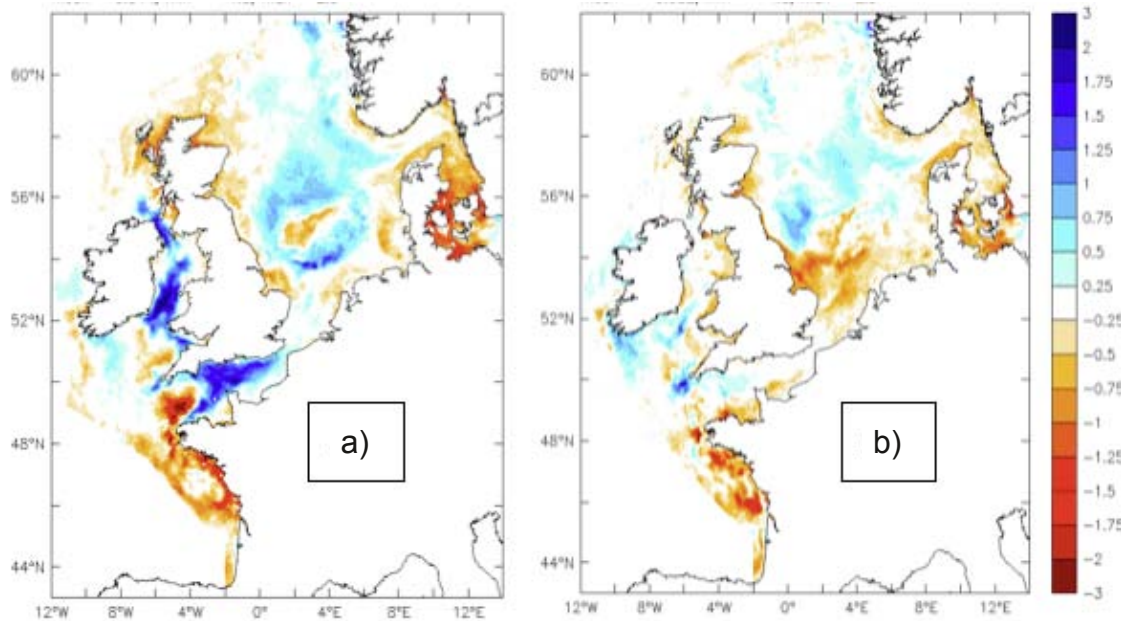


Figure 16: Mean SST bias vs CMS R/S data (Centre de Météo Spatial) in September 2010 (in °C):  
 a) CMS - IBI-OPER , b) CMS - IBI-NUDG .

In Fig. 17 and 18 the SLA bias and RMS significantly decrease from IBI-REF to IBI-NUDG off the shelf. In this area, the large scale and low frequency process SLA is quite well represented by PSY2V4 which assimilates altimetry data and consequently the spectral nudging improves IBI solution. These results complete the previous one (Fig. 16) and confirm the right choice of the tapering function which allows IBI-NUDG to run free in the shelf area.

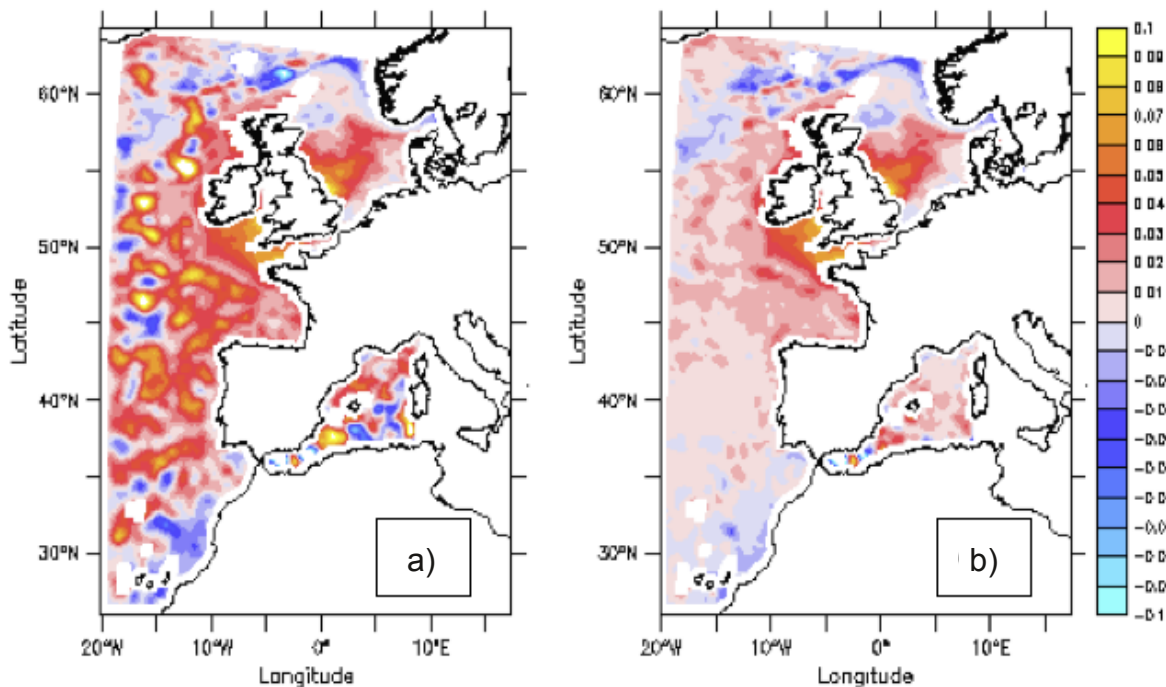


Figure 17: Mean SLA bias vs AVISO (in m) for the run period (2010/03/30 – 2010/10/18) :  
 a) AVISO - IBI-REF , b) AVISO - IBI-NUDG .

Downscaling from Oceanic Global Circulation Model towards Regional and Coastal Model using spectral nudging techniques: application to the Mediterranean Sea and IBI area models

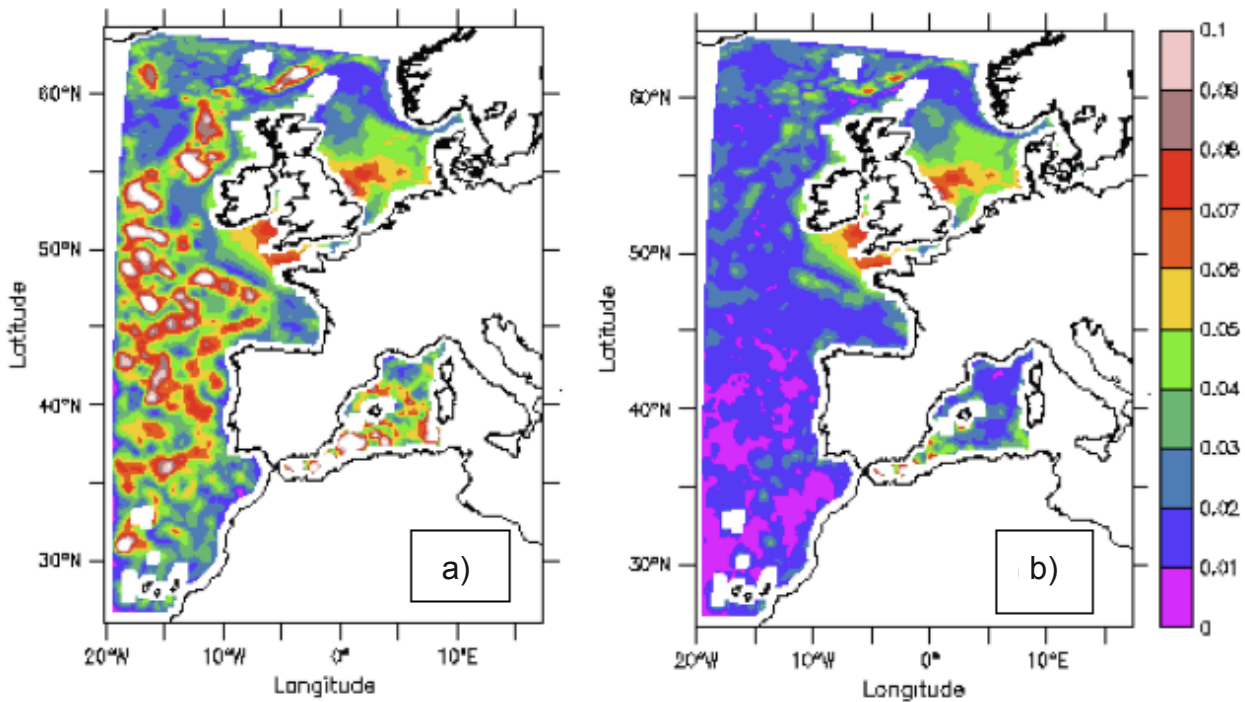


Figure 18: SLA RMS vs AVISO (in m) for the run period (2010/03/30 – 2010/10/18): a) AVISO - IBI-REF , b) AVISO - IBI-NUDG .

We can notice the bias and RMSE of IBI-NUDG seem to increase with the latitude off the shelf and especially along the shelf break. Indeed, the effective resolution of PSY2V4 decreases with the latitude and becomes too low in the high latitudes to resolve meso-scale structures: PSY2V4 is no more eddy-resolving. It can still represent large eddies advected in this area by the North Atlantic Drift (NAD) but not meso-scale eddies generated locally and especially close to the shelf break where slope current or other along break currents can become unstable.

Consequently an improvement of this spectral nudging method would consist in finding a low pass spatial filter depending on the latitude  $\varphi$  ; i.e. with a cut off frequency  $T_c(\varphi)$  increasing with  $\varphi$ . The energy injection scale described previously depends on the Rossby radius which is a characteristic scale of the meso-scale structures (Stammer 97, Penven et al 2005). If we consider in 1<sup>st</sup> approximation the first baroclinic Rossby radius  $R_0$  which decreases in the latitude  $\varphi$  : the higher is  $\varphi$  , the smaller is  $R_0$  and the larger is  $T_c$ . Chelton et al, 1998 generated a global climatology of  $R_0$  from T-S profiles and they established a least squares estimate of the zonally averaged  $R_0$  by regression onto a quadratic function of inverse latitude. As  $T_c$  must increase when  $R_0$  decreases, we can approximate  $T_c$  by a function of inverse of  $R_0$ . In low latitudes,  $R_0$  is large:  $R_0(0^\circ \leq |\varphi| \leq 10^\circ) = R_{0eq} \sim 200\text{km}$  on average according to the climatology of Chelton et al, 1998. If we suppose that the parent system resolution  $\Delta x$  is enough to resolve the large scale structures in the equatorial band, then we can consider  $T_c(0^\circ \leq |\varphi| \leq 10^\circ) = 1 \cdot \Delta x$  . So we can choose the following function:

$$T_c(\varphi) = R_{0eq} \cdot R_0^{-1}(\varphi) \cdot \Delta X \tag{5}$$

This function verifies the value of  $T_c \sim 7\Delta x$  in mid-latitudes as found in this study, with  $R_{0eq} \sim 200\text{km}$  and  $R_0(30^\circ \leq \varphi \leq 40^\circ) \sim 30\text{km}$ . The smoothing can be applied by band of latitude: each band ( $\varphi_0 \leq \varphi \leq \varphi_1$ ) can be defined by a specific integer  $T_c$  which is calculated by Eq. (5).

Mercator Ocean has developed a spectral nudging tool SPECI dedicated for the next IBI operational system version and possibly other regional systems embedded in global one. SPECI takes into account this improvement. Figure 19 sums up the steps of SPECI to generate the nudging fields.

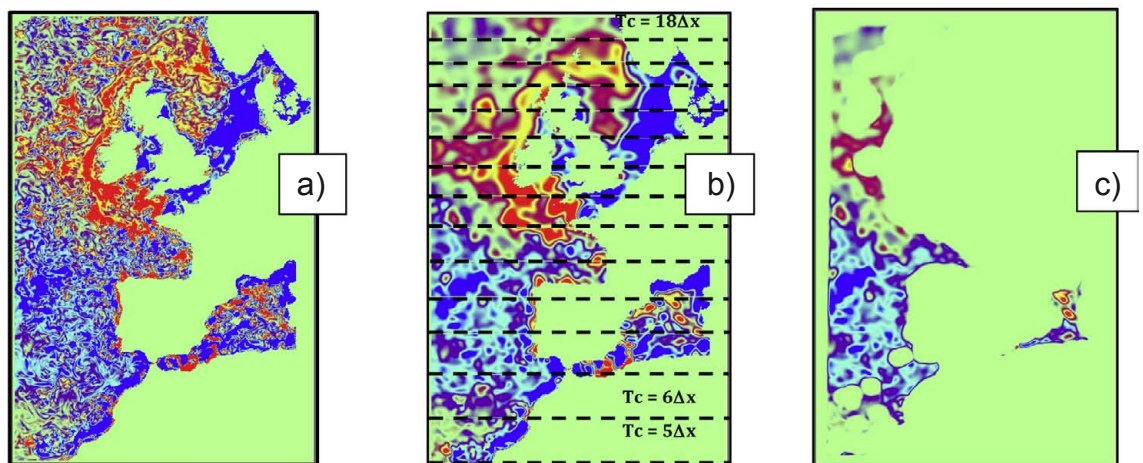


Figure 19: Steps of SPECI for the calculation of  $f(x,y,z) \cdot \langle X_p - X_c \rangle$  . SST is represented here. a) the difference of the weekly means of the SST of PSY2 and IBI, ie.  $X_p - X_c$  . b) the latitude-dependent space Shapiro smoothing of the previous difference, ie.  $\langle X_p - X_c \rangle$  . And c) the application of the tapering function, ie.  $f(x,y,z) \cdot \langle X_p - X_c \rangle$  .

## Downscaling from Oceanic Global Circulation Model towards Regional and Coastal Model using spectral nudging techniques: application to the Mediterranean Sea and IBI area models

### Conclusion - Perspectives

The spectral nudging technique appears as a promising method in order to maintain coherence between regional model and large scale analysis at least over a selected frequency and wavelength band (in this study: the scales  $> 50$  km and  $> 7$  days for the Med Sea case, and the scales  $> 45$  km and  $> 7$  days for the IBI case); it allows to take advantages from data assimilation performed at the global model while maintaining properly the smallest scales variability of the regional model.

Regarding the Med Sea model application, this result was highlighted by diagnostics made through comparisons with observations as satellite SST data which have shown that the bias with observations are reduced in the nudged simulation. The analysis of SSH spectrum over the domain in both simulations also showed that the energy associated to small scales are not significantly affected by the spectral nudging technique. Indeed, only the scales ranged in the frequency and wavelength band selected are nudged toward the global solution, leaving the regional smaller scales free to evolve.

Regarding the IBI model application, comparisons to SLA AVISO, SST CMS and ASPEX section have shown that the nudging has improved IBI model solution off the shelf area where IBI model can really take benefit of the assimilated solution of PSY2V4: the meso-scale eddies are better represented and located due to the SLA assimilation in PSY2V4 among other. Compared to the present operational IBI model (IBI-OPER) which is weekly restarted by PSY2V4 in the whole domain, the SST bias strongly decreases on the shelf where the IBI nudged model (IBI-NUDG) is let free. Indeed, the solution of the high frequency and high resolution IBI model is best on the shelf where data assimilated in PSY2V4 are poor and the resolution of the large model isn't enough. This result is confirmed through the comparison with the ASPEX section on the shelf: the thermocline characteristics of free solution of IBI-NUDG model are far more realistic than PSY2V4 or IBI-OPER.

In addition spectral nudging technique is a low computer cost technique, not intrusive in the code and easy to manage in an operational chain. In this context, the introduction of spectral nudging technique could improve the operational scheme providing an alternative to frequent re-initialisation of the regional model. Besides, spectral nudging could be also a very efficient method useful for regional downscaling of the climate change scenarios.

In terms of perspectives, IBI system nudged by PSY2V4 (and then PSY4) is planned at the end of MyOcean2 first as a demo system and then as a fully operational system for MyOcean Follow On. This update will be applied by Puertos del Estado in the nominal MyOcean IBI system by using a tool SPECI (SPECtral nudging tool) developed by Mercator Ocean. This tool is easy to set up and parameterize, and it generalizes the method applied in the IBI case in this paper since it allows the low pass spatial filter to depend on the latitude.

MANGA system (MANche GAscogne coastal system of PREVIMER) nudged by IBI one is planned too: firstly in reanalysis mode for a 10-year simulation between MANGA and IBIRYS (IBI reanalysis) in the framework of the PPR ENIGME (Evolution Interannuelle de la dynamique dans le golfe de Gascogne et la Manche) lead by IFREMER, and secondly in operational mode. Thus, the downscaling from the large scale global and regional EU systems to the national coastal system will become a reality.

## Downscaling from Oceanic Global Circulation Model towards Regional and Coastal Model using spectral nudging techniques: application to the Mediterranean Sea and IBI area models

### References

- Alexandru, A., R. de Elía, R. Laprise, L. Separovic, and S. Biner, 2009: Sensitivity Study of Regional Climate Model Simulations to Large-scale Nudging Parameters. *Mon. Wea. Rev.*, 137,1666–1686
- Bloom, S. C., Takacs, L. L., Da Silva, A. M. and Ledvina, D., 1996: Data assimilation using incremental analysis updates. *Mon. Wea. Rev.*,124, 1256-1271.
- Cailleau, S., J. Chanut, J.-M. Lellouche, B. Levier, C. Maraldi, G. Reffray, M. G. Sotillo 2012: Towards a regional ocean forecasting system for the IBI (Iberia-Biscay-Ireland area): developments and improvements within the ECOOP project framework. *Ocean Sci.*, 8, 143-159.
- Chelton, D. B., A. R DeSzoeke, M. G. Schlax, 1998: Geophysical variability of the first baroclinic Rossby radius of deformation. *J. Phys. Oceanogr.*, 28, 433-460.
- Eden, C., R. J. Greatbatch, and C. W. Böning, 2004: Adiabatically correcting an eddy-permitting model using large-scale hydrographic data: Application to the Gulf Stream and the North Atlantic Current. *J. Phys. Oceanogr.*, 34, 701– 719.
- Klein, P., Hua, B., Lapeyre, G., Capet, X., Gentil, S. L., Sasaki, H., 2008 : Upper ocean turbulence from high 3-D resolution simulations, *J. Phys Oceanogr.* **38**, 8 1748-1763.
- Lascaratos, A., R. Williams, and E. Tragou, 1993: A mixed layer study of the formation of Levantine Intermediate Water *J. Geo-phys. Res.*, 98 (C8), 14 739–14 749.
- Lazure P., Dumas, F., 2008: An external-internal mode coupling for a 3D hydrodynamical model for applicaitons at regional scales (MARS). *Adv. In. Water Resour.* 31(12): 233-250.
- Le Boyer, A., G. Charria, B. Le Cann, P. Lazure, L. Marié, 2013: Circulation on the shelf and the upper slope of the Bay of Biscay. *Continental Shelf Research*, 55, 97-107.
- Madec G., Delecluse P., Imbard M., Lévy C., 1998: OPA 8.1 Ocean general circulation model reference manual. Institut Pierre-Simon Laplace, 20, p. 91.
- Madec G., 2008: NEMO Ocean General Circulation Model Reference Manuel. Internal Report. LODYC/IPSL, Paris.
- Maraldi C., J. Chanut, B. Levier, N. Ayoub, P. De Mey, G. Reffray, F. Lyard, S. Cailleau, M. Drevillon, E. A. Fanjul, M. G. Sotillo, P. Marsaleix, and the Mercator Research and Development Team .NEMO on the shelf: assessment of the Iberia–Biscay–Ireland configuration. *Ocean Sci.*, 9, 745–771, 2013.
- MEDOC Group, 1970: Observation of formation of deep water in the Mediterranean Sea, 1969. *Nature*, 227:1037-1040.
- Millot, C., 1987: Circulation in the Western Mediterranean. *Oceanol. Acta* 10 2, 143–149.
- Millot C., 1990: The Gulf of Lions' hydrodynamics. *Continental Shelf Research*, 10 (9-11) : 885-894.
- Millot C., 1999: Circulation in the Western Mediterranean Sea. *Journal of Marine Systems*, 20 : 423-442.
- Penven, P and V. Echevin, 2005: Average circulation, seasonal cycle, and mesoscale dynamics of the Peru Current System: a modeling approach. *J. Geophys. Res.*, 110 (C1), 1-21.
- Sheng, J., Greatbatch, R.J., Tang, L., Zhai, X., 2005: A new two-way nesting technique for ocean modeling based on the smoothed semi-prognostic method. *Ocean Dynamic*, 55, 62-17.
- Skamarock, W. C., 2004: Evaluating Mesoscale NWP Models Using Kinetic Energy Spectra. *Mon. Wea., Rev.*, 132, 3019-3032
- Stammer, D., 1997: Global characteristics of ocean variability estimated from regional TOPEX/Poseidon altimeter measurements. *J. Phys. Oceanogr.*, 27, 1743–1769.
- Von Storch, H., H. Langenberg, and F. Feser, 2000: A spectral nudging technique for dynamical downscaling purposes. *Mon. Wea. Rev.*, 128, 3664–3673.
- Wüst, G., 1961: On the vertical circulation of the Mediterranean Sea. *J. Geophys. Res.*, 66, 3261–3271

# EVALUATION OF THE HYDROLOGY AND DYNAMICS OF THE OPERATIONAL MARS3D CONFIGURATION OF THE BAY OF BISCAY

By *H. Berger*<sup>(1)</sup>, *F. Dumas*<sup>(2)</sup>, *S. Petton*<sup>(3)</sup>, *P. Lazure*<sup>(2)</sup>

<sup>1</sup>IFREMER, Brest, France, DYNECO/PELAGOS

<sup>2</sup>IFREMER, Brest, France, DYNECO/PHYSED

<sup>3</sup>IFREMER, L'Argenton, LPI

## Abstract

We present an assessment of the performances of the operational configuration of the Bay of Biscay used in Previmer ; it concerns the hydrology and the dynamics. The model simulation has been validated at different time and space scales by comparing its results with moorings, buoys and satellite data. Recent measurements of sea surface temperature and salinity, bottom temperature and currents on the continental shelf and slope have been used. These comparisons demonstrate the good ability of the model to reproduce the heat content above the continental shelf despite some weak bias, while the results for surface salinity along the coast are satisfactory for all locations. Using the recent ADCP measurements of the ASPEX moorings (Leboyer et al. 2013), we assess the circulation above the continental shelf and the continental slope. Except for extreme events like the strong poleward current in October 2009, the circulation above the shelf is reproduced in a satisfying manner in terms of direction, amplitude and variability. Above the slope, the model is not able to accurately reproduce the observed currents.

## Introduction

Two MANGA (MANche GAscogne) configurations of MARS3D (Model for Applications at Regional Scale, Lazure and Dumas, 2008) have been set up. A medium resolution model with a 2.5km grid and a low resolution model with a 4km grid (MANGAE4000). In the present discussion, we focus on the latter, developed within the PREVIMER project for operational purposes. The MANGAE4000 configuration serves for research purpose on various fields such as physical oceanography, sedimentology, fisheries and biogeochemistry. To be able to provide correct forecasts and conduct researches based on this configuration, we must be able to have an overview of the model capability to reproduce past events. Indeed, being able to correctly simulate the past observations is a necessary step to be confident in the ability to simulate the main physical processes which are at stake in the Bay of Biscay. For these reasons, many comparisons with various observations such as in-situ and satellite measurements for hydrology and ADCP observations for currents have been conducted. This paper is composed as follows. The first part briefly describes the model characteristics. The second part gives a description of the data sets used for validation. The third part presents the validation of the hydrology with temperature comparisons for surface and bottom layers and salinity comparisons for the surface. The fourth part presents a comparison between MANGAE4000 and observed currents. Finally, conclusions and requirements for further investigations are outlined in the fifth part.

## Characteristics of the MANGAE4000 configuration

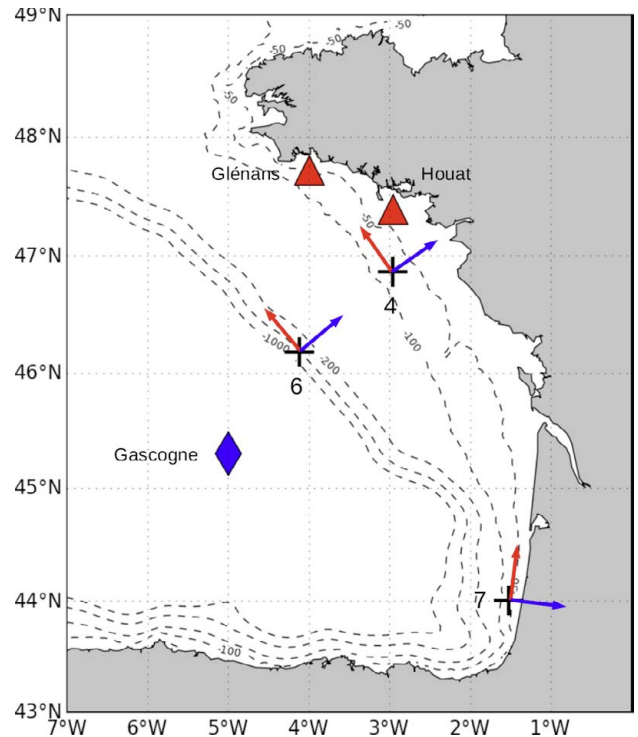
The MANGAE400 configuration encompasses the Bay of Biscay from 18°W to 9.5°E and from 41°N to 55°N with a 30 sigma levels C grid. The domain has been extended to the west to remove unrealistic gyre circulation beyond the continental slope as observed in the previous configuration (Lazure et al., 2008). We use a hindcast of the PREVIMER operational system covering the 2006-2013 period, with the following characteristics. The bathymetry has been filtered out in order to reduce errors in the pressure gradient computation. The tracers advection uses an upwind 5<sup>th</sup> order and multidimensional MACHO3D scheme (Leonard et al., 1996) and the momentum is 3<sup>rd</sup> order QUICK. Vertical advection uses a 5<sup>th</sup> order COMPACT scheme and vertical turbulence is based on a Generalized Length Scale formulation of the k-ε scheme (Umlauf et al., 2005).

The northern, eastern, southern and western open boundaries and the initial conditions are provided by the global analysis from the PSY2V4 Mercator system. Atmospheric forcing are provided by the ARPEGE reanalysis of Météo France (Salas y Méria et al., 2005), with a resolution of 0.5° and 6 hours. Tides are forced along the boundary using the FES 2004 harmonical components (Lyard et al., 2006) and the 72 accounted rivers outflows come from daily observations. Model outputs are saved on an hour basis for all the prognostic variables: temperature, salinity, sea surface height, zonal, meridional and vertical velocities and diffusivity for the whole domain. Three-days mean outputs are also provided to remove tidal frequencies for all outputs thanks to a Demerliac filter (Demerliac, 1973).

## In-situ and satellite data-sets used

Model results for the hydrology along the coast have been compared with SMATCH in-situ SST and SSS measurements from the Island Network (Lazure et al., 2006). This network provides high frequency measurements varying between 10 min and 1h (Charria et al, 2014). Overall, 14 moorings spread along the western French and the northern Spanish coast are available but only Glenans and Houat moorings are discussed here. We also use the Gascogne buoy data which allow comparison of model results with long term SST measurements in the open ocean. Synoptic and climatological SST comparisons from 2008 to 2011 have been done using the SEVIRI satellite observations (Robinson et al., 2004, 11km resolution). Monthly means and monthly climatology were computed using daily observation from 2008 to 2011. Bottom temperatures are extracted from the BOBYCLIM climatology based on all available observations in the Bay of Biscay from the seventies (Vandermeirsch et al., 2010). MANGAE4000 dynamics was compared with the recent ASPEX observations based on ten ADCPs (Leboyer et al., 2013). These moorings are disposed along 3 cross-shore transects and allow an assessment of the model circulation for the alongshore and cross-shore directions at different depths from 10m to 450m. Only ASPEX4, 6 and 7 are discussed here. Both the ASPEX and SMATCH data are filtered out to remove high frequencies (i.e. mostly tides) since we are interested in subtidal circulation. The locations of all of these moorings can be seen on Figure 1.

*Figure 1 : Positions of in-situ observations used. Red triangles represent the Glénans and Houat SMATCH moorings which provide SST and SSS measurements. The blue diamond represents the Gascogne buoy which provides SST measurements. Black crosses represent the position of the ASPEX mooring which provide current measurements. The red line give the alongshore direction while the blue line give the cross-shore direction. The dashed lines present the topography for 50, 100, 200 and 1000 meter depth.*



## Validation of the hydrology

Comparison of the SST for Glenans, Houat and Gascogne moorings are presented on Figure 2 from 2010 to 2011. The large amplitude of the SST seasonal variations are correctly reproduced. Differences between maximum temperature during the summer and minimal temperatures during the winter reach around 10°C along the coast in the model like in the observations ; it reaches only around 9°C at the location of Gascogne buoy, 1°C lower than in the observations because surface temperature during the winter are too warm (around 2°C) in MANGAE4000. Such bias does not appear along the coast and modeled temperatures in winter are accurately reproduced despite temporary differences which do not exceed 0.2°C.

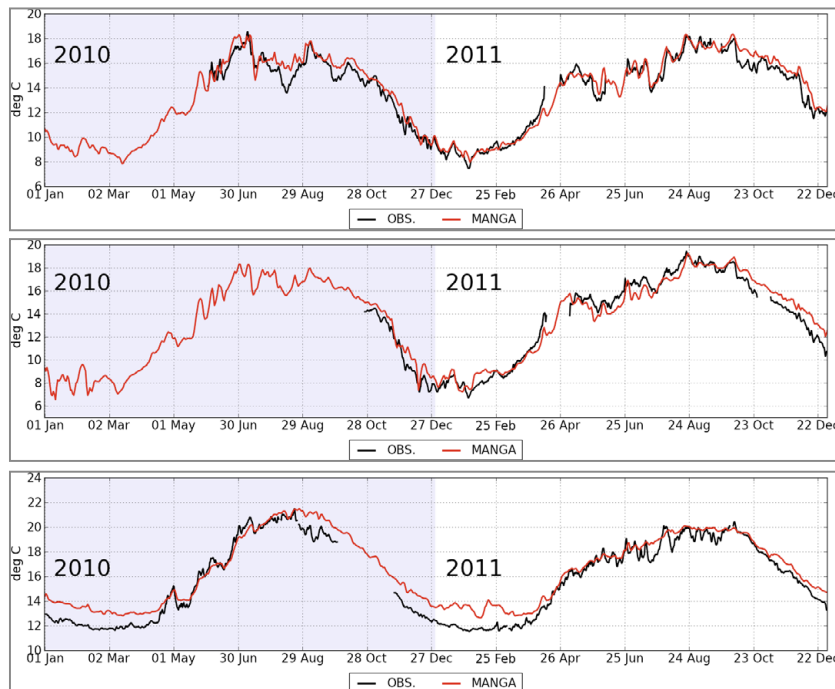


*Figure 2 : Comparison of Sea Surface Temperature time series from July 2010 to July 2011 between the MANGAE4000 outputs and the Island Network moorings Glénans at 4°W 47.72°N (top), Houat at -2.96°W 47.39°N (middle) and with the Gascogne buoy at 5°W 45.30°N. Positions of these moorings appears on Figure 1.*

The increase of the SST from the middle of February to the end of August is also accurately reproduced along the coast and in the open ocean, although a limited cold bias (0.1°C) exists in the model at Houat location. Above the continental shelf (Glénans and Houat), the model is unable to catch at the right time the rapid warming occurring during the middle of April : it is delayed of 10 to 12 days in the model, around April 26<sup>th</sup>. In 2011, after the maximum temperature during August, for all regions, a short 5-6 days warming take place between the end of September and the beginning of October in the observations. This warming, associated with the occurrence of a narrow poleward coastal and warm current from the Spanish coast (Batifoullet et al. 2013), is accurately reproduced in MANGAE4000. However, the following 4-5 days strong cooling is two times larger in the observations (~2°C) than in the model (~1°C). During the autumn, from October to the end of December, a systematic warm bias occurs for all moorings, with increasing differences from the coast (~0.1°C) to the open ocean (~1.5°C) between model and observations. This bias cannot be explained either by the short cooling described previously as it does not occur every year, nor by a time lag as the cooling starts at the right time in the model.

Synoptic comparisons of the climatological SST between SEVIRI and MANGAE4000 data from 2008 to 2011 for February, May, August and November are shown on Figure 3. In February, the model is fairly accurate and misfits above the shelf are rather weak. Mean modeled SST are underestimated along the French coast from 45°N to 47.5°N ( $-0.6/0.8^{\circ}\text{C}$ ) while it is too warm above the rest of the shelf ( $0.4^{\circ}\text{C}$ ). However, beyond the slope, differences are larger and reach more than  $1^{\circ}\text{C}$ , as observed previously at the Gascogne buoy. In May, despite the results between in-situ and model data (Figure 2), a large cold bias is observed in the model for all shallow areas, from the Channel to the continental shelf of the Bay of Biscay. This general bias varies from  $\sim 1/1.2^{\circ}\text{C}$  in the Channel to more than  $1.8^{\circ}\text{C}$  in the Bay of Biscay. For the latter region, a lack of stratification may be responsible of the warming deficit of the SST. Indeed, on average, the stratification in the model does not set in before the second half of April. The simulated SST in August in MANGAE4000 is satisfactory with limited differences, the model being slightly too cold in regions with shallow depth and really close to observations beyond the slope. As mentioned in the previous paragraph, the autumn is characterized by a large warm bias in the model, which increases from the coast ( $\sim 1/1.2^{\circ}\text{C}$ ) to the open ocean ( $\sim 2^{\circ}\text{C}$ ) in November. The origin of this bias is not clear and it may result from several physical processes : the surface heat budget, with an insufficient cooling due to air-sea fluxes, a lack of mixing forced by the atmosphere in the surface layer, or the stratification which remains too strong and delays the surface cooling.

Figure 3 also displays monthly bottom temperature differences above the shelf between BOBYCLIM climatological and MANGAE400 data (observations – model, computed using 2008-2011 monthly fields). Here we only discuss the values above the continental shelf, as the confidence level in the climatological data over the abyssal plain does not allow a valuable assessment of the bottom temperature. In general, in the Bay of Biscay the bottom temperature in the model appears warmer ( $\sim 0.6^{\circ}\text{C}$ ) than the climatology, except in the coastal region between 45°N and 47°N where it is colder (up to  $1.8^{\circ}\text{C}$  in August). In February, May and August, the eastern Channel in MANGAE4000 is colder than in the observations but warmer during November. Outside of the Channel, this warm bias may result from too important mixing or numerical diffusion, the two bringing too much heat to the bottom. Indeed, the negative surface heat budget during this period may not be sufficiently important and may limit the deep cooling before the stratification takes place and isolates the deep water masses. Along the coast, the sources of this cold bias remain undefined, but insufficient mixing between the warm surface water and cold deep waters because of stratification may be an explanation. However, it must be kept in mind that this assessment of bottom temperature relies on a comparison with a climatology which by essence does not take into account the inter-annual variability from 2008 to 2011 only. The lack of long time observations of bottom temperature does not permit a comprehensive assessment of the model errors.

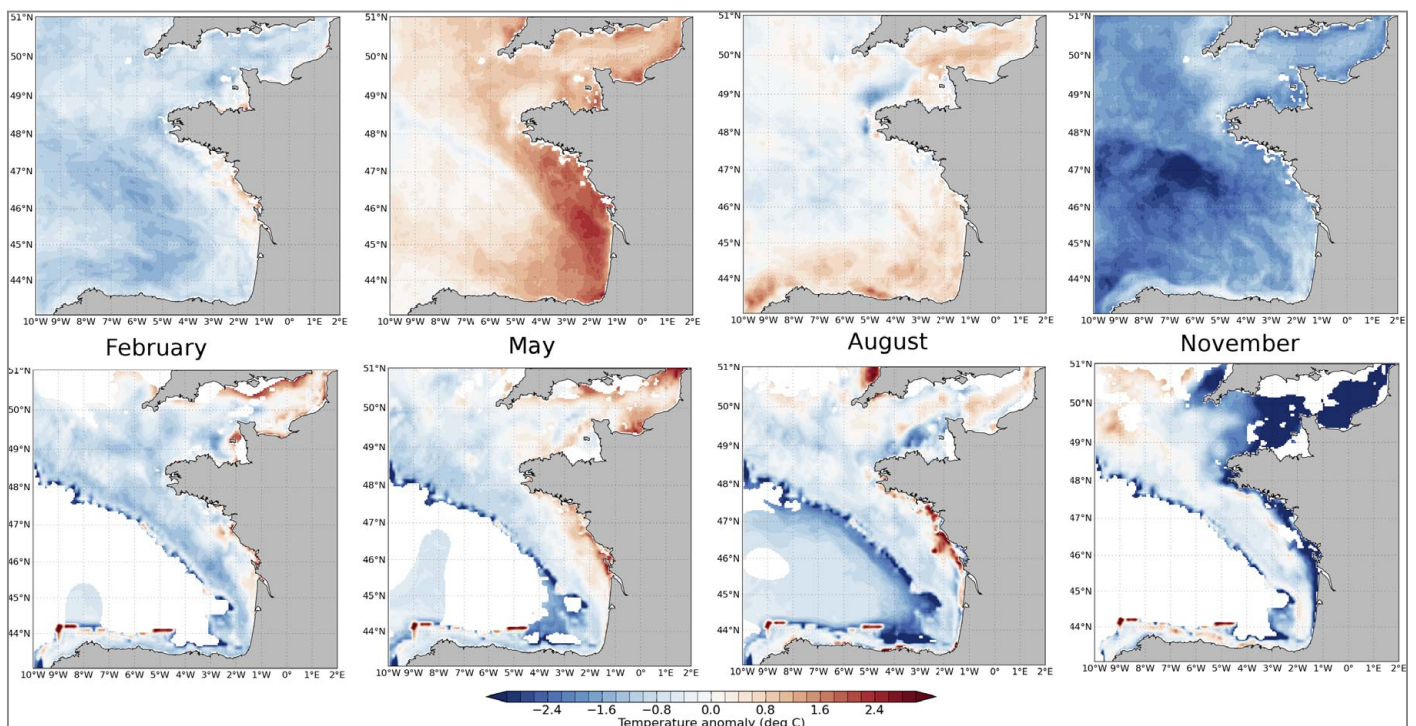


Figure 3 : Temperature anomalies (observation – model) in the Bay of Biscay for the surface (top) and the bottom (bottom) layers for the months of February, May, August and November between Seviri data and MANGAE4000 for the SST and between BOBYCLIM data and MANGAE4000 for the bottom temperature. Anomalies are computed using monthly fields from 2008 to 2012 and observed data have been interpolated on the MANGAE4000 grid.

Comparisons of the interannual SST anomalies between the SEVIRI satellite observations and the model (Figure 4) show that the model SST is always warmer than the observations during February, while August warm and cold bias alternate. During February, the warm bias is relatively large in the open ocean (between 0.8°C and 1.5°C) and limited in the continental shelf (~0.4/0.6°C, sometimes higher locally) in the Bay of Biscay. The cold bias in the regions of freshwater influence (ROFI), is important during November (and the autumn) with more than 2°C, but limited and localized during the other months. These located discrepancies lead us to infer that the vertical mixing which is under the influence of both saline and thermal stratification may not be fully accurate in these complex situations. During August, a cold bias exists in the Channel east of 4°W, but it is only significant in 2009 and 2010. In this region, we clearly see the western front in the Channel, which separates the homogeneous water east of 4.5°W and the stratified waters. During this month, we can also observe a complex structure of the SST anomaly in the Ushant front, with important cold and warm anomalies compared with the surrounding regions. In this case, the 4km resolution does not allow an accurate simulation of the front and may partly explains these large differences. Indeed, as this anomaly exist for all stratified ares, other processes may interfere. For both February and August, the year 2011 exhibits large differences. However, the observed bias with satellite data seems larger than the bias with in-situ measurements which have been shown previously. During these periods, the model SST agree well with in-situ observations except beyond the slope. Such differences between in-situ and satellite observations are intriguing, but are beyond the scope of this paper.

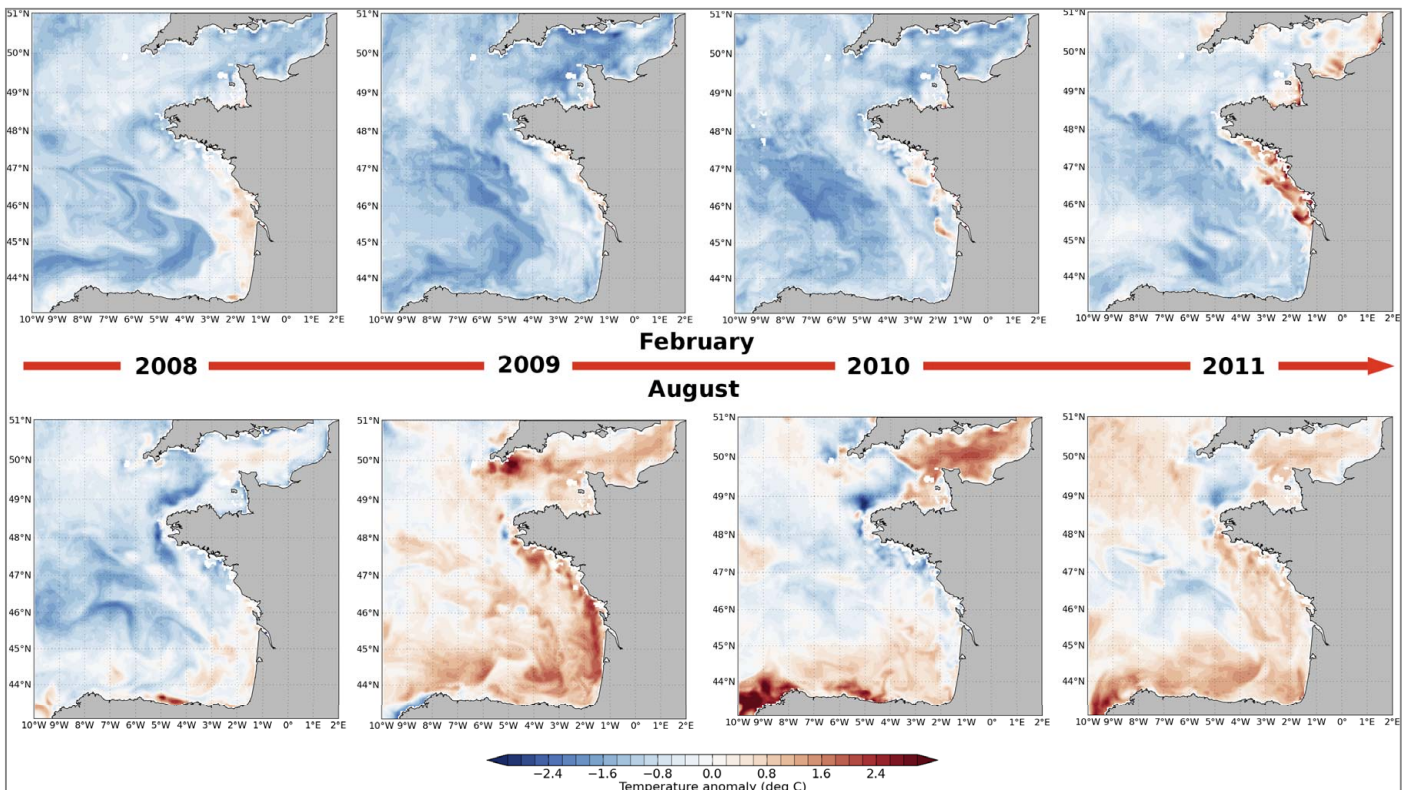


Figure 4 : Interannual variations of the SST anomalies (observations – model) between Sevir satellite observations and MANGAE4000 for February and August from 2008 to 2011. Anomalies are computed using monthly fields from 2008 to 2012 and observed data have been interpolated on the MANGAE4000 grid.

Time series from January 2011 to December 2012 of the observed and modeled Sea Surface Salinity (SSS) at Glénan and Houat are presented on Figure 5. It allows an evaluation of MANGAE4000 ability to reproduce large plume dynamics (i.e. mostly Loire, Gironde, Adour and several other rivers). During winter 2011, heavy precipitations are responsible of extended plumes formation along the coast with moderate salinity at Glénan (33.5 psu min) and Houat (28 psu min) locations. During this period, large but short variations linked to flooding events are noticeable (January 8<sup>th</sup> and 17<sup>th</sup>, February 21<sup>th</sup> at Houat). Model performances during this period vary from place to place. At Glénan, the model is not able to reproduce the drop of the SSS at the beginning of January 2011 and the stabilization which follows. It simulates a regular decrease until the end of February to

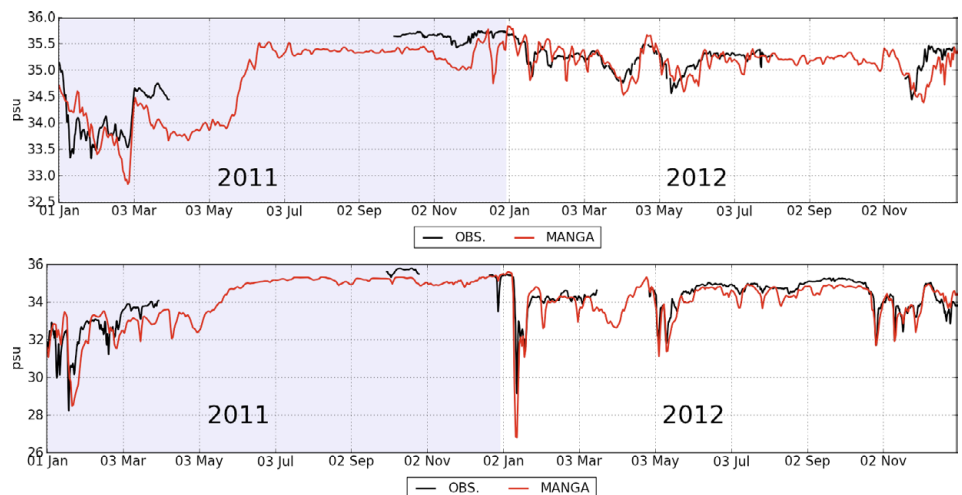


Figure 5 : Comparison of Sea Surface Salinity time series from January 2011 to December 2012 between the MANGAE4000 outputs and the Island Network moorings Glénans at 4°W 47.72°N (top) and Houat at -2.96°W 47.39°N (bottom). Positions of these moorings appears on Figure 1.

reach lower values than in the observations. However, despite error on the amplitude, the model clearly shows the sudden five days increase of the SSS at the beginning of March due to the displacement of the plume. At Houat location, on the other hand, the model has a rather good quality at reproducing the successive SSS drops associated with flooding events, with satisfactory amplitude slightly delayed as regarding the observed time series. For the two locations, very few data are available for the rest of 2011, but it seems that the SSS in MANGAE4000 is biased towards low value. The SSS in 2012 appears largely different compared with 2011 because of limited precipitations ; under this conditions, the representation of the SSS in the model at Glénan and Houat locations is accurate, even if some discrepancies exist occasionally. At Glénan, the SSS during the winter does not decrease as in 2011 and presents a slow decrease from 35.6 psu in January to 34.8 psu in April and misses the high frequency variability. The model is able to reproduce the envelope of the long term evolution, with similar values, but it presents high frequencies variations that are less apparent in the observations. Winter 2012 at Houat is characterized by an extreme and sudden drop of the SSS from 35.3 psu to 29.3 psu within three days (from the 10<sup>th</sup> of January to the 13<sup>th</sup>) and a two steps increase of the SSS until the beginning of February. This rapid drop is well simulated in MANGAE4000 but with a minimum slightly too low. During the rest of the year and particularly during spring and summer, the MANGAE4000 SSS is very accurate at this two locations.

Figure 6 presents the MANGAE4000 SSS in 2012 for the 13<sup>th</sup> and the 22<sup>th</sup> January and illustrates the exceptional variations of the SSS observed at Houat and described previously. First, the drop of the SSS the 10<sup>th</sup> January follows the floodings of the Loire and Vilaine rivers which are maximum the 8<sup>th</sup> of January ( $2600 \text{ m}^3 \cdot \text{s}^{-1}$  for Loire river). The reasons which allow the large amplitude observed this day for the SSS may be a combination of the large amount of freshwater discharge and weak north-easterly winds confining plumes to the west along the coast. After the minimum of SSS on January 13<sup>th</sup>, a first important increase of the SSS occurs on January 14<sup>th</sup> for 4 days and corresponds to the reduction of freshwater discharge by Loire and Vilaine rivers while the second increase from January 19<sup>th</sup> corresponds to north-westerly winds which drives the plume offshore as observed on January 22<sup>th</sup> (figure 8).

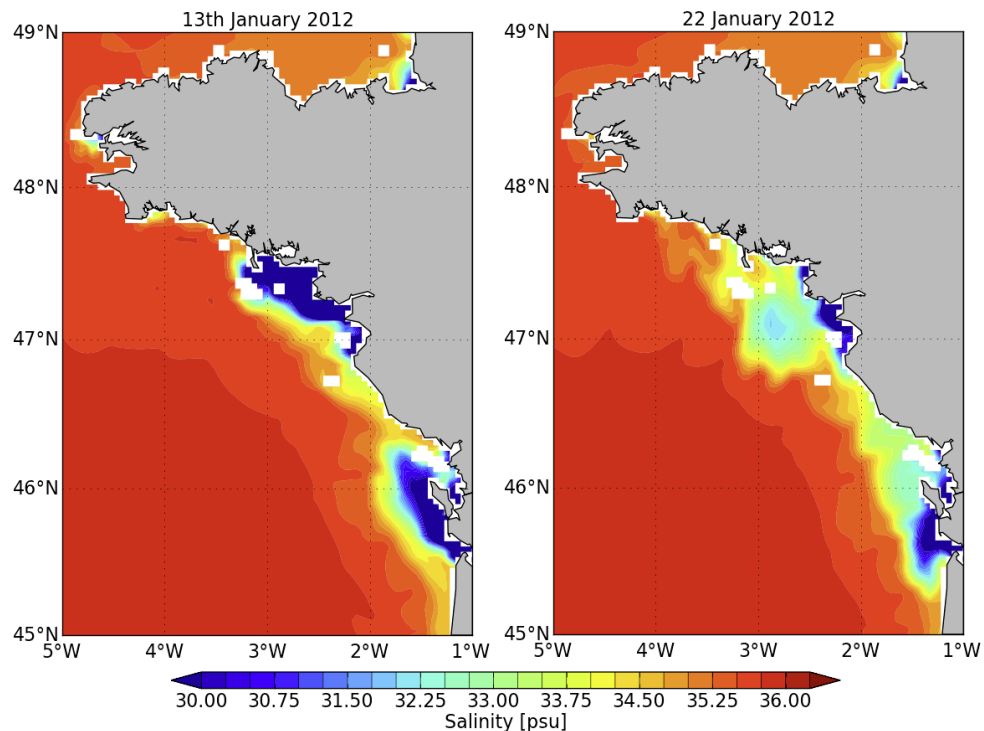


Figure 6 : Daily Sea Surface Salinity in MANGAE4000 for 13th and 22th January 2012 in the north eastern part of the Bay of Biscay. These figures illustrate the exceptional drop of the SSS at Houat and the following dispersion of the plume during the second part of January 2012.

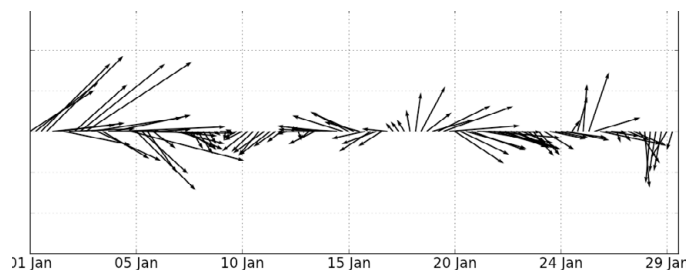


Figure 7 : wind direction from the 1st to the 31th of January 2012 above the Bay of Biscay between 46°N and 48°N and 4°W and 1°W from the ARPEGE reanalysis. Wind direction are northern upwards and eastern clockwise.

## Validation of the dynamics

Previous work of Lazure et al. (2009) about the validation of the MANGA configuration of MARS3D presents only the hydrology because of a lack of observations of the dynamics. Since then, the ASPEX program (Leboyer et al. 2013) brought current measurements above the continental shelf and slope and allow an extensive validation of the model dynamics. Here, we present the results of these comparisons for three of the ten moorings which measured the currents during two periods of time, from July 2009 to May 2010 and from September 2010 to August 2011. Only the 2009-2010 period is discussed here. The currents have been rotated as described in Leboyer et al. (2013) to highlight cross-shore and alongshore circulation (Figure 1).

The circulation above the continental shelf at the location of the ASPEX 4 mooring (Figure 1) is presented on Figure 8 at depth of 10 and 40 meters. Close to the surface, except from September to the end of October 2010, the alongshore and cross-shore MANGAE4000 currents are in good agreement with the observations, for both the variability and the intensity. At this location, the wind driven circulation is mainly alongshore (mainly between 5 and 10 cm.s<sup>-1</sup> vs between 0 and 5 cm.s<sup>-1</sup> for cross-shore circulation), following more or less the topography depending on the season (Leboyer et al. 2013). After the middle of February 2010, the model underestimates the currents intensity and variability (around 5-10 cm.s<sup>-1</sup>), especially in the alongshore direction, but it is able to correctly reproduce the main direction of the circulation. Deeper, at 40 meters, the current intensity is weaker of a few cm.s<sup>-1</sup> and presents less high frequency variability. At this depth the model accuracy is better than at 10 m. The alongshore component of the circulation is also more predominant. The differences between observed and modeled currents in September and October 2010 are intriguing. Indeed, the observations and the model present an important baroclinicity, with stronger currents at 10m than at 40m (up to 20 cm.s<sup>-1</sup> vs 5 cm.s<sup>-1</sup> in alongshore direction) for observations while the model currents are stronger at 40m than at 10m (13 cm.s<sup>-1</sup> vs 5 cm.s<sup>-1</sup> in alongshore direction). However, the mechanisms involved to explain these differences remains not clear : the large oscillation of the observed cross-shore component of the circulation may depend from wind forcing but the winds are weaker at this moment than during the following months. Moreover these oscillations only concern the ASPEX 4 mooring at 10m and only for one year, which may suggest a relation with river plumes and frontal dynamics. Unfortunately, no additional hydrology observations can help us to conclude. Another interesting feature is the representation by the model of the two barotropic events during the middle of January and March 2011, characterized by ~10 cm.s<sup>-1</sup> southward currents. The first event is correctly reproduced by the model, except for the cross-shore component at 40m while the second one is significantly underestimated at the surface in the model.

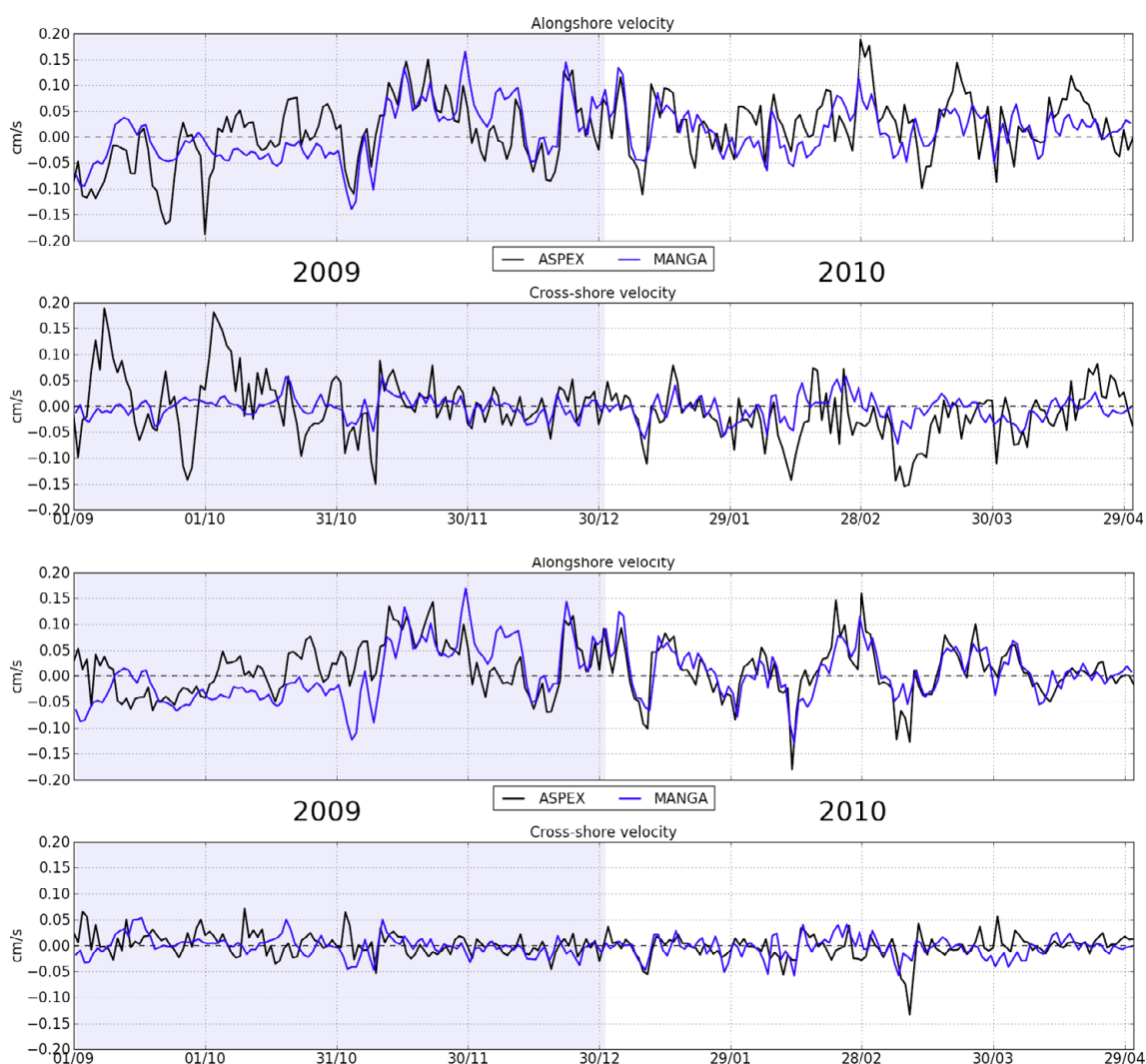


Figure 8 : Comparison of the alongshore and cross-shore components of the circulation at 10 (top) and 40 (bottom) meter depth between ADCP measurements (black) and MANGAE4000 currents at the location of ASPEX 4 (figure 1) above the continental shelf. The orientation of the alongshore and cross-shore components is relative to the bathymetry.

At ASPEX 6 location (Figure 1), above the continental slope (Figure 9), the model dynamics at 60m and 250m is not so efficient than on the shelf. The alongshore circulation clearly dominates for both the observations and MANGAE4000, with an intensity that can reach  $27\text{cm}\cdot\text{s}^{-1}$  vs  $10\text{cm}\cdot\text{s}^{-1}$  for the cross-shore component. On average, the model overestimates the intensity of the alongshore currents at 60m and 250 while the intensity of the cross-shore circulation is satisfying. However, during January 2011, MANGAE4000 alongshore currents remain barotropic while the circulation in the observations seems more baroclinic. This period also corresponds to opposite alongshore dynamics at 60m between observations and model results (north-westward vs south-eastward). During the same time, currents at 250m are in better agreements. It is not the only case of reverse dynamics in the model as it also occurs in September and November 2010. The representation of the topography, the complex forcing mechanisms of the upper slope circulation (Leboyer et al., 2013; Pingree et al., 1989) and the important meso-scale activities in this region do not allow to understand clearly the origins of the model discrepancies. Even realistic boundary conditions cannot insure a proper dynamics because they are too far from the slope and meso-scales dynamics which develops in the model above the abyssal plain can greatly affect the slope dynamics. In addition, the necessity to smooth the bathymetry to avoid errors on the pressure gradient implies that uncertainties are greater in this region. So far, these discrepancies suggest that a realistic simulation of the circulation over the slope of the Bay of Biscay requires an assimilation capability.

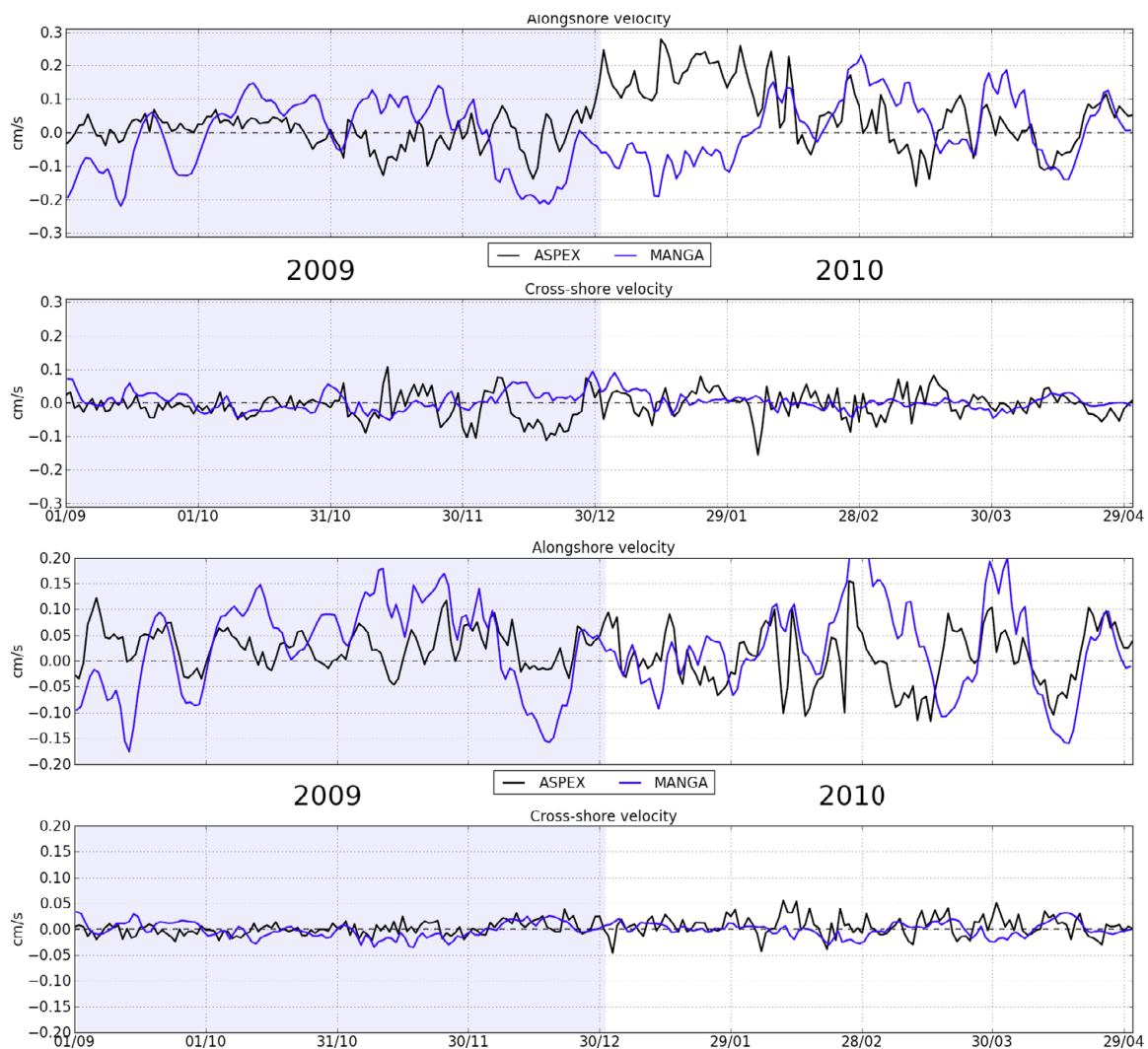


Figure 9 : Comparison of the alongshore and cross-shore components of the circulation at 60 (top) and 250 (bottom) meter depth between ADCP measurements (black) and MANGAE4000 currents at the location of ASPEX 6 above the continental shelf in the south-eastern corner of the Bay of Biscay (figure 1). The orientation of the alongshore and cross-shore components is relative to the bathymetry.

The comparison of observed and modeled currents at ASPEX 7 location (Figure 1) reveals some interesting features (Figure 10). The alongshore currents measured by the ADCP are correctly reproduced in MANGAE4000. Their intensity at 20m is relatively good, apart for the October 2009 and January events where it is underestimated (around  $30\text{cm}\cdot\text{s}^{-1}$ ). Deeper, at 40m, the alongshore component of the circulation is very well reproduced after the September 2009 event, and suffers some discrepancies from September to October 2009. At the end of October 2009, an intense poleward current was measured by ASPEX 7 ADCP (Figure 10). This current and the underlying mechanisms linked to westerlies were described by Batifoulier et al. (2013). This current reach  $50\text{cm}\cdot\text{s}^{-1}$  in the observations at 10 and 40m. At 10m in MANGAE4000, this poleward current emerges few days later ; it peaks at  $20\text{cm}\cdot\text{s}^{-1}$  whereas observations show a peak around  $50\text{cm}\cdot\text{s}^{-1}$  ; it lasts 15 days whereas this phenomenon is observed during 5-6 days. At 40m, the beginning and life time of this event are in better agreement with observations, but its intensity remains too weak ( $\sim 20\text{cm}\cdot\text{s}^{-1}$ ) compared with the observed one. In fact, the MANGAE4000 resolution does not allow to accurately reproduce this strong and narrow coastal current (width around 10-15km). The oscillation of the observed alongshore currents at 10m between January 20<sup>th</sup> and February 9<sup>th</sup> do not exist in MANGAE4000 and remind similar events observed y ASPEX 4 ACDP between September and November 2009 (Figure 8). Again, it only occurs in the surface layer and the mechanisms involved remain not clear.

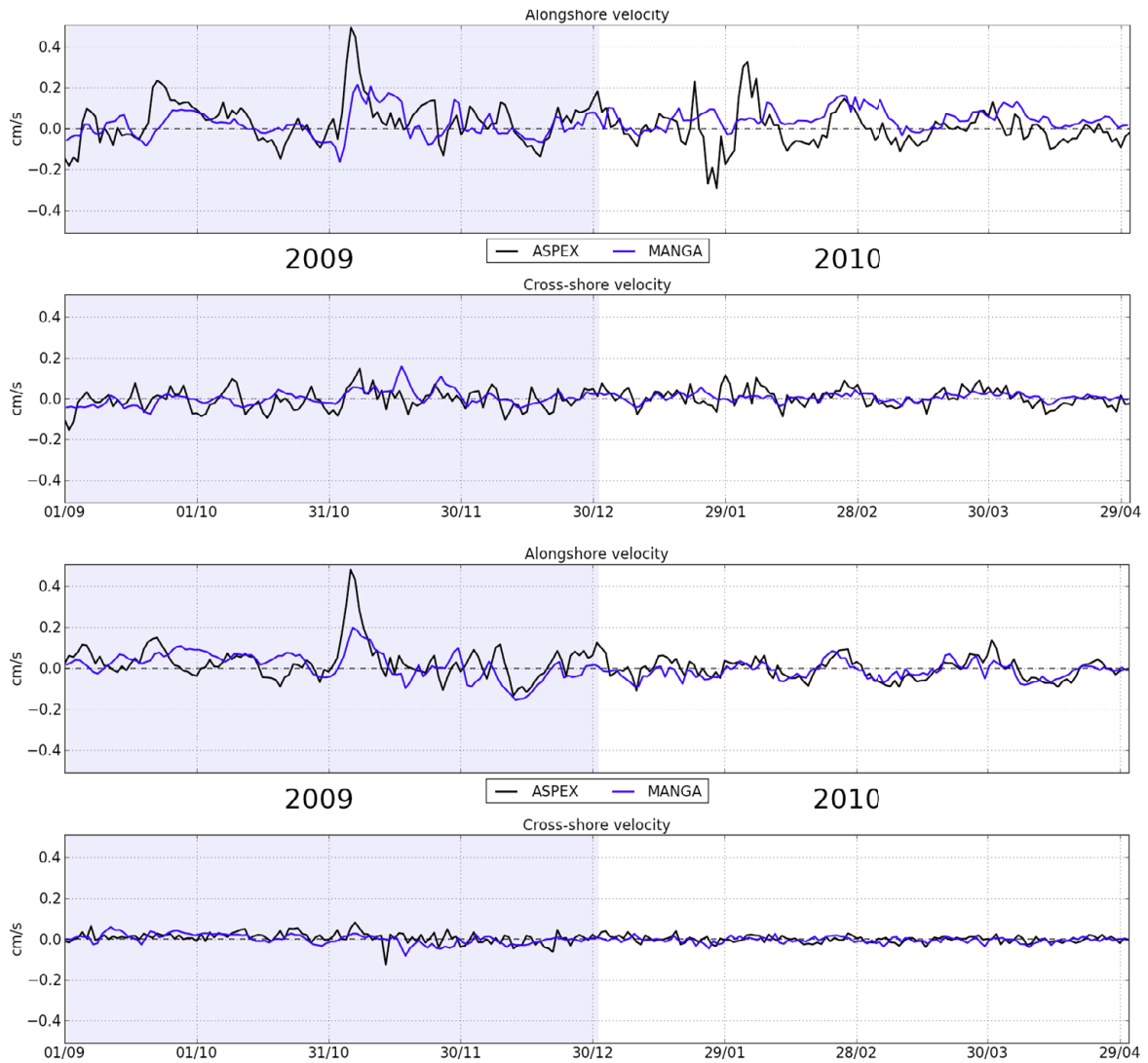


Figure 10 : Comparison of the alongshore and cross-shore components of the circulation at 10 (top) and 40 (bottom) meter depth between ADCP measurements (black) and MANGAE4000 currents at the location of ASPEX 7 (figure 1) above the continental slope. The orientation of the alongshore and cross-shore components is relative to the bathymetry.

## Conclusion

In this paper, we evaluate the hydrology and dynamics of the operational MANGAE4000 configuration of the Bay of Biscay based on MARS3D. Compared with previous work done by [Lazure et al. \(2009\)](#) which do not evaluate the model dynamics because the lack of data : this work leads to a first assessment of the recent progresses done for modeling the Bay of Biscay and the efforts carried out on long time series for currents and hydrology. Concerning the hydrology, MANGAE4000 demonstrate a good ability to reproduce the SST variations at from weekly to seasonal scales. Synoptic and in-situ comparisons shown that despite some limited bias during spring and autumn for the shelf and winter beyond the slope, the MANGAE4000 SST is accurately reproduced. Bottom temperature, although slightly warmer in the model, is very satisfactory above the shelf in the Bay of Biscay. Results for SSS are also satisfactory. Rapid changes of the SSS due to flooding events during the winter are correctly reproduced most of the time and the model no longer underestimates the SSS during spring and summer when river outflow decrease compared with [Lazure et al. \(2009\)](#). About the dynamics, the shelf circulation is well reproduced in terms of amplitude, direction and variability, but the model tends to underestimate some particular events like the strong poleward current of October 2010 ([Batifoulier et al., 2013](#)). Above the slope, model performances are not satisfactory, modelled currents being not close to the observations most of the time and this evaluation raises the requirement either of an assimilation capability to constraint the meso-scale circulation over the abyssal plain of the Bay of Biscay or do modelling without smoothed topography thanks to increased resolution.

## Acknowledgments

The authors wish to thank the PREVIMER project which allows the development of the MANGAE4000 configuration and the disposal of SMATCH in-situ observations. We thank the CDOCO for providing all the hydrological observations presented in this study. We thank Frédéric Vandermeirsch for providing the monthly BOBYCLIM product for bottom temperatures. We thank Louis Marié for providing the ASPEX current measurements.

## References

- Batifoulier, F., Lazure, P. and Bonneton, P 2013 : Poleward coastal jets induced by westerlies in the Bay of Biscay. *J. of Geo. Re.*, vol 117.
- Cailleau, S., Chanut, J., Levier, B., Maraldi, C. and Reffray, G. 2010 : The new regional generation of Mercator Ocean system in the Iberian Biscay Irish (IBI) area. *Quarterly Newsletter, Mercator Ocean*. 39: 5-15.
- Charria, G., M. Repecaud, L. Quemener, A. Ménesguen, P. Rimmelin-Maury, S. L'Helguen, L. Beaumont, A. Jolivet, P. Morin, E. Macé, P. Lazure, R. Le Gendre, F. Jacqueline, R. Verney, L. Marié, P. Jegou, S. Le Reste, X. André, V. Dutreuil, J.-P. Regnault, H. Jestin, H. Lintanf, P. Pichavant, M. Retho, J.-A. Allenou, J.-Y. Stanisière, A. Bonnat, L. Nonnotte, W. Duros, S. Tarot, T. Carval, P. Le Hir, F. Dumas, F. Vandermeirsch, F. Lecornu 2014: PREVIMER: a contribution to in situ coastal observing systems. *Newsletter Mercator*.
- Demerliac, A. 1973 : Calcul du niveau moyen de la mer. *Rapport du SHOM*, 1973.
- Lazure, P., Jégou, A.M., Kerdreux, M. 2006 : Analysis of salinity measurements near islands on the French continental shelf of the Bay of Biscay. *Scientia Marina*. 70S1 : 7-14.
- Lazure P. and Dumas, F., 2008 : An external-internal mode coupling for a 3D hydrodynamical model for applications at regional scales (MARS). *Adv. In. Water Resour.* 31(12) : 233-250.
- Lazure, P.; Garnier, V.; Dumas, F.; Herry, C.; Chifflet, M. 2009 : Development of a hydrodynamic model of the Bay of Biscay. *Validation of hydrology. Continental Shelf Research*, 29, 985-997.
- Leboyer, A.; Charria, G.; Le Cann, B.; Lazure, P.; Marié, L. 2013 : Circulation on the shelf and the upper slope of the Bay of Biscay. *Cont. Shelf Res.*, vol. 55, 97-107.
- Leonard B. P., Lock A. P. and MacVean M.K., 1996 : Conservative Explicit Unrestricted-Time-Step Multidimensional Constancy-Preserving Advections Schemes. *Monthly Weather Review*, 124 : 2588-2605.
- Lyard, F., F. Lefèvre, T. Letellier and O. Francis. 2006 : Modelling the global ocean tides: a modern insight from FES2004. *Ocean Dynamics*, 56: 394-415.
- Pingree, R.D., Le Cann, B. 1989 : Celtic and Armorican slope and shelf residual currents. *Progress in Oceanography*. 23 : 303-338.
- Robinson, I.; Leborgne, P.; Piolle, J.F. And Larnicole, G.2004 : Medspiration products user manual, v1.02, September.
- Salas y Mélia D., Chauvin F., Déqué M., Douville H., Guérémy J.F., Marquet P., Planton S., Royer J.F. and Tyteca S. 2005 : Description and validation of CNRM-CM3 global coupled climate model. *Note de centre GMGEC, CNRM*, 103.
- Umlauf, L. and Burchard, H. 2005 : Second-order turbulence closure models for geophysical boundary layers. A review of recent work. *Continental Shelf Research*. 25 : 795-827.
- Vandermeirsch F., Charraudeau M., Bonnat A., Fichaut M., Maillard C., Gaillard F. and Autret E., 2010 : Bay of Biscay's temperature and salinity climatology. *XII International Symposium on Oceanography of the Bay of Biscay*, 4-6 mai 2010, Plouzané, France.

# MENOR: A HIGH-RESOLUTION (1.2 KM) MODELING OF THE NORTH-WESTERN MEDITERRANEAN SEA ROUTINELY RUN BY THE PREVIMER OPERATIONAL FORECAST SYSTEM

By V. Garnier<sup>(1)</sup>, I.L. Pairaud<sup>(2)</sup>, A. Nicolle<sup>(1,3)</sup>, E. Alekseenko<sup>(1,4)</sup>, M. Baklouti<sup>(4)</sup>, B. Thouvenin<sup>(1)</sup>, F. Lecornu<sup>(1)</sup>, P. Garreau<sup>(1)</sup>

<sup>1</sup>IFREMER, Brest, France

<sup>2</sup>IFREMER, Toulon, France

<sup>3</sup>ENSTA Bretagne, France

<sup>4</sup>MIO, Marseille, France

## Abstract

IFREMER has encouraged for over 15 years the oceanographic modeling of sea waters all around the metropolitan French coasts in order to facilitate environmental coastal studies. In that context, the North-Western Mediterranean Sea configuration (MENOR: 1.2 km – 60 vertical levels) has been introduced in the framework of Previmer operational forecasting system (<http://www.previmer.org/en>). This article gives an insight into the operational applications and scientific research using this MENOR configuration.

## Introduction

Previmer aimed at producing short term forecasts and long term hindcasts of the marine environment all along the French coasts. The Model for Applications at Regional Scale (MARS), used within this context, has been developed by the French Research Institute for Exploitation of the Sea (IFREMER). It is dedicated to simulating environmental coastal dynamics and has been implemented in the area of North-Western Mediterranean Sea at high resolution. The domain extends from 39.5°N to 44.5°N and from Spain to Italy. Such a spatial extension allows simulating the full cyclonic gyre on the abyssal plain in the open of the Gulf of Lions. The realistic simulation of the Northern Current, main component of the general circulation, is also improved. Moreover, the 1.2 km resolution allows the meso-(submeso)scale activity to be fully developed over the plain, along the shelf break, and over the Gulf of Lions (figure 1).

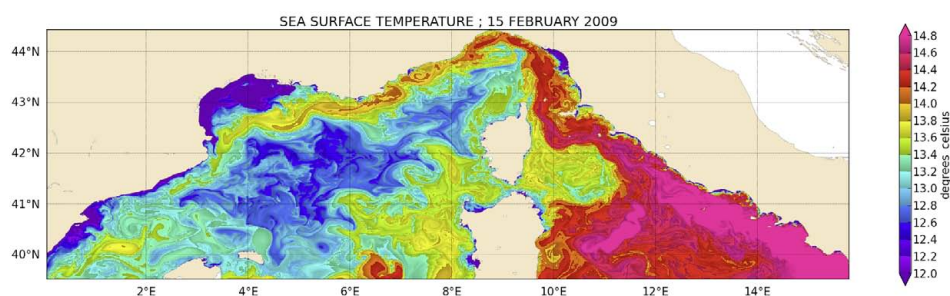


Figure 1: Snapshot of the sea surface temperature on February 15, 2009, simulated by MARS.

## Modeling description

MARS solves the system of incompressible Navier-Stokes equations in the classical Boussinesq approximation with the hydrostatic approximation [Blumberg and Mellor, 1987]. It uses a generalized vertical, terrain-following, coordinate system and has the particularity of resolving the barotropic and baroclinic modes with a common time step, thanks to the alternating direction implicit scheme. The simulation characteristics are summarized in table 1.

area	0-16°E ; 39.5°N-44.5°N
grid	1.2 km resolution generalized vertical, terrain-following, layers (1101x463x60)
forcing	Rivers: 14. The Rhone, Var, Tet, Herault, Aude, Gapeau, Argens, Tech, Lez, Orb river discharges are the observations of the day before. Initial and open boundary oceanic conditions: Mediterranean Oceanography Network for the Global Ocean Observing System (daily fields) Atmospheric forcing: French Met-Office model Arpege (10 km, 3h) No tide
scheme	Bulk turbulent flux: Fairall et al. 2003 Momentum: QUICK (3rd order) Viscosity: Smagorinsky (1963) Tracers: horiz. 5 <sup>th</sup> order, Upwind Compact and Conservative (UCC 5 <sup>th</sup> order), 3D MACHO method (Duhaut and Debreu, 2008, Debreu et al. 2011) Diffusion: centered scheme (1m <sup>2</sup> .s <sup>-1</sup> ) Pressure gradient: density jacobian cubic spline (Shchepetkin and Mc Williams, 2003) Turbulence: GLS (k-epsilon)

Table 1: Characteristics of the MENOR configuration

## MENOR: a high-resolution (1.2 km) modeling of the North-Western Mediterranean Sea routinely run by the Previm operational forecast system

MENOR simulations benefit from progress on numerical schemes following the work of L. Debreu and his colleagues. The remodeled time scheme and barotropic/baroclinic splitting techniques in MARS [Duhaut et al., 2008] allows the dissipation of numerical noise and the simulation of small long-lived coherent eddies. The development of high order schemes for the momentum and advection schemes (3<sup>rd</sup> and 5<sup>th</sup> order respectively) and the 3D extension of the MACHO method (to take into account the crossing terms while solving advection) [Debreu and Duhaut, 2011] have strongly reduced the diapycnal mixing. Lastly, the introduction of a two equation turbulence scheme [Umlauf and Burchard, 2003], used with a suitable rate of dissipation of the turbulent kinetic energy, has improved the conservation of the intermediate and deep water masses hydrological characteristics. In order to improve the simulated sea surface temperature, the radiative atmospheric fluxes penetrate the surface layers according to two different wave lengths. This adjustment improves the correct representation of the sea surface temperature seasonal cycle.

Every day, Previm operational forecasting system imports analyses and forecasts from the French Met-Office model Arpege (10 km, 3h), river discharge observations, daily OGCM fields from Mediterranean Oceanography Network for the Global Ocean Observing System (MONGOOS) and runs the MENOR configuration. Each run produces an analysis for the day before (J-1 at 0 am) and a four day forecast up to J+4 0 am. It saves all the hydrodynamic variables every 3 hours over the global domain and makes result files available to users. Up to January 2013, the atmospheric forcing was provided by ACRI-ST which was running MM5 model (9 km, 3h) as a zoom of the NCEP model.

### Operational applications

MENOR outputs (222 Go a year) are downloaded by File Transfer Protocol (FTP) or openDAP (Open-source Project for a Network Data Access Protocol) by a third of the users interested by hydrodynamic results (which represent 46% of Previm products users) [Pineau-Guillou 2013, Pineau-Guillou et al., 2014, this issue]. The MENOR configuration itself is mainly used in scientific institutes for research applications (58%) while 42% of the requests for access to simulation results come from private companies. Model outputs are used as open boundary and initial fields to force coastal models or for direct analyses. The main domains of applications are flora and underwater fauna (26%), marine water quality (22%), hydro(-sedimento) dynamics (20%), environmental pollution (16%), shipping route optimization (8%), Renewable Marine Energy (6%), and meteorology (2%). Statistics from MENOR output requests suggest that 44% of the user applications have real time objectives.

From feedbacks from Previm users, the MENOR analyses are the most used fields. For instance, they allow investigations on bacteria dispersion due to sewage releases or on drifts of micro-plastics, they provide information to evaluate potential installation of wind mill farms... Real time applications remain relatively marginal but a few can be noticed. A private company used real time forecasts as boundary conditions for an embedded model of the Provençal area, aimed at monitoring Oil Spill drifts during summer. People from LAMA (Tuscany, Italy) used MENOR results for a real time modeling of the Tuscany shelf. Previm team participated to an antipollution exercise managed by the REMPEC (Regional Marine Pollution Emergency Response Centre for the Mediterranean Sea). And lastly Previm provides currents, temperature and salinity for a Mediterranean integrated Oil Spill System in the framework of MEDESS4MS project. Of course, scientists examine the MENOR configuration just before or during a field experiment as a support to manage the data sample strategy.

In 2013, IFREMER participated in HYMEX (Hydrological cycle in Mediterranean Experiment) second Special Observation Period (Feb.-March 2013) effort dedicated to the documentation of dense water formation in the North-Western Mediterranean area. Along with the Laboratory of Aerology (SYMPHONIE-NWMED-111 configuration) and Mercator Ocean (PSY2V4R2 [Lellouche et al., 2013] and IBI36V2R1 [Maraldi et al., 2013] configurations), IFREMER used MENOR operational outputs in order to provide quicklooks describing the hydrological situation of the area and the development of deep convection and dense water formation. Analyses were sent in real time to help the Operational Center of the SOP2 experiment to adjust the deployment of the in-situ measurements. There are available on the <http://sop.hymex.org> website.

### Research applications

MENOR simulates the general circulation, its seasonal and interannual variability, as well as mesoscale processes such as intermittent upwellings, coherent eddies on the shelf itself [Schaeffer et al., 2011] or off Toulon [André et al., 2009] and the Rhone plume dynamics. Over the global domain, IFREMER research studies focus on the hydrodynamics itself and on biogeochemical, benthic and fisheries applications.

### Mesoscale hydrodynamic interpretation

The understanding of the mesoscale structures dynamics is an essential step to consider their contribution to primary production, recruitment of larvae and transfer of contaminants. Numerous hydrodynamical studies have therefore focused on mesoscale eddies, which are observed from satellite, in-situ measurements and lagrangian drifters, and well reproduced in MENOR simulations. Thanks to the simultaneous modeling of both the Gulf of Lions and the abyssal plain, Garreau et al. [2011] explained the dynamics linking the "LATEX" and "CATALAN" eddies. The LATEX eddy is a large anticyclonic structure, fully developed in summer in the southwestern corner of the Gulf of Lions. It was first documented by Millot [1982] and monitored by the Lagrangian Transport Experiment. The "CATALAN" eddies are large anticyclonic gyres of 40-50 km in diameter. They exhibit sub-surface current velocities up to 0.5 m s<sup>-1</sup> and their vertical extension may reach down to 100 m water depth [Rubio et al., 2005]. They occur once to three times a year during summer and autumn in the Catalan Sea. Careful analyses of a particular event in autumn 2007, monitored both by drifting buoys and Jason1's tracks and simulated within MENOR configuration, have allowed Garreau et al. [2011] to conclude (figure 2) that: 1 - the LATEX anticyclonic eddy is a warm and less dense water body, isolated and partially fed by a coastal current carrying warm water from the Catalan Sea during long Tramontane summer events, 2 - that a burst of southeasterlies and/or northerlies appeared to trigger the "LATEX" eddy detachment, which then flowed out of the Gulf of Lions, migrating along the Catalan continental slope before reaching the Balearic Sea where it is known as the "CATALAN" eddy.

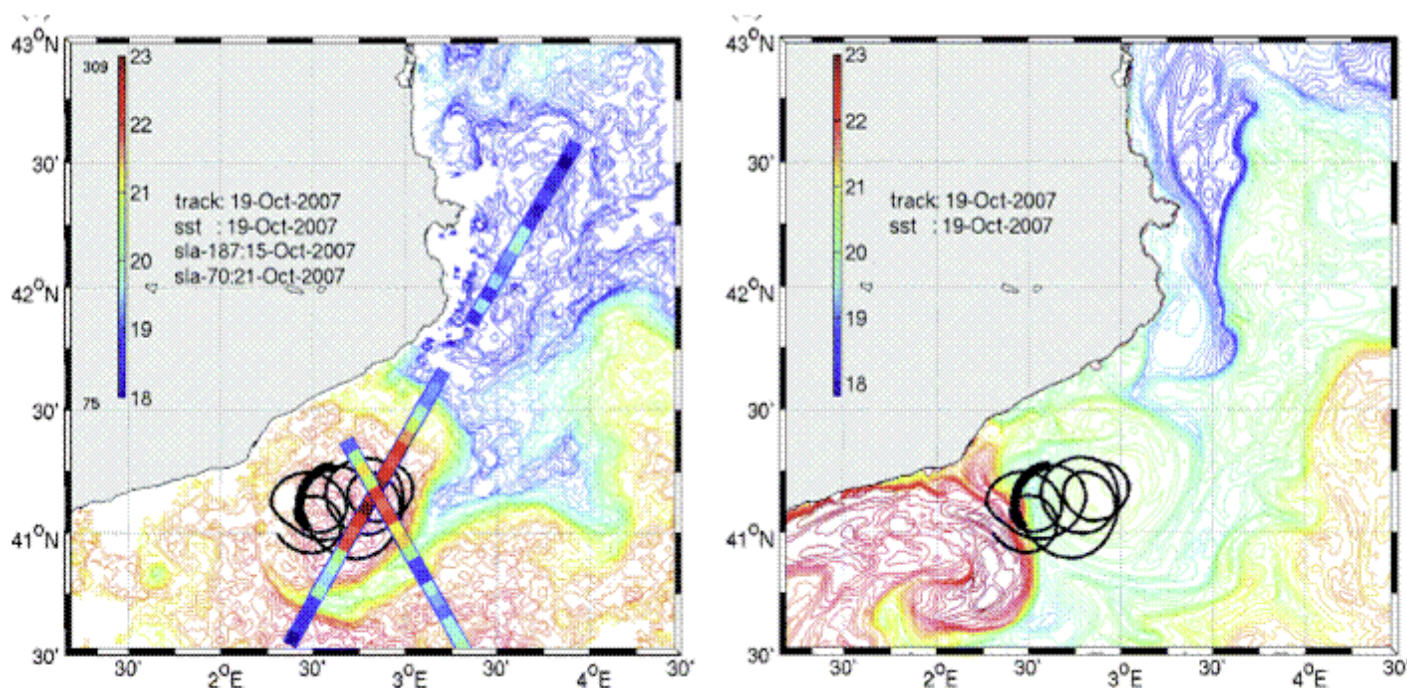
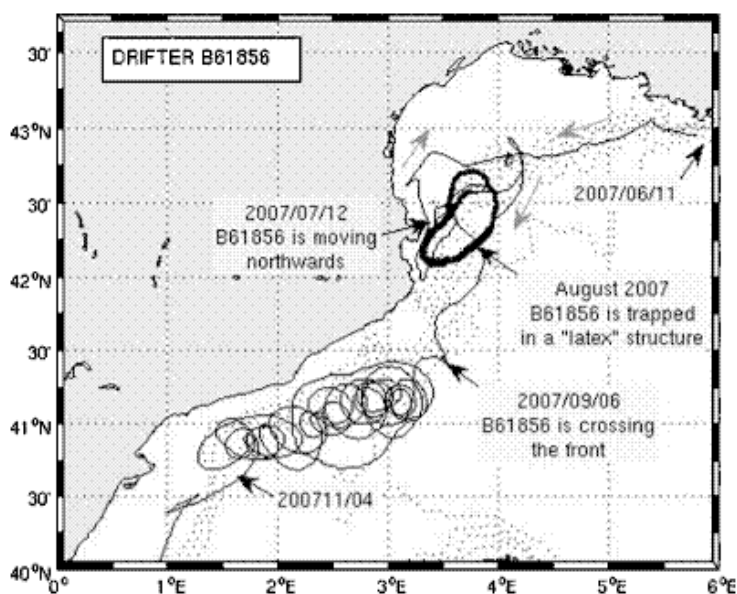


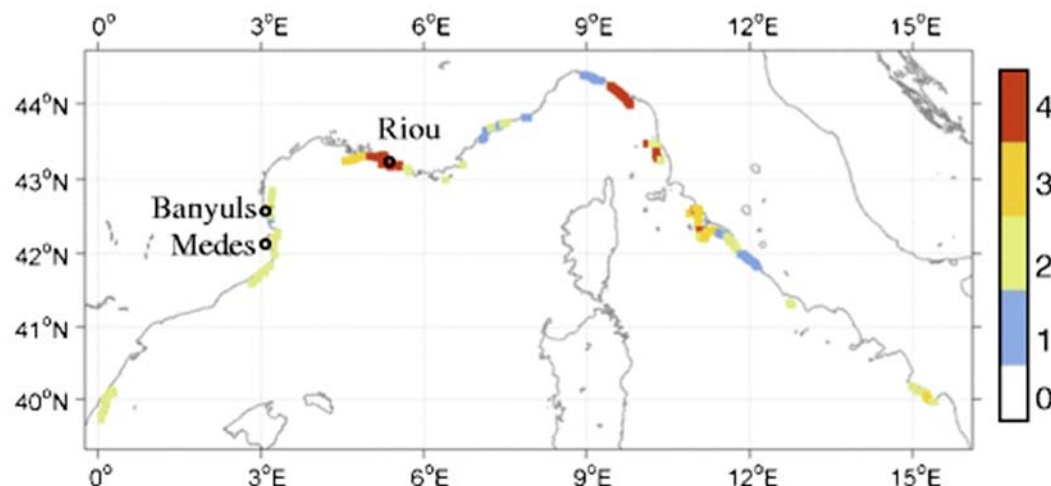
Figure 2: Trajectory of the drifters B61856 dropped on 11 June 2007 off Toulon with a holey sock at 50 m depth: from late July to late August, B61856 is trapped in the southwestern corner of the Gulf of Lions (LATEX area) before being caught by a CATALAN eddy. Sea surface temperature (remote sensed (middle) and modeled (bottom)) and sea level anomaly (sla) along Jason1's tracks on October 19. The left hand side of the color legend represents the scales of the sla (millimeters). The right hand side represents the scale of SST (degrees Celsius). The black line represents the track of the drifter for 10 days centered on the picture time. [Extracted from figures 2 and 6, Garreau et al., 2011]

## Towards applications to climate change impacts

At a decadal-scale, long-term hydrological hindcasts issued from MENOR results also provide an interesting tool to investigate the potential impacts of temperature anomalies induced by climate change on marine benthic biodiversity. Along the rocky coasts of the North-Western Mediterranean Sea, the red gorgonian *Paramuricea-clavata* species (among others) suffered mass mortality events in 1999, 2003 and 2006, while abnormal warming events were reported at the same time. Analyses of the high-resolution T-MedNet temperature time series measured in the Mediterranean coastal waters (0–40 m) have highlighted relationships between the thermal stress and the degree of mass mortality [Bensoussan et al., 2010, Crisci et al., 2011]. A review of available data from aquarium experiments on thermo-tolerance for the red gorgonian *P. clavata* allowed to quantify a thermo-tolerance function linking the exposure to different temperatures (number of days exposed to temperatures ranging from 23 to 28 °C) and the degree of population necrosis. A comparison between MENOR modeled temperature statistics and T-MedNet observations over 2001-2010 confirmed the model's ability to reproduce temperature variations during the stratified periods (with a tendency to underestimate the temperature in subsurface layers). Model temperature hindcasts have then been combined with the thermo-tolerance function and the spatial red gorgonian

**P. clavata** distribution in order to produce maps of mortality risk along the North Western Mediterranean coastline within the 60-m isobath [Pairaud et al., 2014]. Results pointed out that Marseilles and the Gulf of Genoa could be areas the most impacted, while mortality risks were lower along the Catalan coast, especially in the northern part (figure 3). This pattern is in agreement with observed impacts on population carried out during the large mass mortality events in different areas of the northwestern Mediterranean [Crisci et al., 2011]. The methodological approach is therefore validated, although improvements need to be made in the process of mapping the risk of mortality.

*Figure 3: Map of risk for the red gorgonian P. clavata based on integrating the thermo-tolerance thresholds and species geographical and vertical distribution information and using model temperature hindcasts over the period 2001–2010. Scores between 0 and 4 correspond to the risk of mortality: sub lethal (population remains healthy), medium (first signs of necrosis are observed), high (the mortality is important) and extreme (the population is decimated) lethal impact. [Extracted from figure 6, Pairaud et al. 2014]*



## Application to small-scale pelagic recruitment

In the Gulf of Lions and the Catalan Sea, Anchovy (*Engraulis encrasicolus*) is an important commercial species and one of the most abundant pelagic fish. Its recruitment largely depends on hydrodynamics which determines whether the organisms can reach areas favorable to recruitment or are dispersed. MENOR simulated currents and salinity fields have been used as inputs for a lagrangian tool over the 2001-2008 period (ICHTYOP) in order to investigate the transport and fate of anchovy eggs and larvae (hereinafter called "particles") into the North-Western Mediterranean Sea.

According to anchovy spawning observations, 100,000 particles are homogeneously distributed over the Gulf of Lions at 15 m depth. Spawning (release) takes place every week from May 15 to August 15. Recruitment of each cohort is evaluated after 30 days of lagrangian transport because one-month old anchovy larvae have real autonomous swimming movement. Two types of experiments are carried out to take into account the living evolution of anchovy larvae: the passive transport (PT) at 15 m depth corresponds to the behavior of the youngest larvae, while the introduction of a diel vertical migration (DVM) simulates 7-day-old larvae, which moves down to 50 m deep (maximum of chlorophyll) in the daytime (7 a.m.) and move up to the surface at night (7 p.m.).

Surprisingly, although circulation in the Gulf of Lions is strongly influenced by the wind, particles retention in the Gulf of Lions appears to be independent of atmospheric forcing. Actually, the maximum of particles concentration coincides with areas of low salinity and the diel vertical migration intensifies this trend (figure 4). This positive effect complies with observations: located in fresher waters (with more nutrients), larvae have more possibility to survive. Even though the diurnal vertical migration allows more particles to escape the gulf of Lions and reach low salinity areas in the Catalan Sea, the residence time remains relatively high (40 days, an estimate coherent to buoy observations and salt balance) and one can conclude, from a simple method with no real interactions between physical and biological processes, that the Gulf of Lions is a potentially favorable area for anchovy recruitment.

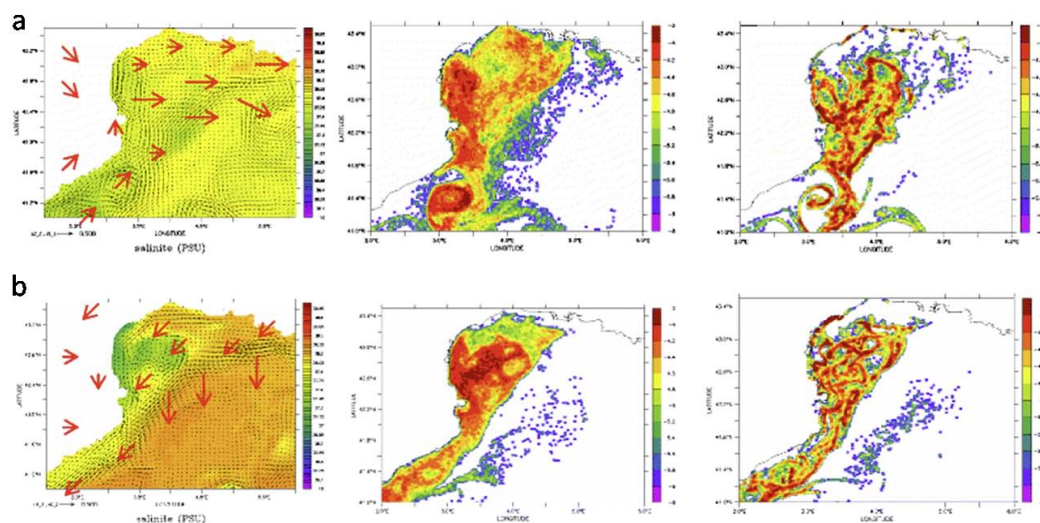


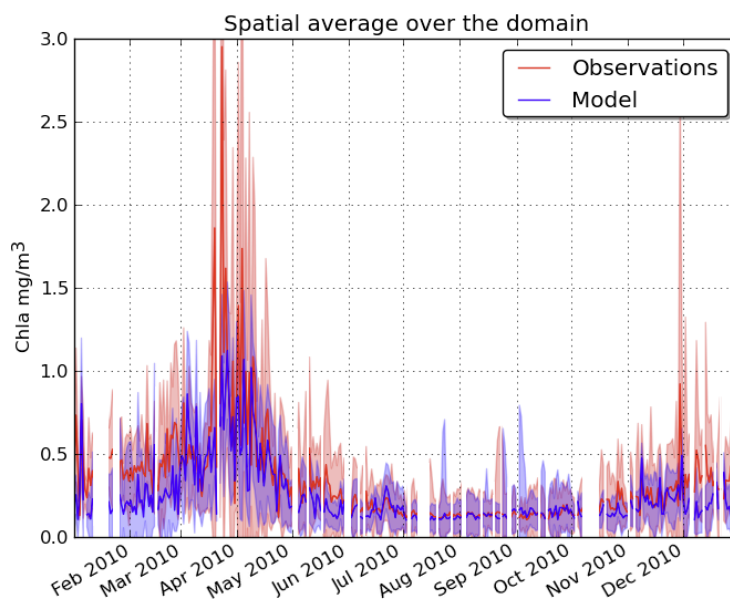
*Figure 4: Currents and salinity at 15 m depth averaged between 16 and 23 June with wind direction (red arrow; left column). Particle concentration (logarithmic scale) after 30 days for passive transport (central column). Particle concentration after 30 days for diel vertical migration (right column). The spawning date is May 22 for a 2003, b 2006. [Extracted from figure 5, Nicolle et al., 2009]*

## Biogeochemical coupling

As the hydrodynamic processes and patterns are simulated with a sufficient accuracy in the MENOR configuration, MARS has been coupled on-line with a 3D bio-geo-chemical model embedded in the Eco3M modular numerical tool [Baklouti et al., 2006a, b]. Eco3M model is a food-web model containing different plankton functional types with a flexible plankton stoichiometry. Such a model is particularly suitable for studies in the Mediterranean Sea since, depending on the season and the geographical position, Nitrogen (N) and/or Phosphorus (P) can limit primary production, and because of the specificity of this sea in terms of N:P stoichiometry [Pujo-Pay et al., 2011].

The hydrodynamic and biogeochemical processes have been simulated from September 1, 2009 to January 31, 2011 [Alekseenko et al., 2014]. Comparisons with two field trips conducted in the Gulf of Lions (ANR COSTAS Project) illustrated a good agreement between modeled and observed patterns of nutrients and Chl-a in spring (Costeau-4: April 27 – May 2, 2010), especially in the eastern half of the Gulf of Lions where the Rhone River has the largest influence, while results were less successful in winter (Costeau-6 : January 23 – January 27, 2011). Comparisons of sea surface chlorophyll with MODIS data showed an accurate phytoplankton productivity in spring, not only on the eutrophic continental shelf of the Gulf of Lions, but also in the open sea area which is separated from the shelf by the low Chl-a waters of the Northern Current. Lastly, a 1-year quantitative comparison of the surface chlorophyll spatially averaged over the global domain (figure 5) concluded to a satisfactory reproduction of the phytoplankton bloom, while modeled Chl-a is slightly underestimated partly due to the general underestimation of small phytoplankton biomass.

*Figure 5: Time variations of averaged chlorophyll over the NW Mediterranean Sea (red line: satellite observations (MODIS), blue line: model results; color shift from lines indicate the minimum and maximum values for the study area; empty spaces correspond to insufficient satellite data for the comparison at these periods) [figure 12 Alekseenko et al., 2014]*



Alekseenko et al. [2014] focused on the temporal and spatial variability of intracellular contents of living and non-living compartments (figure 6). From simulated relative intracellular quotas in phosphorus (P), nitrogen (N), carbon (C), they concluded that each one of the three elements is limiting at some periods of the year [Alekseenko et al., 2014]. In large phytoplankton cells, P is the most limiting element but during winter mixing, C (which depends on light availability) can become more limiting than N. Bacteria are limited by C throughout the year but at the end of the stratified period, P can become more limiting than N.

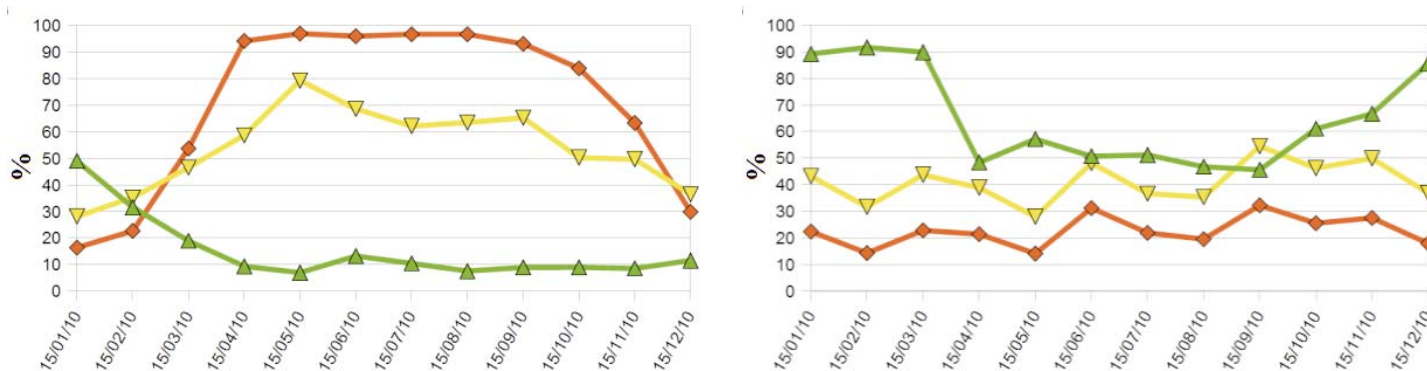


*Figure 6: Relative intracellular quotas (in %) of C (red line), N (yellow line), and P (green line), averaged over the surface layer of the domain of whole NW Mediterranean: - a for large phytoplankton (> 10 μm) - b for bacteria [extracted from figure 18 Alekseenko et al., 2014]*

Although these preliminary results need to be validated by measurements, they illustrate some potentialities offered by the MARS-ECO3M model to explain the functioning of the Mediterranean ecosystem. This model has been further coupled with a contaminant module in order to study PCBs dispersion (Polychlorinated biphenyls) in the Gulf of Lions and their transfer from water to mesozooplankton via biogeochemical processes.

## Conclusion

After sensitivity studies and validation, numerical modeling provides a 4D representation of the environment that complements satellite and in-situ observations. With its large extended domain (0-16°E – 39.5-44.5°N) and its high resolution (1.2 km 60 layers), the MENOR configuration provides powerful results to interpret and study the processes at play in the North-Western Mediterranean sea. The operational Previmer system routinely runs the configuration to provide users - research institutes, universities or private companies - with daily analyses and 4-day forecasts of the area. Operational forecasts will be improved in 2014 thanks to the introduction of the spectral nudging method [Herbert et al., 2014, this issue]. Long-term hindcasts are also published, and this article has briefly reviewed some of the research applications lead by IFREMER and based on MENOR hindcasts. Research applications have confirmed that MENOR is realistic enough to elucidate dynamical behaviors [Garreau et al., 2011], to propose methodologies in order to investigate the potential impact of climate changes [Pairaud et al., 2014], to be coupled with ECO3M model to investigate key biogeochemical processes [Alekseenko et al., 2014] and to interest pelagic fish recruitment [Nicolle et al., 2009].

MENOR main flaw is its incapacity to reproduce the development of deep convection and dense water formation, which are strongly constrained by the initial hydrological conditions in deep water. A new and improved coherent long-term hindcast correcting this bias is therefore needed; it would moreover take advantage of MARS latest significant evolutions and of the experiences shared by all French teams involved in modeling the North-Western Mediterranean sea (within SIMED project). The future hindcast will be forced by CNRM (Centre National de Recherches Météorologiques) ALADIN-climate model (12 km downscaling of ERA-INTERIM [Colin et al., 2010]) and by NEMOMED12 [Beuvier et al., 2012], a NEMO regional simulation at 6-7 km resolution forced by the same atmospheric fields and devoted to the inter-annual variability of the Mediterranean sea. This hindcast will be qualified in 2014 to pursue scientific studies planned within the HYMEX and MedCORDEX programs as well as PPR-GMMC SIMED projects.

## Acknowledgements

Authors thank the Région Bretagne for supporting Previmer, which has driven the construction of the operational system itself (both measurements and modeling) and has allowed significant numerical improvements within MARS. Previmer also allowed a definite rationalization of the modeling methods and tools, from which all environmental scientific studies based on MARS have benefited. Simulations cannot be realistic without the supply of bathymetries, meteorological forcing and realistic OGCM outputs which have been made efficiently available to the scientific community within the Previmer framework: SHOM, the French Met-Office, the Mediterranean Forecasting System as well as PPR-GMMC and the HYMEX program are also thanked for their contributions.

## References

- Alekseenko E., Raybaud V., Espinasse B., Carlotti F., Queguiner B., Thouvenin B., Garreau P. and Baklouti M. (2014): Seasonal dynamics and stoichiometry of the planktonic community in the NW Mediterranean Sea: a 3D modeling approach. *Ocean Dynamics*, 64(02), 179-207.
- André G., Garreau P. and Fraunié P. (2009): Mesoscale slope current variability in the Gulf of Lions. Interpretation of in-situ measurements using a three-dimensional model. *Continental Shelf Research*, 29(2), 407-423.
- Baklouti M., Diaz F., Pinazo C., Faure V. and Queguiner B (2006a): Investigation of mechanistic formulations depicting phytoplankton dynamics for models of marine pelagic ecosystems and description of a new model. *Prog Oceanogr* 71:1-33.
- Baklouti M., Faure V., Pawlowski L. and Sciandra A. (2006b): Investigation and sensitivity analysis of a mechanistic phytoplankton model implemented in a new modular tool (Eco3M) dedicated to biogeochemical modelling. *Prog Oceanogr* 71:34-58.
- Bensoussan N., Romano J.C., Harmelin J.G. and Garrabou J. (2010): High resolution characterization of northwest Mediterranean coastal waters thermal regimes: to better understand responses of benthic communities to climate change. *Estuar Coast Shelf Sci* 87:431-441.
- Beuvier J., Béranger K., Lebeaupin-Brossier C., Somot S., Sevault F., Drillet Y., Bourdallé-Badie R., Ferry N. and Lyard F. (2012): Spreading of the Western Mediterranean Deep Water after winter 2005: time scales and deep cyclone transport. *J. Geophys. Res.-Oceans*. doi:10.1029/2011JC007679.
- Blumberg A.F. and Mellor G.L. (1987): A description of a three-dimensional coastal ocean circulation model. In: Heaps NS (ed) Three-dimensional coastal ocean models. Coastal and estuarine sciences. American Geophysical Union, Washington, pp 1-16.
- Colin J., Déqué M., Radu R. and Somot S. (2010) Sensitivity study of heavy precipitations in Limited Area Model climate simulation: influence of the size of the domain and the use of the spectral nudging technique. *Tellus-A*, 62(5), 591-604. DOI: 10.1111/j.1600-0870.2010.00467.x
- Crisci C., Bensoussan N., Romano J.C. and Garrabou J. (2011): Temperature anomalies and mortality events in marine communities: insights on factors behind differential mortality impacts in the NW Mediterranean. *PLoS ONE* 6(9):e23814. doi: 0.1371/journal.pone.0023814
- Debreu L. and Duhaut T. (2011): Développements numériques pour le modèle MARS : Analyse des schémas d'advection verticaux, réduction de la diffusion diapycnale. *Contrat Previmer – Ref : 09/2 211 097*.
- Duhaut T., Honnorat M., and Debreu L. (2008): Développements numériques pour le modèle MARS. *Contrat Previmer – Ref: 09/2 211 097*.

**MENOR: a high-resolution (1.2 km) modeling of the North-Western Mediterranean Sea routinely run by the Previmer operational forecast system**

- Garreau P., Garnier V. and Schaeffer A. (2011): Eddy resolving modelling of the Gulf of Lions and Catalan Sea. *Ocean Dynamics*, 61(7), 991-1003.
- Herbert G., Garreau P., Garnier V. and Dumas F. (2014): Downscaling from oceanic global circulation model towards regional and coastal model using spectral nudging techniques. Newsletter of Mercator Ocean, this issue.
- Lellouche, J.-M., Le Galloudec, O., Drévillon, M., Régnier, C., Greiner, E., Garric, G., Ferry, N., Desportes, C., Testut, C.-E., Bricaud, C., Bourdallé-Badie, R., Tranchant, B., Benkiran, M., Drillet, Y., Daudin, A., and De Nicola, C. (2013): Evaluation of global monitoring and forecasting systems at Mercator Océan. *Ocean Sci.*, 9, 57-81.
- Maraldi, C., Chanut, J., Levier, B., Ayoub, N., De Mey, P., Refray, G., Lyard, F., Cailleau, C., Drévillon, M., Fanjul, E., Sotillo, M., Marsaleix, P., and the Mercator R&D Team (2013): Nemo on the shelf: assessment of the iberia-biscay-ireland configuration. *Ocean Sci.*, 9:745-771.
- Millot C. (1982): Analysis of upwelling in the Gulf of Lions. In: Nihoul JCJ (ed) Hydrodynamics of Semi-Enclosed Seas: Proceedings of the 13th International Liège Colloquium on Ocean Hydrodynamics. Elsevier Oceanogr. Ser., vol. 34. Elsevier Sc. Pub, Amsterdam, The Netherlands, pp. 143-153.
- Nicolle A., Garreau P. and Liorzou B. (2009): Modelling for anchovy recruitment studies in the Gulf of Lions (Western Mediterranean Sea). *Ocean Dynamics*, 59(6), 953-968.
- Pairaud I., Bensoussan N., Garreau P., Faure V. and Garrabou J. (2014): Impacts of climate change on coastal benthic ecosystems: assessing the current risk of mortality outbreaks associated with thermal stress in NW Mediterranean coastal areas. *Ocean Dynamics*, 64(1), 103-115.
- Pineau-Guillou L. (2013) : Analyse des utilisateurs. Journée de restitution de la phase 2 du projet Previmer. [http://www.previmer.org/espace\\_projet/journee\\_de\\_restitution\\_phase\\_2](http://www.previmer.org/espace_projet/journee_de_restitution_phase_2), talk S3.1.
- Pineau-Guillou L., Lecornu F. and Le Roux J.F. (2014): Analysis of PREVIMER users. Newsletter of Mercator Ocean, this issue.
- Pujo-Pay M., Conan P., Oriol L., Cornet-Barthaux V., Falco C., Ghiglione J.-F., Goyet C., Moutin T., Prieur L. (2011): Integrated survey of elemental stoichiometry (C, N, P) from the western to eastern Mediterranean Sea. *Biogeosciences* 8:883-899.
- Rubio A., Arnau P.A., Espino M., Flexas M.D., Jorda G., Salat J., Puigdefabregas J. and Arcilla A.S. (2005): A field study of the behaviour of an anticyclonic eddy on the Catalan continental shelf (NW Mediterranean). *Prog Oceanogr* 66(2-4):142-156.
- Schaeffer A., Molcard A., Forget P., Fraunié P. and Garreau P. (2011): Generation mechanisms for mesoscale eddies in the Gulf of Lions: radar observation and modeling. *Ocean Dynamics*, 61(10), 1587-1609.
- Umlauf L. and H. Burchard (2003): A generic length-scale equation for geophysical turbulence models. *Journal of Marine Systems*, 61: 235265.

## DEVELOPMENT AND VALIDATION OF A SEDIMENT DYNAMICS MODEL WITHIN A COASTAL OPERATIONAL OCEANOGRAPHIC SYSTEM

By Florence Cayocca<sup>(1)</sup>, Romaric Verney<sup>(1)</sup>, Sébastien Petton<sup>(1)</sup>, Matthieu Caillaud<sup>(2)</sup>, Morgan Dussauze<sup>(2)</sup>, Franck Dumas<sup>(1)</sup>, Jean-François Le Roux<sup>(1)</sup>, Lucia Pineau<sup>(1)</sup>, Pierre Le Hir<sup>(1)</sup>

<sup>(1)</sup>IFREMER, Brest, France

<sup>(2)</sup>ACTIMAR, Brest, France

### Abstract

The rising interest in environmental and ecosystem dynamics have lead coastal oceanographers to not only investigate the “traditional” physical parameters describing the ocean state and its dynamics (e.g. temperature, salinity, currents, water levels in coastal areas), but to also account for the dynamics of parameters describing its biogeochemical components. To that end, MARS3D regional and coastal modelling system has been coupled to ecosystem modules (ECO-MARS3D, ECO3M) as well as sediment dynamics modules (MARS3D-SEDIM): sediment, nutrient and primary production contents can be considered as the lower level environment and ecosystem descriptors of the “biogeochemical” ocean. Early investments into physical and biological analysis at the regional scale have led to the development of several operational configurations within PREVIMER since 2006 for physical and biological parameters, providing 3 to 5-day forecasts as well as hindcasts. The more recent introduction of sediment-related parameters into the operational chain required validating computed sediment transport at the regional scale. Such validation is mostly accessible through indirect measurements – namely turbidity measurements in the water column or derived from satellite data.

This paper describes the main features of MARS3D sediment module, the sensitivity analyses and the validation procedures based on dedicated data acquisition, as well as the assessment of the operational configuration focused on the Bay of Biscay continental shelf. Comparison between *in situ* measurements and satellite data shows a fairly systematic overestimation of the satellite-derived SPM in Southern Brittany; this result stresses the need for further investigation regarding the correct quantitative satellite SPM determination at all times and all places. On the other hand, numerical results highlight the difficulty to simultaneously predict the correct magnitude of bottom and surface concentrations.

### Introduction

Beyond the obvious link between sediment dynamics and sea-floor or coastal morphology, shelf seas environment and ecosystems dynamics is also related to sediment dynamics through 1) turbidity in the water column, which impacts primary production because of light attenuation, and is a proxy for the suspended particulate matter (SPM) as a possible vector of contaminants, 2) benthic habitat structuration. The main difficulties to successfully model sediment dynamics at the shelf scale derive from a relatively poor knowledge of the key parameters driving suspension and deposition processes (e.g. accurate parameterization of the bottom boundary condition - description of the seafloor composition and its consolidation state -, accurate assessment of the erosion fluxes and settling velocities), and from a very limited amount of relevant *in situ* data. The first step in order to propose a reasonable estimate of the sediment dynamics at the regional scale has therefore been to set-up a data acquisition strategy based on long-term moorings investigating the whole water column (Charria *et al.*, this issue). When considering the whole Atlantic / English Channel French continental shelf, an additional difficulty arises from the fact that the Bay of Biscay and the English Channel exhibit very contrasted environments in terms of dynamics (tides and waves), hydrology (stratification) as well as seafloor coverage. *In situ* data and research priorities having been so far focused on the Atlantic coast only, the model assessment will also be focused on the Bay of Biscay continental shelf.

While *in situ* data are scarce, the processing of water colour satellite data provides a fantastic synoptic overview of the surface turbidity, including mineral and organic components. PREVIMER has also ensured the real time processing of MODIS or MERIS spectral reflectance, allowing for daily estimations of chlorophyll and non-algal SPM concentrations according to the methodology described by Gohin (2011). Apart when assessed from water sampling, suspended particulate matter (SPM) quantification (in unit mass per volume) is always indirectly deduced from acoustic or optical measurements. *In situ* measurements – whether acoustic or optical, including longterm time series – usually allow for calibration against actual water samples. This calibration provides a relationship between the recorded signal and a sediment concentration. It is however prone to uncertainties due to the fact that water samples do not span the entire *in situ* data acquisition period: they are most often a one-time procedure, and the calibration they allow is therefore only valid whenever the suspended sediment characteristics match the sediment type that was in suspension during the sampling procedure. However, because of advection or of varying re-suspension intensity, the sediment type in the water column may change in time. Any “steady state” calibration may therefore induce some fairly unknown uncertainty regarding its validity along the recording time. Calibration factors relating the turbidity sensor signal and turbidity inferred from *in situ* samples may for instance vary by a factor 3 at a given position, depending on the tide intensity (spring vs. neap, Verney, 2013). To temper this statement, let us mention that when both acoustic and optical signals are simultaneously recorded and exhibit the same variability, a relative steadiness of the suspended sediment type may be inferred, in which case the calibration may be considered valid over the whole record. SPM quantification deduced from satellite water colour processing exhibits the same kind of uncertainty, not to mention errors linked to atmospheric corrections and/or separation between organic and mineral suspended matter. While Gohin (2011) shows very good agreement between satellite and *in situ* low frequency coastal data (REPHY monitoring network), the availability of long time series Southern Brittany for *in situ* surface turbidity showed that the remote concentration may exceed the *in situ* concentration by a factor 2 to 4. The variability is however remarkably well reproduced; this assessment is essential before validating the numerical model.

The sediment module itself computes sediment erosion, advection and deposition for any number of sedimentary variables that may exhibit a sandy or cohesive behaviour. These different types of particles are mixed in the sediment compartment, where their combination affects the mixture behaviour. On the other hand, the use of a large number of sedimentary variables allows a detailed description of the sea floor sedimentary facies. The sediment

module conceptual framework allows taking into account fairly complex processes, including flocculation, consolidation and fine vertical discretization of the silt/clay mixtures within the bed. While permitting the representation of a realistic behaviour thanks to accounting for a large range of processes, this complexity also makes model results highly sensitive to initial conditions and parameterization driving the evolution of layers thicknesses. Particularly since these initial conditions and parameters are poorly known at the shelf scale, the modelling strategy consisted in opting for a fairly simple (or even simplistic) configuration, so as to ensure more robust results and a reasonable amount of sediment parameters to investigate.

### In situ data and satellite analysis

Because of the scarcity of *in situ* turbidity data along the continental shelf, the project first focused on pertinent data acquisition. Figure 1 shows the location of the long term moorings used for model validation all based on the use of vertical acoustic Doppler current profilers. Greater water depths impose lower acquisition frequency, hence reduced vertical resolution, and a shift in the grain size refraction peak decreasing from about 100  $\mu\text{m}$  for 100kHz down to about 150  $\mu\text{m}$  for 150 kHz. PREVIMER-D4 moorings spanned 7 winter months in 2007-2008 and 5 months in 2009-2010. They were moored at 15 m and 25 m water depths, using 1000 kHz current profilers (also measuring waves, the backscatter signal being used to assess SPM concentrations in the water column). Their design is detailed in Charria *et al.* (this issue). Other moorings were not conceived with any real time data transmission and were more lightly designed, namely with a bottom current profiler (150 kHz, 300 kHz or 600 kHz for water depths ranging from 40 to 150 m), a bottom turbidity sensor and a surface turbidity sensor for the shallower point, in 2011 and 2012. These moorings provided up to one year long time series.

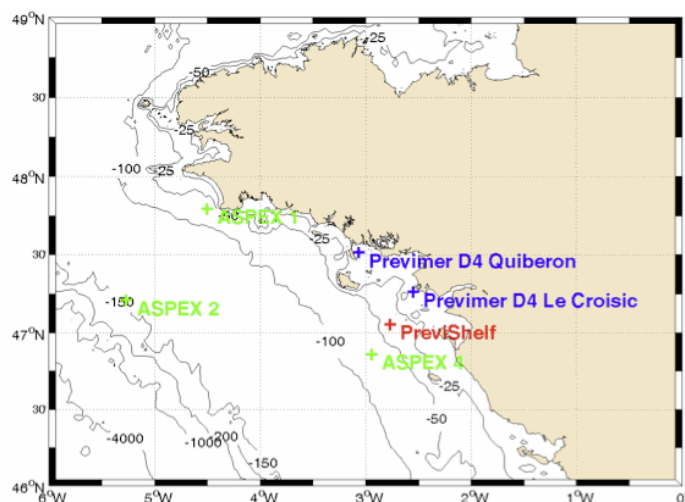


Figure 1: Position of the long term moorings used for model validation.

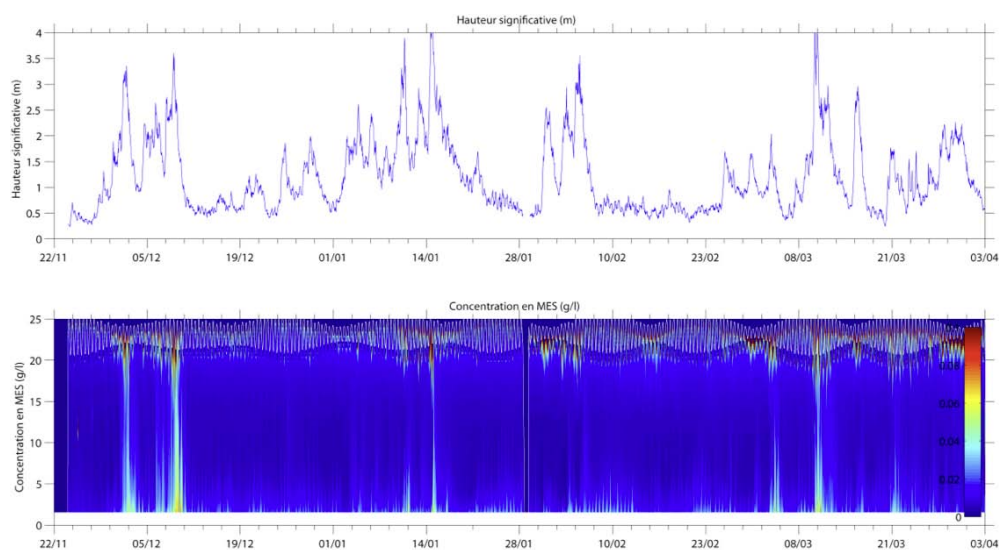


Figure 2 - Top: significant wave height measured from the profiler (m); bottom: calibrated SPM concentration deduced from the profiler backscatter (mg.l-1). PREVIMER-D4 LE Croisic 2007-2008

The strategy behind the use of bottom profilers lies in their capacity to provide wave and current data as well as an estimate of the suspended concentration over the whole water column (Figure 2). The simultaneous use of a near-bottom optical turbidity sensor aims at carrying out some kind of backscatter “calibration” accounting for attenuation with distance and particle load. Once the optical sensor has been calibrated against *in situ* water samples, the backscatter processing is constrained so as to obtain the best possible fit between the optical SPM time series and the profiler SPM time series at the same elevation above the bed. This procedure may lead to reasonable correlation coefficients (e.g. Figure 3,  $R^2=0.78$ ; in cases where suspended sediment composition greatly varies in time, this correlation may be extremely poor, in which case the backscatter signal cannot be used to assess turbidity). The standard deviation in this particular case leads to a factor 2 in the SPM concentration estimate. Figure 3 shows the correspondence between acoustic and optical bottom SPM time series for PREVIMER-D4 Le Croisic. The high frequency oscillations are related to the tide while waves significantly drive the lower frequency signal (Figure 2 and Figure 3 illustrate the same dataset).

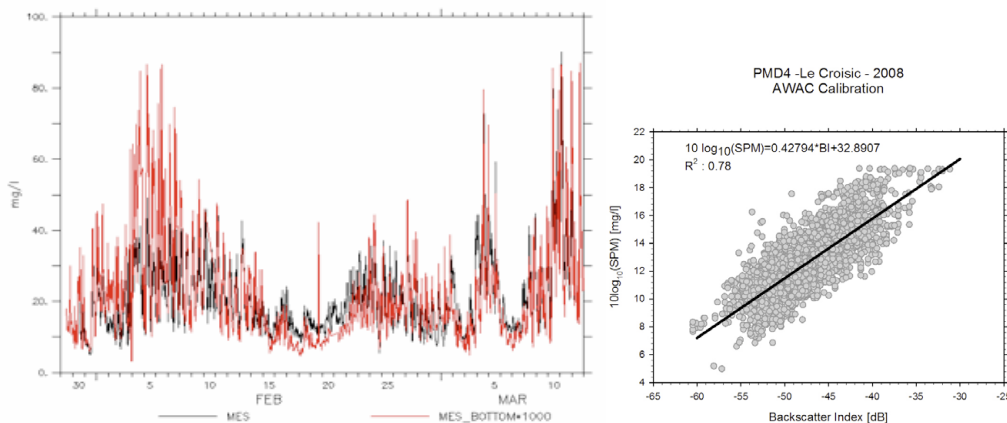


Figure 3 - Left : Bottom SPM concentration (mg/l) measured from the turbidity sensor (red) and from the current profiler at the same elevation (black). Right : Scatter plot showing the optical SPM concentration ( $\log_{10}(\text{mg.l}^{-1})$ ) against the so-called backscatter index (in dB, to be converted to acoustic SPM concentration). PREVIMER-D4 LE Croisic 2007-2008

The use of profiler-derived SPM concentration is however much less reliable in the higher part of the water column, for various reasons including the presence of bubbles at the surface (hence perturbing the acoustic signal), the increase with distance in the attenuation corrections errors and a possible difference in particle size between the upper and the lower parts of the water column (the backscatter calibration is based on bottom SPM only, while finer particles may typically be found higher up in the water column, depending on the local seabed composition, resuspension dynamics and possible advected matter). Only the use of surface turbidity sensors therefore allows a sound assessment of the satellite-derived mineral SPM concentration estimate. Figure 4 shows this comparison for PREVIMER-D4 Le Croisic. Satellite data are only available once a day (with a 500m resolution for MERIS while *in situ* concentrations are recorded hourly (the horizontal print of theinsonified cell increases with distance from the sensor, and reaches about 1 m<sup>2</sup> in 20 m water depth). At that location and for the winter conditions encountered from December 2007 to march 2008, the satellite data systematically overestimates the *in situ* measurement, even when the *in situ* turbidity signal is averaged daily in order to smooth out high frequency peaks. The ratio between the two signals varies between 2 and 4 over the investigated period (although Gohin (2011) shows much better agreement between satellite and *in situ* data, but for a lower range of concentrations). A similar ratio between satellite and *in situ* data was found

during PREVIMER-D4 Quiberon mooring (2009-2010). Several reasons may explain this discrepancy. One of them lies in the fact that the satellite data processing algorithm is uniform in space all along the French coast, and does not account for the changes in particle reflectance depending on the location. Similar type discrepancies were observed along the Belgium coast on satellite data processed with a different algorithm, and were interpreted as arising from the particular high reflectance of the surface sediments in that area (Fettweiss, *pers. comm.*). It is beyond the scope of this paper to investigate any further the reasons explaining this finding (more *in situ* surface data would be required) or to improve the satellite signal processing (more research would be required). It is however important to remember, when using satellite data to validate surface SPM concentrations 1) that the satellite provides low frequency information compared to *in situ* sensors records and model outputs, 2) that the overall dynamics of the satellite signal is nonetheless very well correlated to *in situ* data, but the quantitative estimates must be considered with care. Their uncertainty may greatly depend on time and space, and more surface *in situ* data (long term time series and surface transects) would be necessary to better qualify the satellite outputs over the whole continental shelf.

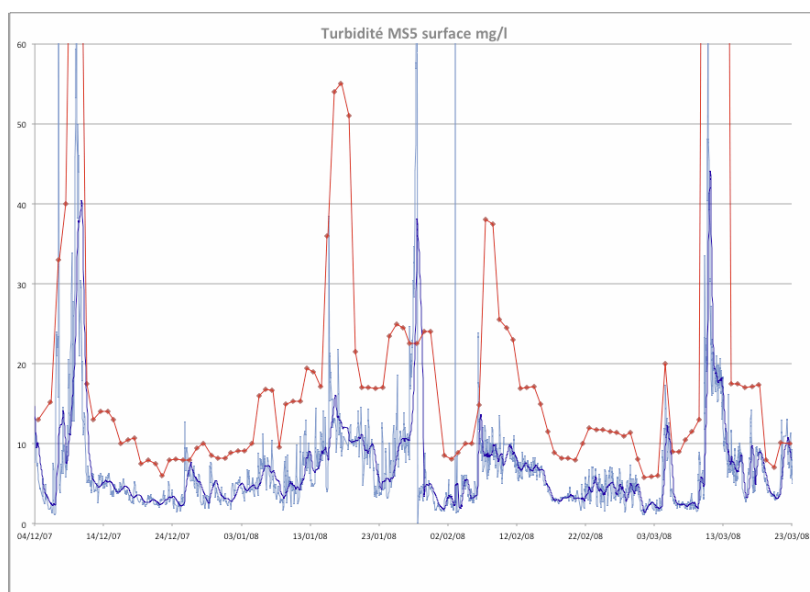


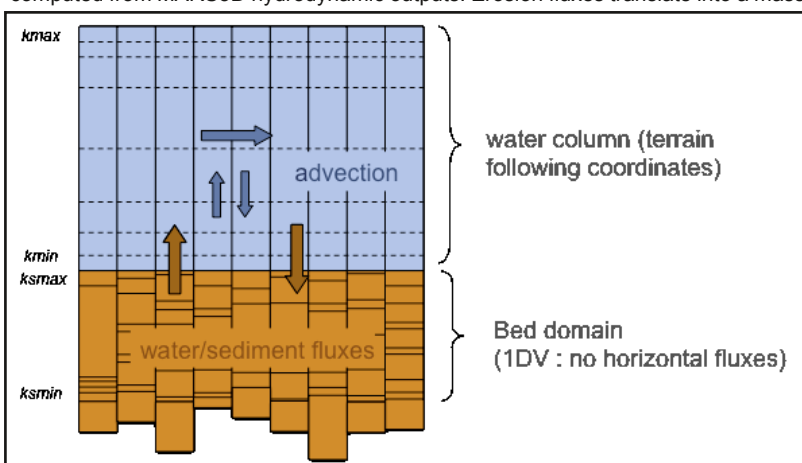
Figure 4: *in situ* surface turbidity (hourly, light blue; daily average, dark blue; PREVIMER-D4 LE Croisic 2007-2008) and satellite turbidity at the same location (red) mg.l-1.

Model validation described in this paper will focus on the December 2007 – March 2008 period, during which several storms were recorded, separated by long calm spans, hence covering a large variety of situations.

## Sediment model description

### Model domain and overall principle

The sediment dynamics compartment consists in a juxtaposition of 1DV models simulating the bed “under” each of the hydrodynamic cells (that may be rectangular or curvilinear in MARS3D, Figure 5). The total bed thickness may vary in time and space, and is discretized in cells of irregular thickness, each cell being characterized by its composition (sediment mixture). Depending on the sediment exchanges between the bed and the water column, the overall bed thickness and number of cells may change over time and from place to place, so as may each individual cell thickness and composition. Erosion and deposition processes are driven by the bottom shear stress that is computed from wave and current forcing: wave-induced shear stress is given by WW3 (Ardhuin *et al* this issue) outputs interpolated on the computation grid, while current-induced shear stress is computed from MARS3D hydrodynamic outputs. Erosion fluxes translate into a mass transfer from the bed compartment into the water column. Once



in suspension, the sediment is advected along with other dissolved or particulate variables. High settling velocities however require the use of an upwind scheme in the vertical, unlike for other variables (see Berger *et al.*, this issue, for general information regarding numerical schemes). Changes in water density due to high sediment concentrations and changes in bottom roughness may optionally be fed back into the hydrodynamic model. Settling particles eventually reintegrate the bed compartment. Their arrangement in the bed is managed according to Le Hir *et al* (2011).

Figure 5: MARS3D-SEDIM grid setting: the bed is discretized in each “sediment column” independently from the neighbouring cells in the horizontal. *kmin* and *kmax* are the vertical min and max cell indices in the water column. *ksmin* and *ksmax* are the vertical min and max cell indices in the bed compartment

### Sediment model

The model computes the dynamics of any number of sediment classes defined for each run. Realistic sediment composition in the bed may therefore be finely described, each facies being represented by a mixture of several sediment classes, in various proportions and concentrations. Sediment classes may exhibit a sandy behaviour ("sands", no cohesion) or muddy behaviour ("muds", cohesive behaviour). The critical shear stress for any mixture depends on the sand/mud proportion in the bed, and the critical erosion shear stress for mud and sand (as a function of bed concentration). Erosion fluxes for mud and sand depend likewise on the individual erosion flux for each sediment type and on the proportions of each type in the bed. Settling velocity for sands is only related to the grain diameter while settling velocity for muds may depend on the concentration in the water column (hindered settling processes) and on flocculation.

The use of terrain-following coordinates in the water column translates into bottom cells of varying thickness in time and space. Deposition fluxes are classically computed as the product between the concentration in the bottom layer (computed in the middle of the cell) and the settling velocity. However, whenever vertical gradients are strong (as is the case for high settling velocities) or when the bottom cell is thick, the actual near bottom concentration – classically computed at a given "reference height" above the bed (2 to 10 times the grain size diameter, van Rijn, 1993) –, is likely to be greater than the concentration in the middle of the cell. An extrapolation technique is therefore used in order to assess the concentration at the reference level, hence the deposition. Horizontal concentration fluxes in the bottom cell are also modified so as to account not only for vertical concentration gradients in that cell, but also for vertical velocity gradients (Waeles *et al.*, 2007; Vareilles *et al.*, submitted). The reference height being arbitrarily chosen, the deposition magnitude depends on this reference height, and so does the erosion flux. While flume and numerical experiments using monodisperse sediment make it possible to actually derive an expression of the erosion flux variations as a function of the reference height, the erosion flux for realistic configurations remains one of the tuning parameters.

Accounting for suspended sand transport in large realistic configurations may lead to unmanageable computational times because of large settling velocities imposing small time steps for vertical advection. Another particularity of the model is the possibility to compute vertically integrated sand concentration (and advection) in the water column, while all other particles are computed in three dimensions. Following a strategy similar to the strategy described above in order to take into the concentration gradients in the bottom cell, classical equilibrium sand concentration profiles are assumed in the water column (Rouse profile) so as to take into account higher sand concentrations near the bed, and compute realistic deposition. Horizontal sand fluxes also mostly occur near the bed, and would be greatly underestimated if they were computed within a 2D-framework. They are therefore computed as the product over the water column of the "re-constructed" sand concentration profile and a 3D- velocity profile (Vareilles *et al.*, submitted).

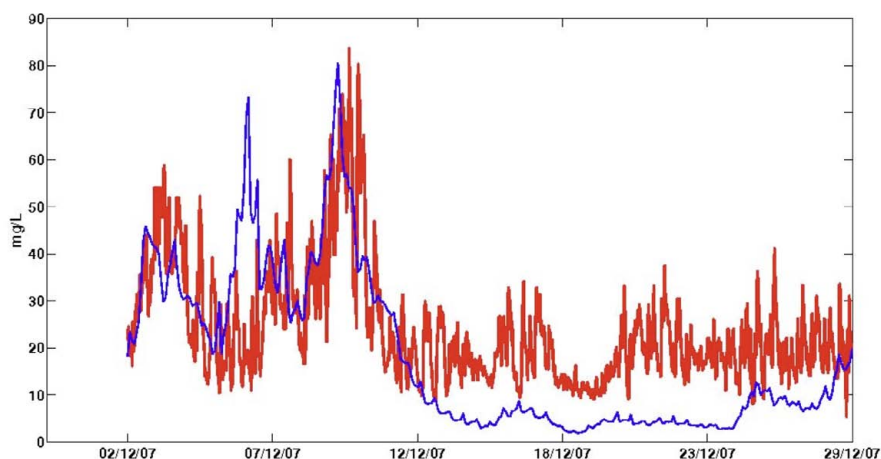
### Operational framework

Operational runs for sediment dynamics are carried out at the same time as the hydrodynamic computations for the English Channel and Atlantic coast area (MANGAE4000, Berger *et al.*, this issue). The import of real-time hydrodynamic forcing (river discharge, meteorological forcing, offshore boundary conditions) is managed by the operational hydrodynamic framework. The sediment-related added features consist in assigning river sediment discharges (from empirical relationships relating solid discharge with liquid discharge for each river), importing real-time PREVIMER WW3 wave outputs, and initializing the bed composition. Additional model outputs consist in the time varying concentration of all sediment variables in the water column (hourly). The bed composition changes are saved at a lower frequency (daily). The number of sediment cells in the sediment compartment may be fairly large, and a most interesting output of the sediment model lies in keeping track of surface bed evolutions. The decision was thus made to only save the composition of the sea bed integrated over a given thickness. For research purposes, the whole sediment grid may of course be saved at a higher frequency.

## Sensitivity analysis and model calibration

A first configuration consisted in ignoring coarse sediments, and considering two cohesive sediment classes: one class representative of river inputs (clay-like, settling velocity of  $0.02 \text{ mm}\cdot\text{s}^{-1}$ ) and one class representing the initial sea bed coverage (silt-like,  $0.1 \text{ mm}\cdot\text{s}^{-1}$ ). Critical erosion and deposition shear stresses were set to respectively  $0.15 \text{ N}\cdot\text{m}^{-2}$  and  $12 \text{ N}\cdot\text{m}^{-2}$ , erosion flux to  $4.10\text{-}6 \text{ kg}\cdot\text{m}^{-2}\cdot\text{s}^{-1}$ , initial bottom bed concentration set to  $400 \text{ kg}\cdot\text{m}^{-3}$ . No consolidation was taken into account. The initial bed coverage respected realistic data (no initial sediment in areas mostly covered with sands, pebbles or rocks). Figure 6 shows reasonable agreement between the near bottom turbidity sensor and the model magnitude during the December 2-12 storm, but the model significantly underestimates the observation after the storm. The same trend is seen from comparing surface model results to satellite data (Figure 7): while computed and observed magnitudes agree during the storm, the model seems to predict much more rapid settling than suggested by the satellite observation.

Figure 6 – Time series for the measured (red, optical turbidity sensor) and simulated (blue) bottom turbidity ( $\text{mg}\cdot\text{l}^{-1}$ ). PREVIMER-D4 Le Croisic 2007.



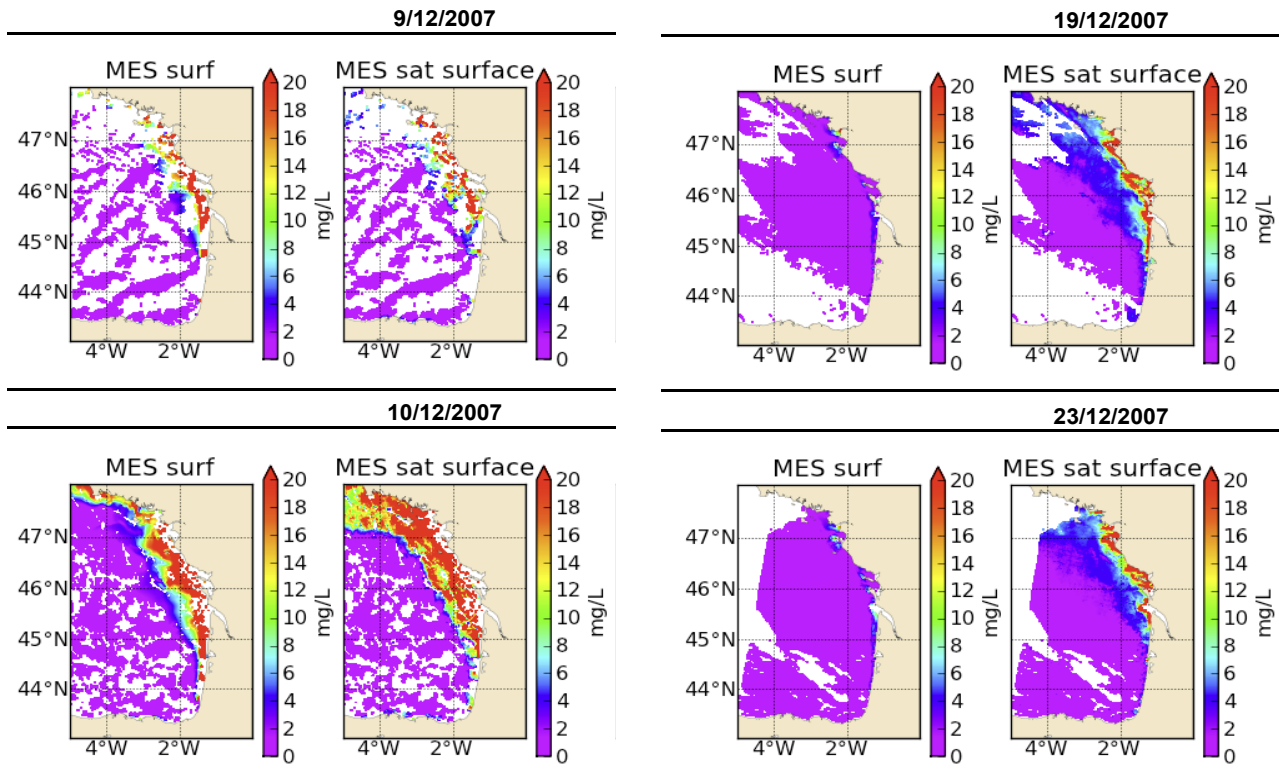


Figure 7 – Left: modelled and satellite surface concentration during the 2-12 December 2007 storm; Right: modelled and satellite surface concentration after the storm.

Vertical modelled and observed *in situ* profiles however suggest excessive vertical mixing in the water column during the storm, insufficient resuspension during the following calm period, and an almost complete absence of remaining SPM in the water column after December 13 (Figure 8). These initial results suggested to carry out several sensitivity tests on critical shear stress, erosion flux, initial bottom density, settling velocity. The use of an additional sandy variable and an experiment starting from a uniform initial bed composition made of 50% silt and 50% sand were also tested. Satisfactory results were obtained thanks to the use of 3 variables (sand – vertically integrated computation –, silt and clay, settling velocities of 5 mm.s<sup>-1</sup>, 0.5 mm.s<sup>-1</sup> and 0.02 mm.s<sup>-1</sup>) and an identical erosion flux for all variables, set to 8.10<sup>-6</sup> kg.m<sup>-2</sup>.s<sup>-1</sup> (configuration later referred to as "reference run"): Figure 9 exhibits encouraging results displaying the monthly average of surface turbidity provided by the model and by satellite data over December 2007. This representation, which was chosen by Sykes and Barciela (2012) when they assessed the quality of their operational POLCOMS turbidity model, is indeed much more forgiving than a thorough investigation of high frequency outputs over the water column. However, it may hide some model (and/or data) discrepancies. In our case, since the satellite absolute SPM concentration seems to be overestimated by a factor two, correct model results may have to predict half the value given by the satellite data (but that may not be true in the English Channel). Moreover, this parameterization induces a significant overestimation of the bottom concentration when compared to moorings.

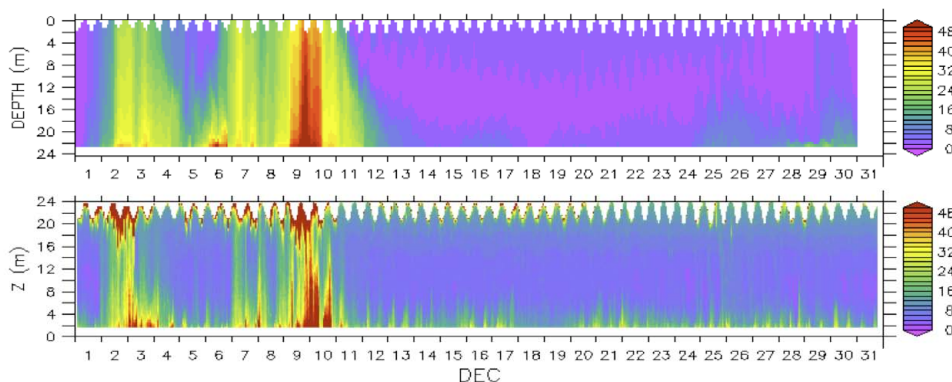


Figure 8 - Upper panel: modelled turbidity in mg.l-1 as a function of time and water depth ("reference run"). Bottom panel: profiler calibrated turbidity (mg.l-1). The red areas near the water surface in the observations represent noise in the acoustic signal. The data can only be reliable up to about 5 m under the surface (for this record)-PREVIMER-D4 Croisic 2007.

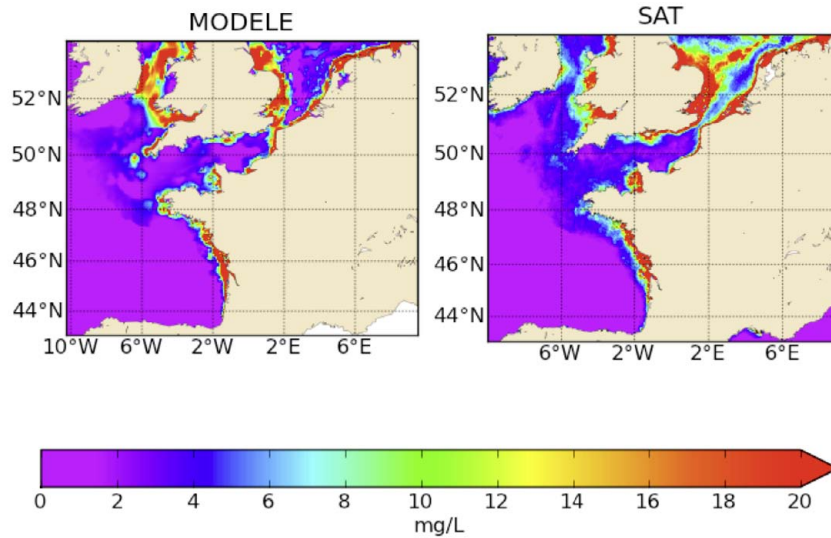


Figure 9 - Computed (left) and satellite (right) surface SPM concentration averaged over December 2007 (mg.l-1)

#### Sea bed evolution

One of the goals of the regional sediment dynamics model is to assess the variability of the seabed composition. Coastal areas, sandy beaches or muddy tidal flats do exhibit a very strong variability in their seabed morphology and composition, with the creation of temporary fluid mud layers after storms for instance (a maybe more spectacular and visible expression of this variability is the seasonal sand loss on beaches every winter, turning summer sandy beaches into winter pebble fields). The seasonal or interannual sea floor variability at the shelf scale and its possible impact on habitat is however unknown. Predicting this variability should be possible with our model, provided the management of seabed layers is carefully assessed. The influence of the minimum and maximum layer thicknesses allowed in the bed compartment was therefore investigated. In case of sediment mixtures, these parameters may greatly influence results, in particular because the model behaviour is drastically different for a sandy surface sediment or muddy surface sediment. In particular, the active layer thickness changes with the choice of these parameters. The thinner the layers are allowed to be, the more chances there will be of having superimposed layers of pure sand and pure mud (because of their different settling velocities for instance), whereas larger layers will lead to systematic mixing of all sediment types. This investigation showed that the minimum layer thickness had to be of the order of  $5 \cdot 10^{-2}$  mm or smaller for results to not depend on this thickness anymore, while a maximum thickness of the order of 0.5 mm was more prone to allow the creation of laminations. Figure 10 illustrates how bed thickness and concentration evolve in time (initial 1 cm bed thickness,  $10^{-6}$  mm minimum layer thickness,  $10^{-4}$  m maximum layer thickness).

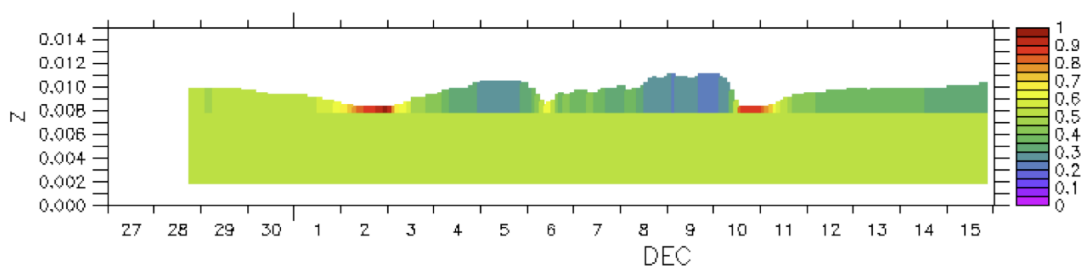


Figure 10 – Time evolution of the bed thickness in a given cell (sediment height in m). The initial bed was a 1 cm thick sediment mixture of 50% sand and 50% clay. The color represents the sand fraction in the mixture. Erosion periods lead to thinning and sand enrichment (going towards warmer colors) while deposition events lead to thickening and mud enrichment (going towards colder colors).

New sensitivity tests were carried out on sediment-related parameters with this better control of the seabed dynamics. For this investigation, priority was given to the comparison between modelled turbidity and *in situ* time series. The initial sediment coverage was derived from a spatial sand and silt repartition obtained after a 4 month long spin-up run, so as to use a bottom description in equilibrium with the model dynamics. This sand and silt repartition exhibits the same overall features as the sedimentological maps of the area (Figure 11). However, this bed sediment distribution corresponds to a situation in the spin-up run when fine sediments were in suspension in the whole domain; since new runs usually start from clear water (apart from the background turbidity), 50 kg.m<sup>-3</sup> clay were added to this initial sediment coverage so as to not create immediate fine sediment "drainage" from the seabed as soon as resuspension occurs, which would induce artificial sand enrichment in the bed.

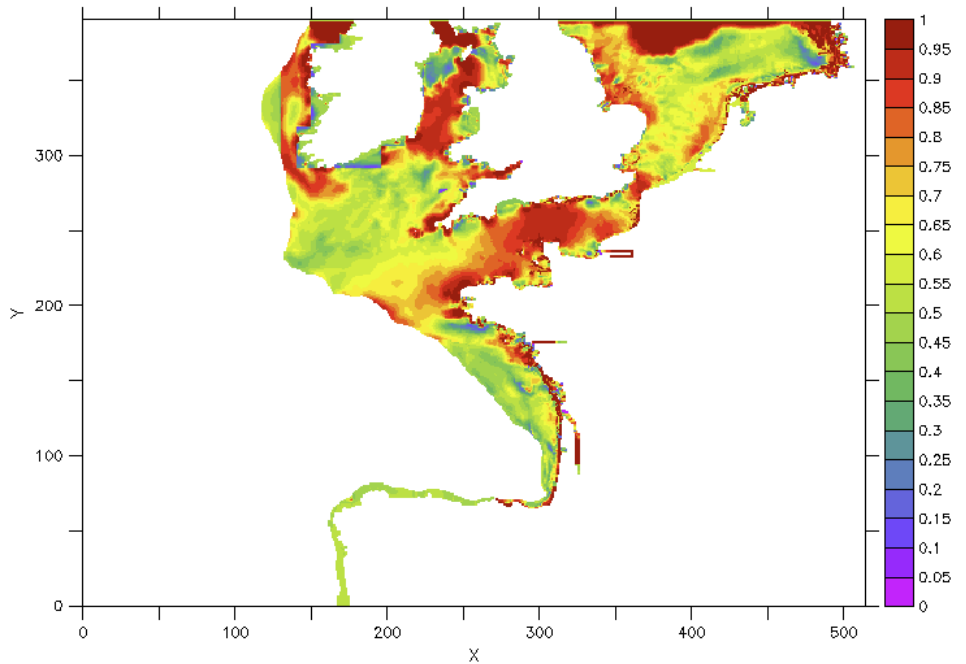


Figure 11 – Sand fraction used in the initial bed composition

The choice was made to adjust results for 3 variables (clay, silt and sand). The offshore background surface turbidity level was also imposed in the model through the initial seeding of clay-like particles in the whole domain (concentration of 1.5 mg.l<sup>-1</sup>).

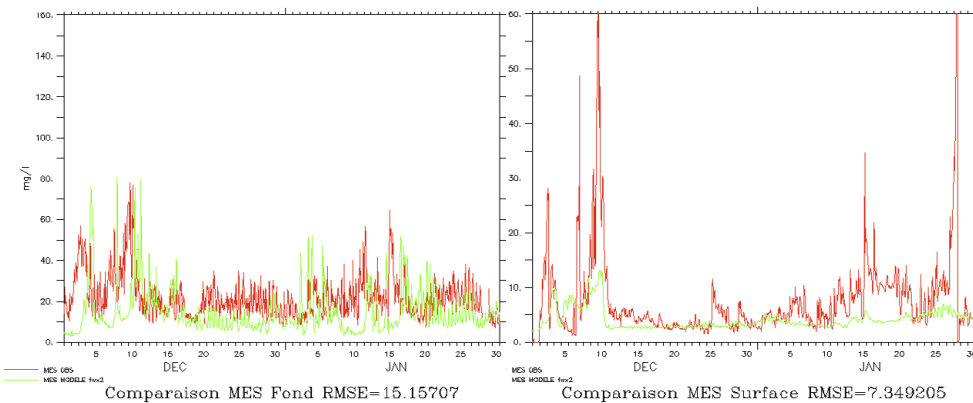
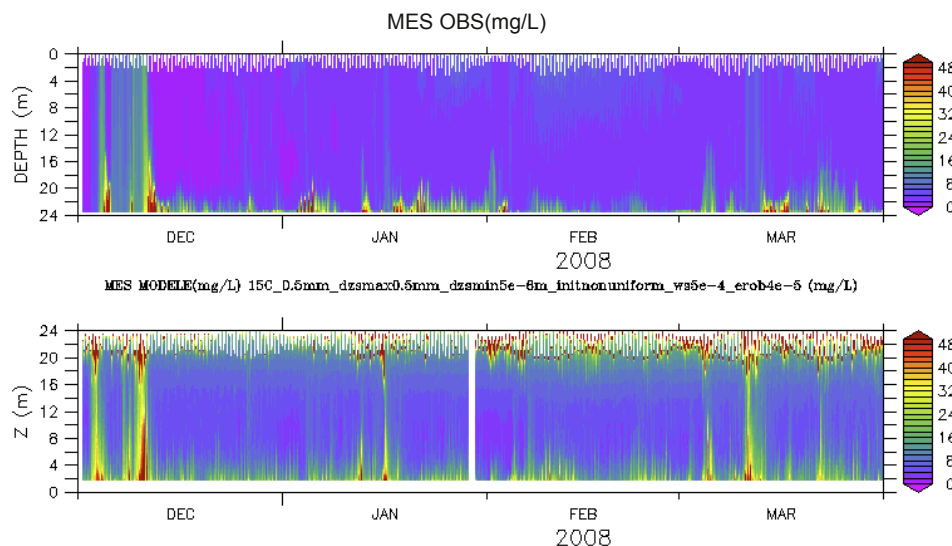


Figure 12 – Measured (red, optical turbidity sensor) and modelled (green) SPM concentration for PREVIMER-D4 Le Croisic (operational parameterization). Left: bottom concentration; Right : surface concentration. z0=0.5 mm. fwref from Soulsby (1993)15:15



The investigated parameters used to calibrate the turbidity signal were once again settling velocity, bottom erosion flux and bottom shear stress, which usually have to be simultaneously adjusted. Settling velocities are chosen so as to reproduce the correct time scale during which suspended sediment stays in the water column after a storm. They were kept to 5 mm.s<sup>-1</sup>, 0.5 mm.s<sup>-1</sup> and 0.02 mm.s<sup>-1</sup> for the three variables (*i.e.* flocculation not accounted for). The amount of eroded sediment is driven by the chosen values for the erosion flux and the bottom shear stress. Changing the erosion flux however does not allow differential weighting of the waves and/or tides contributions. These contributions may be assessed when comparing the different suspended dynamics observed in the English Channel (tide-dominated) or along the French Atlantic coast (wave-dominated): the turbidity signal frequency may indeed be more or less correlated to tides or waves. While theoretical or empirical formulations exist to determine tide- and wave-related friction factors (and they are used as first guesses), their accurate estimate can only be assessed through *in situ* turbulence measurements, and their values may greatly vary in time and space. That is the reason why they are still commonly used as calibration factors for resuspension in regional sediment dynamics models.

Figure 13 – Modelled (top) and measured (bottom) SPM vertical concentration profile as a function of time (mg.l<sup>-1</sup>). PREVIMER-D4 Le Croisic (operational parameterization)

## Development and validation of a sediment dynamics model within a coastal operational oceanographic system

After inspection, the erosion flux was set to  $8 \cdot 10^{-6} \text{ kg} \cdot \text{m}^{-2} \cdot \text{s}^{-1}$ . The bed roughness used to compute current-induced bottom shear stress was unchanged ( $z_0=0.5 \text{ mm}$ , uniform in space) while the wave friction factor was doubled compared to the reference run (where it was set to Soulsby (1997)'s formulation), therefore increasing resuspension during storms. This parameterization leads to results shown on Figure 12 and Figure 13. The computed turbidity magnitude and variability are satisfactory on the bottom and the lower part of the water column, but they are still underestimated at the surface. Figure 14 shows that increasing tide-induced resuspension manages to increase surface concentration variability and magnitude, but leads to great overestimation in the bottom (which was one of the early "reference run" bias, see Figure 8).

An ultimate comparison between model results and satellite data (while being aware of the possible bias between satellite and *in situ* data) suggested a systematic underestimation of the turbidity along the British south coast, and the Belgian and Eastern Channel French coasts. Model results, *in situ* horizontal profiles using a towed fish, and satellite images of the English Channel after strong storms (Gohin, *pers. comm.*) suggest that advection may not be a major process in driving the spatial distribution of sediment suspension at the shelf scale: the seabed composition is on the other hand a strong determining factor. The deficit of coastal turbidity was therefore attributed to a lack of muddy sediments in the bed (the initial bed was indeed quite sandy along the coast, which is not conform to reality), which was corrected by changing the sand/silt proportion below 20 m water depth in the aforementioned areas.

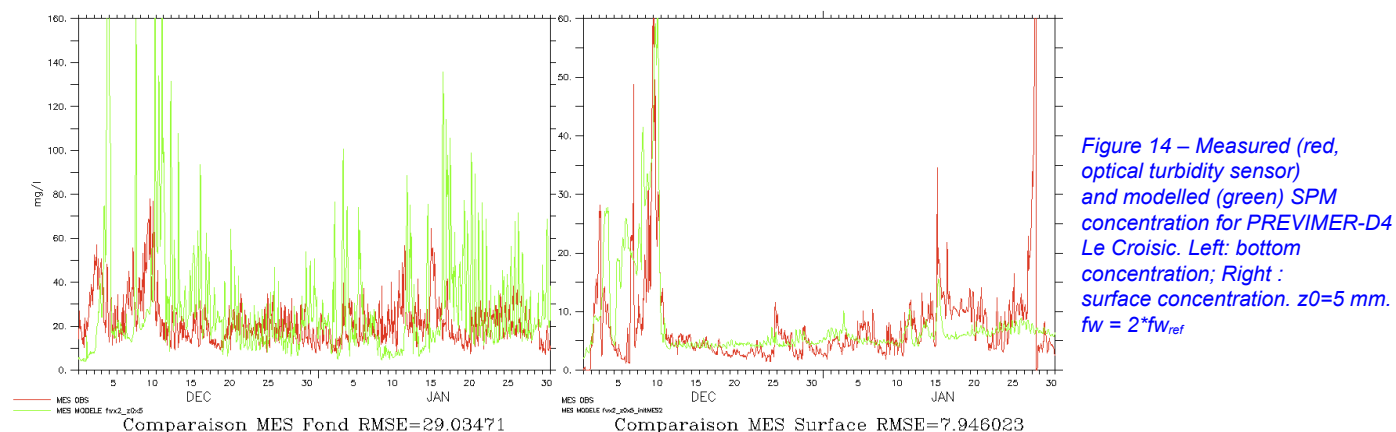


Figure 14 – Measured (red, optical turbidity sensor) and modelled (green) SPM concentration for PREVIMER-D4 Le Croisic. Left: bottom concentration; Right: surface concentration.  $z_0=5 \text{ mm}$ .  $fw = 2 \cdot fw_{ref}$

This latter parameterization was chosen for operational runs, which have been computed since September 2013. Further comparisons to existing data need to be carried out in order to improve this parameterization, and a systematic calibration/validation procedure would greatly benefit from a more systematic data acquisition strategy covering French coastal waters. More *in situ* surface concentration data would be of utmost importance so as to improve the confidence we can have in satellite-derived SPM concentrations, which remain a precious source of systematic (cloud dependant) synoptic coverage.

#### Influence of horizontal grid resolution

Particularly along the French Atlantic coast, sediment resuspension is highly related to wave action. While bathymetric gradients on the shelf are usually fairly smooth, they are obviously much sharper in shallow areas, precisely where wave influence is felt the most. The horizontal resolution of most regional models (of the order of 2-3 km for structured grids) usually remains fairly coarse compared to the bathymetric gradients encountered for water depths lower than 20 to 40 m. The sediment dynamics model does exhibit a spatially variable behaviour (because of the space variability in sea bed composition or even bed roughness), but this parameterization does not account for any sub-grid processes. A first investigation of the effect of resolution on turbidity results has therefore been attempted, using a local coastal two-way zoom of 500 m resolution inserted into a 2500 m resolution operational configuration (GirondePertuis500 inserted into MANGAE2500). Figure 15 shows the bathymetric schematization in both configurations. WW3 operational computations (see Ardhuin *et al.*, this issue) are run on an unstructured grid of about 200 m resolution near the coastline, and take into account current and water depth refraction computed from a 2D MARS hydrodynamic configuration (see Pineau *et al.*, this issue). Identical wave model outputs were projected on to the 500 and 2500 m grids, and used to compute wave-induced bed shear stress in both models. Figure 16 illustrates, for several depth ranges, the relative wave-induced shear stress variation only due to grid refinement. The refinement induces a quasi systematic increase in wave-induced shear stress, of increasing magnitude as water depth gets shallower. Over January 2010, this increases amounts to 80 to 200% for a bathymetry of 5-10 m below mean sea level, 40-110% for 10-20 m bathymetry, up to 50% for 20-40 m bathymetry. The figure 16 also shows the spatial distribution of differences for a given date: the coarse resolution not only prevents waves from propagating in areas sheltered by islands, but also significantly underestimates wave action as soon as water depth reaches 15-20m (e.g. west coast of the islands).

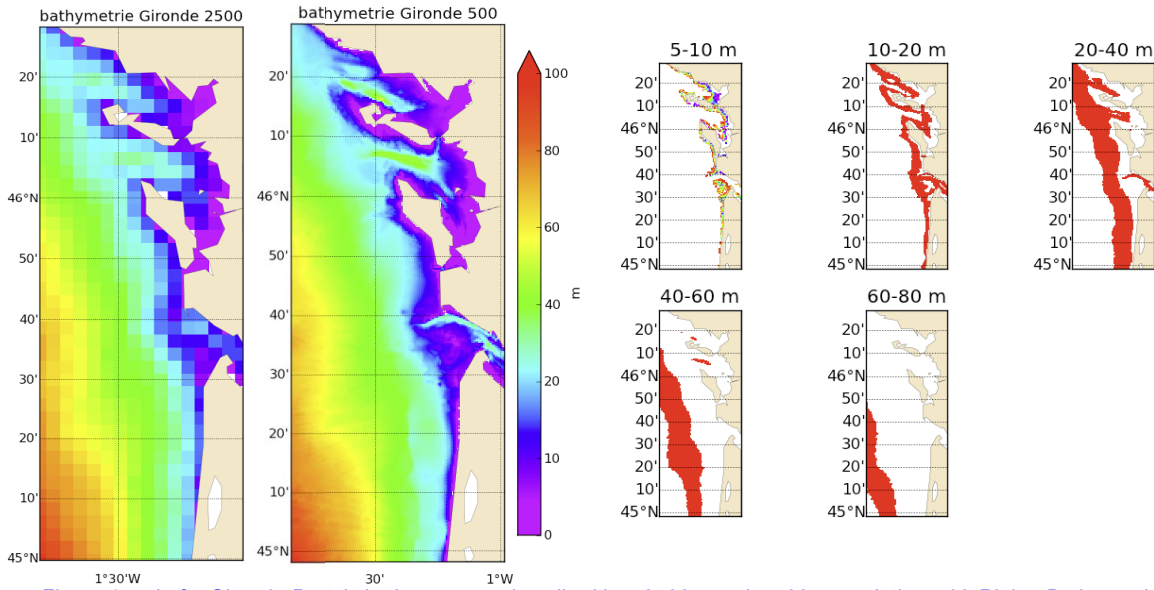


Figure 15 – Left : Gironde-Pertuis bathymetry as described in a 2500m and a 500m resolution grid. Right : Bathymetric strata used to compare model outputs on both resolutions according to water depth.

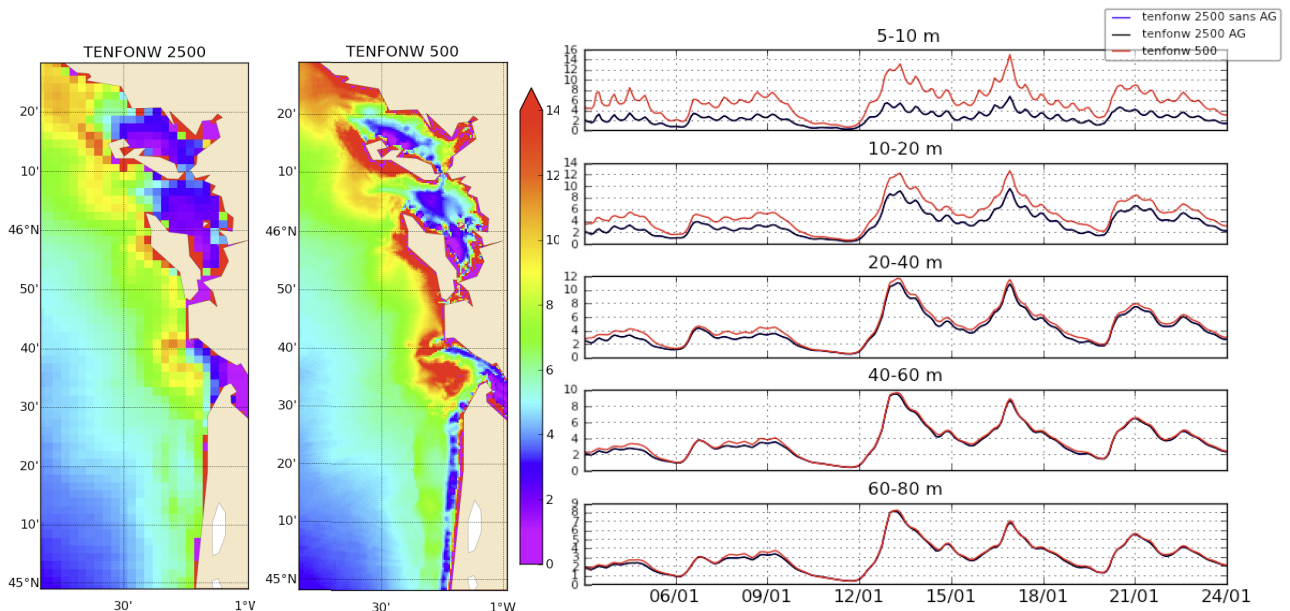
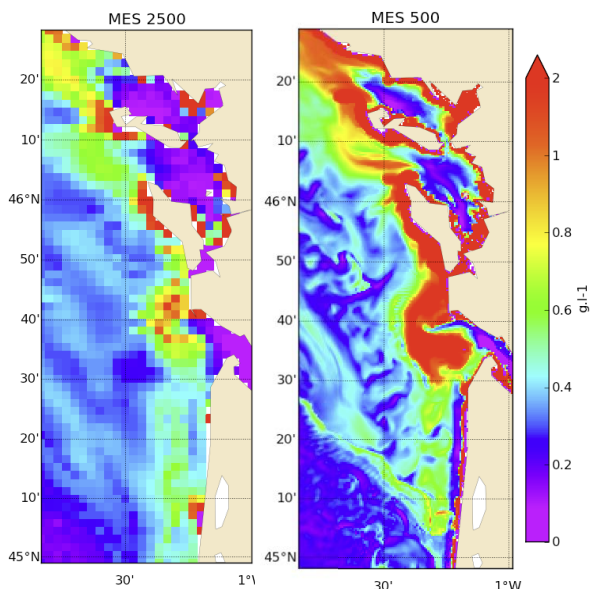


Figure 16 – Left : Wave-induced shear stress ( $N.m^{-2}$ ) as described in a 2500m (left) and a 500m (right) resolution grid. Right : Wave-induced shear stress averaged over 5 ranges of water depth, as a function of time, computed on the 500m resolution grid (red) and the 2500m resolution grid (black).



In these conditions, otherwise identically parameterized configurations for sediment dynamics will predict very different SPM concentration patterns. Differences will not only result from a different expression for forcing parameters: while current-induced shear stresses are almost identical for both configurations, the refined circulation exhibits structures that are likely to also impact overall sediment fluxes. Apart from the sharp differences in SPM concentration magnitude, Figure 17 for instance exhibits how the increased resolution allows the representation of submesoscale structures. Their influence on long term sediment budgets and fluxes remains to be investigated.

Figure 17 - Modelled near-bottom concentration on January 16, 2010. Left: 2500m grid; right : 500m grid (identical parameterization for both configurations)

## Conclusion

A sediment dynamics model predicting turbidity levels and monitoring seabed coverage evolutions has been coupled to MARS3D MANGAE4000 operational configuration. The model computes erosion, transport and deposition of 3 types of variables, namely sand, silt and clay. Several sensitivity tests were carried out on two kinds of parameters: 1) parameters driving the vertical discretization in the sediment compartment, and describing the initial distribution of sediments in the domain, 2) parameters driving the sediment behaviour in the water column (mostly erosion and settling). While the repetitiveness of satellite data make them a precious source of information for model validation, errors linked to their absolute quantification are not fully known, which makes it hazardous to fully rely on this source to validate the model. However, their time variability was shown to exhibit very good agreement with surface SPM concentration measured from optical turbidity sensors.

In situ data from moorings were so far privileged in order to parameterize the configuration, knowing this parameterization does not allow any convincing comparison with satellite data (Sykes and Barcilea (2012) mention similar discrepancies between buoys and satellite data). We made it a definite choice to use fairly simple formulations for the bottom shear stress and bed roughness computations, erosion fluxes (which were identical for all sediment types) and settling velocity. Ignoring processes such as flocculation and consolidation was also a definite choice: the uncertainty regarding the space variability of all parameters required to properly take into account these processes is so large, that it was considered more reasonable to focus on adjusting a more reduced number of parameters, and judge whether or not such simplifications could still lead to reasonable results. A few experimental runs (not shown) took into account flocculation in the determination of settling velocity, using empirically determined flocculation parameters. Those runs led to fairly different results from those shown here, and that would have required new adjustments for all other parameters driving sediment dynamics (erosion fluxes, critical erosion threshold) without necessarily adding any more realistic results. Including the most advanced state of the art formulations for all sediment related processes is another challenge, particularly when trying to validate procedures on well constrained academic configurations (see Warner *et al.* (2008), for instance, for some aspects such as wave-current interaction or the use of ripple predictors). But the benefits of this complexity to simulate fairly unknown dynamics at a regional scale remains to be addressed.

On the other hand, the influence of some fairly “fundamental” features such as the impact of turbulence schemes and resolution require immediate attention. The model apparent incapacity to simultaneously reproduce accurate bottom and surface magnitudes for SPM concentration for instance suggests insufficient vertical mixing in some cases. Whether increasing horizontal resolution in shallow water is likely to modify overall sediment fluxes at the shelf scale still has to be inferred – which would impose either a two-way zoom strategy as allowed thanks to AGRIF, or the use of unstructured grids.

## Acknowledgements

The authors wish to thank Region Bretagne for financially supporting this work, and thank PREVIMER project lead team for its support. The French hydrographic service (SHOM) is thanked for providing data on the sediment coverage at the regional scale.

## References

- Ardhuin F., M. Accensi, A. Roland, F. Girard, J.-F. Filipot, F. Leckler, J.-F. Le Roux, 2014, Numerical wave modeling IN PREVIMER: multi-scale and multi-parameter DEMONSTRATIONS, Mercator Ocean Newsletter #49, this issue.
- Berger H., F. Dumas, S. Petton, P. Lazure 2014, Evaluation of the hydrology and dynamics of the operational mars3d configuration of the bay of Biscay, Mercator Ocean Newsletter #49, this issue.
- Charria G., M. Repecaud, L. Quemener, A. Ménesguen, P. Rimmelin-Maury, S. L'Helguen, L. Beaumont, A. Jolivet, P. Morin, E. Macé, P. Lazure, R. Le Gendre, F. Jacqueline, R. Verney, L. Marié, P. Jegou, S. Le Reste, X. André, V. Dutreuil, J.-P. Regnault, H. Jestin, H. Lintanf, P. Pichavant, M. Retho, J.-A. Allenou, J.-Y. Stanisière, A. Bonnat, L. Nonnotte, W. Duros, S. Tarot, T. Carval, P. Le Hir, F. Dumas, F. Vandermeirsch, F. Lecornu, 2014, PREVIMER: a contribution to In situ coastal Observing systems, Mercator Ocean Newsletter #49, this issue.
- Gohin, F., 2011, Joint use of satellite and in-situ data for coastal monitoring, Ocean Sci. Discuss., 8, 955–998, 2011, [www.ocean-sci-discuss.net/8/955/2011/](http://www.ocean-sci-discuss.net/8/955/2011/), doi:10.5194/osd-8-955-2011
- Le Hir, P, Cayocca, F., Waeles, B., 2011, Dynamics of sand and mud mixtures: A multiprocess-based modelling strategy, Continental Shelf Research, 31(2011) S135-S149, doi:10.1016/j.csr.2010.12.009
- Pineau-Guillou L., F. Dumas, S. Theetten, F. Ardhuin, F. Lecornu, J.-F. Le Roux, D. Idier, H. Muller, R. Pedreros, 2014, PREVIMER: improvement of surge, sea level and currents modelling, Mercator Ocean Newsletter #49, this issue.
- Soulsby, R., 1997, Dynamics of marine sands – Thomas Telford Publications, - ISBN 072772584-X, 249pp.
- Sykes, Peter A. and Rosa M. Barciela, 2012, Assessment and development of a sediment model within an operational system J. Geophys. Res, VOL. 117, C04036, doi:10.1029/2011JC007420, 2012
- van Rijn, L.C., 1993, Principles of sediment transport in rivers, estuaries and coastal seas, Amsterdam: Aqua Publications – ISBN 90-800356-2-9
- Verney, R.; Voulgaris, G.; Manning, A.; Deloffre, J. and Bassoullet, P. (2013) Quantifying SPM Dynamics in estuaries : Combining acoustic and optical approaches : the FLUMES experiment. Proceedings of the 12th International Conference on Cohesive Sediment Transport Processes (INTERCOH), October 21-24; Gainesville, Florida
- Vareilles, J., Cayocca, F., Le Hir, P., 2014, Modelling the long-term morphological evolution of mixed-sediments beds, submitted
- Waeles, B., Lesueur, P., Le Hir, P., 2006, Modelling sand/mud transport and morphodynamics in the Seine river mouth (France): an attempt using a process-based approach, Hydrobiologia (2007) 588:69–82, DOI 10.1007/s10750-007-0653-2
- Warner, J., C., Christopher R. Sherwood, Richard P. Signell, Courtney K. Harris, Hernan G. Arang, 2008, Development of a three-dimensional, regional, coupled wave, current, and sediment-transport model, Computers & Geosciences 34 (2008) 1284–1306

# OPERATIONAL MODELLING OF NUTRIENTS AND PHYTOPLANKTON IN THE BAY OF BISCAY AND ENGLISH CHANNEL.

By A. Ménesguen<sup>(1)</sup>, M. Dussauze<sup>(2)</sup>, F. Lecornu<sup>(1)</sup>, F. Dumas<sup>(1)</sup>, B. Thouvenin<sup>(1)</sup>

<sup>1</sup>IFREMER, Brest, France

<sup>2</sup>ACTIMAR, Brest, France

## Abstract

Nitrate loadings to the French coastal waters of the Bay of Biscay and the English Channel have increased from 5 to 10 times during the four last decades, due to runoff on intensively fertilized agricultural watersheds. Eutrophication of this coastal zone is now a recurrent problem, with well-known direct impacts (Ulva "green tides" on beaches, excessive phytoplanktonic blooms responsible for "coloured waters" and bottom hypoxia events offshore), but also indirect enhancement of the toxicity of some phytoplankton species, caused for instance by increased N:Si ratio in the coastal sea. In order to better guide the decision makers about nutrient loading reduction, Ifremer uses the so-called ECO-MARS3D biogeochemical-hydrodynamical model to simulate the present situation in terms of phytoplanktonic biomasses and oxygen concentrations, along with more specific information: concentrations of 3 harmful phytoplanktonic species (*Pseudo-nitzschia*, *Karenia*, *Phaeocystis*) and ASP toxin (domoic acid) in the sea water. The simulations of recent years have been compared favorably to satellite images and field measurements, and an operational version currently runs on the previmer.org site. An original tracking method of nitrogen (or phosphorus) coming from any source allows the assessment of the quantitative role of the 3 main rivers (Seine, Loire, Gironde) nitrogen loads in the phytoplankton blooms. The model points out the bay of Vilaine as very sensitive to bottom oxygen depletion in summer, and can be compared on-line to the automatic measurements coming from the MOLIT buoy. Through the appearance of too high N :Si ratio in the nutrients, the model also provides some explanation to the patchy location of ASP toxin recorded by the REPHY monitoring network.

## The French coastal eutrophication in the European context

The terrestrial loadings on the European coastal shelf have varied during the last century in a nearly independent way for the three main nutrient Nitrogen N, Phosphorus P and Silicon Si. Whereas Si remained quasi-constant or slightly declined due to partial trapping by settling freshwater diatoms upstream of dams, P increased until the nineties, and then decreased thanks to polyphosphate banning in detergents and phosphate removal in sewage plants (Billen and Garnier, 2007); N increased continuously during the second half of the 20<sup>th</sup> century, but began to slightly decrease during the last decade due to European directives.

The first global impact of coastal eutrophication is an increase of phytoplankton biomass in the enriched areas, mainly in the plumes of rivers. In temperate seas, a characteristic of eutrophicated waters is the apparition of additional blooms in summer, between the two classical blooms (the main one in spring and the secondary one in autumn). The sedimentation and decomposition of high phytoplanktonic biomasses in stratified and calm areas may lead to severe oxygen depletions in bottom waters, as in the bay of Vilaine, in July 1982 (Merceron, 1988). Besides these quantitative effects, some qualitative changes in the flora may be induced by the changing balance N/P/Si. In the eastern English Channel and the southern North Sea for instance, undesirable blooms of the Haptophyte *Phaeocystis globosa*, which forms spherical colonies with foam as by-product, invades every spring (April-May) the coastal strip from the Bay of Somme up to Belgium (Lancelot, 1995). These Haptophytes are known to follow the classical early-spring diatom bloom (Rousseau et al., 2002) when a remaining excess of nitrate allows their rapid growth, even if phosphate conditions are low (Lancelot et al., 1987), because this species is able to use organic forms of phosphorus (Veldhuis et al., 1991). Along the Atlantic and English Channel coasts, several harmful species of phytoplankton have been recorded for a while, because they produce diseases in human consumers of shellfishes. Some of them are dinoflagellates (*Dinophysis* sp., *Alexandrium* sp.), and may have been triggered by summer excess nutrient in the coastal plumes, as mentioned by Guillaud and Ménesguen (1998); in case of *Dinophysis* sp., the link between nutrients and the dinoflagellate seems to be indirect, through intermediate ciliates used as preys by the heterotrophic dinoflagellate (Souchu et al., 2013). Recent episodes of long-term Amnesic Shellfish Poisoning have severely hampered the scallop fisheries in the eastern English Channel and the northern Bay of Biscay (first event in December 2004 in Bay of Seine and Brittany, very strong and persistent contamination in the northern Bay of Biscay following the Xynthia hurricane); they are due to domoic acid production by several diatom species belonging to the genus *Pseudo-nitzschia*. Several papers have clearly related the biomass increase of these species to the increase of nitrogen delivery by rivers (Parsons and Dortch, 2002), as well as the enhancement of toxin production by excess of nitrogen availability relatively to silicon or phosphorus (Fehling et al., 2004).

Thanks, first, to the Water Framework Directive WFD (2000), then to the Marine Strategy Framework Directive MSFD (2008), the European Commission has compelled European countries to periodically assess the status of their coastal waters relatively to the eutrophication process (Ferreira et al., 2011). For the WFD, coastal water masses have been delineated following the "1 nautical mile from shoreline" rule, which can miss the most part of wide eutrophicated areas: in a large river plume, the turbidity near the coast and the estuary is often too high to allow strong primary production, whereas enriched surface waters more offshore, after settling of suspended particles, can host very productive communities. For the MSFD, the "ecological status" has to be monitored on the whole shelf, in a few large sub-regions, for which dense sampling at sea becomes too expensive and unaffordable. Modelling the eutrophication on the European shelves then becomes an attractive way to fill the gap, as well as satellite remote sensing.

## The ECO-MARS3D tool

The biogeochemical modelling component (ECO-MARS3D) of the French Previmer project of Coastal Operational Oceanography is based on the MARS3D hydrodynamical code (Lazure and Dumas, 2008). The current application to the French Atlantic shelf is based on a regular grid with 4x4 km meshes and 30 sigma levels, which covers the Bay of Biscay, the English Channel and the southern part of the North Sea, up to the Rhine estuary; it extends from 8.13°W to 5.0°E, and from 43.17°N to 52.75°N (Fig. 1). This running version is an extended and re-calibrated version of a first model of the same space resolution, but limited to the Bay of Biscay, which was built as a Previmer demonstrator. This has been run operationally during 6 years (2007-2012) on the previmer.org site, and used also for a long off-line run (1972-2008) for an environmental approach of pelagic fish fluctuations (Huret et al., 2013).

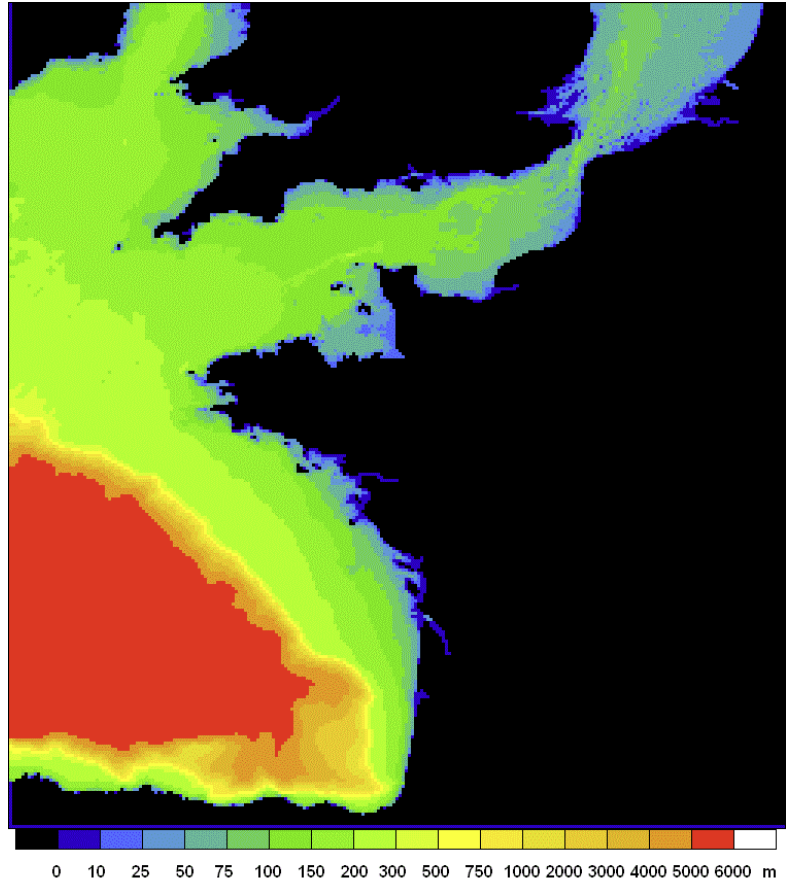


Figure 1: Bathymetry (mesh: 4x4 km) of the English Channel and Bay of Biscay model domain.

Mechanical forcing of the MARS3D hydrodynamical model is made by barotropic sea-level oscillation at the oceanic boundaries (provided by a 2D model covering the whole North-East Atlantic), and wind and atmospheric pressure at the sea surface; these are provided by the Arpege model of Météo-France with a 30 km and 6 h space-time resolution. Measured daily discharges as well as monthly river temperatures are provided on line by the Seine-Normandie, Loire-Brittany and Adour-Garonne River Basin Agencies, for the 5 main French rivers: Adour, Gironde, Loire, Vilaine and Seine. For all the other rivers in the domain, only discrete measurements of flow rates made in recent years are available for validation; in operational mode, the daily flow rate of these rivers is deduced from the measured flow rate of the nearest main river by linear regression. River daily concentrations for inorganic and organic dissolved nutrients are computed from empirical statistical relationships involving flow rate and time fitted to historical data (Guillaud and Bouriel, 2007). Suspended particulate matter is set to the maximum of ambient climatological monthly mean distribution derived from satellite data (Gohin et al., 2005) and the suspended matter brought by the rivers, which is simply simulated as a particulate conservative tracer, with uniform and constant settling velocity. At the open boundaries, all the biogeochemical state variables are imposed following a zero gradient condition.

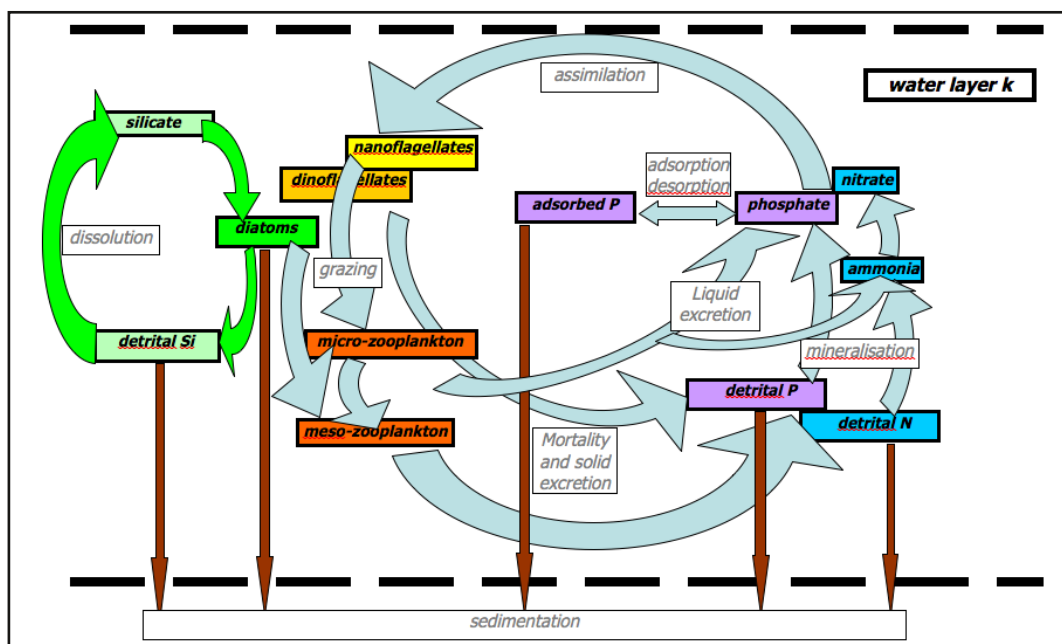


Figure 2: Flow diagram of the biogeochemical model.

The basic biogeochemical model (Fig. 2) contains 17 state variables, describing the nitrogen, phosphorus and silicon cycles and the dissolved oxygen in the pelagic ecosystem. Three limiting dissolved inorganic nutrients are considered: nitrogen, with nitrate and ammonium separately, phosphorus, and silicon. Phytoplankton is divided into 3 groups: diatoms, dinoflagellates and nanoflagellates, with concentrations expressed in nitrogen currency. In order to mimic pigment adaptation to the ambient mean light, chlorophyll is deduced from the nitrogenous state variables of the model by an empirical Chl:N ratio, computed as a Smith-like formula depending on the local extinction coefficient. There are two zooplanktonic components, expressed in nitrogen units: the microzooplankton, which eats nanoflagellates and detrital particulate matter everywhere, along with diatoms in oceanic regions (depth > 200m), and the mesozooplankton, which eats diatoms, dinoflagellates and microzooplankton. So, in this model, diatoms do sink, whereas nanoflagellates and dinoflagellates do not (they are considered as able to maintain at any depth in calm water, thanks to motility). Three particulate detrital variables (detrital N, detrital P, detrital Si) close the biogeochemical cycles, and settle in the water column; in the bottom layer, each settling fraction is partially transferred to a fixed state variable, which can give back to the water layer some particulate material through erosion by currents, and some dissolved equivalent after remineralisation.

Some advanced features are also provided on the Previmer website. Three harmful phytoplanktonic species or genus have been added in competition with the three basic bulk phytoplanktonic variables: the diatoms *Pseudo-nitzschia* sp. responsible for Amnesic Shellfish Poisoning of human consumers of infected bivalves, the dinoflagellate *Karenia mikimotoi* responsible for marine invertebrate and fish kills, and the prymnesiophyte *Phaeocystis globosa* responsible for mucus and foam production. For *Pseudo-nitzschia*, following Davidson and Fehling (2006) and Pénard (2009), the importance of the internal Si:N ratio in triggering the toxin secretion led to the adjunction of 2 state variables to the basic nitrogen mass: the silicon mass and the toxin (domoic acid) concentration. The limiting effect of silicon on the growth is now depending on Si:N ratio (Si internal quota) in a Droop's formulation, whereas the N and P limiting effect remain dependent on the water nutrient concentration in a classical Michaelian manner. As in the Davidson and Fehling's model, when the internal Si/N ratio goes below a certain threshold, the continuous secretion of domoic acid is activated; the toxin then decays following a simple first order process. Finally, in order to highlight the respective roles of the three main tributaries of the domain in sustaining the phytoplanktonic production, a numerical tracking technique (Ménèsquen et al., 2006) has been applied to the inorganic nitrogen loads of the Seine, Loire and Gironde rivers, allowing to track dynamically the fraction of phytoplanktonic nitrogen fuelled by these three tributaries.

Numerous data have been gathered for validation purposes. They come mainly from REPHY, MAREL and SOMLIT monitoring networks for the French coastal zone, from CEFAS and WCO (Western Channel Observatory) for the U.K coastal zone, from the BMDC (Belgian Marine Data Center) for the Belgian coastal zone, as well as from some French oceanographic cruises (MODYCOT). A unique time-series of dissolved oxygen in surface and bottom waters has been measured in the bay of Vilaine by the MAREL buoy named "MOLIT". NOAA AVHRR measurements of Sea Surface Temperature and MODIS colour measurements are collected by Ifremer's Nausicaa browser automat and processed thanks to the OC5 algorithm (Gohin et al., 2002), with a subsequent merging of images collected during the 4 last days, in order to partially fill the holes caused by cloud covering.

## Some results

A detailed validation of the hindcasts of this wide application of the coastal ECO-MARS3D is under progress. A first global overview of the surface chlorophyll can be obtained from the comparison between the mean values during the growing season (March to October) obtained from satellite images and from the model respectively (Fig. 3). The computed mean annual chlorophyll concentration reproduces the great difference between the productive French coastal strip of the Bay of Biscay and the eastern English Channel (enriched by the nutrient loadings of Gironde, Loire, Vilaine and Seine rivers) and the poor zones located over the abyssal plain, on the outer shelf or in the western English Channel; but the scatterplot clearly shows a strong dispersion of simulated values at large measured value, i.e. in front of estuaries.

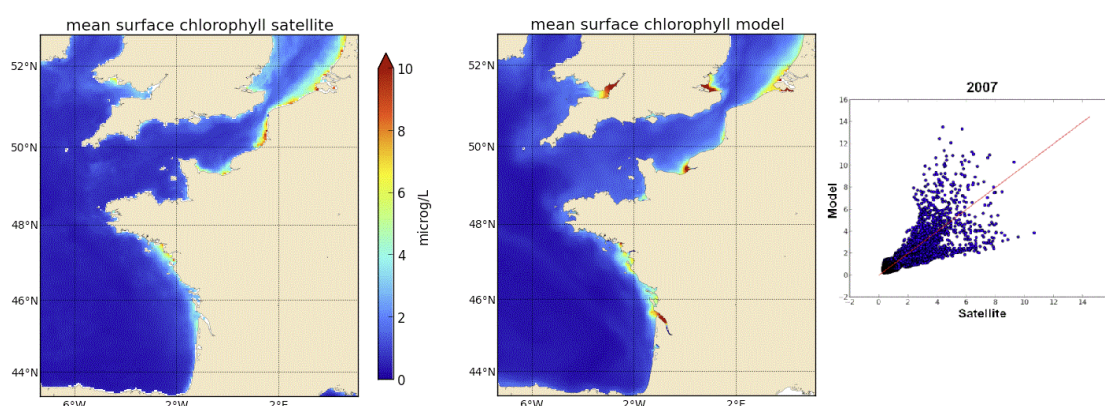


Figure 3: Observed (MODIS satellite) and simulated mean surface chlorophyll during the period March–October 2007.

Even when nutrients are correctly simulated, this damped behaviour of simulated chlorophyll relatively to the observed one can be retrieved in the decadal validation of the simulation of main nutrients ( $\text{NO}_3$ ,  $\text{NH}_4$ ,  $\text{PO}_4$ ,  $\text{Si(OH)}_4$ ) and total chlorophyll at the Cabourg station (Bay of Seine, eastern Channel), which can be considered as presenting some characteristic features of an eutrophicated place (Fig. 4)

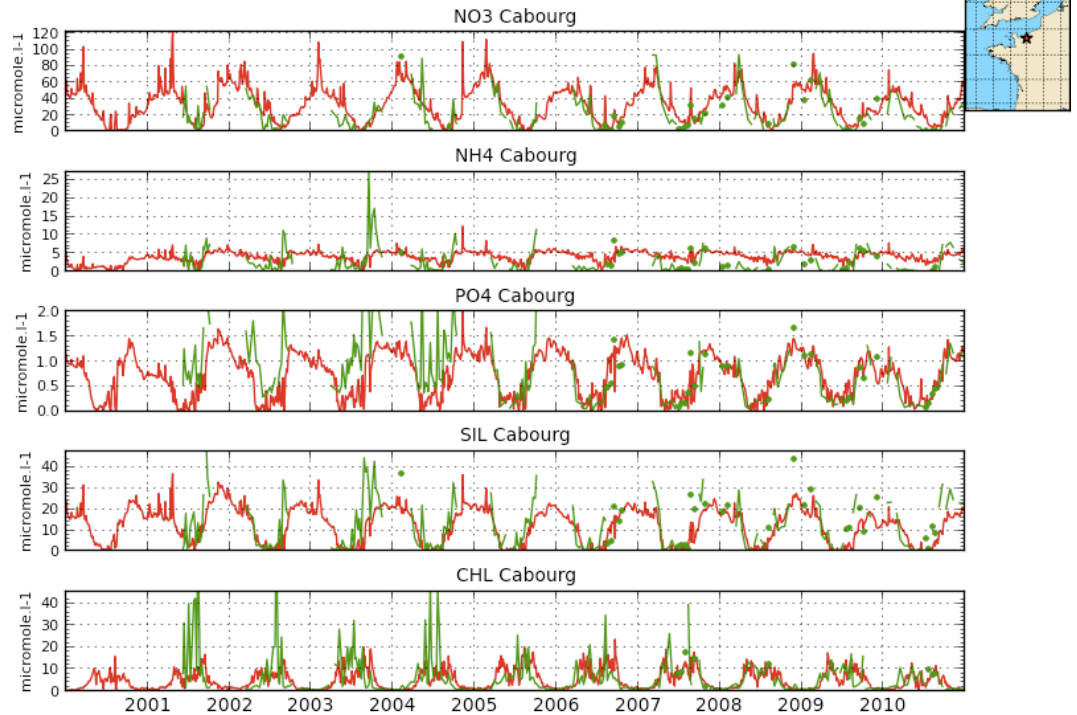


Figure 4: Decadal validation of the simulation of main nutrients ( $\text{NO}_3$ ,  $\text{NH}_4$ ,  $\text{PO}_4$ ,  $\text{Si(OH)}_4$ ) and total chlorophyll at the Cabourg station (Bay of Seine, eastern Channel)

As mentioned earlier, oxygen depletion in bottom waters is a crucial parameter in defining the ecological status of water mass relatively to the eutrophication process. The model has been validated with the unique long and high frequency series of bottom oxygen concentration measured by the Previmer's MOLIT buoy in the bay of Vilaine. Even if the model fails to reproduce some short episodes of over-saturation, especially in the surface layer, it reproduces the gradual decrease of oxygen concentrations measured near the bottom during spring and summer (Fig. 5), which can lead to repeated episodes of hypoxia down to  $2\text{mg/L O}_2$ , which is clearly considered as being deleterious for animal physiology (Gray et al., 2002).

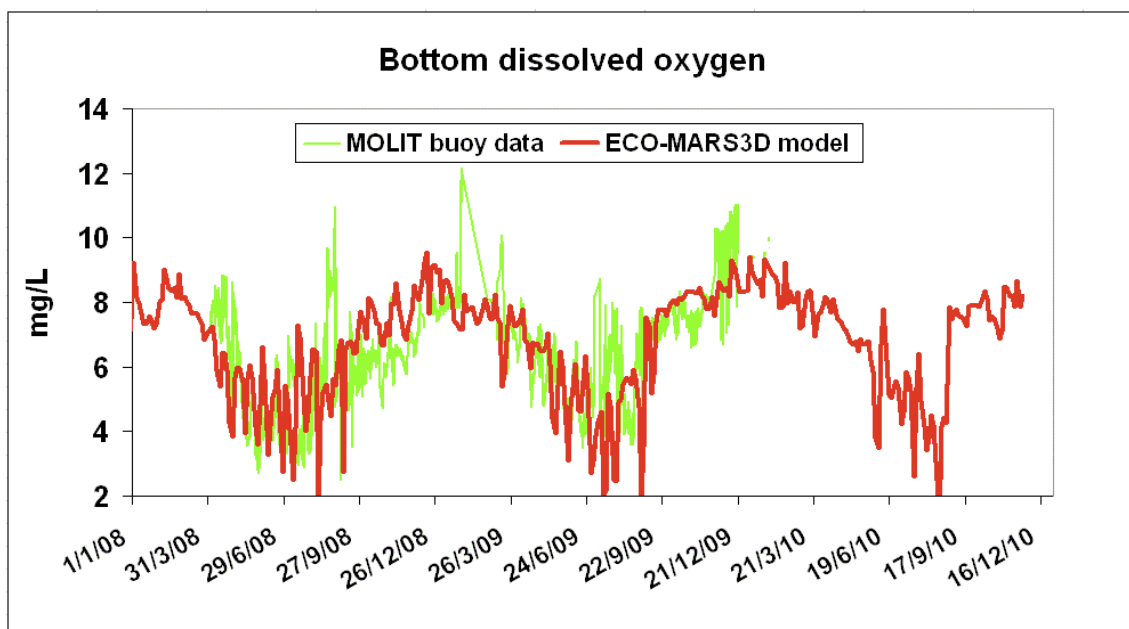
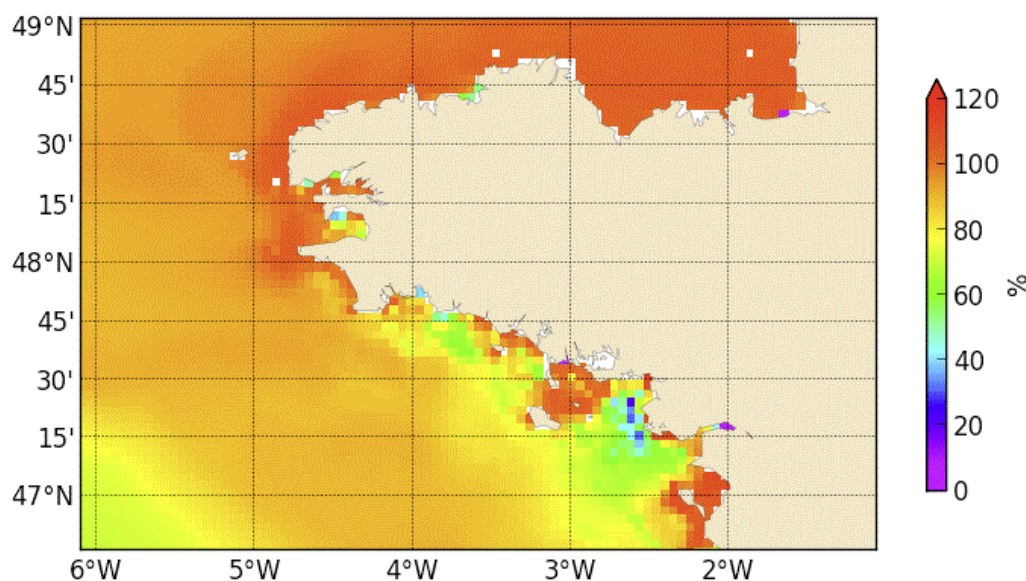


Figure 5: Measured (MOLIT buoy) and simulated oxygen concentration in bottom water in the Vilaine bay (French Atlantic coast).

## Oxygen saturation in bottom water



Since 2007, the model has provided on the previmer.org website daily maps of bottom oxygen saturation in southern Brittany, which reveal (Fig. 6) that the bay of Vilaine is the hot point of a more extensive area subject to recurrent hypoxia during summer. A recent study based on the same ECO-MARS3D results has put forward the hypothesis that some acute hypoxia episodes may trigger high mortality (e.g. in August 2006) of the ground-farmed oysters of the nearby bay of Quiberon (Stanisière et al., 2013).

Figure 6: Simulated oxygen saturation in bottom waters on August, 1st, 2009.

Modelling the change induced in phytoplankton biodiversity by eutrophication is the future challenge for biogeochemical models. A first limited step in that direction has been recently made on the Previmer operational version of ECO-MARS3D model by introducing three types of HAB species (Harmful Algal Blooms species) which are commonly found on some parts of the French Atlantic-Channel coast (Fig. 7). These additional components compete for light and nutrients with the three basic bulk components, but each of them has narrower ecological preferences than its non-specialised bulk homolog. The *Pseudo-nitzschia* diatom component, for instance, has a temperature optimum about 14°C and lower half-saturation constants for nutrient uptake that allows it to bloom in May-June, i.e. after the decay of the main diatom spring bloom. The simulated ASP toxin content of *Pseudo-nitzschia*, caused by silicon depletion of cells, reproduces the spatial distribution of toxicity measured in shellfishes by the REPHY monitoring network and its apparent lack of correlation with the abundance of *Pseudo-nitzschia*. For instance, in contrast with the southern Brittany, the northern Brittany remains almost free of contamination in spite of a common spring occurrence of this diatom genus.

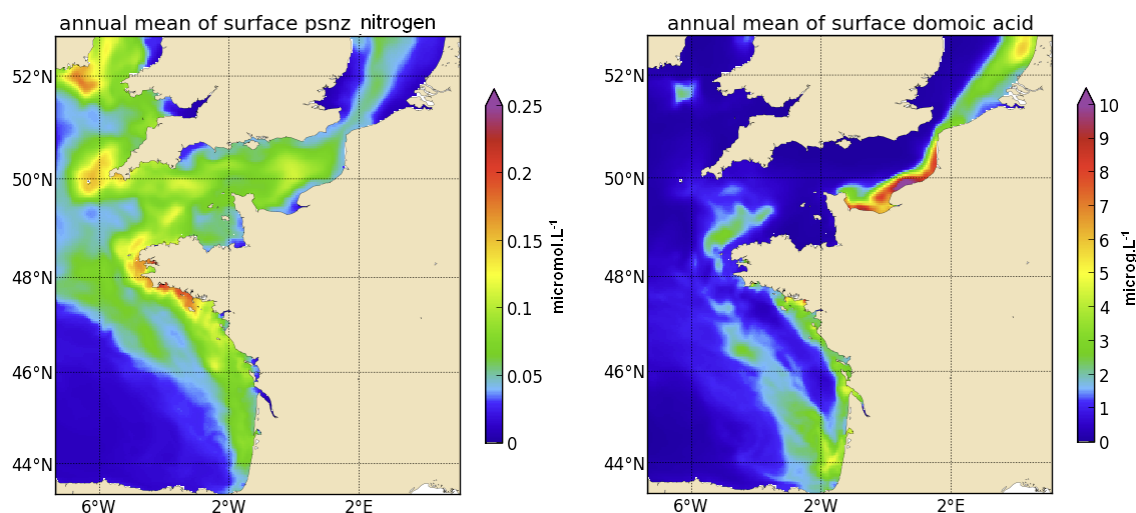


Figure 7: Simulated mean annual distribution of *Pseudo-nitzschia* biomass (left) and ASP toxin-domoic acid (right)

Improving the ecological status of eutrophicated water masses (Water Frame Directive and Marine Strategy Framework Directive) or moving from (potential) problem to non-problem areas (OSPAR) implies assessing the responsibility of any terrestrial input of nutrient in the coastal zone enrichment. OSPAR commission has a particular interest in the transboundary transport of nutrients, and the ICG-EMO working group has devoted a special session to its modelling (OSPAR, 2009). Thanks to a tracking and aging technique applied to the entire nitrogen cycle in the model, the Previmer website provides daily maps of the part of phytoplankton nitrogen which comes respectively from the Seine, Loire and Gironde rivers, along with the mean time elapsed from its entrance in the marine ecosystem. These maps bring to light the long-range marine imprint of big rivers, which may change location following winds and flow rates (Fig.8 left & middle), and the relatively long residence time of these inputs over the continental shelf. Roughly speaking, the Seine nitrogen imprint on phytoplankton entering the North Sea is about one year old, whereas the Loire imprint is three years old (Fig.8 right).

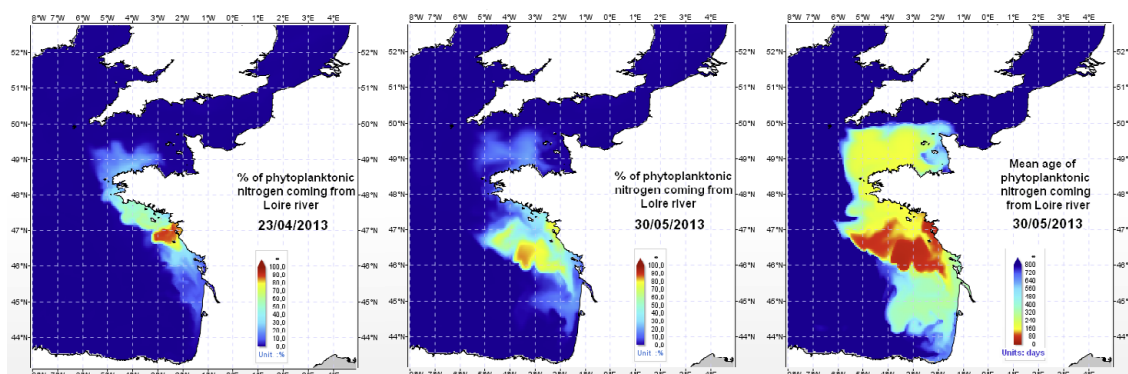


Figure 8: Distribution of phytoplanktonic nitrogen coming from Loire river on April, 23th and on May, 30th, with its mean age at this last date.

## Conclusion

An ecological model of the nutrients and phytoplankton on the Bay of Biscay/English Channel area (i.e. covering a large part of the IBI-ROOS domain) has been validated on a ten year period by comparison to various data (remotely sensed images of SST and surface chlorophyll, samples from monitoring stations, data from a buoy). Globally speaking, the model was able to reproduce the geographical pattern as well as the seasonal mean time course of nutrients and total chlorophyll. It reproduces also the occurrence of strong hypoxia events in the bottom layer of the bay of Vilaine, as observed by an automatic buoy. Since the end of 2013, this model has been turned into an operational mode, for the previmer.org website, to replace the previous versions limited to the Bay of Biscay shelf and Brittany. Some new products have been added to help the understanding of the influence of the three main French rivers (Seine, Loire, Gironde) on the global phytoplankton production, as well as on the triggering of some HAB episodes (foam produced by *Phaeocystis*, ichthyotoxin from dinoflagellate *Karenia* and amnesic toxin from diatoms *Pseudo-nitzschia*).

Apart from the immediate interest of such on-line information, this operational tool does provide over the years a growing bank of daily simulated situations, which will be used to build a statistical description of the “mean” nutrient and phytoplanktonic annual cycle in these coastal areas, as well as to define what can be designated as being “extreme” events. This information will feed the Water Frame Directive report for the French water masses, and will help to assess the ecological status of the French sub-regions defined in the Marine Strategy Frame Directive.

## Acknowledgements

The authors wish to thank the Agence de l'Eau Loire-Bretagne for her financial contribution to the off-line validation and applications of the ECO-MARS3D model, as well as the Région Bretagne for her financial support to the operational version put on the web site: [http://www.previmer.org/previsions/production\\_primaire](http://www.previmer.org/previsions/production_primaire).

The authors are also indebted to their Ifremer colleagues in charge of oxygen measurements (Jean-Pierre Allenou and Michel Répécaud) and satellite image processing (Francis Gohin).

## References

- Billen G., Garnier J., 2007. River basin nutrient delivery to the coastal sea: assessing its potential to sustain new production of non siliceous algae. *Mar. Chem.*, 106:148-160.
- Davidson K., Fehling J., 2006: Modelling the influence of silicon and phosphorus limitation on the growth and toxicity of *Pseudo-nitzschia seriata*. *African Journal of Marine Science*, 28(2): 357-360.
- Fehling J., Davidson K., Bolch C.J. and Bates S.S., 2004: Growth and domoic acid production of *Pseudo-nitzschia seriata* (Bacillariophyceae) under phosphate and silicate limitation, *J. Phycol.* 40: 674–683.
- Ferreira J.G., Andersen J.H., Borja A., Bricker S.B., Camp J., Cardoso da Silva M., Garcés E., Heiskanen A.S., Humborg C., Ignatiades L., Lancelot C., Ménesguen A., Tett P., Hoepffner N. and Claussen U., 2011: Overview of eutrophication indicators to assess environmental status within the European Marine Strategy Framework Directive. *Estuarine, Coastal and Shelf Science*, 93: 117-131.
- Gohin, F., Druon, J.N. and Lampert, L., 2002: A five channel chlorophyll concentration algorithm applied to SeaWiFS data processed by SeaDAS in coastal waters. *International Journal of Remote Sensing*, 8(23): 1639-1661.
- Gohin, F., Loyer, S., Lunven, M., Labry, C., Froidefond, J.-M., Delmas, D., Huret, M. and Herbland, A., 2005: Satellite-derived parameters for biological modelling in coastal waters: Illustration over the eastern continental shelf of the Bay of Biscay. *Remote Sensing of Environment*, 95: 29–46.
- Gray J. S., Shiu-sun Wu R. and Or Y. Y. 2002. Effects of hypoxia and organic enrichment on the coastal marine environment. *Mar. Ecol. Prog. Ser.*, 238: 249–279.
- Guillaud J.-F. and Bouriel L., 2007: Relationships between nitrate concentration and river flow, and temporal trends of nitrate in 25 rivers of Brittany (France). *Revue des Sciences de l'Eau*, 20(2): 213-226.
- Guillaud J.F. and Ménesguen A., 1998: Modélisation sur vingt ans (1976-1995) de la production phytoplanktonique en Baie de Seine (France), *Oceanol. Acta*, 21(6): 887-906.
- Huret M., Sourisseau M., Petitgas P., Struski C., Léger F. and Lazure P., 2013: A multi-decadal hindcast of a physical–biogeochemical model and derived oceanographic indices in the Bay of Biscay. *Journal of Marine Systems*, 109, S77-S94.
- Lazure P. and Dumas F., 2008: An external–internal mode coupling for a 3D hydrodynamical model for applications at regional scale (MARS). *Advances in Water Resources*, 31(2), 233-250.
- Lancelot, C., 1995. The mucilage phenomenon in the continental coastal waters of the North Sea. *Science of the Total Environment*. 165: 83-112.
- Lancelot, C., Billen, G., Sournia, A., Weisse, T., Colijn, F., Veldhuis, M., Davies, A. and Wassman, P., 1987: *Phaeocystis* blooms and nutrient enrichment in the continental coastal zones of the North Sea. *Ambio* 16: 38-46.
- Ménesguen A., Cugier P., Leblond I., 2006: A new numerical technique for tracking chemical species in a multi-source, coastal ecosystem, applied to nitrogen causing *Ulva* blooms in the Bay of Brest (France). *Limnol. Oceanogr.*, 51: 591-601. ([http://aslo.org/lo/toc/vol\\_51/issue\\_1\\_part\\_2/0591.pdf](http://aslo.org/lo/toc/vol_51/issue_1_part_2/0591.pdf))
- Merceron, M. 1988: Baie de Vilaine: juillet 1982. Mortalité massive de poissons. L'analyse des causes et des mécanismes du phénomène., les propositions d'action. *Equinoxe* 21: 4-9.
- OSPAR, 2009: Report of the 3rd OSPAR Workshop on eutrophication modelling (Transboundary Nutrient Transport), Brussels, 7-9 September 2009. 10p. + annexes.
- Parsons M.L., Dortch Q., 2002. Sedimentological evidence of an increase in *Pseudo-nitzschia* (Bacillariophyceae) abundance in response to coastal eutrophication. *Limnol. Oceanogr.*, 47(2): 551-558.
- Pénard C., 2009: Détection satellitaire et modélisation opérationnelle de la production végétale non-fixée (phytoplankton et ulves) dans la bande côtière bretonne. PhD thesis, Université de Bretagne Occidentale, 227 p. + annexes.
- Rousseau V., Leynaert A., Daoud N., Lancelot C., 2002. Diatom succession, silicification and silicic acid availability in Belgian coastal waters Southern North Sea. *Marine Ecology Progress Series*, 236: 61–73.
- Souchu P., Le Maguésse A., Lassus P., Séchet V. and Oger-Jeanneret H., 2013: DINOPHAG (janvier 2011-juin 2012). Programme de recherche sur *Dinophysis* dans les eaux littorales des Pays de la Loire, rapport final Ifremer, 32 p. (<http://archimer.ifremer.fr/doc/00172/28368/26660.pdf>)
- Stanisière J.-Y., Mazurié J., Bouget J.-F., Langlade A., Gabellec R., Retho M., Quinsat K., Leclerc E., Cugier P., Dussauze M., Ménesguen A., Dumas F., Gohin F., Augustin J.-M., Ehrhold A., Sinquin J.-M., Goubert E. and Dreano A., 2013: Les risques conchylicoles en Baie de Quiberon (3<sup>ème</sup> partie): le risque d'hypoxie pour l'huître creuse *Crassostrea gigas*. Rapport final du projet Risco 2010-2013. Rapport Ifremer RST/LER/MPL/13.21, 73 p.
- Veldhuis MJW, Colijn F and Admiraal W., 1991: Phosphate utilization in *Phaeocystis pouchetii* (Haptophyceae). *Mar Ecol Prog Ser* 12(1): 53-62.

# BMGTOOLS: A COMMUNITY TOOL TO HANDLE MODEL GRID AND BATHYMETRY

By *S. Theetten*<sup>(1)</sup>, *B. Thiébaud*<sup>(2)</sup>, *F. Dumas*<sup>(1)</sup>, *J. Paul*<sup>(3)</sup>

<sup>1</sup>IFREMER, Brest, France

<sup>2</sup>ARTENUM, Toulouse, France

<sup>3</sup>MERCATOR OCEAN, Toulouse, France

## Abstract

A software called BathyMeshGridTools is proposed to facilitate the construction of gridded bathymetry data for hydrodynamic ocean models from global to coastal scales. These tools consist of a graphical interface written in Java and a computational core written in FORTRAN, which are freely distributed under LGPL and GPL licenses (<http://www.ifremer.fr/bmgtools>). The process of gridded bathymetry creation relies on three successive tasks: (1) creation of structured grid using graphic user interface for positioning, resizing and creating a hierarchy of nested model grids on a map; (2) data interpolation using a grid-to-grid interpolation algorithm for interpolation of Digital Terrain Model and kriging algorithm for bathymetric sounding data interpolation; (3) visual inspection and manual editing of the interpolated bathymetry field. These three steps can be used in the same process of construction of bathymetry gridded data and can also be used independently (e.g. one can use only the visualization tool for checking and modifying manually a bathymetry field previously created with an other tool).

## Introduction

Before launching numerical simulations, it is necessary to perform various preprocessing tasks to prepare the input fields. The BMGTools (BathyMeshGridTools) are a set of pre-processing tools that helps to create, check and modify bathymetric grids in an easy, fast and interactive way. CreateBMG is a part of the BMGTools package. Its purpose is to help create a hierarchy of nested grids on a map, resize them and interpolate bathymetry data on the created model grids, either from bathymetric sounding measurements or from digital terrain model. CheckBMG is also part of the BMGtools package. Its purpose is to help to visualize bathymetric grids created with CreateBMG - or with other applications - and to check the relevance of the interpolation. If necessary, the users can modify the grid manually in the aim to correct the interpolation algorithm errors.

## BathyMeshGridTools: a tool to handle model grid and bathymetry

Both graphical user interfaces that handle the grid creation and the visualization/correction of the interpolated bathymetry on the grid are entirely written in JAVA which gives them a good portability and which ensures an easy installation. CheckBMG and CreateBMG runs under Unix/Linux 32/64 bits, Mac OSX and Windows 32/64 bits operating systems using the suitable JAVA library which is integrated in the distribution. The computational part on data interpolation is written in Fortran90 so the user can read, understand and modify the code as they wish. In order to facilitate the compiling task on each platform, a user can handle the cross-platform, open-source build system CMake<sup>1</sup> to generate the appropriate Makefile. Bmgtools is composed of three distinct features. These three features are: the creation of grids, the interpolation of data grids and the verification of interpolated bathymetric grids. These three features can be used independently.

- Grid creation (CreateBMG)

Within BMGTools software, CreateBMG aims at facilitating the creation of model grids with the help of a Graphical User Interface (GUI) and by using some geographic information system functionalities. To adjust the geographical domain, several geomorphic elements like coast line, isobath or physical field can be displayed. Modification of mesh grid resolution or creation of a hierarchy of embedded grids, as required for the AGRIF<sup>2</sup> refinement method for instance, are interactively and rapidly achieved through the GUI (Figure1). The createBMG tool can handle various C-Arakawa type model grid such as rectangular grid used by several modeling codes and especially by the MARS3D<sup>3</sup> code used in the PREVIMER operational system or more complex grid such as the ORCA grid. Thus, this tool allows to create sub-grid by calling a fortran code use in building the NEMO<sup>4</sup> grid (i.e. ORCA grid). The horizontal mesh grid files are written in netcdf format. The netCDF format uses the COMODO<sup>5</sup> convention (<http://pycomodo.forge.imag.fr>) to be compliant with most of ocean models (MARS, NEMO, SYMPHONIE<sup>6</sup>, ROMS<sup>7</sup>, HYCOM<sup>8</sup>).

<sup>1</sup> CMake : <http://www.cmake.org>

<sup>2</sup> AGRIF : Adaptive grid refinement in Fortran - <http://www-ijk.imag.fr/MOISE/AGRIF>

<sup>3</sup> MARS3D: coastal ocean numerical model developed in Ifremer - <http://www.ifremer.fr/mars3d>

<sup>4</sup> NEMO : Nucleus for European Modelling of the Ocean - <http://www.nemo-ocean.eu>

<sup>5</sup> COMODO : French Numerical Ocean Modelling Community - <http://pycomodo.forge.imag.fr>

<sup>6</sup> SYMPHONIE : <http://sirocco.omp.obs-mip.fr/outils/Symphonie/Accueil/SymphoAccueil.htm>

<sup>7</sup> ROMS : Regional Oceanic Modeling System - <http://www.romsagrif.org/index.php>

<sup>8</sup> HYCOM : HYbrid Coordinate Ocean Model - <http://hycom.org>

<sup>9</sup> SCRIP : Spherical Coordinate Remapping and Interpolation Package - <http://climate.lanl.gov/Software/SCRIP>

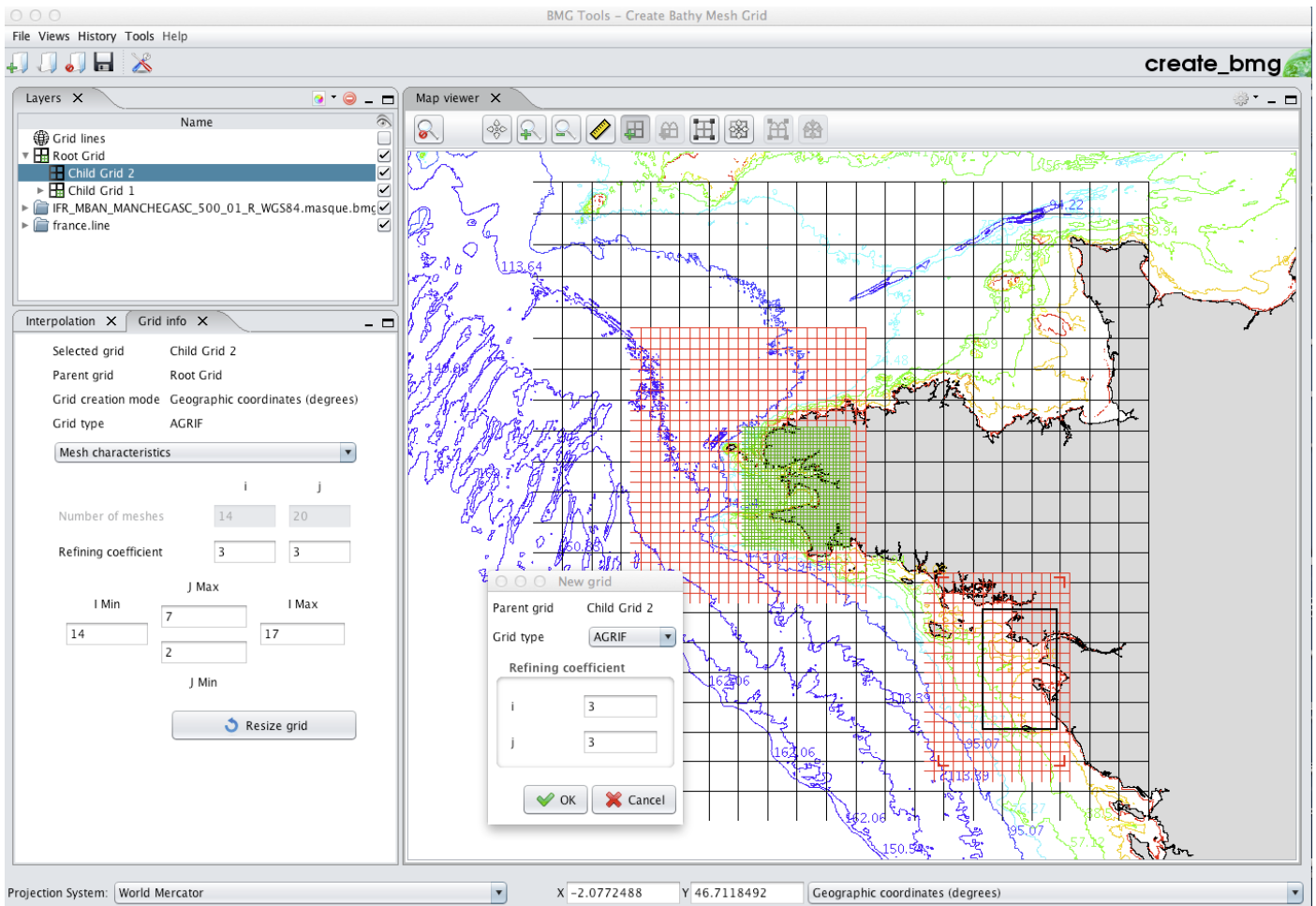
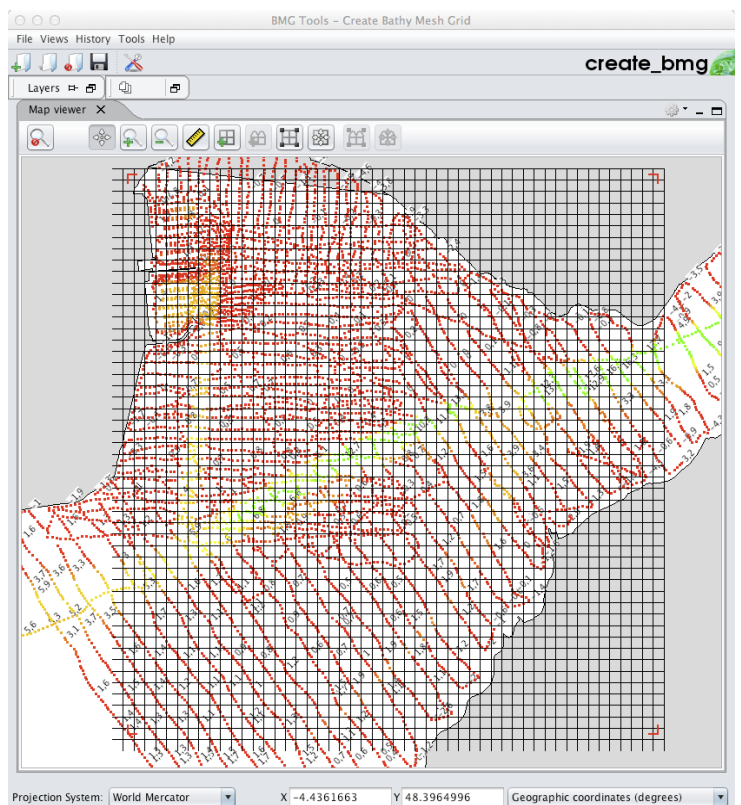


Figure 1: Screenshot of the CreateBMG Graphical User Interface used to create a hierarchy of AGRIF embedded grids

- Data interpolation (CreateBMG)

CreateBMG can also be used to generate a gridded bathymetry, either from sounding data coming from oceanographic survey or from digital terrain models. The use of sounding data is often preferred for high resolution coastal hydrodynamic models (grid-cell size less than 1 km) whose realism strongly depends on the realism of the gridded bathymetry. In that case, spatial distribution and density of sounding points are first compared to the grid resolution and to its geographical extension (Figure 2). Sounding data are then interpolated following the data preprocessing methodology and the kriging algorithm described in Bailly du Bois (2011). For a larger geographical extension and coarser grid resolution, the interpolation of one or several digital terrain model is usually made. In this case, the structured digital terrain models are interpolated by using the SCRIP<sup>9</sup> algorithm. Both interpolation codes are written in Fortran offering the possibility to users to read, understand and modify (even improve) the codes. The GUI makes a system call to the Fortran executable. It implies that the Fortran executable can be used without the CreateBMG GUI on any suitable machine if more memory is needed to interpolate a large amount of data.

Figure 2: Visualization of a set of soundings and grid before interpolation in the CreateBMG Graphical User Interface



- Visual inspection, manual editing and some other useful tools (CheckBMG)

The second graphical user interface called CheckBMG is certainly the most popular and the most used within the ocean modeler community. CheckBMG provides many functionalities that helps in working on the bathymetry grid. Here are some examples :

- The fastidious task of visualization and checking the interpolated bathymetry grid is now greatly facilitated by using this tool. The JAVA developments that have been made allow fluidly and interactive visualization of large grids (benchmarked up to 1000x1000 grid points). In addition, the display performance remains satisfactory even when different layers of geographic information, like coastline or physical fields (Figure 3), are added. The user may realize many intuitive actions with the computer mouse like zoom, unzoom, display or not of geographic information layers. By playing with the range of the color bar, the user can explore the interpolated bathymetry values more finely. In case of working on larger bathymetry grids or with a insufficiently powerful computer, the user can also only work on a sub-region in order to decrease the memory and cpu needs.

- Sometimes because of limitation in the interpolation algorithms or because of the poor data quality, the user has to modify interpolated values "by hand". The user could also want to modify the bathymetry for specific purpose. For example, fill an estuary or a bay that is not relevant for a given application, dig an artificial channel with the objective to test the influence of a bathymetric modification on the model solution; modify the bottom depth values in some area in order to improve the physical solution of the model. Owing to CheckBMG, this bathymetric values modification process is both quick and easy : the user selects a point or a set of points with the mouse and enters the new value. This change is then updated automatically and instantaneously in the NetCDF file.

- Based on these previous features other tools are available to the user for perform other manipulation on the grid. Thus, one can create and modify the runoff locations on the grid. One can also selects specific points on the grid, save it in a text file for use in the model or in another application.

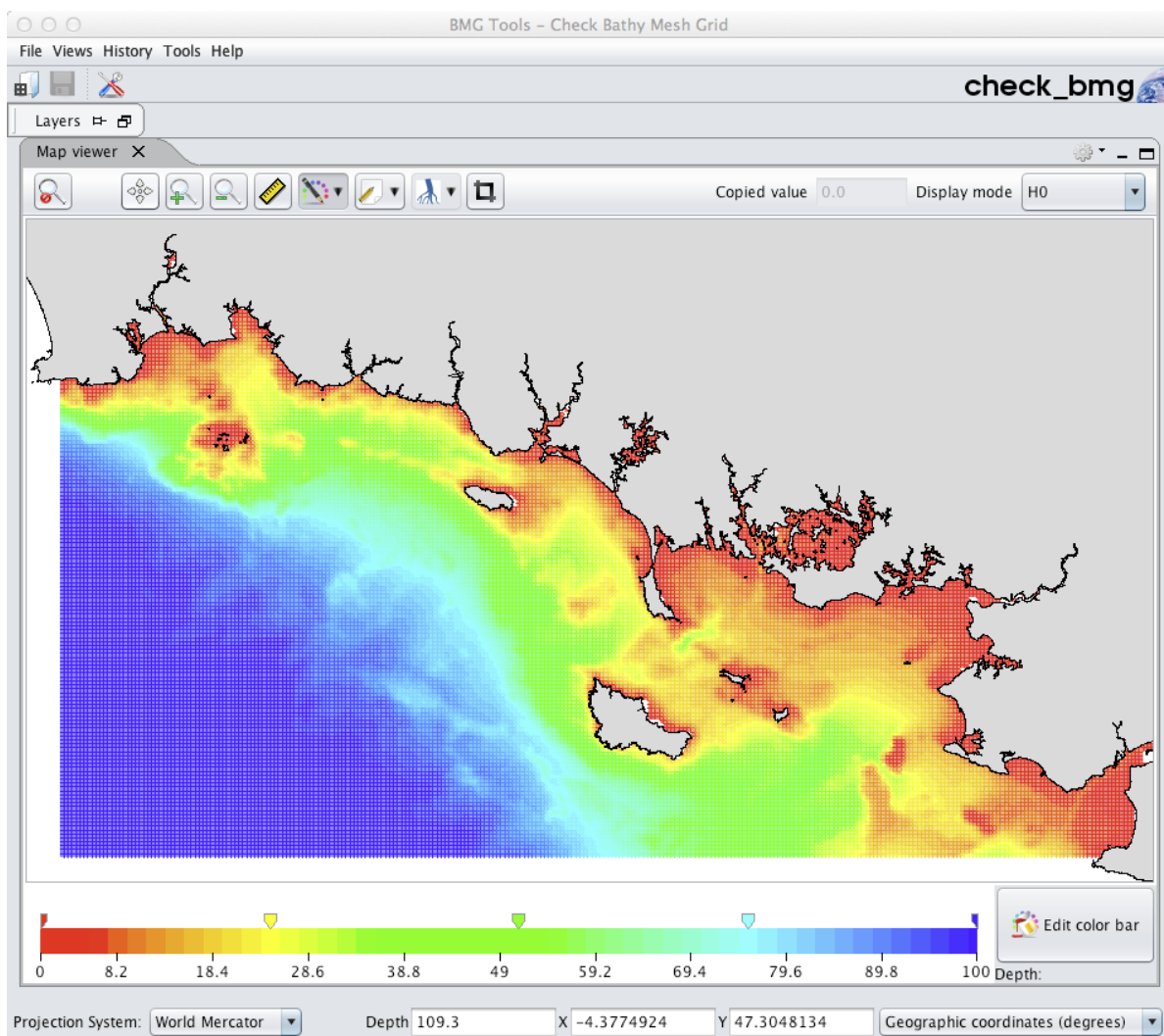


Figure 3: Visualization of interpolated bathymetry for checking and manual modifying process

## BathyMeshGridTools: a pre-processing community tool. Two examples of application in operational systems

- Operational Coastal Oceanography system : PREVIMER<sup>10</sup>

Many model configurations are required to cover the metropolitan France coastal zone and overseas regions. Each of those model configurations have different resolution (*i.e.* 4 km to 50 meters) and also different spatial extension (*e.g.* Bay of Biscay to the Rade de Brest (Figure 4)). To build all those model configurations we need robust and reliable tools to generate all the input fields required for the simulation. In the case of PREVIMER, the whole BathyMeshGridTools package is used. The grid are built with createBMG and both interpolation algorithms (SCRIP grid-to-grid interpolation for digital terrain model and kriging algorithm for sounding data) are used. CheckBMG is used in the last step specially to check the proper definition of shallow water bathymetry near the coast.

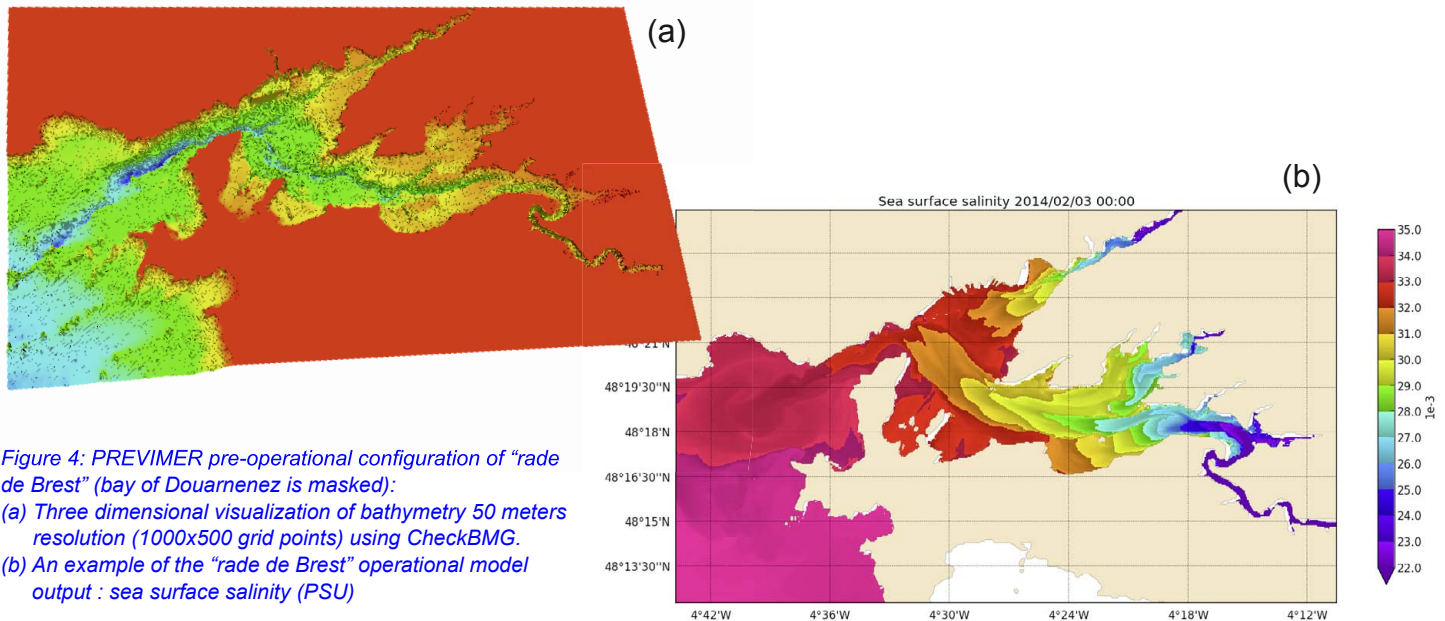


Figure 4: PREVIMER pre-operational configuration of "rade de Brest" (bay of Douarnenez is masked):  
 (a) Three dimensional visualization of bathymetry 50 meters resolution (1000x500 grid points) using CheckBMG.  
 (b) An example of the "rade de Brest" operational model output : sea surface salinity (PSU)

- MERCATOR OCEAN<sup>11</sup>

The CheckBMG tool is integrated to the Mercator Ocean System and Interface RElocatable Nesting tools (SIREN). SIREN allows users to create a new configuration embedded in a larger one. To do so, it creates merged bathymetry, initial state and boundary conditions. In a first step, SIREN extracts fine grid bathymetry over the domain of interest and merge it at boundaries with coarse grid bathymetry. In this context, CheckBMG is used to check and to adjust locally the bathymetry created for the new regional configuration.

For example, Mercator Ocean develops, in collaboration with CLS, an operational system over the Indonesian archipelago named INDES0. SIREN was used to create it. This configuration is based on the ORCA12 grid. First, the data collected during the INDOMIX Campaign have been included in the ORCA12 bathymetry (Figure 5). Moreover, to improve the transport in LUZON (LST: Luzon Strait Transport) several straits have been corrected, *e.g.* Surigao strait, Mindoro strait. CheckBMG was also used to correct the Mindanao strait and other Island position (like Sibutu island). All these changes have been made from Googleearth, ETOPO 1 and the GSHHG - A Global Self-consistent, Hierarchical, High-resolution Geography coast line.

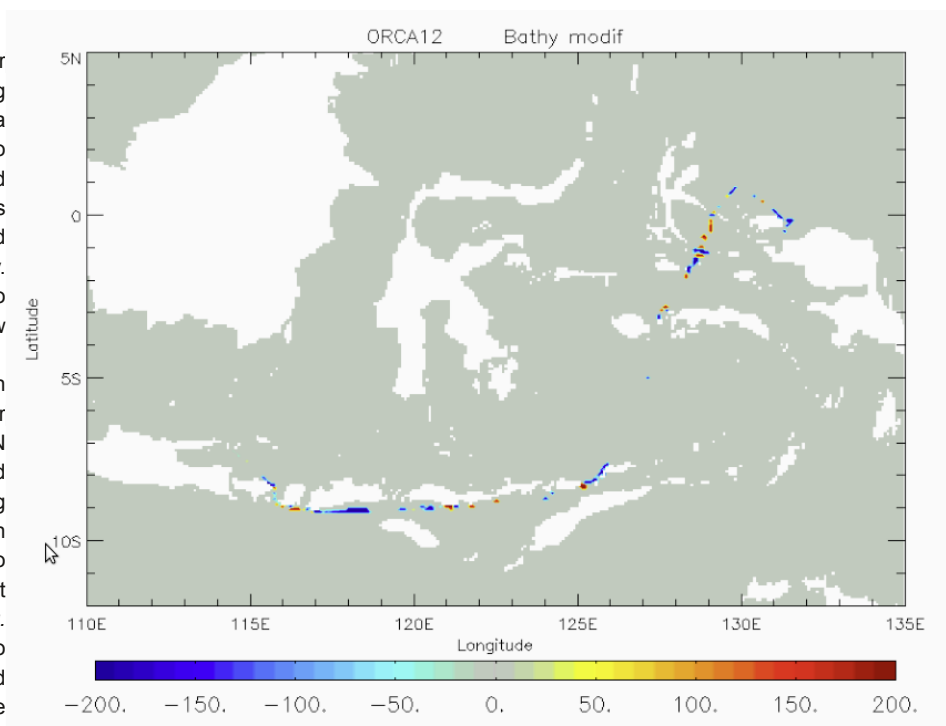


Figure 5: Modification of the bathymetry ORCA12, thanks to the consideration of the data collected during the INDOMIX cruise.

Mercator Ocean also used CheckBMG to improve the bathymetry of the Iberian Biscay Irish (IBI, Maraldi *et al.*, 2013; Cailleau *et al.*, 2012) operational system. Indeed some anomalous points (less than a dozen) along the coast of Brittany and in the Irish Sea have been corrected with CheckBMG by reverting those to the GEBCO 1' bathymetry values. In the Gulf of Cadiz, a suspicious mountain at 6.92°W 36.45°N (near PdE Cadiz buoy), has been suppressed by reverting to GEBCO 1' bathymetry in this area. Finally, data compilation from the SWIM project (Zitellini *et al.*, 2009) and data from GMRT (Global Multi-Resolution Topography, Ryan *et al.* 2009, [http://www.marine-geo.org/tools/maps\\_grids.php](http://www.marine-geo.org/tools/maps_grids.php)) has been used to correct the original bathymetry in the Gulf of Cadiz and in the Gibraltar strait. All those corrections were made easily with the use of CheckBMG.

## Conclusion

These tools have already proven their operational capability in the community of modelers using MARS3D code. These reliable tools are used either in research or in operational oceanography applications as PREVIMER or MERCATOR. Their compatibility with the C-Arakawa grid and the use of a standard netCDF file format with common conventions make them usable with other oceanic circulation model. These tools belong to the family of pre-processing tools as ROMSTOOLS (Penven *et al.*, 2007) who are designed to facilitate modelers' work.

## Acknowledgements

The authors wish to thank Fabrice Lecornu and the PREVIMER project that allowed developments and improvements of the BMGtools software. A special thanks to the Artemum developers for their availability and reactivity, and two anonymous reviewers for their useful comments.

## References

- Bailly du Bois P. (2011). Automatic calculation of bathymetry for coastal hydrodynamic models. Computers and Geosciences, Volume 37, Issue 9, p. 1303-1310. <http://dx.doi.org/10.1016/j.cageo.2010.11.018>
- Cailleau S., Chanut J., Lellouche J.-M., Levier B., Maraldi C., Refray G., and Sotillo M.-G., 2012. Towards a regional ocean forecasting system for the IBI (Iberia-Biscay-Ireland area): developments and improvements within the ECOOP project framework. Ocean Sci., 8, 143-159
- Penven P., P. Marchesiello, L. Debreu, and J. Lefevre, 2007: Software tools for pre- and post-processing of oceanic regional simulations. Environ. Model. Softw., 23, 660-662.
- Maraldi C., Chanut J., Levier B., Ayoub N., De Mey P., Refray G., Lyard F., Cailleau S., Drevillon M., Fanjul E. A., Sotillo M. G., Marsaleix P., and the Mercator Research and Development Team .NEMO on the shelf: assessment of the Iberia-Biscay-Ireland configuration. Ocean Sci., 9, 745-771, 2013.
- Ryan, W. B. F., *et al.* (2009), Global Multi-Resolution Topography synthesis, Geochem. Geophys. Geosyst., 10, Q03014, doi:10.1029/2008GC002332.
- Zitellini *et al.*, 2009: The quest for the Africa-Eurasia plate boundary west of the Strait of Gibraltar, Earth Planet. Sci. Lett., doi:10.1016/j.epsl.2008.12.005.

## VACUMM – A PYTHON LIBRARY FOR OCEAN SCIENCE

By S. Raynaud<sup>(1)</sup>, G. Charria<sup>(2)</sup>, J. Wilkins<sup>(1)</sup>, V. Garnier<sup>(2)</sup>, P. Garreau<sup>(2)</sup>, S. Theetten<sup>(2)</sup>

<sup>1</sup>ACTIMAR, Brest, France

<sup>2</sup>IFREMER, ODE/DYNECO/PHYSED, Brest, France

### Abstract

VACUMM is an open-source Python library for processing data from observations and numerical models. The library is now used for several years in research and operational contexts, for instance for producing figures and reports, validating models, converting data, or making simple or advanced diagnostics. In this paper, we introduce how the library is built, and we present two applications of its use: one in an operational context and one in a research context.

### A generic library

VACUMM (Validation Analysis Comparisons Multi-Models) is a Python library and collection of scripts that has been mainly designed to validate the MARS3D<sup>1</sup> numerical simulations. However, VACUMM is now used for both processing of ocean and atmosphere data in general, including model and observations. It has a complete dedicated documentation that includes the full list of modules and scripts, and a large collection of tutorials, examples, gallery and test cases: <http://www.ifremer.fr/vacumm>. It is open-source software with a CeCILL<sup>2</sup> licence, and is open to new contributions.

VACUMM is written in the Python language, an interpreted language widely used for a long time in the ocean/atmosphere/climate community. This object-oriented language suits both computer experts and scientists, with applications going from the interactive side to the batch or operational sides. The low performance of an interpreted language are generally not a concern with Python since it can be easily interfaced for instance with C or Fortran languages, as it is the case in VACUMM for some interpolation routines. VACUMM has been written as a layer on the top of the CDAT<sup>3</sup> and Matplotlib libraries. CDAT (or UV-CDAT<sup>4</sup>) is used in the climate data analysis community, mainly for facilitating the comparisons between CMIP<sup>5</sup> climate models; it uses the high performance numerical library Numpy, and adds geographical and time informations, regridding capabilities of the ESMF<sup>6</sup>, and a collection of climate tools. Matplotlib provides a Matlab<sup>®</sup> like interface to produce high quality figures. VACUMM typically makes an intensive use of CDAT variables that have a similar structure to those of NetCDF variables, with numerical data, axes and attributes. This makes it easy to exploit them such as when plotting a map of Sea Surface Temperature (SST) calling “`map2(sst)`” with axes, title and units properly formatted, or regridding the same variable “`regrid2d(sst, newgrid)`”.

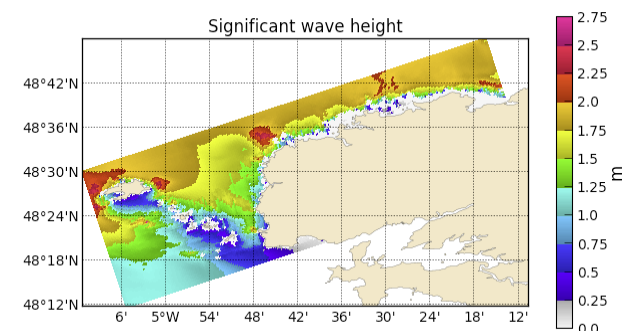


Figure 2: Example of a map of significant wave height generated using VACUMM function (source code: <http://www.ifremer.fr/vacumm/tutorials/misc.plot.advanced.swan.html>).

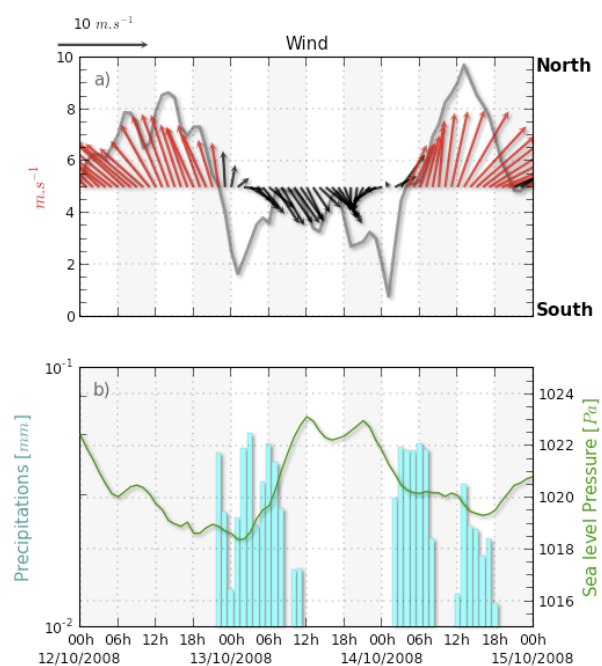


Figure 1: Example of 1D time series of meteorological data including wind vectors, wind intensity (grey line), sea surface pressure (green line), and precipitation bar plot plotted using VACUMM functions (source code: <http://www.ifremer.fr/vacumm/tutorials/misc.plot.advanced.meteo.html>).

<sup>1</sup> MARS3D: coastal ocean numerical model developed in Ifremer - <http://www.ifremer.fr/mars3d>

<sup>2</sup> CeCILL license, compatible with GPL license: [http://www.cecill.info/licences/Licence\\_CeCILL\\_V1.1-US.html](http://www.cecill.info/licences/Licence_CeCILL_V1.1-US.html)

<sup>3</sup> Climate Data Analysis Tools - <http://uvcdat.llnl.gov/>

<sup>4</sup> Ultrascale Visualization Climate Data Analysis Tools - <http://uvcdat.llnl.gov/>

<sup>5</sup> Coupled Model Intercomparison Project

<sup>6</sup> Earth System Modeling Framework

The library is made of a generic component and several specialized ones. The generic part has tools for dealing with most common 1D and 2D plots (Fig. 1 and 2), regridding (even between curvilinear grids), for interpolating and masking, for time conversions, formatting and splitting, for plotting, for easily reading NetCDF and other formats, for filtering data or performing statistics on huge datasets (Fig. 3). The generic subpackage also offers more advanced tools, for instance for working with remote files, managing advanced configurations, logging, working with xml and namelists. VACUMM also contains specialized interfaces to deal with *in situ* profiles or satellite data (see following section). In addition, a generic interface to specialized gridded data such as outputs from oceanic (MARS3D, NEMO, HYCOM) and atmospheric models (WRF), that facilitates post-processing, has been integrated. Retrieving the mixed layer depth becomes as simple as `mld=DS('output.nc', 'mars').get_mld(mode='deltadens')`. This interface uses an extension to CF (Climate and Forecast) conventions that helps discovering variables in NetCDF files and format in-memory variables. The generic interface integrates some advanced diagnostics part of other more thematic subpackages: bathymetry and shorelines, tidal diagnostics, spectral analyses, and physical diagnostics like geostrophic velocity (Fig. 4) or mixed layer depth.

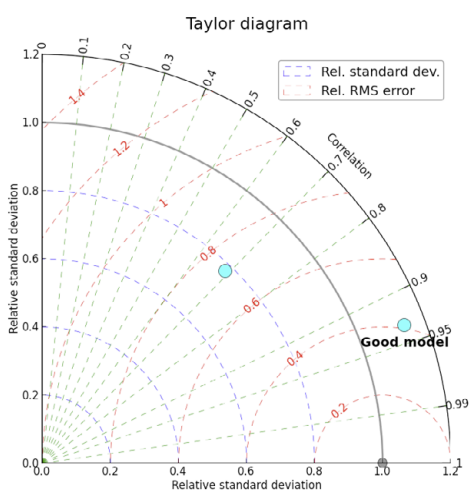


Figure 3: Example of a Taylor diagram to compare standard deviation and correlation between two datasets plotted using VACUMM library (source code: <http://www.ifremer.fr/vacumm/tutorials/misc.plot.basic.taylor.html>).

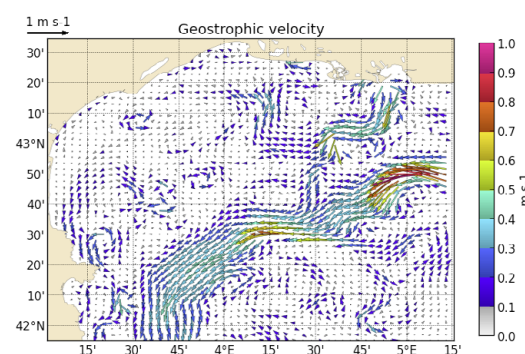


Figure 4: Example of geostrophic velocities computed from MARS3D modelled sea surface height using VACUMM library (source code: [http://www.ifremer.fr/vacumm/tests/test\\_dataset\\_get\\_uvbt\\_menor.html](http://www.ifremer.fr/vacumm/tests/test_dataset_get_uvbt_menor.html)).

## Application for operational oceanography: modeled sea surface temperature validation and real time cruise support

### Modeled sea surface temperature validation

One way to illustrate the VACUMM library is to show examples of applications. For example, in the frame of the PREVIMER<sup>7</sup> project, we developed an application to validate the modeled Sea Surface Temperature (SST) using remotely sensed observations. This tool is mainly dedicated and designed for operational oceanography but it has also been used and applied on longer interannual simulations in the frame of research projects.

The algorithm follows a classical scheme divided in 4 steps:

- Getting model and observation data (e.g. from remote data server),
- Collocation of model and observations,
- Statistic computation (e.g. spatial and temporal mean, standard deviation, correlation, root mean square, ...),
- Plotting and generating validation report (e.g. figures, web page).

Based on SEVIRI Sea Surface Temperature remotely sensed data (METEOSAT SST provided by OSI-SAF belong to EUMETSAT), PREVIMER Bay of Biscay and Northwestern Mediterranean simulations are qualified on a daily basis. Results available on the PREVIMER website (<http://www.previmer.org/produits/qualifications>) display temporal average of the modeled and observed sea surface temperature, the time-averaged bias (Fig. 5), the time series of the spatial average temperature (observed and modeled) with the amount of cloud free observations (Fig. 6) to sustain our interpretation of qualification results. The algorithm is also able to provide Root Mean Square, Standard Deviation and Correlation statistics. Furthermore, the algorithm design allows adding new diagnostics quickly and applying analysis on a different dataset (e.g. the tool has already been used for surface chlorophyll concentrations).

<sup>7</sup> <http://www.previmer.org>

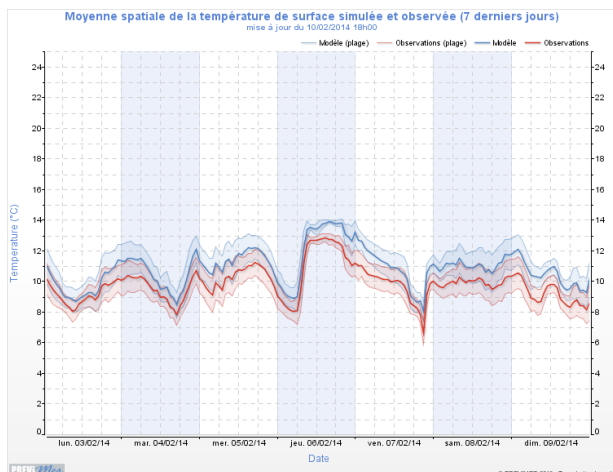


Figure 5: Spatial mean of observed and modeled Sea Surface Temperature from the 3rd to the 9th February 2014.

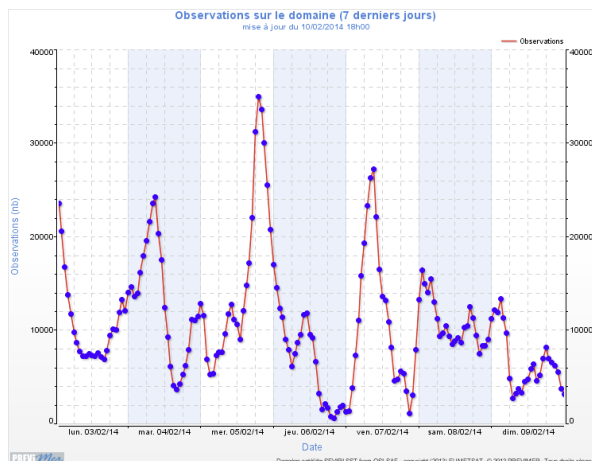


Figure 6: Number of Sea Surface Temperature cloud free pixels from the 3rd to the 9th February 2014.

In the example, we show the time-averaged bias for the week between the 3rd and the 9th February 2014 (Fig. 5). During this period, the model (covering the Bay of Biscay and Channel region - Berger *et al.*, 2014) overestimates the sea surface temperature compared with satellites observations. The bias is around 1°C. The standard deviation is in agreement with observations. Strong variations appear during the period and have to be cross-analyzed with the data availability (Fig. 6). Indeed, lowest temperatures are linked with a smaller number of observations and, then, the average is limited on specific regions.

Based on a similar approach, a tool has been developed to compare model simulations with *in situ* vertical profiles (e.g. from RECOPECA program - not shown).

**Real time cruise support**

In 2013, the Operational Center of the SOP2 experiment (February-March 2013 - Hydrological cycle in Mediterranean Experiment program) asked PREVIMER to provide synthetic “quick-looks” describing the hydrological situation of the Northwestern Mediterranean sea and the development of deep convection and dense water formation. They focused on two areas - NWMED [0-12°E; 38.1-44.5°N] and GOL [2-8°E ; 41-43.8°N] - and were of different types: surface-300m-1000m depth 2D snapshots, hovmöller diagrams or time series graphs at key points and glider sections. The documented fields were atmospheric (radiative and turbulent fluxes, wind stress, evaporation, precipitation) and hydrodynamical (temperature, salinity, density, currents). The “quick-look” specification was extremely well precise in terms of colorbar definition, scaling, units, as well as criteria to extract diagnostics (e.g. the mixed layer depth was defined according to 3 different ways: turbulent, density or temperature criteria).

“Quick-look” scripts have been developed from the VACUMM library and allowed to complete the type of available graphs available, to improve the graphical parameterization and to validate the genericity of the model output reading and vertical interpolation. During the experiment, the PREVIMER system routinely created and sent to the SOP website more than 2000 snapshots a day (see Figure 7 as an example), extracted from MARS (PREVIMER configuration) or NEMO (MONGOOS configuration in which MENOR is embedded) outputs.

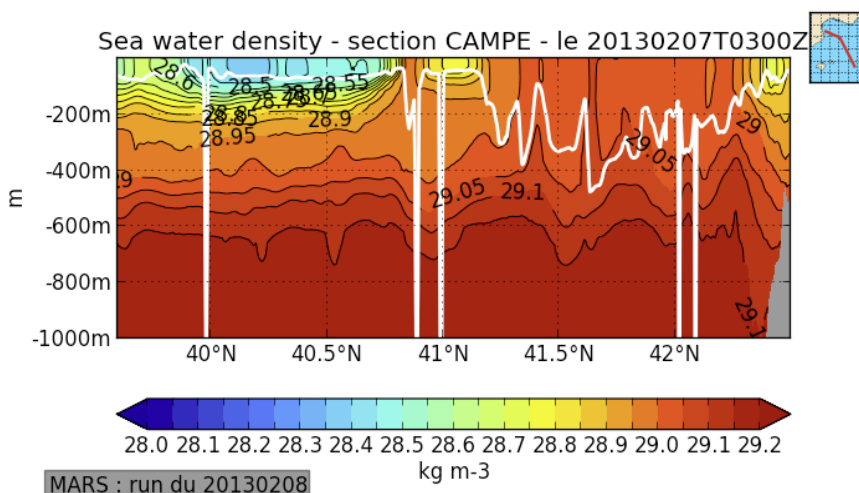
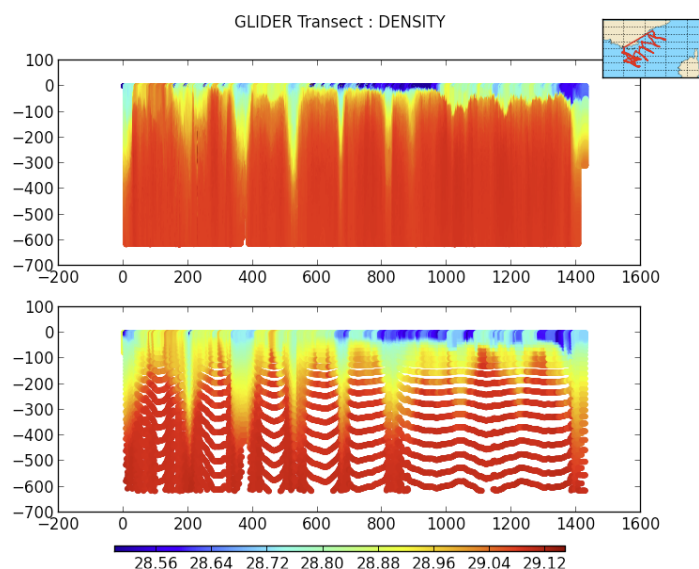


Figure 7: Example of density vertical section from MARS3D numerical simulations for the 7th February 2013 ([http://sop.hymex.org/mars.php?current=20130207&nav=MarsSection&expected=DENS\\_CAMPE](http://sop.hymex.org/mars.php?current=20130207&nav=MarsSection&expected=DENS_CAMPE)). The white line represents the mixed layer depth. Section position is displayed as a red line on the small map.

## Application for research experiment: model validation from glider section

Taking advantage of the possibility to manage both ASCII files (Microsoft Excel or CSV) through Python modules and “xyz” coordinates from Netcdf’s outputs of ocean numerical model through UV-CDAT, VACUMM library is particularly designed to facilitate the collocation of *in situ* data and gridded results. It is now straightforward to compare, for example, glider data stored in Coriolis database (<http://www.coriolis.eu.org/>) as a succession of profiles with 3 hourly outputs of numerical models. During the IMEDIA cruise (March 2012) a glider recorded salinity and temperature along the French Provençal coast in the Mediterranean Sea monitoring a density current flowing along the continental slope from the Ligurian Sea to the Balearic Sea. This current called “North Current” exhibits warmer and fresher water along the coast. On the density field, the North Current is characterized by a lower density vein (until 400m depth) when the glider is close to the coast (Fig. 8). This current is also present in the model. The range in density is correct; nevertheless the vertical mixing seems to be overestimated in the numerical model leading to an important mixed layer depth offshore. Its clearly highlights that the observation vertical resolution is higher than the model one !

*Figure 8: Density profile along a glider trajectory during IMEDIA cruise experiment (Mach 2012). The glider profile read in Coriolis data base (top) is compared to a co-localised numerical model results (MARS3D-MENOR configuration)(bottom).*



## Conclusion

The open-source VACUMM library appears as an efficient toolbox to process ocean data (numerical models and observations) in the frame of research project or to sustain operational systems. Development prospects could for example include an improved interfacing with usual oceanographic and atmospheric models and datasets, or the implementation of new physical or numerical diagnostics, algorithms or schemes. The library is open to new contributors to ensure that it meets at least the requirements of a wide oceanographic community.

## Acknowledgements

The authors wish to thank Fabrice Lecornu and the PREVIMER project that allowed developments and improvements of the VACUMM library. A special thanks to all other junior or advanced developers: Mickaël Garo, Julie Gatti, Pierre Garreau, Serguei Skrypnikov-Laviolle, Sébastien Petton, Jean-François Le Roux. Remotely sensed Sea Surface Temperature data are provided by OSI-SAF (<http://www.osi-saf.org/>) belongs to EUMETSAT.

## References

Berger, H., F. Dumas, S. Petton, and P. Lazure, Evaluation of the hydrology and dynamics of the operational MARS3D configuration of the Bay of Biscay : MANGAE4000, Coriolis - Mercator Ocean Quarterly Newsletter, this issue, 2014.

## A TOOL FOR COASTAL OCEAN FORECASTER

By *M. Faillot<sup>(1)</sup>, J. Lagadec<sup>(1)</sup>, D. Jourdan<sup>(1)</sup>, B. Le Squère<sup>(2)</sup>, J.-M. Léculier<sup>(2)</sup>*

<sup>1</sup> SHOM, Toulouse, France

<sup>2</sup> SHOM, Brest, France

### Abstract

PREVIMER, as a case study for an Operational Coastal Oceanographic Capacity, aimed at providing observation data, modeling tools and real time forecasts as required by a fast growing number of users in coastal areas. One of the inputs from SHOM in this project was to provide the PREVIMER ocean forecasters with an appropriate and user-friendly data management tool in order to manipulate, display, qualify and deliver their expertise on coastal ocean environmental data and forecasts in the timeframe of an operational service.

This task was carried out by SHOM relying on its long term experience in operational oceanography forecasts and its operational ocean forecasting system SOAP ("Système Opérationnel d'Analyse et Prédiction") (Jourdan et al., 2003).

This paper shortly presents SHOM's activities in operational oceanography and how SOAP system has been adapted to PREVIMER and coastal ocean data.

### What is ocean forecasting at SHOM?

SHOM's vocation is to provide with the best qualified information about the ocean physical environment to meet both civilian and military requirements.



Figure 1: Military and civilian applications

In order to achieve this goal, SHOM has been operating ocean forecasting systems for the last 15 years. As a naval agency for military hydro-oceanography, SHOM is responsible for the provision of hydrographic and oceanographic information to support military operations and exercises, and brings as well its expertise to the development and use of military weapons systems and Command and Information Systems (CIS).

SHOM delivers real time ocean forecasting services on a daily basis over the areas of interest of the French Navy. These services are tailored to the various Navy users (Anti-Submarine Warfare, Amphibious and coastal operations) and different sensors (active and passive sonars). This capacity relies on a strong experience and knowledge of the operational issues through daily exchanges with military end-users, but also a strong academic commitment through R&D oceanographic activities (processes studies, numerical improvements, configuration and validation of ocean forecasting models), oceanographic research campaigns at sea, and many collaborations with other French and international operational and research bodies: Mercator Ocean, HYCOM consortium, US National Research Laboratory (NRL), Ifremer, French Met office Météo-France...

The SHOM operational ocean center is located at Brest and Toulouse. This second location is close to the joint defense METOC center and the French Met Office Météo-France.

Figure 2: SHOM operational oceanographic centre



A team of eight forecasters is responsible for delivering 7 days a week the oceanographic information required by the French Navy. These forecasters are working with the SOAP System in order to routinely compute, qualify, prepare and deliver value added military products (Jourdan and al., 2011). The SOAP system allows:

- "to adopt" and retrieve all useful information from different sources: model outputs (oceanographic, meteorological), observations data (in situ, satellite),
- "to produce" value-added products and check-out the production,
- "to qualify". model outputs and products,
- "to serve" "package" user orders,
- "to supervise" the production chains and monitor the system functions and performances.

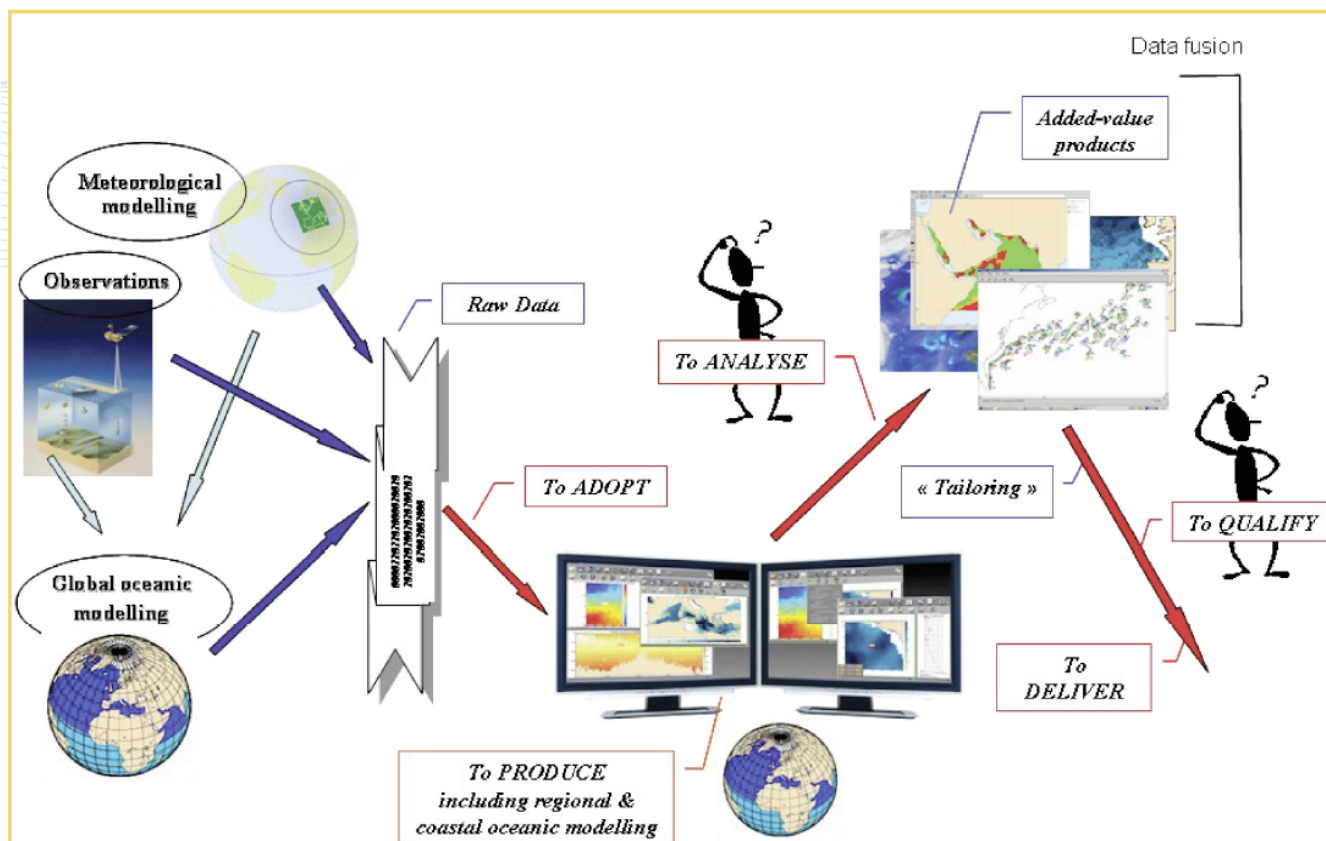


Figure 3: SOAP in one picture

For PREVIMER, SHOM has chosen the SOAP system as a foundation on which the coastal production capability could be built and "plugged in" (Maraldi et al., 2013).

## Adaptation for PREVIMER

The issue was to adapt the SOAP system, initially designed for mesoscale dynamics, to high resolution coastal data in PREVIMER. The objective was that the system shall be used by a forecaster as a unique integrated and modular tool in order to provide the best description and analysis of the coastal ocean state based on PREVIMER model outputs.

In order to meet this goal, the different core functions of SOAP were modified as follows:

- "To adopt": all the input and output data available in PREVIMER can be acquired in the system (adaptation of internal pivot format, NetCDF4 library, etc.):
  - o model outputs (MARS3D, MARS2D, HYCOM, WaveWatch III, meteorological models, etc.),
  - o In situ data:
    - time series (Marel, Molit, tide gauges, meteorological buoys, river runoffs, drifting buoys, etc.)
    - profile data (Recopesca, Argo profilers, TESAC, Gliders, etc...)
    - HF radar data
  - o Satellite data
  - o Coastal environmental climatologies
- "To produce": in the new system, it is now possible to analyze time series, sea state models, spectra, sigma level model.

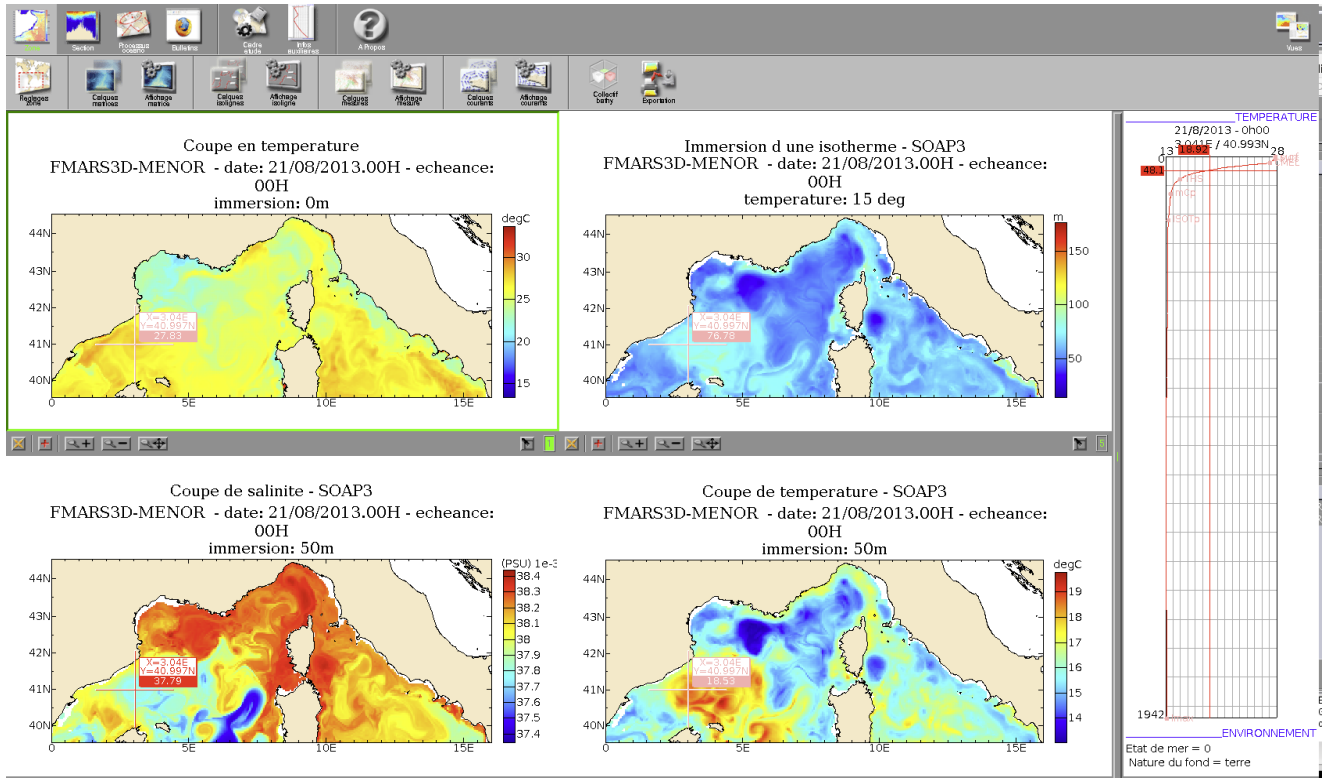


Figure 4: Simultaneous visualisation of different parameters with geolocalisation synchronisation

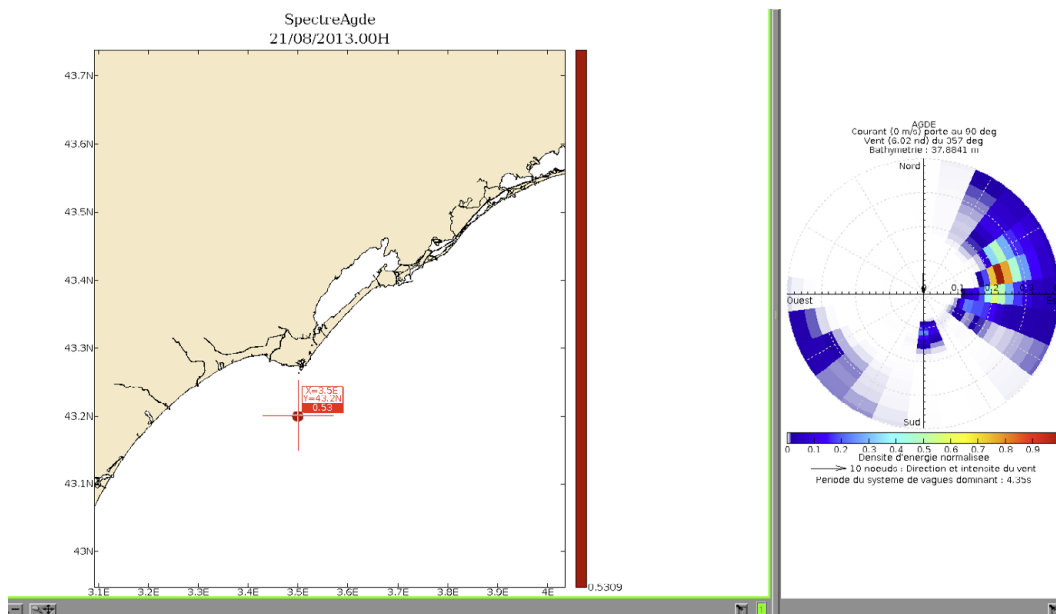
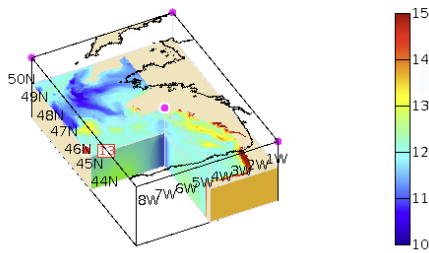


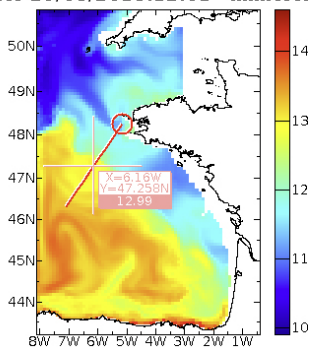
Figure 5: Wave spectrum visualisation

- "To qualify" – thanks to this software, a coastal forecaster can now quickly project sigma level model on different Z coordinate grids, intuitively move inside a 3D matrix of output model, and easily compare different kinds of *in situ* data with models outputs and climatologies.

Temperature eau de mer  
 PREVIMER-D3-ECOMARS3D-GDGE du  
 29/05/2013.12.01 ech. 00H zone "Atlantique"  
 resolution 0.053



PREVIMER-D3-ECOMARS3D-GDGE Temperature  
 eau de mer 29/05/2013.12.01 - immersion 50m



Radiale Golfe Gascogne -  
 PREVIMER-D3-ECOMARS3D-GDGE Temperature  
 eau de mer 29/05/2013.12.01

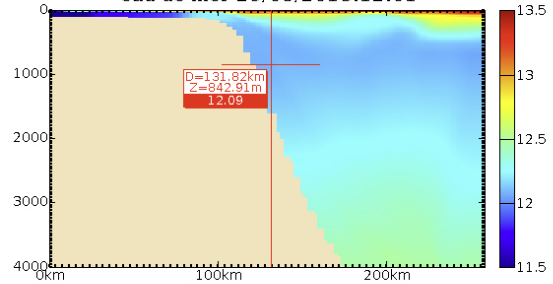


Figure 6: 3D visualisation, transect

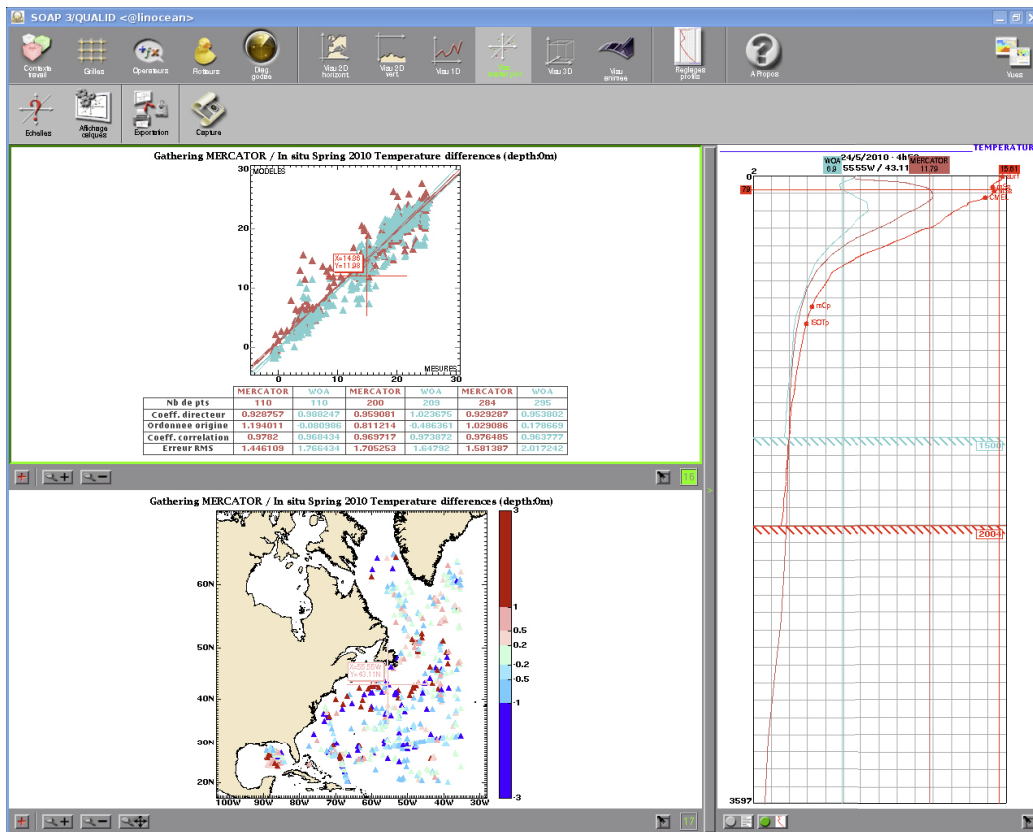


Figure 7: Intercomparison Mercator Ocean/ World Ocean Atlas WOA climatology / in situ data. For each in situ profile, equivalent model and climatological profile are computed.

## Conclusion

SHOM has used its experience and skill in operational oceanography in order to specify and develop a post-production and expert system dedicated to coastal ocean forecasters. This modular, integrated and intuitive tool aims at helping the forecasters to improve on a daily basis their knowledge and expertise of the coastal ocean situation. In particular, this system is able to handle "multi-model" and "multi-scale" (cascade of nested high resolution models) production and consequently to deliver a better quality ocean assessment by taking advantage of the comparison of the "same" reality as viewed by different ocean models and in situ data.

## References

Jourdan D, Lucion C, **2003**: Defense-related applications for operational oceanography: the SOAP system. Building the European capacity in operational oceanography, Elsevier Oceanography Series, 69, 579-585

Jourdan D, Faillot M, Maraldi C, **2011**: SOAP-3: An example of integrated oceanographic information system for naval applications, Vol. 13, EGU2011-8793

Maraldi C, Corréard S, Louazel S, Faillot M, Jourdan D, **2013**: An example of defence service using HYCOM output of the bay of Biscay, Vol. 15, EGU2013-9244, 2013